The Direct Pd-Catalyzed C(sp^3)–H Functionalization of Aliphatic Carboxylic Acids

Dissertation

zur Erlangung des Doktorgrades

der Mathematisch-Naturwissenschaftlichen Fakultät

der Christian-Albrechts-Universität zu Kiel

vorgelegt von

Tianxiao Xu

Kiel 2025

Erster Gutachter: Prof. Dr. Manuel van Gemmeren

Zweite Gutachterin: Prof. Dr. Thisbe K. Lindhorst

Tag der mündlichen Prüfung: 09.05.2025

Zum Druck genehmigt: 12.05.2025

gez. Prof. Dr. Frank Kempken, Dekan

This work was performed between

September 2021 and March 2022 at the Organisch-Chemisches Institut in

University of Münster

April 2021 and December 2024 at the Otto-Diels-Institut für Organische Chemie in

Christian-Albrechts-Universität zu Kiel (Kiel University)

in the working group of

Prof. Dr. Manuel van Gemmeren

Parts of this work have already been published in

T. Xu[1], S. Mal[1], M. van Gemmeren, The Direct Pd-Catalyzed γ-Lactonization of Aliphatic Carboxylic Acids. *Acs Catal.* **2025**, 2735-2741. ([1] These authors contributed equally)

S. Mal[1], T. Xu[1], M. van Gemmeren, The Direct Pd-Catalyzed β-C(sp^3)–H Hydroxylation of Aliphatic Carboxylic Acids. *Submitted* ([1] These authors contributed equally)

Declaration

I, Tianxiao Xu, hereby declare that I have completed this dissertation independently and solely using the sources and tools specified. Apart from the advice provided by my supervisor, Prof. Dr. Manuel van Gemmeren, I have conducted and written this work on my own. Parts of this dissertation result from collaborations with other scientists—any contributions not made by me are clearly marked in the respective sections of this dissertation. This dissertation has not been submitted in any other examination process, nor has any academic degree been revoked. This work has been conducted in compliance with the rules of good scientific practice of the German Research Foundation (DFG). This is my first attempt at obtaining a doctoral degree.

City, Date

Tianxiao Xu

Eidesstattliche Erklärung

Hiermit erkläre ich, Tianxiao Xu, die vorliegende Dissertation selbstständig und ausschließlich unter Zuhilfenahme der angegebenen Quellen und Hilfsmittel angefertigt zu haben. Abgesehen von der Beratung durch meinen Betreuer, Prof. Dr. Manuel van Gemmeren, habe ich diese Arbeit eigenständig erarbeitet und verfasst. Teile der Arbeit gingen aus Kooperationen mit anderen Wissenschaftlern hervor – Leistungen, die nicht von mir selbst erbracht wurden sind an den entsprechenden Stellen der Arbeit immer als solche gekennzeichnet.Die Arbeit hat an keiner anderen Stelle im Rahmen eines Prüfungsverfahren vorgelegen und mir wurde kein akademischer Grad entzogen. Diese Arbeit ist unter Einhaltung der Regeln guter wissenschaftlicher Praxis der Deutschen Forschungsgemeinschaft entstanden. Dies ist mein erster Promotionsversuch.

Ort, Datum

Tianxiao Xu

The Use of Assistive Tools in This Thesis

In this thesis, two assistive tools were used: ChatGPT was employed to enhance language expression, following a publicly available reference (Gruda D. Three ways ChatGPT helps me in my academic writing. *Nature*. **2024** Apr 8. DOI: *10.1038/d41586-024-01042-3*). And Deepl was utilized to translate English into German. These tools were strictly used to improve writing efficiency and refine language clarity. The core content, research conclusions, and academic viewpoints presented in this thesis were independently developed by me and were in no way influenced or replaced by any tool.

Ort, Datum

Tianxiao Xu

Der Einsatz von Hilfsmitteln in dieser Arbeit

In dieser Arbeit wurden zwei Hilfsmittel verwendet: ChatGPT wurde eingesetzt, um den sprachlichen Ausdruck zu verbessern, in Anlehnung an eine öffentlich zugängliche Referenz (Gruda D. Three ways ChatGPT helps me in my academic writing. *Nature*. 2024 Apr 8. DOI: *10.1038/d41586-024-01042-3*). Und Deepl wurde verwendet, um Englisch ins Deutsche zu übersetzen. Diese Hilfsmittel wurden ausschließlich dazu verwendet, die Effizienz des Schreibens zu verbessern und die sprachliche Klarheit zu verfeinern. Der Kerninhalt, die Forschungsergebnisse und die akademischen Standpunkte, die in dieser Arbeit dargelegt werden, wurden von mir unabhängig entwickelt und in keiner Weise durch irgendein Tool beeinflusst oder ersetzt.

Ort, Datum

Tianxiao Xu

Acknowledgement

I would like to express my sincere gratitude to my supervisor, Prof. Dr. Manuel van Gemmeren. Thank you for welcoming me into your team and guiding me throughout my research. I deeply appreciate your patience and persistence, especially during times when our work faced unfair treatment. Your support and made great efforts to ensure our work was published. I have always been amazed by your clear and skillful explanations of mechanisms in our synthesis group meetings. Your passion for research and deep knowledge of chemistry have shown me what it truly means to be a chemist. I feel very lucky to have you as my supervisor—you will always be my role model.

Many thanks to Prof. Dr. Thisbe K. Lindhorst and Prof. Dr. Alessandro Ruffoni for kindly agreeing to serve as candidates for the second examier of my thesis.

I also sincerely appreciate Ms. Svenja Röwer and Ms. Angelika Merten for their invaluable assistance with administrative and document-related matters.

I am also deeply grateful to all the members of the Otto Diels Organic Institute research groups. Thank you for sharing the chemical library, which was a great help to my work. I would also like to extend my gratitude to Mr. Jakob Schweitzer, Mr. Markus Luft, and the entire staff of the NMR, MS, and IR departments—without your help and support, I would not have been able to complete my project.

To my colleagues in the research group—I am truly grateful to have you all as my colleagues and friends. Your support has meant the world to me, and I wouldn't have made it this far without you. Sourjya, my most important work partner and a friend who endured the tough times with me—you are the most humble yet hardest worker in the lab. Your diligence made it possible for us to complete our projects together. And Darte, Simon, and Jyotirmoy, thank you for being such kind and supportive lab mates, tolerating my bad habits, and always being there to help. A special thanks to Fritz, a warm-hearted and handsome person—the first group member I met. And Rita, whose bright and contagious laughter made the lab feel like home. Thank you both for always caring about me and helping me. We created so many wonderful memories together, and I will cherish them always. Thank you, Alex, Arup, and Sabine, for your valuable advice and support at the start of my PhD. To Mirxan, I truly loved your Christmas gift—it was so useful! To Isaac, I appreciate your insights on academic and professional life, and Kerstin, thank you for sharing synthesis materials. To Tommaso, the

funniest guy, and Edis, thanks for the fitness tips, and Tobias, I appreciate your help with lab courses, Joshua, the only person I know who drinks hotpot soup! And Friedrich, Maria and Monika, thank you all—I truly enjoyed our time together in the lab. To Shangze and Hongmei, thank you for inviting me to cook and eat together and for your kind words about my cooking.

To my dear friends, especially Zhe Wang and Honghua Zuo, I am so grateful for your support, advice, and all the fun travels we shared.

Above all, my deepest thanks go to my family—my parents and brother—for always being there for me. Your unwavering love and support have made everything possible.

Abstract

The functionalization of C(sp³)–H bonds has become a key strategy in modern organic synthesis, enabling the efficient construction of complex molecules from simple precursors. In this thesis, I introduced the fundamental principles of C(sp³)–H activation, summarizing prior advancements, limitations, and ongoing efforts in the field. Chapter 2 (**Scheme A.a**) explores β-C(sp³)–H amination of free carboxylic acids. Despite extensive optimization, the desired β-amino acid products were not obtained, but the findings provide insights for future research. Chapter 3 (**Scheme A.b**) presents a palladium-catalyzed β-C(sp³)–H hydroxylation, enabled by pyridone-based ligands. This method shows broad functional group tolerance and works well with α-non-quaternary carboxylic acids. Chapter 4 (**Scheme A.c**) describes γ-C(sp³)–H lactonization using sodium percarbonate and a β-alanine-derived ligand. This one-step reaction efficiently converts various carboxylic acids, including β-non-quaternary substrates, into γ-lactones, offering a valuable tool for synthesis.

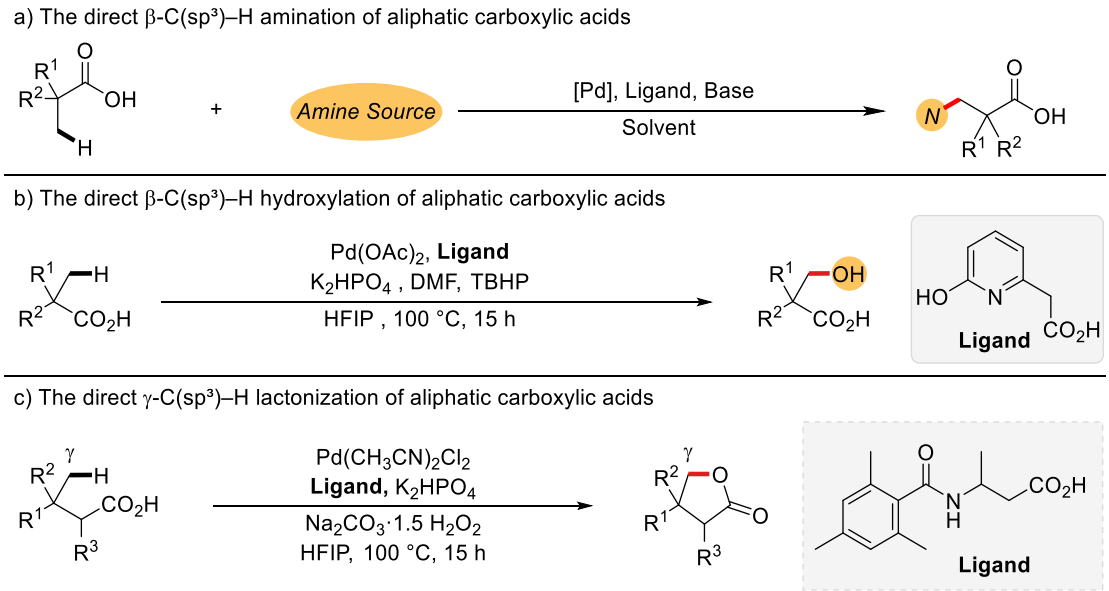

Scheme A. Abstract of this thesis.

Zusammenfassung

Die Funktionalisierung von C(sp³)–H-Bindungen ist zu einer Schlüsselstrategie in der modernen organischen Synthese geworden, die den effizienten Aufbau komplexer Moleküle aus einfachen Ausgangsstoffen ermöglicht. In dieser Arbeit habe ich die grundlegenden Prinzipien der C(sp³)–H-Aktivierung vorgestellt und frühere Fortschritte, Einschränkungen und laufende Bemühungen auf diesem Gebiet zusammengefasst. Kapitel 2 (**Schema A.a**) erforscht die β-C(sp³)–H-Aminierung von freien Carbonsäuren. Trotz umfangreicher Optimierungen konnten die gewünschten β-Aminosäureprodukte nicht erhalten werden, aber die Ergebnisse bieten Einblicke für zukünftige Forschung. In Kapitel 3 (**Schema A.b**) wird eine Palladium-katalysierte β-C(sp³)–H Hydroxylierung vorgestellt, die durch Pyridon-basierte Liganden ermöglicht wird. Diese Methode zeigt eine breite Toleranz gegenüber funktionellen Gruppen und funktioniert gut mit α-nicht-quaternären Carbonsäuren. In Kapitel 4 (**Schema A.c**) wird die γ-C(sp³)–H-Laktonierung unter Verwendung von Natriumpercarbonat und einem von β-Alanin abgeleiteten Liganden beschrieben. Diese einstufige Reaktion wandelt verschiedene Carbonsäuren, einschließlich β-nicht-quaternärer Substrate, effizient in γ-Lactone um und bietet damit ein wertvolles Werkzeug für die Synthese.

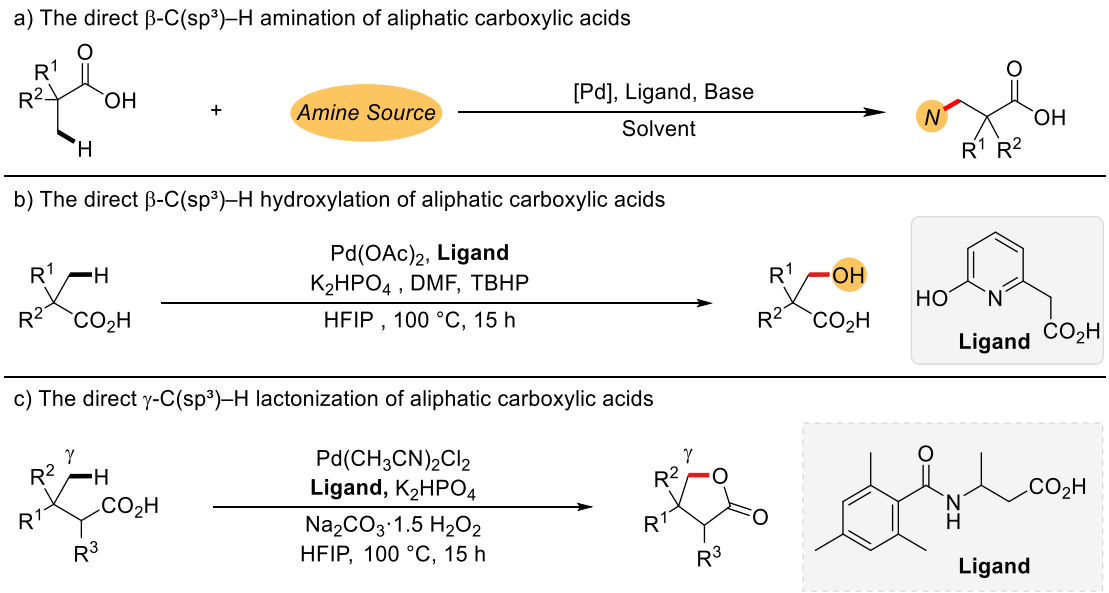

Scheme A. Zusammenfassung dieser Arbeit.

Contents

List of Abbreviations **1**

1 Introduction **6**

1.1 General Introduction 6

1.2 C–H Activation and C–H Functionalization 7

1.3 Mechanism of C–H Activation 8

1.4 Different Catalytic Manifolds in Pd-Catalyzed C–H Activation and Functionalization 12

1.5 Challenges in Pd-Catalyzed C(sp^3)–H Activation 16

1.6 Advantages of Carboxylic Acids as Substrates 20

1.7 The Development of Pd-catalyzed C(sp^3)–H Activation/Functionalization: The Strategies and Influencing Factors 21

1.7.1 Pd-Catalyzed C(sp^3)–H Activation/Functionalization by the Use of Directing Group Strategies 22

1.7.2 Native Carboxylic Acid Group Directed Strategy 25

1.8 Key Developments in the Direct C(sp^3)–H Activation/Functionalization of Free Carboxylic Acids 30

1.8.1 Arylation 30

1.8.2 Olefination 36

1.8.3 Alkynylation 39

1.8.4 Carbonylation 39

1.8.5 Dehydrogenation 40

1.8.6 Deuteration 45

1.8.7 Halogenation 46

2 The Direct Pd-Catalyzed β-C(sp^3)–H Amination of Aliphatic Carboxylic Acids **48**

2.1 Background 48

2.2 Project Goals 53

2.3 Reaction Design 54

2.4 Results and Discussion 56

2.4.1 The Target Product Synthesized Using Hydroxylamine as Amine Source 56

2.4.2 Testing of Using Hydroxyamines as Amine Source 58

2.4.3 Testing of Using Free Amines as Amine Source 61

2.5 Conclusion 66

3 The Direct Pd-Catalyzed β-C(sp^3)–H Hydroxylation of Aliphatic Carboxylic Acids 68

3.1 Background 68

3.2 Project Goals 71

3.3 Optimization of the Reaction Conditions 72

3.4 Substrate Scope 85

3.4.1 Scope of the β-C(sp^3)–H Hydroxylation of Aliphatic Carboxylic Acids 85

3.5 Mechanistic Studies 88

3.6 Conclusion 92

4 The Direct Pd-Catalyzed γ-C(sp^3)–H Lactonization of Aliphatic Carboxylic Acids 94

4.1 Background 94

4.2 Project Goals 98

4.3 Optimization of the Reaction Conditions 99

4.3.1 Optimization for β-Quaternary Carboxylic Acids 99

4.3.2 Optimization for β-Non-Quaternary Carboxylic Acids 120

4.4 Substrate Scope 124

4.4.1 Substrate Scope for β-Quaternary Carboxylic Acids 124

4.4.1 Substrate Scope for β-Non-Quaternary Carboxylic Acids 128

4.5 Synthetic Applications 129

4.5.1 Scale-up Reaction (2.0 mmol scale) 129
4.5.2 Derivatization of the Lactone Product 130
4.6 Proposed Catalytic Cycle 131
4.7 Limitations 132
4.8 Preliminary Evaluation of an Enantioselective Variant 133
4.9 Conclusion 135
5 Experimental Section 136
5.1 General Information 136
5.2 Ligand Synthesis 139
5.3 Pd-Catalyzed Direct β-C(sp^3)–H-Amination of Free Carboxylic Acids 145
5.4 Pd-Catalyzed Direct β-C(sp^3)–H–Hydroxylation of Free Carboxylic Acids 151
5.5 Pd-Catalyzed Direct γ-C(sp^3)–H-Lactonation of Free Carboxylic Acids 158
5.5.1 Scope of the Free Carboxylic Acids 158
5.5.1 Scope of the lactones 163
6 References 176

List of Abbreviations

Å	Ångström
Ac	Acyl
ATP	Adenosine triphosphate
Ala	Alanine
amyl	*n*-pentyl
Ar	Aryl
atm	physical atmosphere
BDE	Bond Dissociation Energy
Boc	tert-Butyloxycarbonyl
BQ	1,4-Benzoquinone
Bu	butyl
cat.	Catalytic
°C	degrees Celsius
CMD	Concerted Metalation Deprotonation
Cy	Cyclohexyl
d	doublet
δ	chemical shift
DCE	1,2-dichloroethane
DFT	Density Functional Theory

DG	Directing Group
DMF	Dimethylformamide
DMSO	Dimethyl sulfoxide
EDG	Electron Donating Group
Equiv.	equivalent
ESI	Electron Spray Ionization
Et	Ethyl
et al.	Latin phrase *"et alia"* means and others
EWG	Electron Withdrawing Group
e.r.	enantiomeric ratio
FG	Functional group
FID	Flame Ionization Detector
FT	Fourier Transformation
GC	Gas Chromatography
Gly	Glycine
h	hour(s)
HFIP	1,1,1,3,3,3–Hexafluor-2-propanol
HPLC	High Performance Liquid Chromatography
HRMS	High Resolution Mass Spectrometry
i	iso

i.e.	id est (it means “in other words”)
Ile	Isoleucine
IR	Infrared Spectroscopy
IUPAC	International Union of Pure and Applied Chemistry
J	Coupling constant
k	Rate of the reaction
κ	coordination mode
KIE	Kinetic Isotope Effect
L	Ligand
LDA	Lithium diisopropylamide
LG	Leaving group
μ	Micro
m	meta or multiplet
M	Metal or Molar
MS	Molecular sieves
m/z	mass/charge
Me	Methyl
MHz	Megahertz
min	minute(s)
MW	Molecular Weight

NaHFIP	Sodium 1,1,1,3,3,3–Hexafluoro-2-propanolate
nm	nano meter
NMR	Nuclear Magnetic Resonance
o	ortho
p	para
Ph	Phenyl
Phe	Phenylalanine
phth	Phthaloyl
Bpin	Boronic acid pinacol ester
Piv	Pivaloyl
pos	positive
ppm	parts per million
Pr	Propyl
q	quartet
quint	quintet
rac	racemic
RCM	ring closing metathesis
R.T.	room temperature
s	singlet
sept	septet

T	Temperature
t	time or triplet
t	tert
Troc	2,2,2-trichloroethoxycarbonyl
TFA	Trifluoroacetyl
THF	Tetrahydrofuran
TMS	Trimethylsilane
UV	Ultraviolet
vs	versus
Val	Valine
ref. data	reference data

1 Introduction

1.1 General Introduction

Over the past several centuries, chemistry has profoundly impacted fields such as medicine, electronics, materials science, energy, agriculture, and cosmetics. Key breakthroughs have enabled the development of more effective drugs, durable or biodegradable materials, and biofuels, supporting advancements that were previously out of reach.[1] Therefore, the continuous improvement of chemical processes has consistently been a focal point of research and innovation.

Modern synthetic chemistry seeks not only to discover new compounds but also to refine methods for creating known compounds more efficiently. Current research aims to streamline chemical synthesis by reducing costs, minimizing reaction steps, and enhancing atom economy, thereby making synthesis both more accessible and environmentally sustainable.

The role of catalysis has been central to these advancements. Catalysts provide alternative reaction pathways that require less energy, effectively lowering activation energy barriers and making previously inaccessible reactions feasible.[2] This catalytic control allows chemists to steer reactions toward specific outcomes with increased precision, yielding desired products while avoiding unnecessary byproducts.[3]

Functional group interconversion, the strategy of converting one functional group into another through substitution, addition, elimination, oxidation, or reduction, stands as a cornerstone in organic synthesis, empowering chemists to precisely transform functional groups and construct complex target molecules.[4] Compared to the highly versatile transformations available with functional groups, the presence of inert C–H bonds often seem inconspicuous. However, as noted by researchers such as Goldberg and Goldman, C–H bonds, though generally considered "unfunctionalized,"[5] are far more ubiquitous and accessible than typical functional groups.

Although these principles have been well-known and applied for many years, they have become increasingly important as interest in developing new, efficient synthetic methods continues to grow. Thus, opportunities now exist to develop novel catalytic methods that can utilize more abundant starting materials or enable the formation of target scaffolds in a single step rather than multiple steps (**Scheme 1.1**). It is evident that if the selective functionalization

of C–H bonds is fully developed, it could become one of the most efficient, versatile, and powerful transformations in organic synthesis,[6] expanding the toolkit beyond traditional functional group interconversions. Transition-metal-catalyzed C–H bond functionalization has emerged as a key strategy in this area.[7]

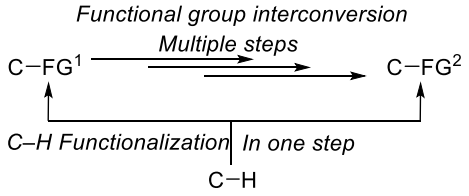

Scheme 1.1 Functional group interconversion and C–H functionalization

1.2 C–H Activation and C–H Functionalization

In this thesis, these two terms that may seem very similar will be used extensively. Although they are often confused in many contexts within the chemical community, it is essential to distinguish between the terms "C–H functionalization" and "C–H activation" in this study to avoid misunderstandings (**Scheme 1.2**).[8]

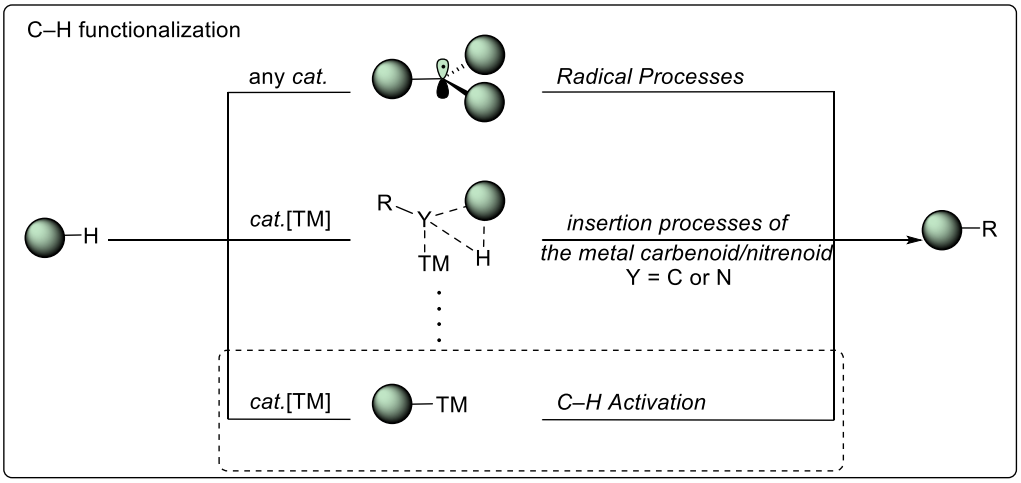

Scheme 1.2 Distinction between the terms "C–H functionalization" and "C–H activation"

In general, the term "C–H functionalization" describes the entire transformation process from the initial C–H bond to the final non-C–H bond. During these transformations, the C–H bond is cleaved, ultimately forming new C–C or C–Heteroatom bonds. The method of C–H bond

cleavage is not emphasized and may include reactions proceeding via radical,[9] ionic (Friedel-type) mechanisms or insertion of the metal carbenoid/nitrenoid, as well as C–H activation reactions.[10]

The term "C–H activation" was used to describe a mechanistic step in C–H functionalization: the process of C–H bond (especially a non-acidic C–H bond (approx. p*K*a > 25)) cleavage via a (transition)metal-mediated reaction, forming a C–M bond. This differs from radical or ionic mechanisms and was thus specifically named "C–H activation."[8] After a C–H activation step, the substrate forms an organometallic species intermediate with the transition metal, which can subsequently react with other species to form additional bonds or undergo further functionalization. In summary, extensive research has demonstrated that transition metals can react with C–H bonds to generate C–M bonds, a process referred to as "C–H bond activation".

1.3 Mechanism of C–H Activation

The modern development of homogeneous C–H functionalization catalyzed by transition metals began with Shilov's platinum chemistry research in the 1970s.[11] Over the past half-century, a range of transition metals has been investigated for their potential in C–H functionalization.[7a, 12] The properties and oxidation states of metals largely determine the C–H activation mechanisms employed in reactions. Historically, understanding these mechanisms relied on experimental techniques to isolate reaction intermediates; and now, extensive research recognizes density functional theory (DFT) as a reliable tool for investigating organometallic reactivity.[13] Although distinctions between mechanisms are sometimes subtle, understanding fundamental mechanistic processes remains essential. Here, we discuss the most common C–H activation mechanisms:

i. Oxidative addition (**Scheme 1.3**) is the most common mechanism for C–H bond cleavage, resulting in the formation of C–M and M–H bonds. The process begins as the C–H bond coordinates to a vacant site on the metal, with electrons from the C–H σ-orbital transferring to the metal's d-orbital. Simultaneously, electrons from the metal's d-orbital transfer cooperatively into the σ* orbital of the C–H bond, weakening the bond. This mechanism raises the metal's formal oxidation state by +2. The resulting metal complex then typically undergoes reductive elimination and product release, returning to its original oxidation state.[14] This pathway is favored in electron-rich, low-valent complexes of late transition

metals (e.g., Re, Fe, Ru, Os, Ir, Pt), where both the increased oxidation state and the geometric shifts needed for new bond formation are energetically favorable.

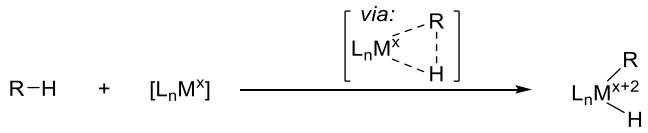

Scheme 1.3 Oxidative addition

ii. σ-Bond metathesis (**Scheme 1.4**): Transition metals with a d^0 electron configuration (such as those in groups 3 and 4, as well as lanthanides and actinides)[15] cannot undergo oxidative addition due to their inability to back-donate from d orbitals into the σ* orbital of the C–H bond. Instead, σ-bond metathesis is the preferred mechanism, often involving alkyl or hydride complexes.[16] In σ-bond metathesis, chemical bonds are exchanged between two reactive species. This concerted pathway involves the simultaneous formation of M–R and R–H bonds while M–R and R–H bonds break in the transition state, keeping the metal's oxidation state unchanged throughout. σ-Bond metathesis is especially favorable in systems with bulky ligands that reduce coordination sites, facilitating this pathway.

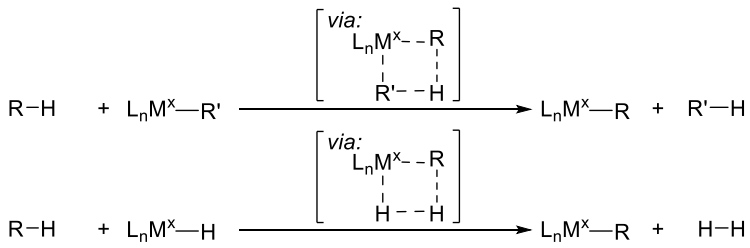

Scheme 1.4 σ-Bond metathesis

iii. Concerted Metalation-Deprotonation (CMD) (**Scheme 1.5a**) is considered a plausible mechanism for most Pd-catalyzed C–H activations. The term CMD was first formally introduced in the early 2000s when Keith Fagnou and David Lapointe[17] defined this base-mediated, simultaneous process of C–H bond cleavage and C–M bond formation. However, the CMD concept dates back to 1955, when Winstein and Traylor initially hypothesized this mechanism while studying the acetolysis of diphenylmercury in acetic acid.[18] Later, in 1968, Davidson and Triggs recognized similarities between palladation and mercuration in benzene while investigating the Pd-catalyzed formation of biphenyl.[19]

Subsequent studies have further clarified the general CMD pathway: in CMD, a hydrogen atom transfers as a proton to a base through either an intramolecular or intermolecular route. Lone electron pairs on heteroatoms within the ligand assist in proton abstraction, while late transition metals (e.g., Ir, Pd, Pt) form a sigma bond with the alkane. Thus, the ligand acts both as a Lewis base and as a Brønsted base. Since C–H bond cleavage occurs in a coordinated step, a primary kinetic isotope effect (KIE) is often observed in CMD processes. A closely related mechanism is ambiphilic metal-ligand activation (AMLA),[20] which, like internal base-assisted C–H cleavage, involves cooperative interactions between the metal center and ligand. Both mechanisms are gaining increasing significance in homogeneous catalysis, particularly for alkane activation.

iv. Electrophilic mechanisms (**Scheme 1.5b**):A key guiding principle in viewing C–H activation as an electrophilic mechanism is the involvement of a neighboring heteroatom's lone pair in proton abstraction during the transition state.[8] This characteristic differentiates the electrophilic substitution (ES) mechanism from σ-bond metathesis, which also involves a four-centered transition state but lacks lone pair participation. Electrophilic C–H activation typically occurs with positively charged late transition metal complexes where the metal's oxidation state remains constant during the C–H activation step. However, the term "electrophilic activation" alone does not capture the variety of possible transition states, which are now more specifically classified into categories such as electrophilic substitution (ES),[21] electrophilic concerted metalation-deprotonation (eCMD).[22] Regardless of the transition state, this mechanism involves a positively charged metal center approaching the C–H bond of the substrate, followed by a concerted hydrogen abstraction.

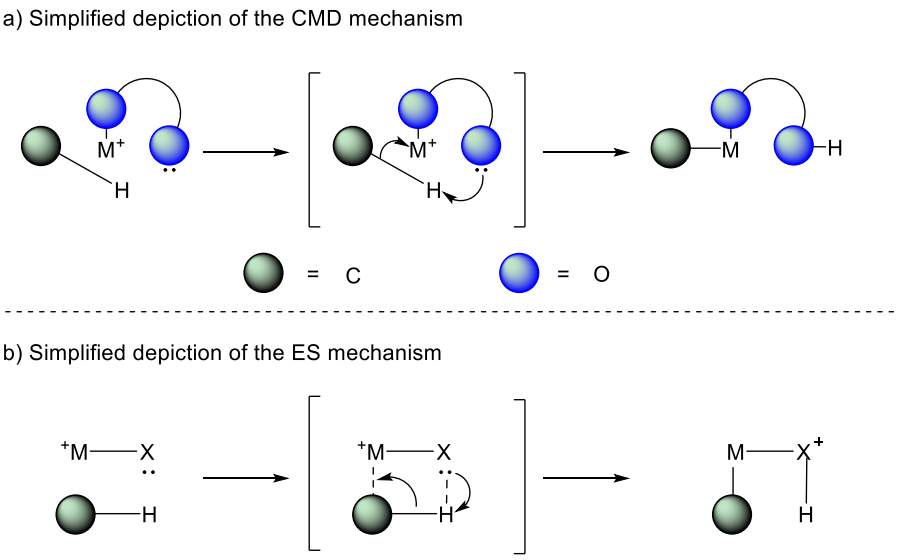

Scheme 1.5 The electrophilic mechanisms: CMD and ES

Literature surveys indicate that among transition metals, palladium—often regarded as the champion catalyst in coupling chemistry[23] —is also one of the most extensively studied metals in C–H activation.[24] Research highlights the critical role of selecting the appropriate palladium source for achieving optimal reactivity.[25] Palladium acetate is particularly favored, as its acetate ligand offers unique advantages in cyclometalation: its larger effective volume compared to chloride facilitates solvation of reaction intermediates,[26] and it enhances the electrophilicity of the Pd^{II} center by acting reversibly as either a bidentate or monodentate ligand.[27] A significant publication by Sakaki and colleagues in 2000 showed that, while carboxylates are essential for reactivity, the reaction rate is unaffected by the strength of an external base, indicating that proton abstraction occurs via the acetate ligand on palladium rather than through an external base.[28] Organopalladium compounds are highly versatile, exhibiting a wide range of chemical properties and standing out as some of the most accessible, easily synthesized, and manageable transition metal complexes. This versatility stems from palladium's ability to undergo redox reactions across multiple oxidation states and to coordinate and dissociate readily with various ligands and substrates. Furthermore, palladium's broad compatibility with multiple functional groups distinguishes it from many other transition metal complexes.[26]

While C–H activation represents only one step in the broader process of C–H functionalization, palladium plays a pivotal role in facilitating these pathways. Its effectiveness in driving C–H functionalization lies in its ability to adopt multiple catalytic modes, which will be illustrated

in the following discussion.

1.4 Different Catalytic Manifolds in Pd-Catalyzed C–H Activation and Functionalization

Extensive research has identified four primary catalytic modes by which Pd facilitates C–H to C–R bond formation: Pd^{II}/Pd^{0}, $Pd^{0}/Pd^{II}/Pd^{IV}$, Pd^{0}/Pd^{II}, and Pd^{II}/Pd^{IV}. Although other oxidation states of Pd complexes have been reported in recent years,[29] these remain less studied and will not be covered in the following discussion.

i. Pd^{II}/Pd^{0} catalytic cycle

This catalytic cycle is exemplified in C–C bond-forming reactions where organometallic compounds serve as reaction partners. In this mode (**Scheme 1.6**), Pd^{II} mediates the activation of a C(sp^3)–H bond in the first step, converting it into a reactive C–Pd bond. Subsequently, an organometallic reagent, with a partially negative charge on its carbon, acts as a nucleophile and undergoes transmetallation with the Pd center, forming a key Pd cycle intermediate. This intermediate then undergoes reductive elimination, releasing the target product and regenerating Pd^{0}. When an alkene is used instead of an organometallic reagent, the π-electrons of the double bond coordinate with the metal center, followed by an insertion reaction and β-hydride elimination to release the product. Under basic conditions, reductive elimination then occurs, leading to the formation of Pd^{0}. In both cases, an external oxidant (also called terminal oxidant) is required to reoxidize the resulting Pd^{0}, completing the catalytic cycle.

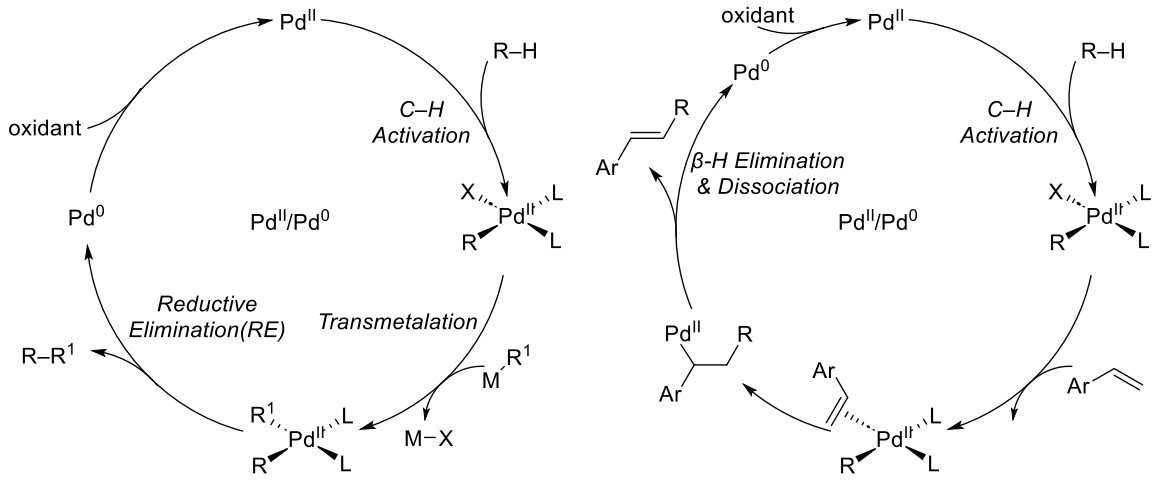

Scheme 1.6 Pd^{II}/Pd^{0} catalytic cycle for the C–H functionalization.

ii. Pd^{0}/Pd^{II} catalytic cycle

This catalytic cycle (**Scheme 1.7**) is initiated by Pd^{0}, making the first step similar to that in cross-coupling reactions, with reaction partners typically being halides or pseudohalides with oxidizing potential. In 1994, Dyker published a pioneering report on activating inert C(sp^3)–H bonds in aryl iodides to synthesize polycyclic systems via this catalytic mode. [30] A more notable example followed in 2003, when Baudoin reported the first synthesis of fused four-membered carbocycles through intramolecular C(sp^3)–H arylation of aryl bromides.[31] In this catalytic mode, Pd^{0} undergoes oxidative addition with the aryl halide to form C–Pd intermediate . Then the C–H bond was activated to produce a key Pd cycle intermediate, which undergoes reductive elimination to yield the product and regenerate the Pd^{0} species.

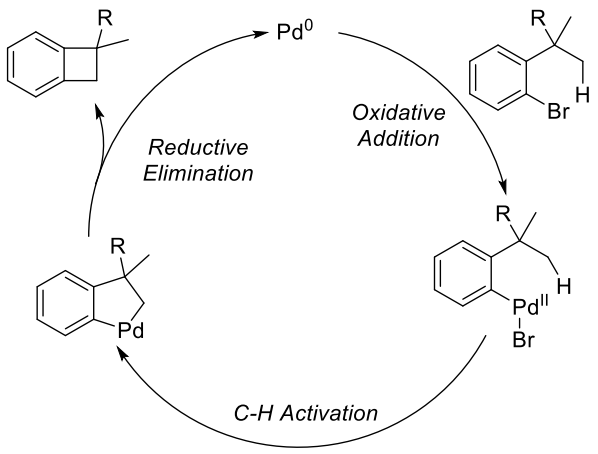

Scheme 1.7 Example of Pd^0/Pd^{II} catalytic cycle for the C–H functionalization

iii. Pd^{II}/Pd^{IV} catalytic cycle

To facilitate C–H activation, strong donor atoms are often used to stabilize the carbon-palladium intermediate. However, this strong chelation effect results in a thermodynamically stable Pd cycle intermediate, which can reduce reactivity in subsequent steps and hinder further transformations. A strategy to address this issue involves employing a Pd^{II}/Pd^{IV} catalytic cycle (**Scheme 1.8**) with highly oxidizing, electrophilic coupling partners (such as alkyl or aryl iodides). In the Pd^{II}/Pd^{IV} catalytic cycle, C–H activation occurs in the first step, followed by oxidative addition with an electrophilic partner to form a highly reactive Pd^{IV} species. This high-energy Pd^{IV} intermediate is typically unstable and quickly decomposes, yielding the Pd^{II} species and the desired product. Removal of the halogen requires the assistance of silver salts and base.

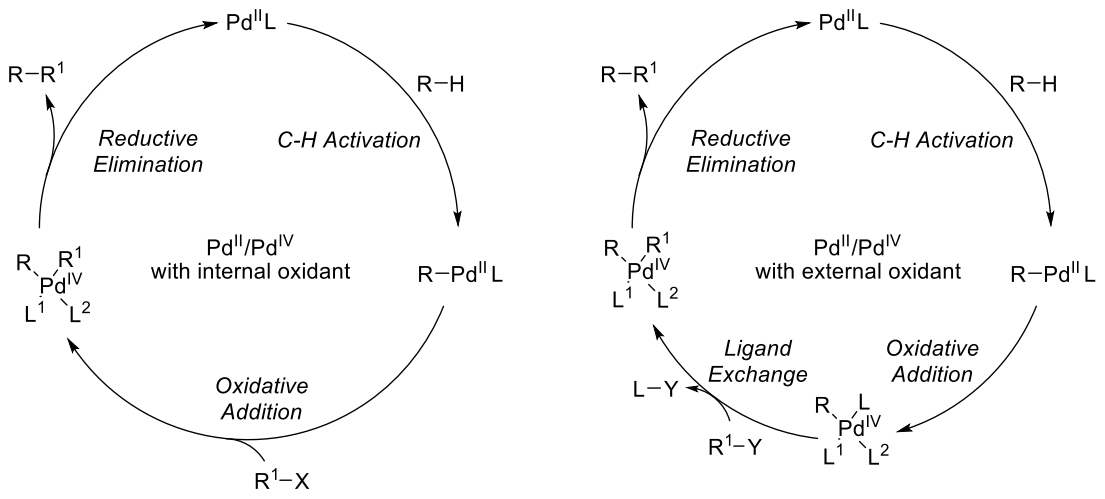

Scheme 1.8 Pd^{II}/ Pd^{IV} catalytic cycle for the C–H functionalization

iv. $Pd^0/Pd^{II}/Pd^{IV}$ catalytic cycle

This catalytic mode (**Scheme 1.9**) is commonly observed in Catellani-type reactions. In this process, a Pd^0 species initiates the reaction by undergoing oxidative addition with the substrate, typically an aryl halide, to form the Pd^{II} intermediate **Int-I**. Due to the rigidity and optimal planar bending angle of norbornene (NBE), **Int-I** then migrates into the norbornene, generating **Int-II**. **Int-II** facilitates the activation of the C–H bond adjacent to the C–Halide bond, forming the key intermediate **Int-III** (an aryl-norbornyl-Pd cycle). This active intermediate, **Int-III**, is then oxidized by an electrophilic reagent to generate the Pd^{IV} intermediate **Int-IV**, which undergoes reductive elimination to form **Int-V**. **Int-V** subsequently undergoes β-carbon elimination and extrusion of norbornene, yielding intermediate **Int-VI**. Finally, **Int-VI** reacts with various nucleophiles to complete the catalytic cycle and regenerate Pd^0.

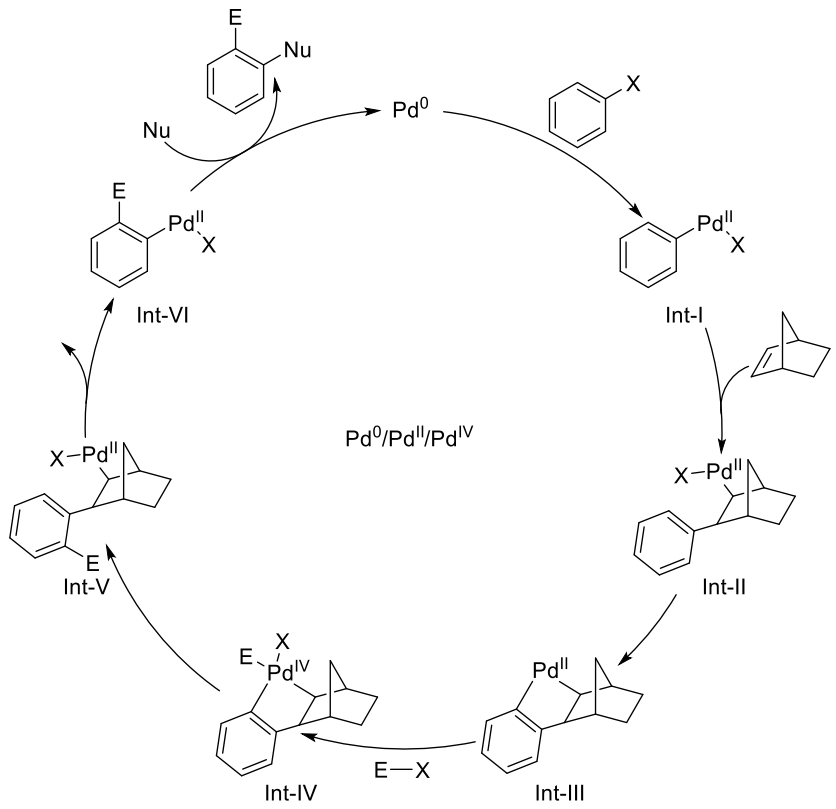

Scheme 1.9 $Pd^0/Pd^{II}/Pd^{IV}$ catalytic cycle for the C–H functionizatin

1.5 Challenges in Pd-Catalyzed C(sp³)–H Activation

As outlined in the previous discussion, the mechanism of Pd-catalyzed C–H activation has been extensively studied. However, inherent and challenging issues remain in Pd-catalyzed functionalization of $C(sp^3)$–H bonds that cannot be overlooked.

The reactivity of C–H bonds in chemical reactions is influenced by several factors, with bond dissociation energy (BDE) and p*K*a being two of the most critical.

Bond Dissociation Energy (BDE) refers to the energy required to homolytically cleave a specific bond, where each atom involved retains one bonding electron, resulting in the formation of two neutral radicals.[32] Bonds with lower BDE values are generally more reactive, particularly in radical-mediated reaction pathways.[33] On the other hand, p*K*a is the negative logarithm of the acid dissociation constant for a molecule.[32] A lower p*K*a value corresponds to a stronger acid. For C–H bonds, an high p*K*a indicates lower acidity, greater bond strength, and higher resistance to deprotonation, often necessitating stronger bases or catalysts for

activation.

Type of Bond	BDE (kcal/mol)	p*K*a	Examples
Alkane C(sp^3)–H	~104	~50	Methane (CH_4), Ethane (C_2H_6)
Benzylic C(sp^3)–H	~87	~41	Toluene ($C_6H_5CH_3$)
Allylic C(sp^3)–H	~88	~43	Propene (CH_2=$CHCH_3$)
Alkene C(sp^2)–H	~110	~44	Ethylene (CH_2=CH_2)
Aromatic C(sp^2)–H	~113	~43	Benzene (C_6H_6)
Alkyne C(sp)–H	~131	~25	Acetylene (HC≡CH)
Methyl Adjacent to Carbonyl C(sp^3)–H	~94	~20	Acetone (CH_3COCH_3)
α-C(sp^3)–H in Aldehydes	~90	~17	Acetaldehyde (CH_3CHO)
C–Halogen (C–Cl)	~84		Chloromethane (CH_3Cl)
C–O Single Bond (C–O)	~85		Dimethyl ether (CH_3OCH_3)
C–S Single Bond (C–S)	~65		Dimethyl sulfide (CH_3SCH_3)
Nitriles C(sp^3)–H	~88–91	~25–30	Acetonitrile (CH_3C≡N, ~25)
Amides C(sp^3)–H	~90–93	~15–20	Acetamide (CH_3CONH_2, ~16)

Table 1.1 Bond dissociation energy (BDE) at 298 K and p*K*a of common Carbon–Heteroatom (C–X) and Carbon–Hydrogen (C–H) bonds[34]

The table (**Table 1.1**) summarizes the bond dissociation energies (BDEs) and p*K*a values for common Carbon–Heteroatom (C–X) and C–H bonds.[34] C–H bonds generally exhibit higher BDE, consistent with their inherent in many reactions; however, their reactivity is also influenced by p*K*a. Notably, BDE and p*K*a trends may oppose one another under distinct mechanistic regimes. For instance, in radical or thermally driven processes, BDE determine reactivity due to the homolytic bond cleavage step, which typically favors the weaker tertiary

C(sp^3)–H bonds. Conversely, in ionic or metal-mediated mechanisms (e.g., base-assisted deprotonation pathways), p*K*a predominates because proton abstraction depends on acidity. For example, aryl C(sp^2)–H bonds, despite their higher BDE, display enhanced reactivity compared to unactivated C(sp^3)–H bonds.

Also, unactivated C(sp^3)–H bonds lack low-energy vacant orbitals or high-energy filled orbitals close to the metal orbitals.[35] The tetrahedral geometry of the C(sp^3) carbon further reduces the accessibility of C(sp^3)–H bonds to the metal center. These combined effects contribute to the inertness of C(sp^3)–H bonds.

Additionally, the narrow differences in BDE and p*K*a values among unactivated C(sp^3)–H bonds complicate regioselective activation of specific positions. In such cases, their activation potential varies depending on their position within the molecular structure. Taking 2,3-dimethylheptanoic acid as an example (**Scheme 1.10**): the C–H bond on β- and γ-methyl groups are inequivalent due to the different distance with the electron-withdrawing carboxyl group (–COOH). During C–H activation, the coordination of the metal center with the different carbons (β- or γ-position) results in Pd cycle intermediates with different stabilities.[36] Specifically, under identical conditions, the five-membered Pd cycle intermediate (from β-C–H activation) is generally lower in energy and more stable than the six-membered Pd cycle intermediate (from γ-C–H activation). Larger Pd cycles are higher in energy and less stable, making the activation of more distant C–H bonds significantly more challenging.[37]

Moreover, compared to primary C(sp^3)–H bonds, methylene groups (–CH_2–) equidistant from the carboxyl group are even less prone to activation, despite their relatively diminished BDE and p*K*a values. This difference arises from the steric effects of the resulting Pd cycle intermediate[36]: methyl C–H bonds form Pd cycles with lower steric hindrance and thus lower energy than those involving methylene C–H bonds.[37d, 38]

These are general guidelines, but of course crossed selectivities are also observed. In addition, other factors such as ring strain, conformational effects and last but not least ligand effects can alter the usual selectivity.[36]

The possible forms of palladacycle intermediates generated after palladium-catalyzed C–H activation.

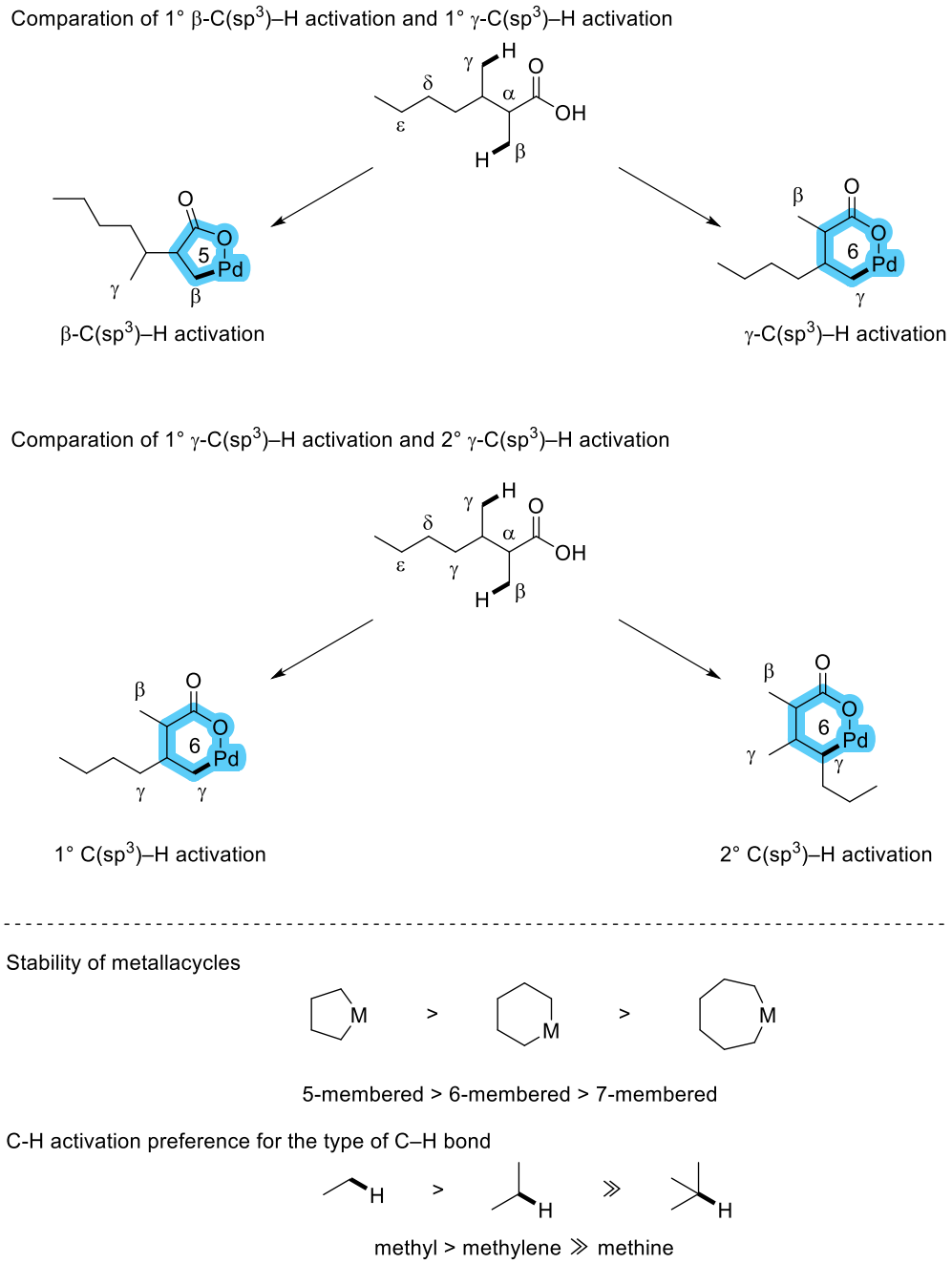

Scheme 1.10 Elaboration of the challenge of C–H activation selectivity: the example of 2,3-dimethylheptanoic acid

In addition, the reactivity of C(sp³)–H bonds can be further enhanced by the presence of functional groups introduced through prior C–H functionalization. Alternatively, in aliphatic molecules with multiple branching groups, similar chemical environments may arise—for

instance, the presence of two β-methyl groups—leading to overreaction and the formation of multiple products (mono-, di-, or tri-functionalized).[39] One potential solution to mitigate overreaction is to employ statistical control. By increasing the concentration of other reaction partners, selective mono-functionalization can be statistically favored.

Additional challenges include reproducibility and scalability. While small-scale laboratory reactions can be optimized for high efficiency and selectivity, scaling these reactions to an industrial level often presents high catalyst and/or ligand loadings and reproducibility issues.[40] Furthermore, applying C–H activation in highly complex environments, such as in total synthesis, introduces additional difficulties. As molecular complexity rises, the number of intramolecular functional groups and accessible C–H bonds also increase, placing high demands on reaction tolerance and selectivity. Finally, addressing sustainability remains a critical challenge.[7b]

1.6 Advantages of Carboxylic Acids as Substrates

Understanding the class of carboxylic acids and the key reactions of the –COOH group is foundational in introductory chemistry. Carboxylic acids are available in a wide range of structures, are easy to store, and simple to handle.[41] They can be prepared through established methods, such as nitrile hydrolysis, malonic ester alkylation, or olefin carbonylation, and may also be sourced from renewable natural materials or synthesized via the oxidation of naturally occurring alcohols.[42] Consequently, carboxylic acids are accessible at low cost from both natural and synthetic sources and offer extensive structural diversity.[43] These versatile properties make carboxylic acids highly promising starting materials for chemical synthesis.

The unique physical properties of the carboxyl group—acidity, polarity, and surface characteristics—contribute to its significant applications in organic chemistry and industry.[44] These applications span materials science, pharmaceuticals, agrochemicals, coatings, the food industry, cosmetics, disinfectants, and other chemical products.[45] For instance, decarboxylation reactions involving carboxyl groups have gained significant prominence in the field of organic synthesis,[46] demonstrating versatility across various catalytic modes, including photocatalysis and electrocatalysis.[47] Thus, modifying the structure of substrates containing carboxyl groups while retaining the carboxyl functionality would be highly beneficial, as it would allow the advantageous properties of the carboxyl group to be

maintained while introducing new functional characteristics.

1.7 The Development of Pd-catalyzed C(sp³)–H Activation/Functionalization: The Strategies and Influencing Factors

Industrial-scale C–H functionalization, such as the synthesis of methanol from methane, is conducted on a large scale, where the efficiency and scalability of catalysts and reaction conditions are critical concerns.[48] Given the inherent simplicity of substrates and the absence of chemically distinct functional groups, extreme reaction conditions are often applied to cleave both C–H and C–C bonds, without specific recognition of individual C–H bonds.

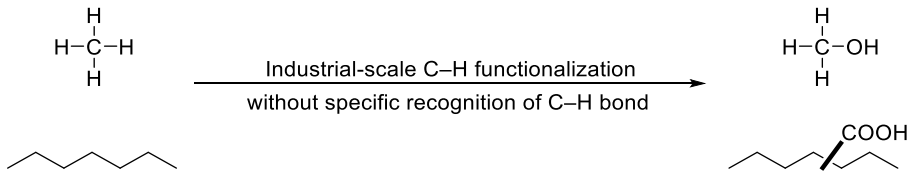

Scheme 1.11 Industrial-scale C–H functionalization

Introducing different functional groups into a molecule can alter the reactivity of its C–H bonds, leading to differentiation—one of the fundamental challenges of C–H activation and functionalization previously mentioned. A common approach to address this challenge is to use directing groups that coordinate with palladium, enabling the formation of a stable palladacycle with the substrate molecule through C–H activation.[37a, 49] Ideally, utilizing naturally occurring functional groups, such as amines, carboxylic acids, and alcohols, to achieve this goal would be the optimal strategy. However, these natural groups, particularly free acids and alcohols, interact weakly with Pd and are ineffective in promoting C–H activation when using simple palladium salt catalysts. To enhance coordination between metal catalysts and substrates, additional nitrogen-containing chelating arms were initially introduced. This led to the development of directing group (DG) assisted C–H functionalization. In this strategy, naturally occurring functional groups are transformed into ligands capable of coordinating with transition metals.

1.7.1 Pd-Catalyzed C(sp³)–H Activation/Functionalization by the Use of Directing Group Strategies

The strategy of directing group-assisted C–H functionalization can be traced back to pioneering works in the mid-20th century.[50] These studies laid the groundwork for the development of this approach.

The core principle of this strategy involves utilizing functional groups with strong coordinating abilities to facilitate C–H bond cleavage both kinetically and thermodynamically. Kinetically, these functional groups increase the local concentration of the metal complex at the target site, enhancing the reaction rate. Thermodynamically, they stabilize the activated intermediate, such as the metallacycle, through a chelation effect, thereby lowering the energy barrier for C–H bond activation.[8, 51] Nitrogen-containing functional groups were initially considered due to their strong coordinating properties. However, the scarcity of naturally nitrogen-based structures meeting this criterion led to the development of directing groups (DG) installation. These involve coupling nitrogen-containing functionalities with naturally occurring groups, such as carboxylic acids and 8-aminoquinoline,[52] or alkylamines and pyridine carboxylic acids.[53] This hybrid design enables C–H activation and functionalization in systems[54] where native functional groups alone would fail to achieve C–H bond recognition. The directing group is subsequently removed to complete the desired molecular modification (**Scheme 1.12**).[55]

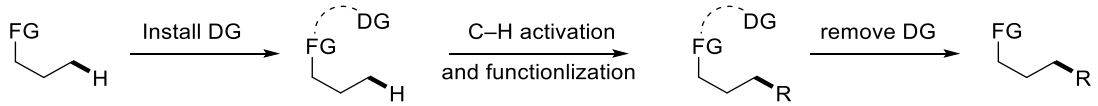

Scheme 1.12 C–H functionalization assisted by the use of directing group strategies

To date, a wide variety of functional groups, including amides, imines, azacycles, amines, oximes, and functional groups containing sulfur, phosphorus, and silicon, as well as π-coordinating groups, have been developed as directing groups, significantly expanding the substrate scope for C–H activation and functionalization (**Scheme 1.13**).[56]

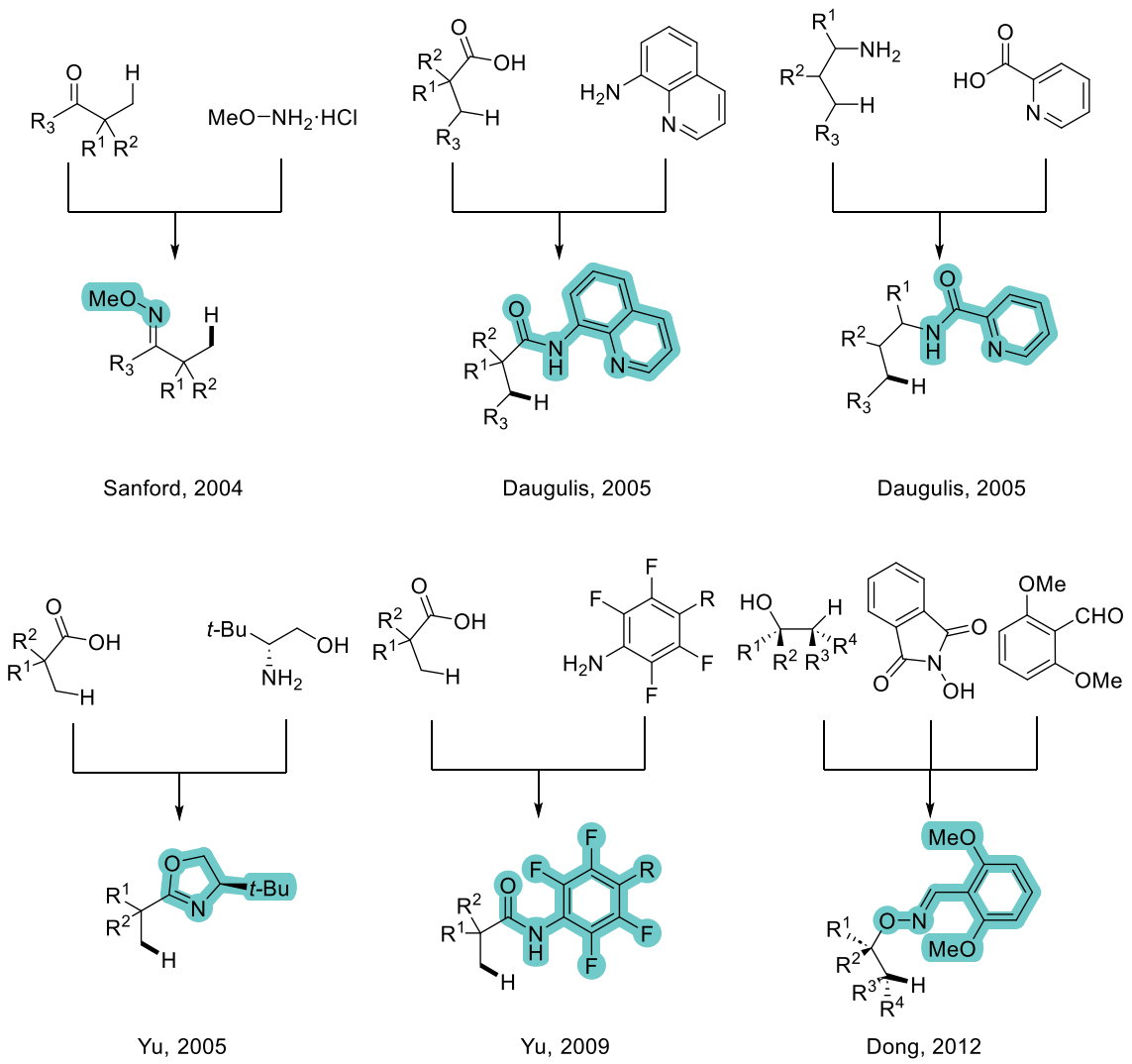

Scheme 1.13 Examples of common directing group

While the use of directing group (DG) strategies has opened the new door to the field of C–H activation, the requirement for DG installation and removal has limited their broader application. The emerging strategy, temporary directing group (TDG), offer an alternative approach.

The temporary directing group (TDG) strategy is an evolution of the traditional DG approach, addressing the cumbersome steps of pre-installation and post-reaction removal. In the TDG method, DG installation, functionalization, and removal occur sequentially in one pot.[57] This approach retains the advantages of traditional DG methods while alleviating their limitations. For instance, amine-containing TDGs can convert weakly coordinating ketone groups into stronger σ-donor imine moieties. After the C–H activation and functionalization are complete,

the imine intermediate decomposes within the same reaction vessel, yielding the desired product (**Scheme 1.14**).[57b]

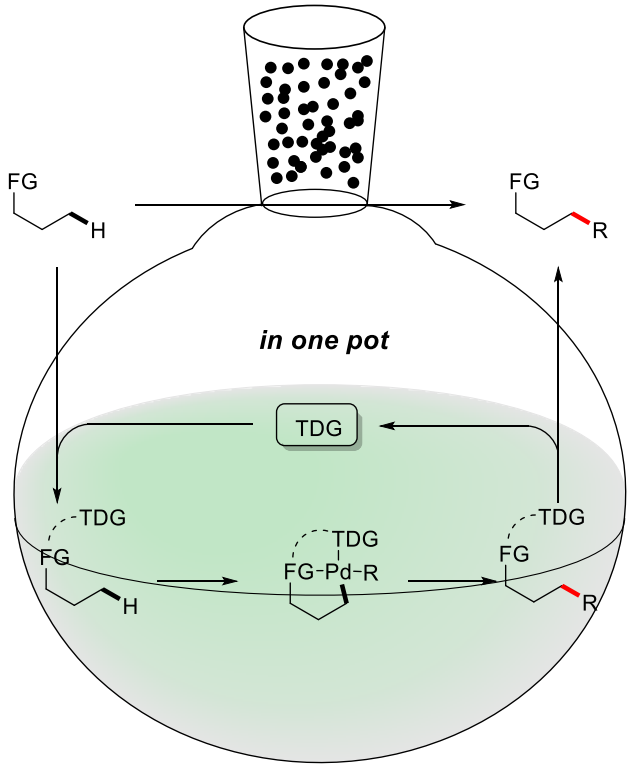

Scheme 1.14 C–H functionalization assisted by using of transient directing group (TDG) strategies

A successful TDG strategy must meet several critical criteria. The formation of the TDG should be reversible, enabling its installation and removal in the same reaction vessel. Additionally, the TDG must be compatible with the reaction system before and after installation, avoiding interference with the target product or other reagents. Most importantly, the TDG should ensure high chemical and site selectivity in the resulting product.[58]

To date, the formation of imines via in situ condensation reactions has been one of the most successful TDG strategy for C(sp³)–H functionalization (**Scheme 1.15**).[59] For example: For aliphatic aldehydes/ketones, α- or β-amino acids and their derivatives have been used as TDGs.[60] For aliphatic amines, TDGs such as amino acids or glycolic acid have been employed.[59a, 61]

Despite the advantages of the TDG approach, its application remains limited to a few substrate types and single functionalization events, significantly hindering its broader practical adoption.

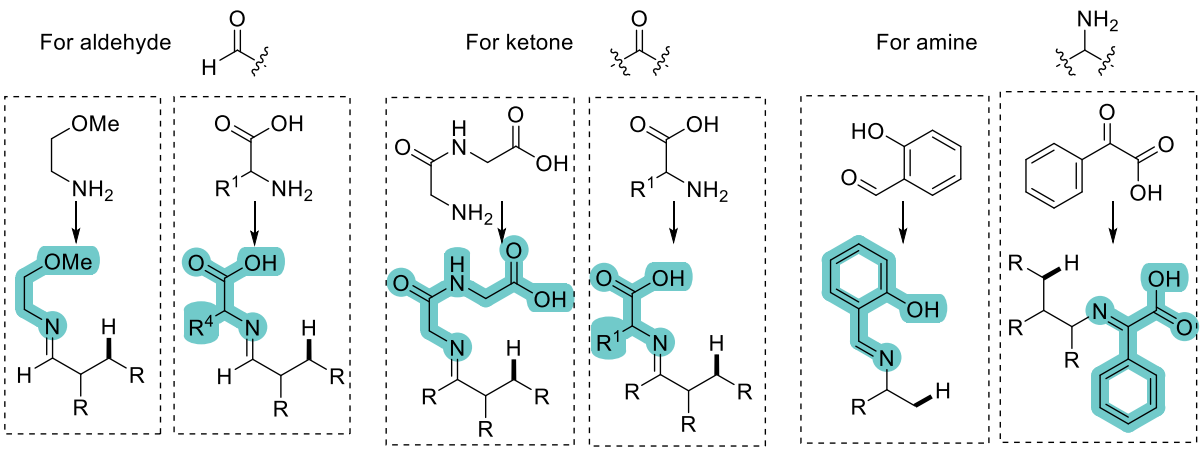

Scheme 1.15 Examples of common transient directing group (TDG)

The use of temporary or removable directing groups faces significant practical limitations. However, years of development have provided substantial insights into direct C(sp³)–H activation facilitated by native functional groups.

1.7.2 Native Carboxylic Acid Group Directed Strategy

Utilizing the native functional groups present in aliphatic compounds to promote C–H activation is conceptually one of the most attractive approaches, as it eliminates the need for external directing groups, making it the most step- and atom-economical method. However, as previously mentioned, the weak coordination of native functional groups with Pd makes achieving selective C–H activation challenging. Ironically, this limitation presents an opportunity for reaction design: the weakly coordinating native groups prevent the formation of overly stable palladium complexes, thereby facilitating more efficient functionalization steps. Due to the various advantages of native carboxylic acids as substrates and products, they have been extensively studied.

The first study to use carboxyl groups as directing groups for aliphatic C–H activation was based on lactonization via potassium tetrachloroplatinate. In 1991, Kao and Sen demonstrated that various aliphatic carboxylic acids could be converted into lactones in deuterium oxide (**Scheme 16**).[62] However, the reaction showed low efficiency and required stoichiometric platinum. Nevertheless, this pioneering discovery supported further research.

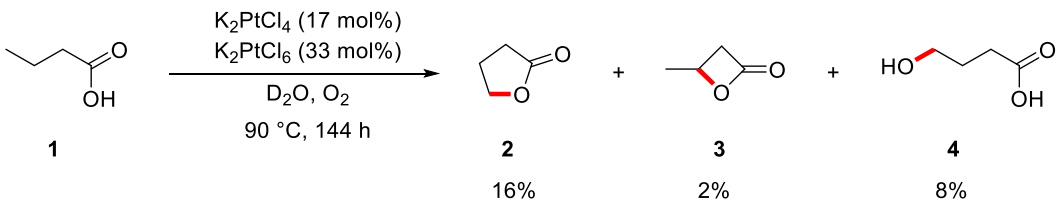

Scheme 16. Lactonization of aliphatic carboxylic acids developed by Kao and Sen.

In 2007, Yu and co-workers developed the first example of an intermolecular C–H activation/functionalization using carboxyl groups as native directing groups (**Scheme 17**).[63] The authors showcased arylation using both organoboron and aryl iodide reagents, proposing reliable mechanistic insights for both approaches. Notably, a key factor for achieving reactivity under these conditions was the addition of sodium and potassium salts. Although the role of these countercations was unclear at the time, this discovery was an important milestone in subsequent palladium-catalyzed functionalization of alkyl carboxylic acids. Today, the effect is generally referred to as the countercation effect.[64]

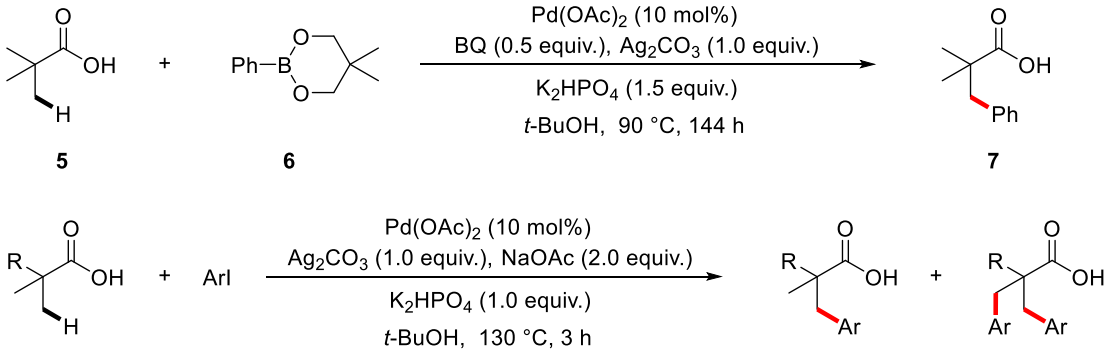

Scheme 17. Direct β-C–H arylation of α-quaternary carboxylic acids by Yu.

Countercation Effect of Alkali Metals

It is known that carboxylates can coordinate with transition metals in two distinct binding modes: κ^1 and κ^2. In the κ^2 mode (**Scheme 1.18**), the metal coordinates with both oxygen atoms of the carboxyl group, thereby locking the transition metal in a position that prevents proximity to the C–H bond that is to be activated.[65] In contrast, in the κ^1 binding mode (**Scheme 1.18**), the metal coordinates with only one of the carboxylate oxygen atoms, forming a coordination environment conducive to C–H functionalization. However, coordination via the κ^2 mode is generally more favorable for palladium. The presence of inorganic or organic counterions, such as Na^+, K^+, Cs^+, forces the palladium-carboxylate complex to transition from the κ^2 to the κ^1

mode.

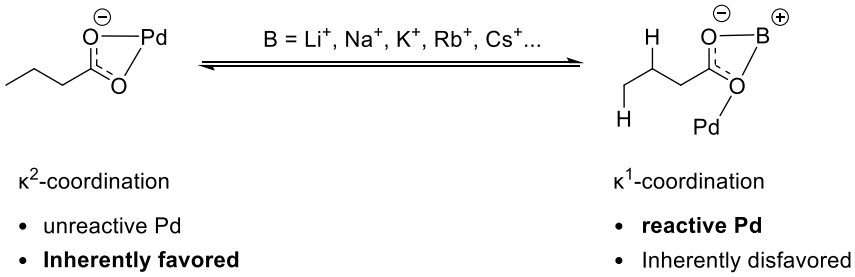

Scheme 1.18 Competitive coordination modes of the carboxylate moiety and the countercation effect of alkali metals to carboxylate directed C–H activation

The countercation effect facilitates coordination of the carboxylate substrate to the palladium in a form that can undergo C–H activation. However, the inherently weak coordination of carboxylates with palladium often results in dissociation before the C–H activation step is completed. Suitable ligands play an essential role in accelerating the C–H activation step, allowing the formation of a more stable palladacycle intermediate.

The Role of Ligands

In transition metal-catalyzed coupling reactions, ligands have been highly regarded for their ability to tune the electronic properties of the catalytic center, alter steric hindrance, and thus control the reaction outcome.[66] The enhancement of catalytic performance is heavily influenced by the nature of ancillary ligands, making the search for novel ligand scaffolds a central pursuit in all subfields of homogeneous catalysis.[67]

In the early development of the C–H activation field, researchers employed simple Pd^{II} salts (such as $Pd(OAc)_2$, $Pd(TFA)_2$, PdI_2) as catalysts, and these basic systems enabled several initial C–H transformations. However, many challenges remained unresolved, including issues of stereoselectivity and regioselectivity. It also became clear that the reactivity of these simple palladium complexes was insufficient for the diverse range of transformations desired, especially in cases involving weakly coordinating directing groups.

The turning point occurred in 2010 when Yu and co-workers found that, in the alkenylation and cross-coupling of phenylacetic acid, only electron-rich substrates underwent C–H activation in the absence of ligands.[68] However, through extensive ligand screening, they

observed that bidentate mono protected amino acids such as Boc-Val-OH could enable C–H activation in electron-deficient substrates (**Scheme 1.19**).

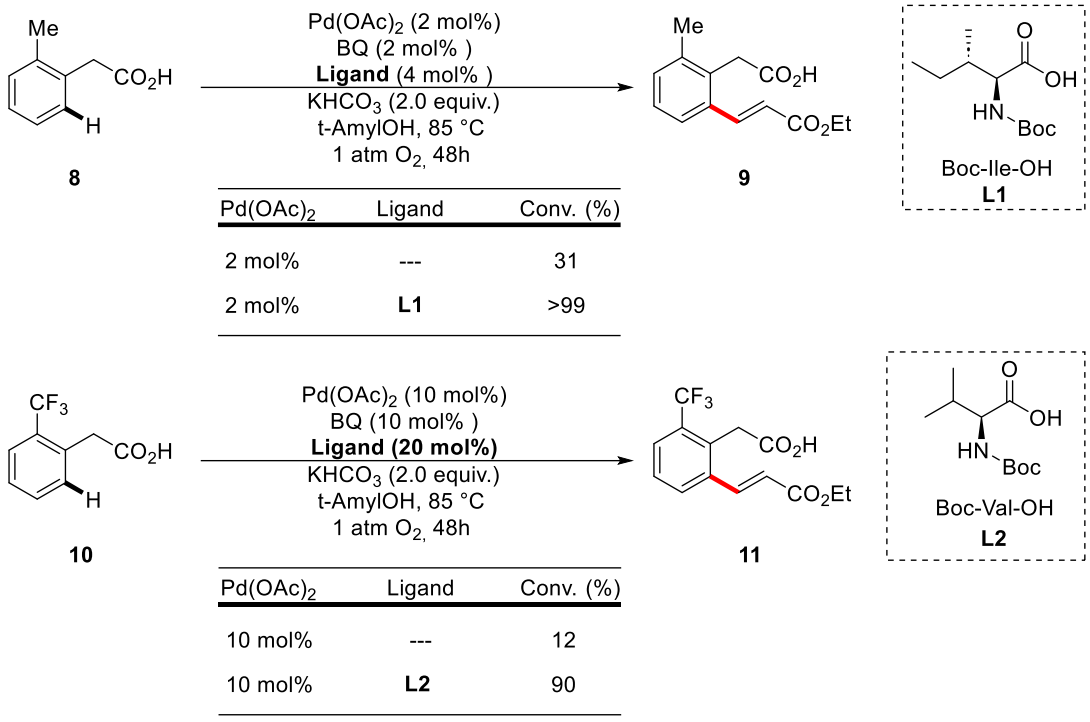

Pd(OAc)$_2$	Ligand	Conv. (%)
2 mol%	---	31
2 mol%	**L1**	>99

Pd(OAc)$_2$	Ligand	Conv. (%)
10 mol%	---	12
10 mol%	**L2**	90

Scheme 1.19 Amino acid ligand-enabled C–H olefination with Pd(OAc)$_2$ in electron-deficient substrates.

The first test of amino acids derivate ligands were conducted in enantioselective C–H activation reactions to control the stereochemical ratio of the products.[69] Subsequent mechanistic studies and DFT study revealed that, unlike the typical electrophilic palladation pathway that favors electron-rich substrates, the Pd and amino acids derivate ligand system proceeds via a concerted metalation-deprotonation (CMD) mechanism.[70] Compared to acetate, the amide group has significantly higher basicity and lower steric hindrance, resulting in a lower activation barrier (by 4 kcal/mol) for C–H cleavage when using amino acids derivate ligands.[71] These observations revealed that amino acids derivate ligands actively participate in the C–H cleavage transition state itself, thus accelerating catalysis, rather than merely modulating the electronic and steric properties of the palladium catalyst, as is typical for many ligands in cross-coupling reactions.

These findings were quickly applied to diverse C–H functionalizations, particularly for the activation of C(sp^3)–H bonds using weakly coordinating directing groups.[72] The development

greatly accelerated the field of carboxyl-directed C–H activation, and further studies continued to showcase the power of these ligands.[73] More CMD-based ligands have been designed and synthesized, typically consisting of highly customizable components: the donating group (Do) part, which can be anionic or neutral, anchoring the bidentate ligand to the metal, the internal base part facilitating C–H deprotonation, and the backbone or bridging segment connecting these elements (**Scheme 1.20**).[74] This high degree of customization allows the ligands to be tailored to meet the specific needs of different transformations and reaction conditions, providing greater versatility and adaptability in catalytic applications.[75]

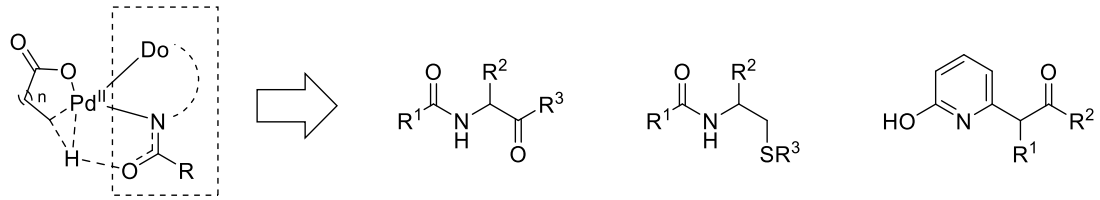

Scheme 1.20 CMD-based ligand design

Oxidants in the Pd(II/IV) Cycle

Ligands accelerate the C–H activation step, and the resulting carbon-metal bond can either undergo migratory insertion or reductive elimination from Pd^{II} to form a new chemical bond. However, in the Pd(II/IV) cycle, an oxidant is needed after C–H activation to oxidize Pd^{II} to Pd^{IV}, a crucial step for subsequent functionalization. High-valent palladium intermediates which can undergo reductive elimination serve as powerful tools for C–H functionalization, enabling the formation of various carbon–Heteroatom bonds.

Oxidants can be categorized by their role in the transformation: external oxidants do not contribute directly to the product, whereas internal oxidants also serve as reaction partners, often undergoing oxidative addition to convert Pd^{II} to Pd^{IV}, with parts of the oxidant becoming incorporated into the product structure (see **1.7 Pd^{II}/Pd^{IV} catalytic cycle**). Notably, several studies have shown that the choice of oxidant significantly impacts reaction efficiency, yield, and selectivity.[76]

Other influencing factors

To achieve complete C–H functionalization, many other factors also come into play, such as

the effect of solvents. To date, hexafluoroisopropanol (HFIP) possibly has been found to be the most suitable solvent in this field, due to its strong hydrogen-bond donating ability, high polarity, and low nucleophilicity, which stabilize key intermediates and lower activation energy.[77] And its excellent solubilizing ability ensures a homogeneous reaction environment. These properties collectively enhance reaction efficiency, selectivity, and control over the reaction pathway.

Moreover, in certain reactions, additives have been found to positively impact reaction outcomes. These additives may participate or not in the mechanism but improve reaction yield or efficiency. For example, silver salts are often added to regenerate the active palladium species or to act as halide scavengers.[78] By removing halides from the catalyst, silver salts help maintain the catalyst in an active form, indirectly enhancing yield. Halide salts also fall into this category. Such additives are generally used as enhancers, providing benefits like increased solubility, stabilization of intermediates, or optimization of reaction conditions, thereby improving the overall yield.

Through these methods and strategies, the scientific community has made significant progress in addressing the challenges of direct C–H activation and functionalization of native carboxylic acids, achieving notable preliminary successes in this field.

1.8 Key Developments in the Direct C(sp^3)–H Activation/Functionalization of Free Carboxylic Acids

This section provides an overview of key developments in this field but does not cover all advances. For a comprehensive review, see the reviews of Larrosa,[7a] Yu[71] or Maiti.[58b, 73c, 79]

1.8.1 Arylation

Arylation was among the earliest reaction types explored in this field. As mentioned above, the Yu group first reported the arylation of free carboxylic acids in 2007. However, the methodology at that time has some limitations.

Some years later, as a powerful complement of Yu's original method, Zhao and coworkers reported a palladium-catalyzed direct arylation of carboxylic acid β-C(sp^3)–H bonds (**Scheme 1.21**) in 2017.[80] This approach utilizes N-acetylglycine as a ligand and employs the carboxylic

acid moiety as an native directing group. The method demonstrates broad applicability across various substrates and functional groups, including amino acid analogs and liner aliphatic acids like propionic acid. Its compatibility with challenging substrates underscores its potential for late-stage functionalization in complex molecule synthesis.

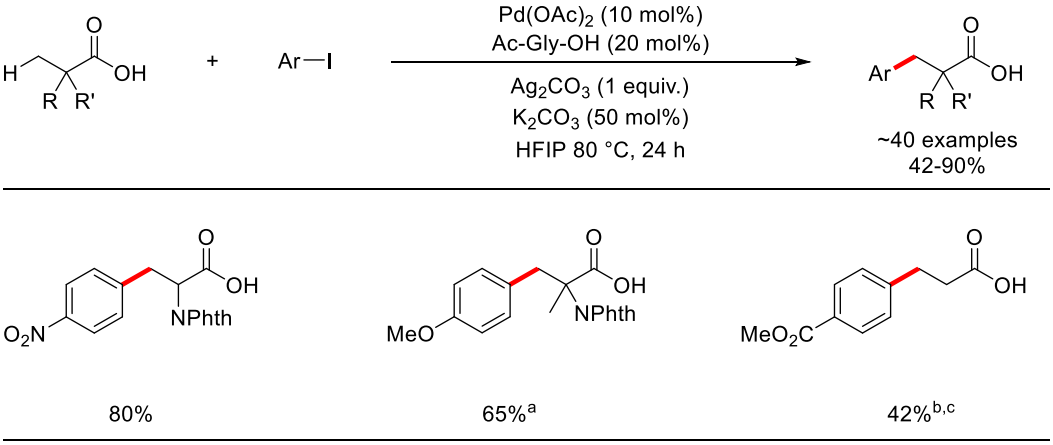

Scheme 1.21 Pd-catalysed ligand-enabled carboxylate-directed highly regioselective arylation of aliphatic acids. [a]100 °C. [b]60 h. [c]150 °C

Around the same time, the Yu and coworkers reported similar ongoing research,[81] achieving β-C(sp³)–H arylation of Phth-protected alanine and related substrates using pyridine- or quinoline-based ligands(**Scheme 1.22**). For some specific substrates, the authors performed fine-tuning of the reaction conditions (such as changing base or ligand combinations) to obtain optimal product yields. Additionally, preliminary attempts at methylene C–H arylation and remote γ-position arylation were explored, though with limited success. Despite these challenges, scale-up experiments and applications to drug molecules highlighted the method's potential for practical use.

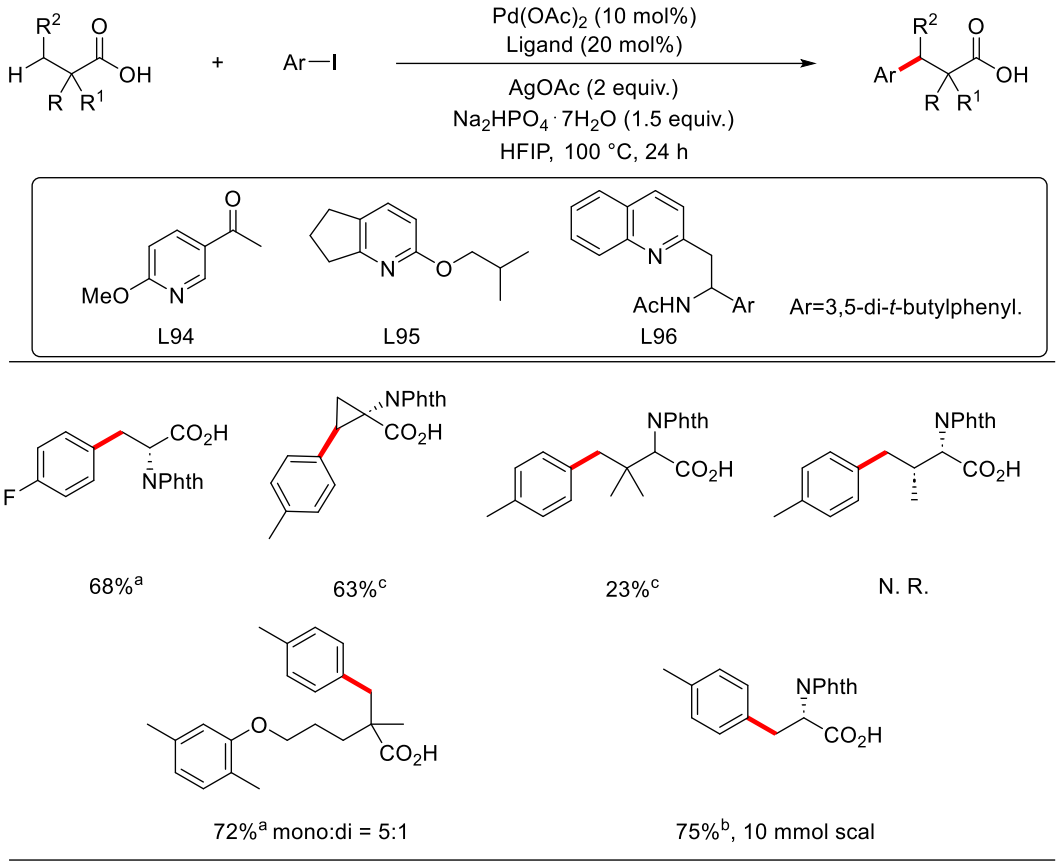

Scheme 1.22 Ligand-enabled β-C–H arylation of α-amino acids without installing exogenous directing groups [a]**L95** was used. [b]**L95**(10 mol%) + **L94** (10 mol%) were used. [c]**L96** was used.

In the later of 2017, the van Gemmeren group developed a broadly applicable method for the β-C(sp^3)−H arylation of free aliphatic acids (**Scheme 1.23**).[82] This approach was not only suitable for α-quaternary acids but also particularly effective for α-non-quaternary and even the challenging propionic acid. The broad applicability of aryl iodide reagents further demonstrated the synthetic utility of this method.

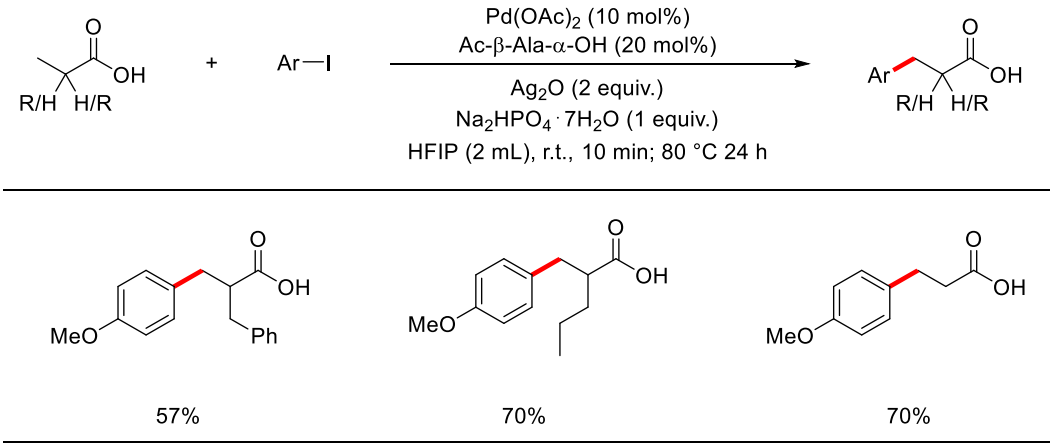

Scheme 1.23 Pd-catalyzed β-C(sp^3)−H arylation of propionic acid and related aliphatic acids

These arylation efforts were reported successively within the same year. Although each approach differs slightly, they all have a common limitation: incompatibility with heteroaryl iodides as reaction partners. To overcome this challenge, the Yu group introduced a β- and γ-C(sp^3)–H heteroarylation strategy for aliphatic acids in 2023 (**Scheme 1.24**).[83] The key point of this transformation was the use of pyridine-pyridone ligands. Moreover, the strategy is nearly unaffected by the electronic properties of the heterocyclic iodide, consistently yielding the target product with high mono-selectivity in most cases. Additionally, the authors successfully generated stereocenters with heteroaryl groups through successive C–H bond activation on the same substrate, highlighting the reaction's remarkable versatility and practical utility.

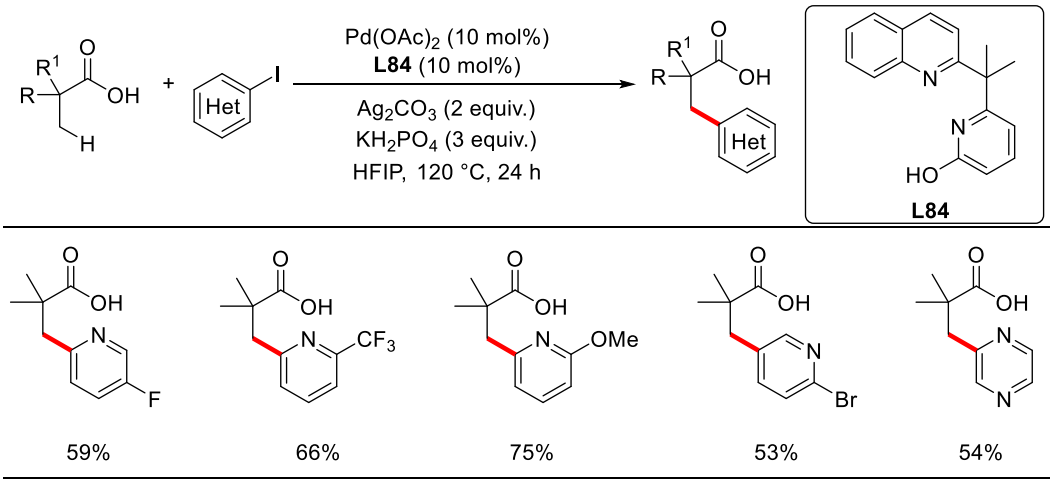

Scheme 1.24 β- and γ-C(sp^3)−H heteroarylation of free carboxylic acids: A modular synthetic platform for diverse quaternary carbon centers

As previously discussed, methylene C–H bonds are more difficult to activate. To address this challenge, in 2022, the Yu group developed the first direct Pd-catalyzed β-methylene C(sp^3)–H arylation of free aliphatic acids (**Scheme 1.25**).[38d] The success of this method was attributed to the use of a bidentate pyridyl-pyridone ligand and precise control over its bite angle. The broad substrate scope provided a novel bond-cleavage strategy for the preparation of diverse arylated carboxylic acids from simple starting materials.

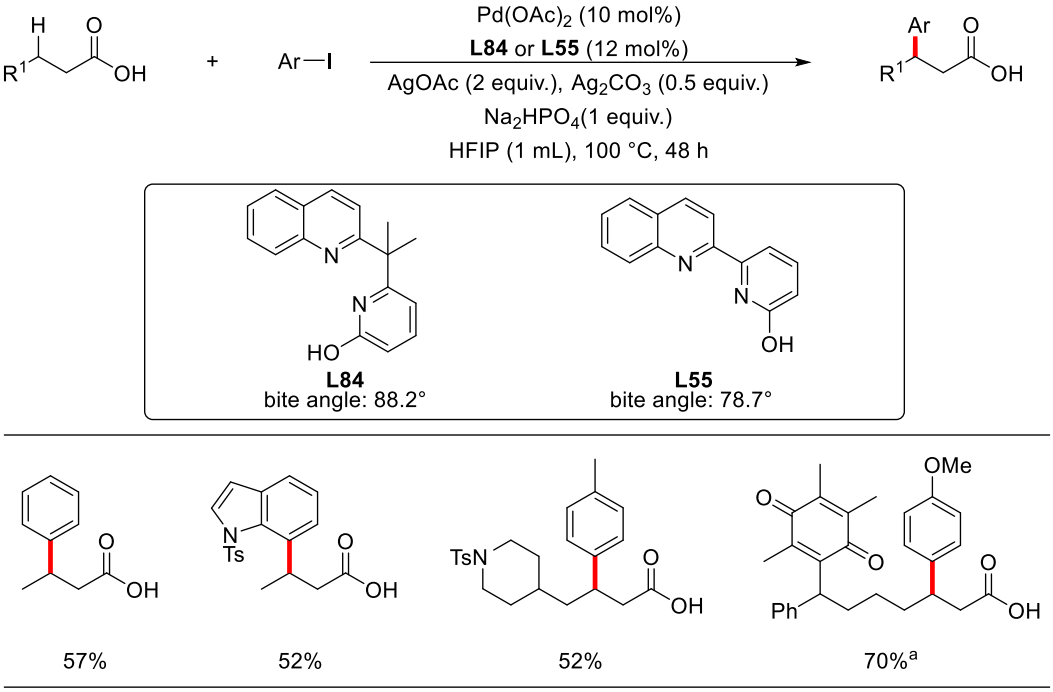

Scheme 1.25 Ligand-enabled Pd(II)-catalyzed β-methylene C(sp^3)–H arylation of free aliphatic acids. [a] The reaction was run at 110 °C

Furthermore, in 2023, the Yu group achieved transannular γ-methylene C–H arylation of cycloalkyl carboxylic acids using a quinoline-pyridone ligand, as well as a double C–H activation strategy employing sulfonamide-pyridone and monodentate pyridone ligands (**Scheme 1.26**).[84] Various cycloalkyl carboxylic acids, ranging from four- to eight-membered rings, exhibited good functional group tolerance with different (hetero)aryl iodides and arene coupling partners. This method demonstrates excellent compatibility with the more reactive β-C–H bonds while achieving highly regioselective transannular γ-arylation. It enables the synthesis of a series of valuable compounds that previously required up to 10 steps. The significant biological activities of cyclic aliphatic acids and their derivatives underscore the particular importance of this methodology in medicinal chemistry.

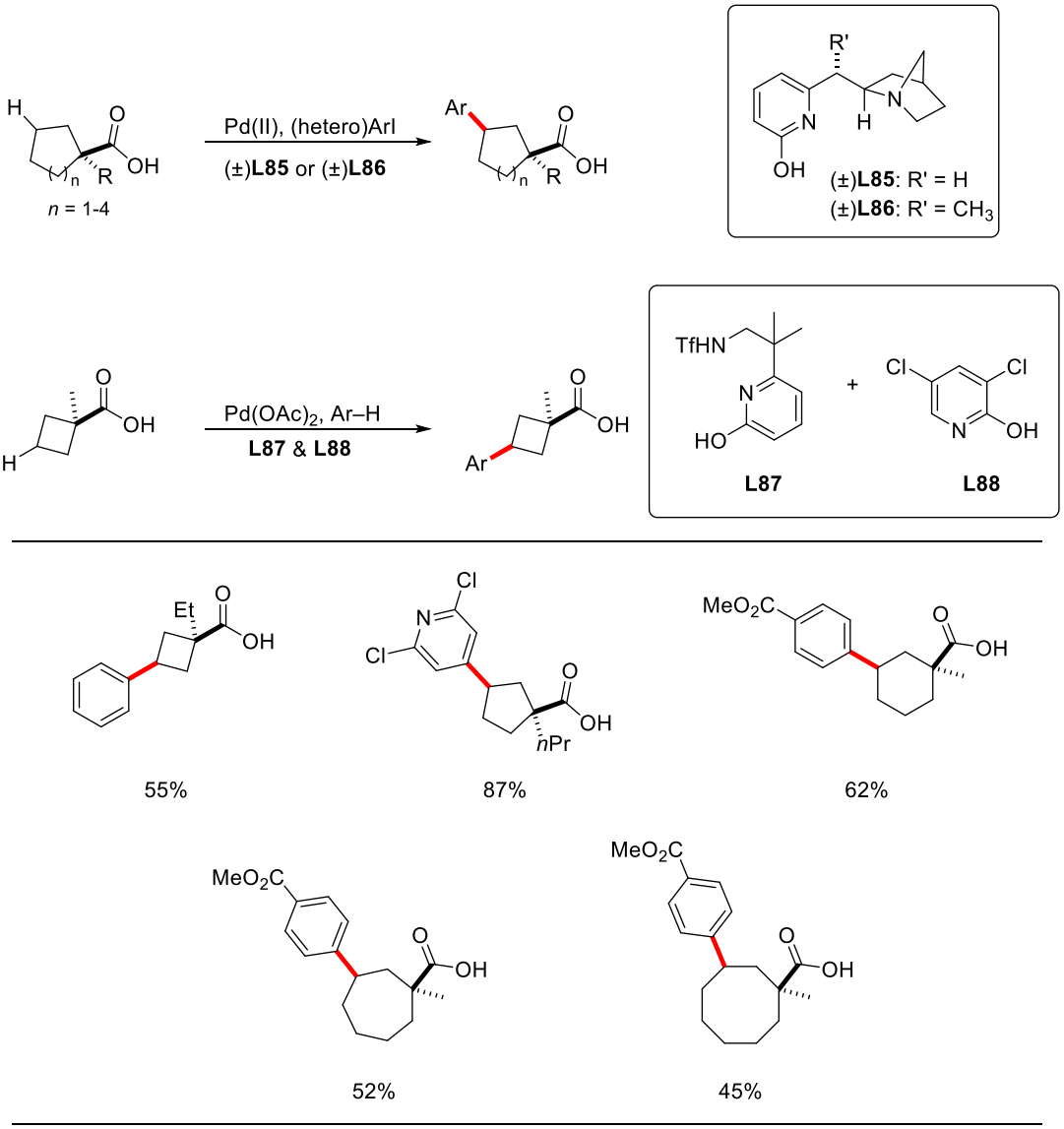

Scheme 1.26 Transannular C–H functionalization of cycloalkane carboxylic acids

1.8.2 Olefination

In 2018, the Yu group first reported the direct β-C(sp^3)–H alkenylation of free carboxylic acids by using an acetyl-protected aminoethyl phenyl sulfide ligand (**Scheme 1.27**).[85] This method exhibited broad substrate scope include various alkyl carboxylic acids and high functional group tolerance, affording lactone products in moderate to good yields. The synthetic utility of this approach was further demonstrated through gram-scale reactions and the conversion of lactones into structural building blocks.

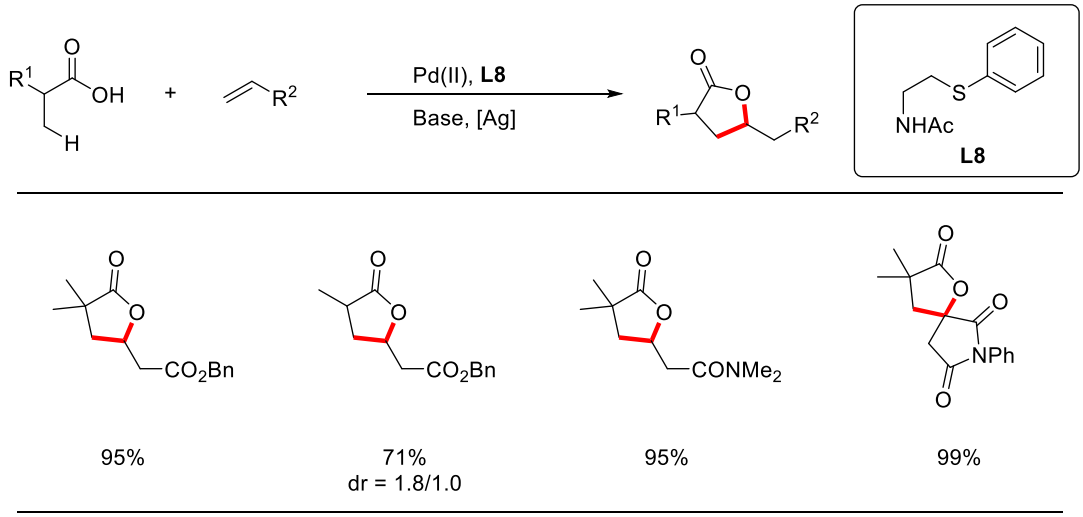

Scheme 1.27 Ligand-enabled β-C(sp^3)–H olefination of free carboxylic acids

In 2020, the van Gemmeren group disclosed a γ-C(sp^3)–H alkenylation strategy for aliphatic acids, applicable to diverse aliphatic acids and activated olefins, yielding six-membered lactones in moderate to good yields (**Scheme 1.28**).[86] The use of simple, readily available ligands enhanced the practicality of this method.

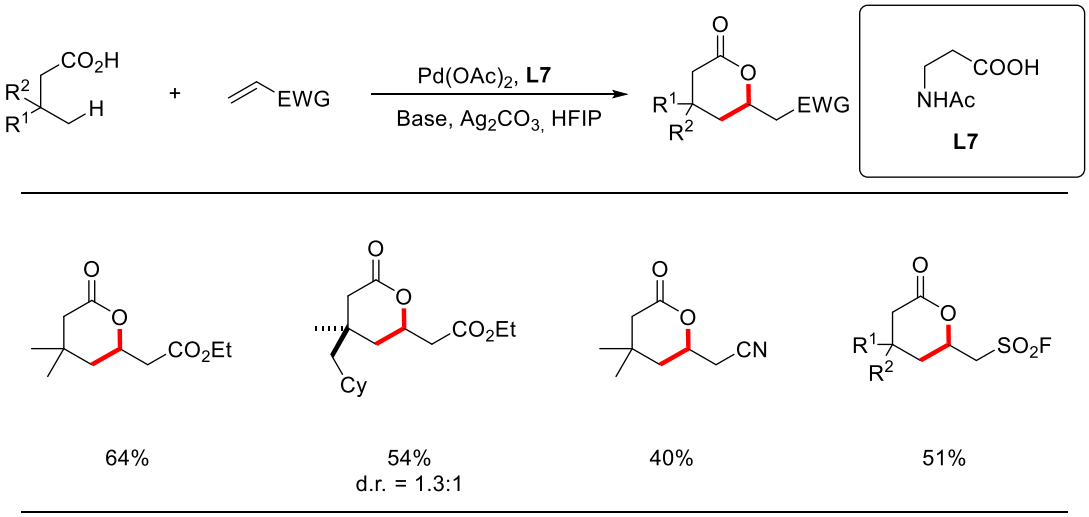

Scheme 1.28 Ligand-enabled γ-C(sp^3)−H olefination of free carboxylic acids

Meanwhile, The Maiti group developed another γ-C(sp^3)–H olefination strategy to directly generate lactone products from aliphatic acids using N-Ac-Val as a ligand (**Scheme 1.29**).[87] A diverse range of olefinic partners, including acrylates, vinyl sulfones, nitriles, and acetylenic ketones, enabled the formation of six-membered lactones in good to excellent yields. Notably, using maleimide as an olefinic partner provided direct access to seven-membered lactones.

Additionally, Yu's group reported a highly similar approach around the same time.[88]

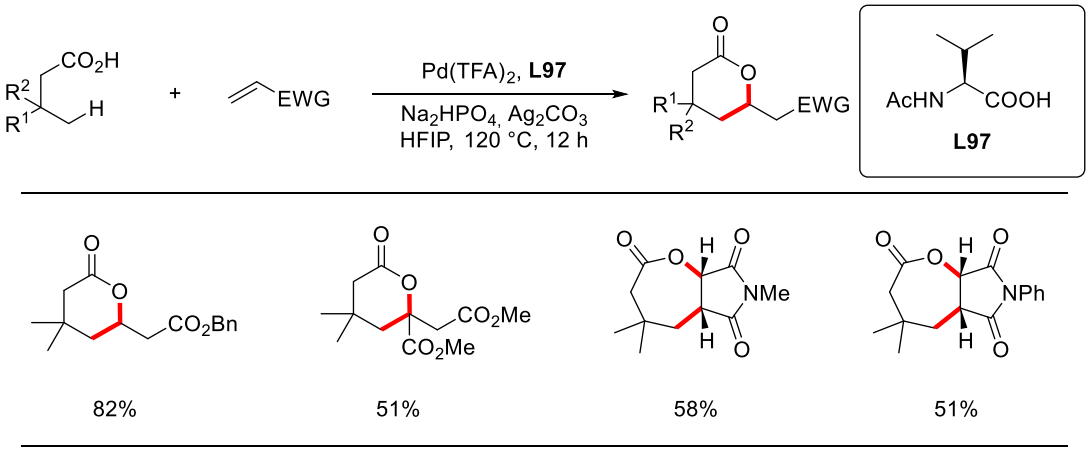

Scheme 1.29 A direct route to six and seven membered lactones via γ-C(sp^3)–H activation: a simple protocol to build molecular complexity.

Furthermore, Maiti and colleagues demonstrated the first example of Pd-catalyzed dual γ-1,1-C(sp^3)–H activation of free carboxylic acids with allylic alcohols as coupling partners, forming highly substituted γ-lactones (**Scheme 1.30**).[89] The bidentate N-Ac-*t*Leu ligand played a crucial role in this transformation, and a range of aliphatic acids, including long-chain acids, were compatible with this method. Mechanistic studies indicated that the reaction proceeded via sequential C–H activation: initial γ-C–H activation followed by allylic C–H activation, culminating in reductive elimination to afford the final product.

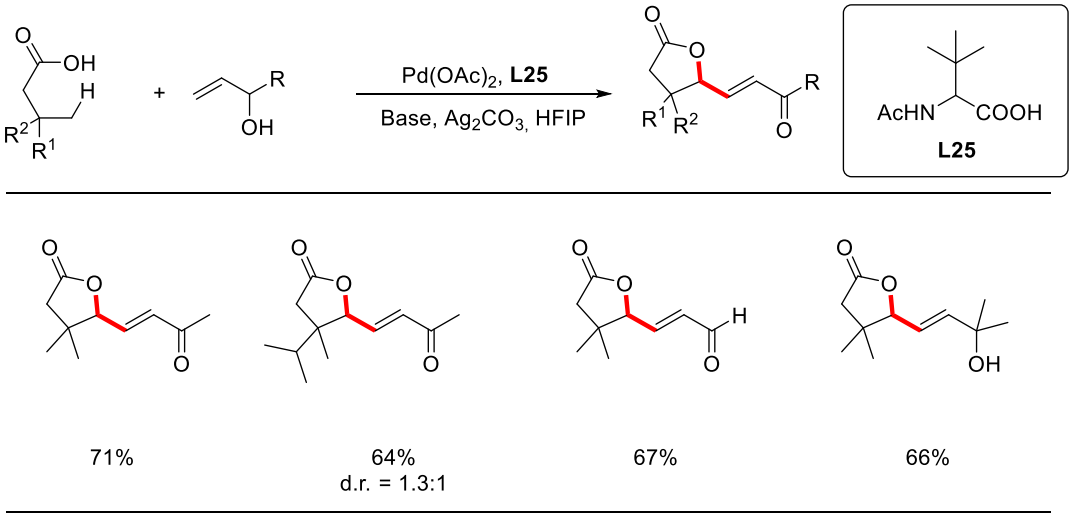

Scheme 1.30 Pd-Catalyzed dual-γ-1,1-C(sp^3)–H activation of free aliphatic acids with Allyl–O moieties

1.8.3 Alkynylation

In 2020, the van Gemmeren group reported the first alkynylation of free aliphatic acids, employing 1-bromo-2-(triisopropylsilyl)acetylene as the alkynylation regent (**Scheme 1.31**).[90] This study revealed the catalytic activity of ethylenediamine-derived ligands in direct C–H activation of alkyl carboxylic acids. The reaction condition can be used for α-non-quaternary carboxylic acids and even distal γ-C(sp^3)–H bonds, providing access to the desired alkynylation products in synthetically useful to moderate yields.

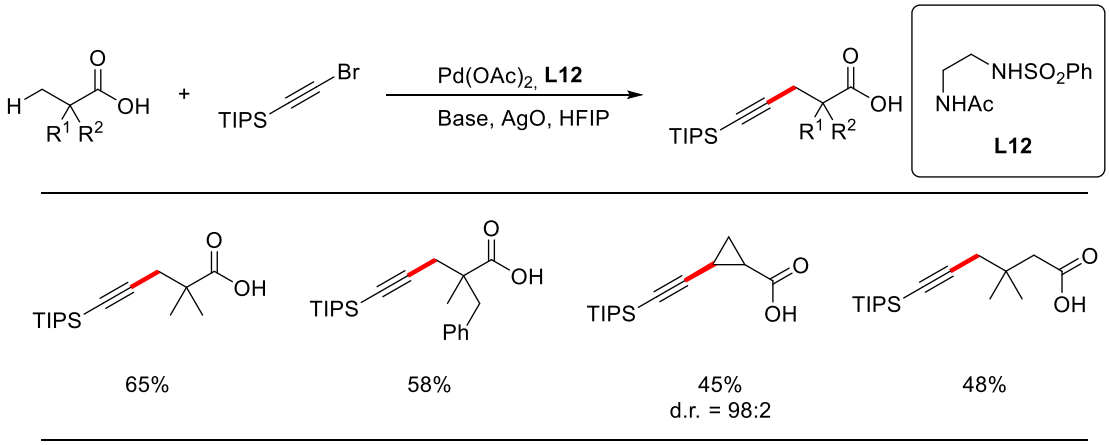

Scheme 1.31 Direct β- and γ-C(sp^3)−H alkynylation of free carboxylic acids

1.8.4 Carbonylation

In 2021, the Yu group reported a Pd(II)-catalyzed direct C–H carbonylation of aliphatic acids using bidentate ligands (**Scheme 1.32**).[91] This reaction employed $Mo(CO)_6$ as a convenient solid CO source, producing various cyclic anhydrides. The high reactivity of these products facilitated the synthesis of structurally diverse carboxylic acid derivatives. The approach was readily extended to the γ-C−H bonds of alkyl carboxylic acids, and, using chiral bidentate thioether ligands, enabled enantioselective C–H carbonylation of cyclopropanecarboxylic acids.

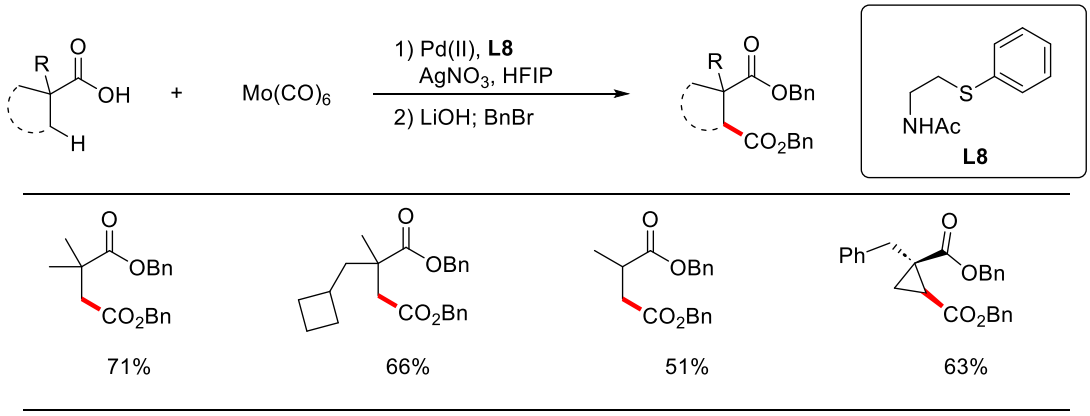

Scheme 1.32 Synthesis of cyclic anhydrides via ligand-enabled C–H carbonylation of simple aliphatic acids

1.8.5 Dehydrogenation

In 2021, the Yu group developed a Pd-catalyzed dehydrogenation of linear alkyl carboxylic acids, converting free aliphatic acids into α,β-unsaturated acids or γ-alkylidene butenolides (**Scheme 1.33**).[92] The formation of these distinct products was highly dependent on the use of bidentate pyridyl-pyridone ligands with different bite angles (five- vs. six-membered chelates), highlighting the crucial role of ligand design in this field.

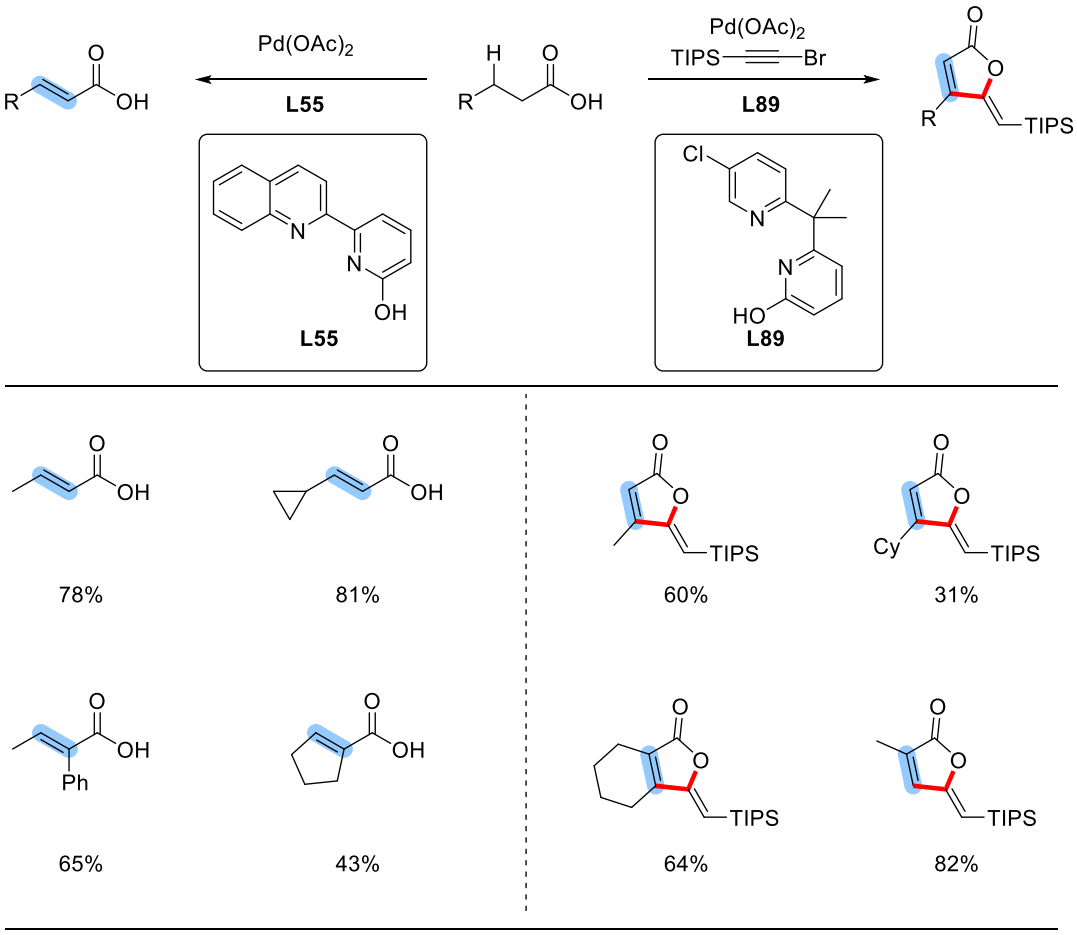

Scheme 1.33 Ligand-controlled divergent dehydrogenative reactions of carboxylic acids via C–H activation

Additionally, the Yu group achieved an efficient tandem reaction enabling sequential β,γ-dehydrogenation and vinyl C–H alkenylation of free aliphatic acids (**Scheme 1.34**).[93] This strategy provided a one-step route to diverse β-alkylidene-γ-lactones. The tailored bidentate methoxy-pyridone ligands were essential for this tandem transformation.

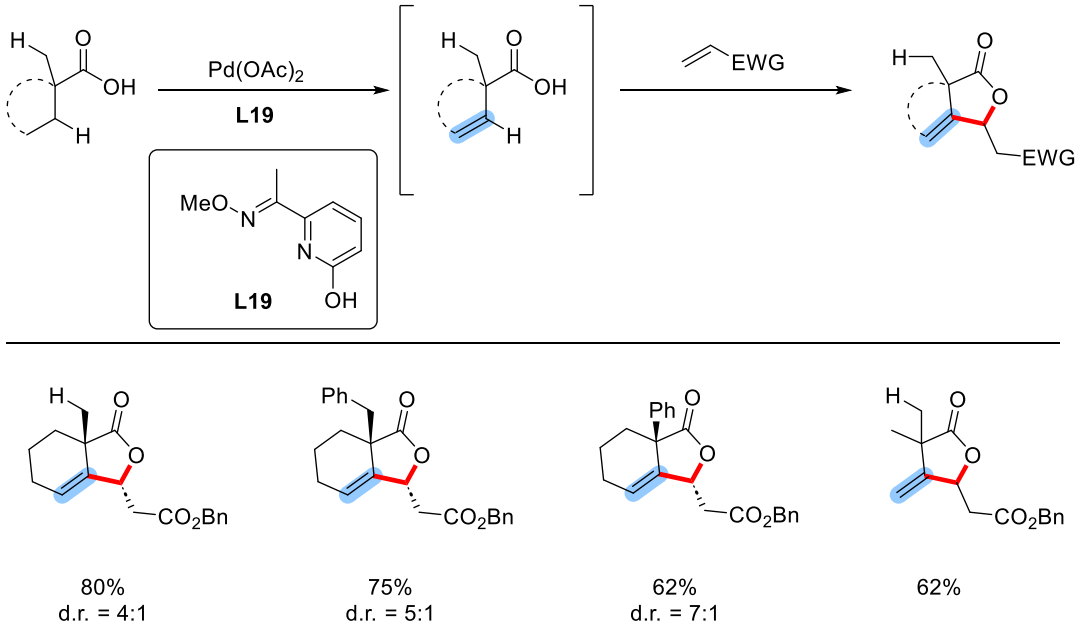

Scheme 1.34 One-step synthesis of β-alkylidene-γ-lactones via ligand-enabled β,γ-dehydrogenation of aliphatic acids

The aforementioned reactions yielded unsaturated alkyl carboxylic acids as products, which are inherently reactive intermediates. Designing suitable reaction conditions to utilize these intermediates for further structural elaboration allows access to more complex compounds.

For example, in 2023, the Yu group developed a regioselectively controlled [2+2] reaction that facilitated the synthesis of benzofused four-membered rings (**Scheme 1.35**), structures that are difficult to construct using traditional methods. This reaction was compatible with a range of free aliphatic acids, including linear and cyclic carboxylic acids. Mechanistic studies indicated that the dehydrogenation product served as a key intermediate in the reaction.

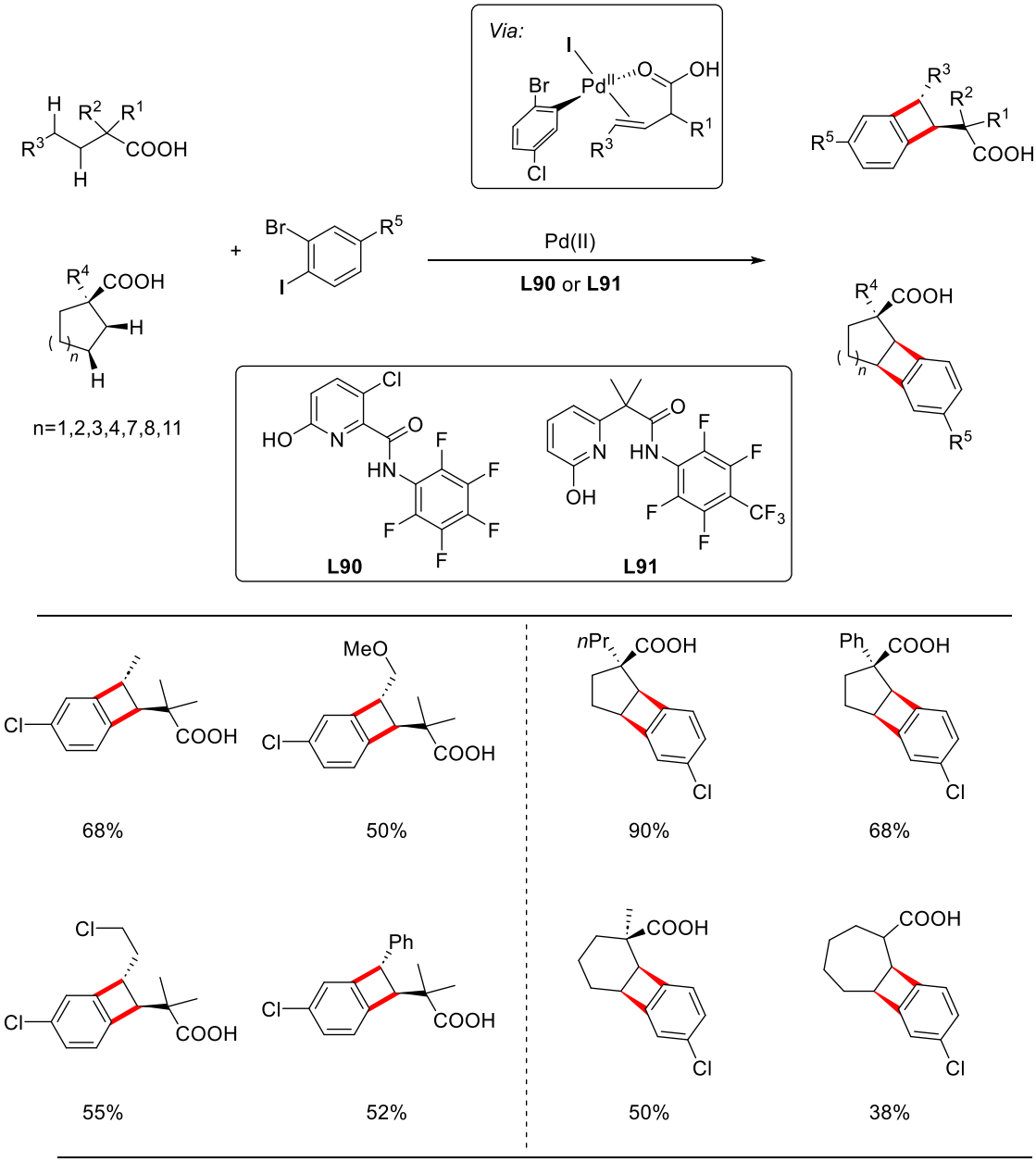

Scheme 1.35 Regio-controllable [2+2] benzannulation with two adjacent C(sp^3)–H bonds

Additionally, the Yu group developed a Pd(II)-catalyzed tandem γ-C(sp^3)−H arylation and γ-lactonization of aliphatic acids (**Scheme 1.36**). The key to this reaction was the use of a bidentate pyridone ligand, enabling the one-step synthesis of diverse γ-arylated γ-butyrolactones from simple carboxylic acids. The proposed reaction mechanism involved the formation of a crucial dehydrogenated intermediate.

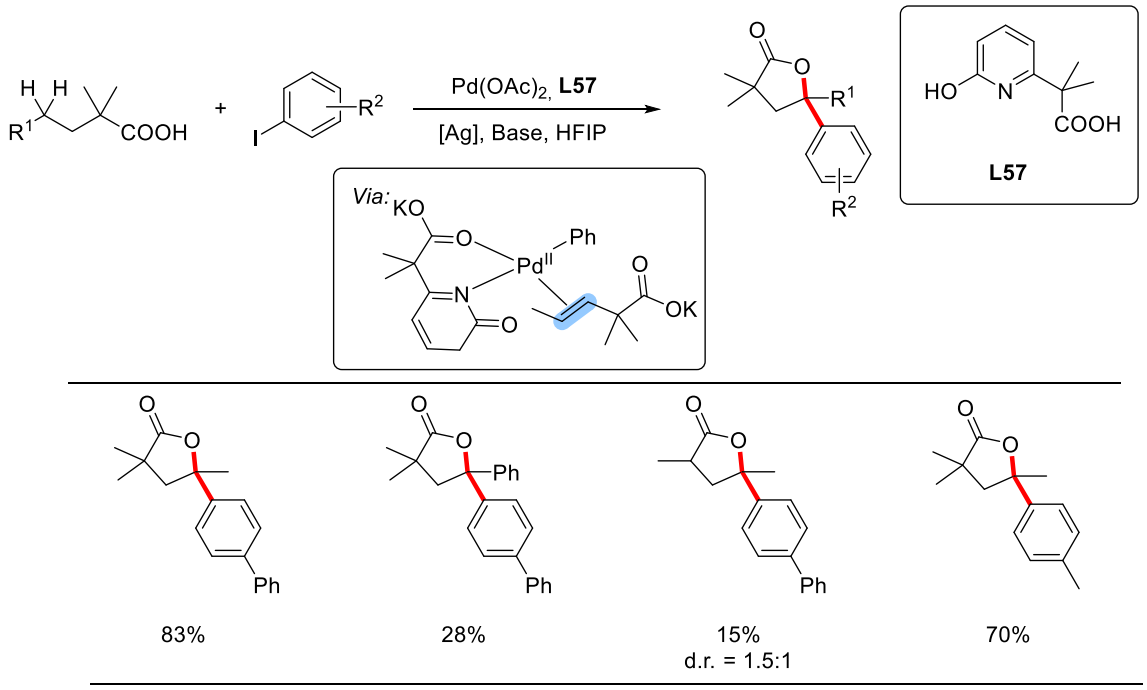

Scheme 1.36 Ligand-enabled double γ-C(sp^3)−H functionalization of aliphatic acids: one-step synthesis of γ-arylated γ-lactones

Similarly, in 2023, the Maiti group reported a cascade C–H activation reaction, in which an intramolecular reaction formed unsaturated bicyclic lactones, while an intermolecular reaction with olefins or allylic alcohols led to one-step γ-alkenylated lactone formation (**Scheme 1.37**). The proposed mechanism also involved the formation of a key unsaturated carboxylic acid intermediate.

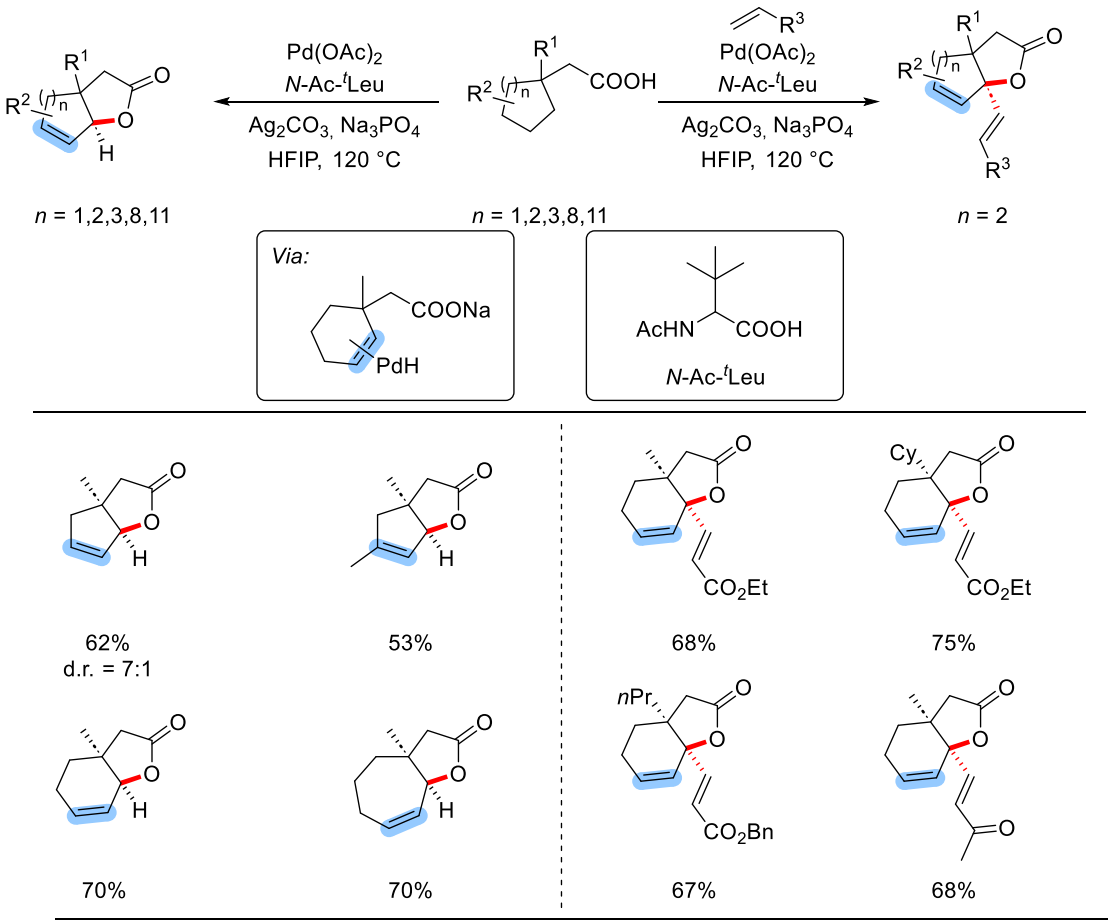

Scheme 1.37 Access to unsaturated bicyclic lactones by overriding conventional C(sp^3)–H site selectivity

1.8.6 Deuteration

In 2021, the van Gemmeren group reported a late-stage C(sp^3)–H deuteration of free carboxylic acids using an ethylenediamine-based ligand and deuterated hexafluoroisopropanol (d_1-HFIP) as the deuterium source (**Scheme 1.38**). The broad substrate scope included multiple biologically active molecules, highlighting the method's utility for drug discovery.

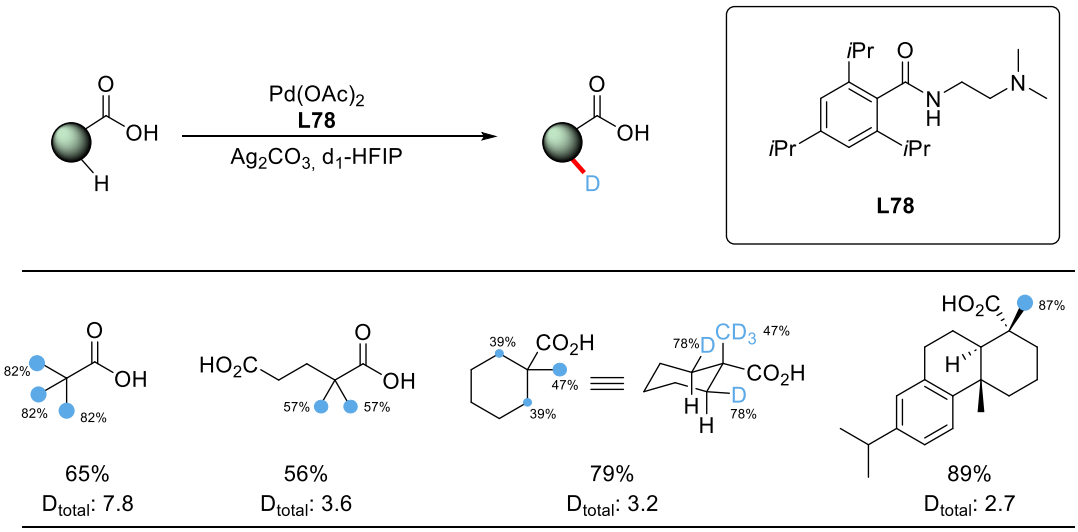

Scheme 1.38 Late-stage β-C(sp^3)–H deuteration of carboxylic acids

1.8.7 Halogenation

In 2024, the Yu group reported a Pd-catalyzed β-C(sp^3)–H bromination of free carboxylic acids using hydrogen-bond donor pyridyl ligands (**Scheme 1.39**).[94] The broad substrate scope and synthetically useful halogenated products demonstrated the strategy's potential. The key to success was the design and synthesis of new ligand types capable of interacting with the carboxyl directing group.

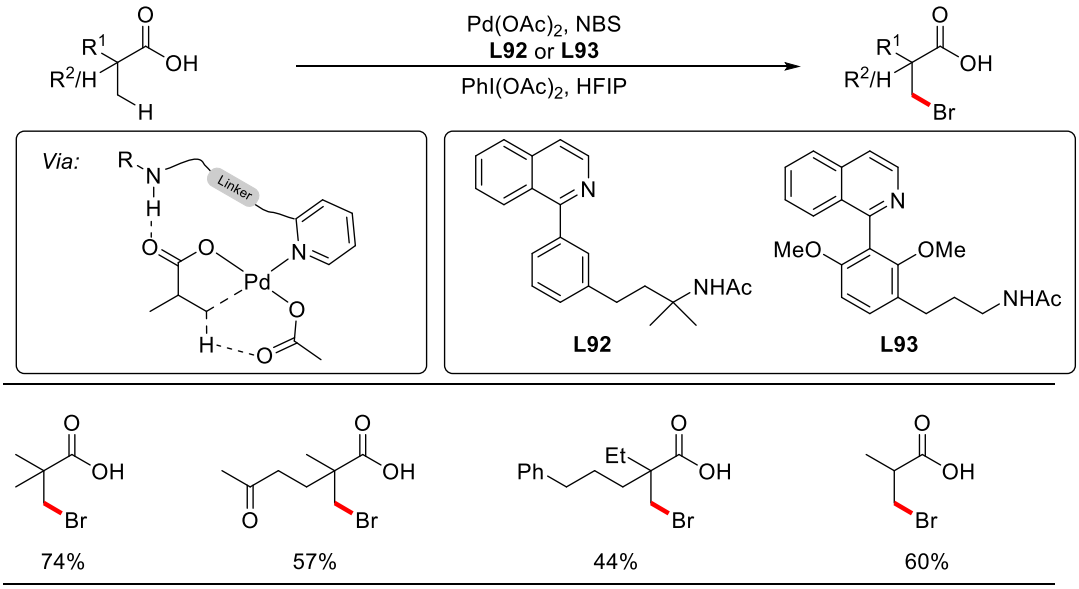

Scheme 1.39 Enhancing substrate–metal catalyst affinity via hydrogen bonding: Pd(II)-catalyzed β-C(sp^3)–H bromination of free carboxylic acids

In the same year, the van Gemmeren group developed a direct β-C(sp^3)–H fluorination of free carboxylic acids using a combination of nucleophilic fluorine sources and external oxidants (**Scheme 1.40**).[76e] This method was applicable to both simple β-quaternary carboxylic acids and the more challenging α-non-quaternary carboxylic acids, demonstrating remarkable functional group tolerance. The rational design of the oxidant was crucial to the reaction's success.

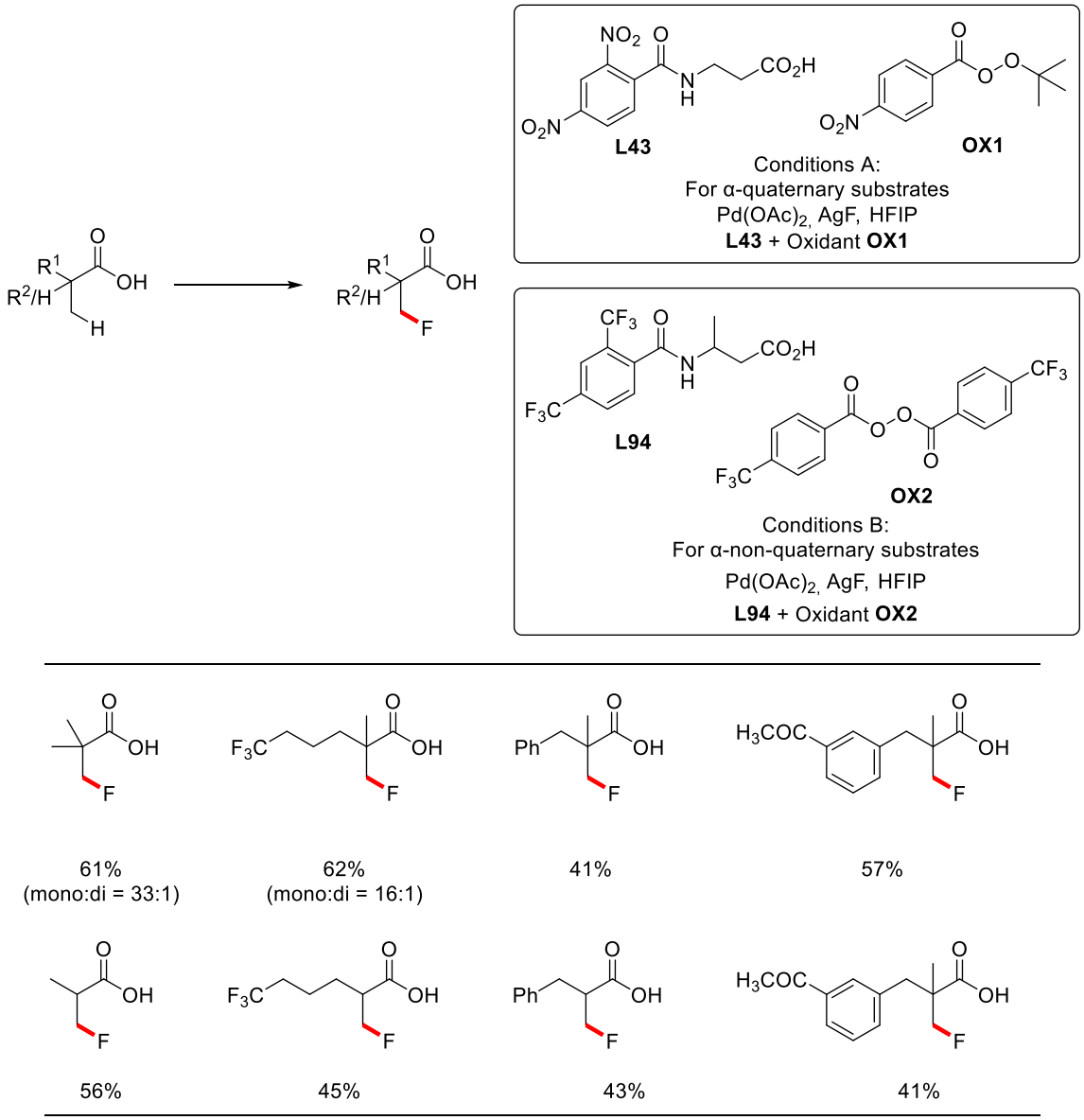

Scheme 1.40 Transannular C–H functionalization of cycloalkane carboxylic acids

2 The Direct Pd-Catalyzed β-C(sp^3)–H Amination of Aliphatic Carboxylic Acids

2.1 Background

Nitrogen-containing functional groups exist in various forms, including primary amines, amides, and nitrogen heterocycles, and are widely recognized as key pharmacophores in bioactive compounds (**Scheme 2.1**).[95] For instance, an analysis of the structures and properties of 321 unique nitrogen-containing heterocyclic small-molecule drugs approved by the FDA between 2013 and 2023 shows a remarkable trend: the proportion of drugs containing at least one nitrogen heterocycle has increased from 59% over the past half-century to an impressive 82%.[96] Beyond pharmaceuticals, nitrogen-containing fragments with diverse structures are also extensively utilized in fine chemicals and functional materials.[97] A significant subset of these structures involves bonds between nitrogen residues and saturated carbon atoms, highlighting the critical importance of developing efficient methods for constructing C(sp^3)–N bonds in both academic and industrial settings.

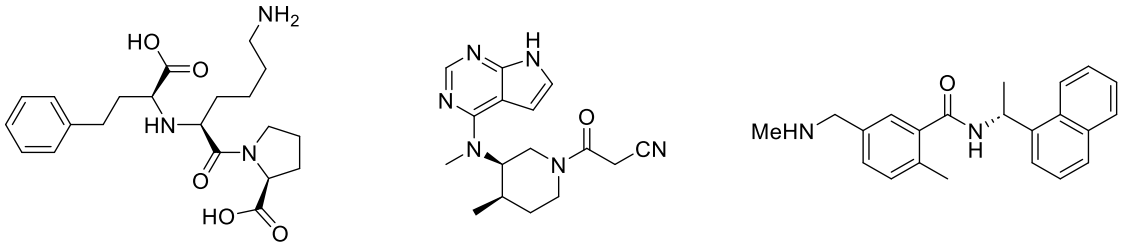

Lisinopril
ACE inhibitor

Xeljanz
Immunosuppressant

SARS-CoV PLpro inhibitor

Scheme 2.1 Selected examples of pharmaceuticals containing nitrogen-containing functional groups

In traditional organic synthesis, a classical approach to forming C–N bonds is N-alkylation via alkyl (pseudo)halides, relying on S_N2 (bimolecular nucleophilic substitution) chemistry. However, in complex molecular environments, this reactivity faces significant limitations. Certain less reactive amine substrates may require harsh conditions, such as strong bases and high temperatures, which often result in low yields and competing E2 elimination reactions, leading to undesired alkene byproducts. In recent years, transition-metal-catalyzed C–N bond

formation strategies have significantly advanced this traditional approach (**Scheme 2.2**).[98] These methods have garnered substantial attention due to their high catalytic efficiency and broad substrate compatibility.[99] Additionally, classical reactions such as the Mannich type reaction[100] and aza-Michael addition[101] remain effective alternatives for constructing C–N bonds in various synthetic contexts.

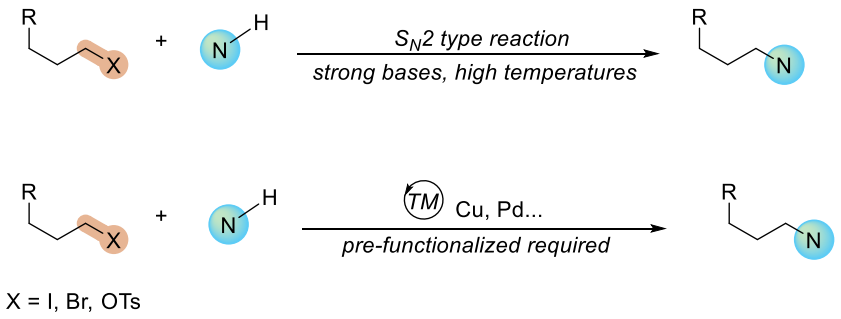

Scheme 2.2 Traditional method for forming C–N bonds via SN2 chemistry and transition-metal-catalyzed C–N bond formation strategies

However, these methods share a significant limitation: the alkyl portion of the substrate often requires pre-functionalization to participate in the reaction, and sensitive groups frequently need protection. These drawbacks restrict the substrate scope. In contrast, transition-metal-catalyzed sp^3 C–H amination has emerged as a novel strategy that circumvents the need for pre-functionalized groups, simplifying the synthetic process and broadening substrate compatibility.[35a, 102]

Despite its potential, this approach poses considerable challenges. Beyond the inherent difficulties of C–H activation, issues such as the coordination of the amine source and the resulting aminated product to the metal catalyst often lead to catalyst deactivation or side reactions.[102-103] This is particularly problematic for aliphatic amines, which typically exhibit strong coordination capabilities. Primary and secondary amines, in particular, readily form stable bis(amine) Pd^{II} complexes that are poorly reactive in subsequent C–H activation steps, effectively stalling the reaction. Additionally, once coordinated, aliphatic amines may undergo β-hydride elimination, resulting in oxidative degradation of the substrate and reduction of the palladium catalyst, further hindering the reaction progress (**Scheme 2.3**). Due to these significant challenges, the development of C–H activation and amination represents a major milestone in the fields of organic and organometallic chemistry.

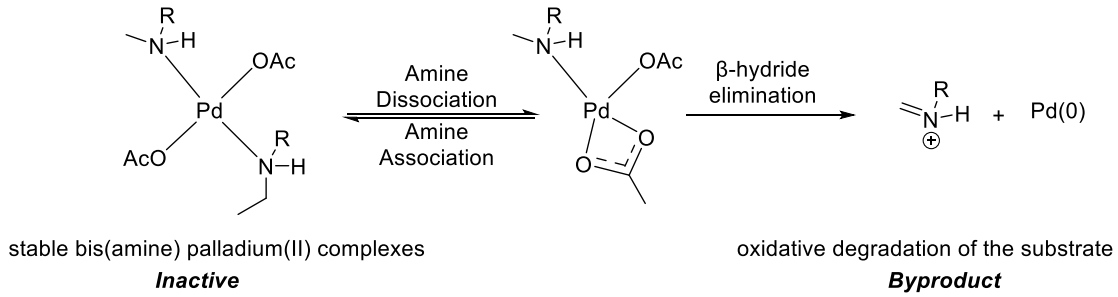

Scheme 2.3 The challenges of C–H amination

The development of palladium-catalyzed amination of unactivated C(sp³)–H bonds began in 2006, when Che and Yu described the intermolecular amidation of unactivated sp³ C–H bonds using primary amides and potassium persulfate as reagents (**Scheme 2.4**).[104] In this reaction, an oxime or pyridine group was employed as a directing group to facilitate C–H bond activation. The process proceeded via the formation of a cyclopalladated intermediate, which subsequently reacted with a reactive nitrene species generated by oxidative activation of the primary amide with persulfate. This approach demonstrated excellent chemical and regioselectivity, providing a foundation for further advancements in C(sp³)–H amination strategies.

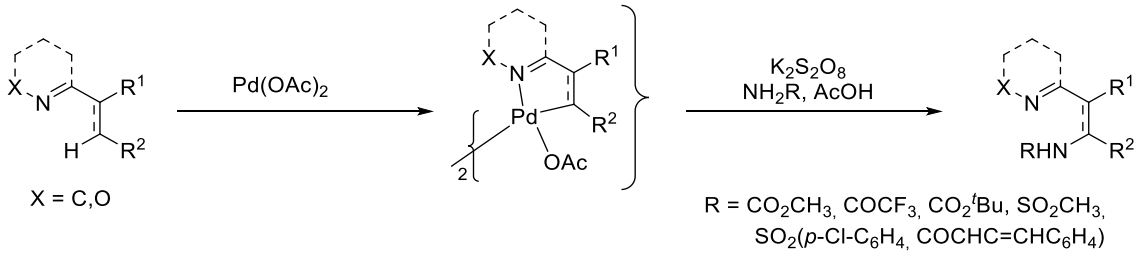

Scheme 2.4 Amination of unactivated C(sp³)–H bonds using primary amides

Subsequently, in 2009, Glorius and colleagues reported a palladium-catalyzed, amide-directed intramolecular amidation of unactivated C(sp³)–H bonds (**Scheme 2.5**).[54c] Remarkably, this reaction demonstrated a high degree of selectivity for the functionalization of C(sp³)–H bonds even in the presence of C(sp²)–H bonds. Notably, this was the first example of an unactivated C(sp³)–H bond activation and C(sp³)–N bond formation process that did not involve a nitrene intermediate, marking a significant advancement in the field.

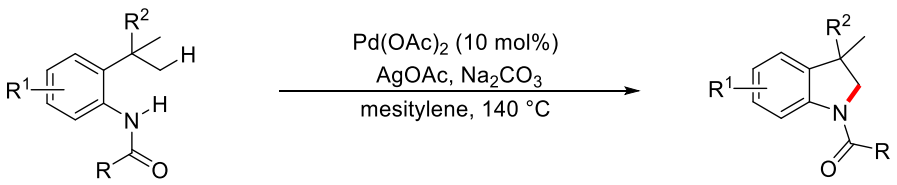

R = Me, H, C_2H_5, C_3H_7 R^1 = H, OMe, STol, Br, CHO, NO_2,... R^2 = Me, *i*Pr

Scheme 2.5 Pd-catalyzed, amide-directed intramolecular amidation of unactivated C(sp³)–H bonds

With the advancement of directing group and transient directing group strategies, significant progress has been made in C(sp^3)–H activation and C(sp^3)–N bond formation reactions. A noteworthy contribution involved a Pd^0/triarylphosphine-catalyzed C(sp^3)–H amination reaction, primarily designed for synthesizing β-amino acids derivatives with a perfluoro-DG (**Scheme 2.6**). This reaction proceeded via the oxidative addition of Pd^0 with O-benzoylhydroxylamine, followed by C(sp^3)–H bond cleavage by the palladium-amino intermediate. The catalytic cycle resembled that of Pd-catalyzed C–H arylation, requiring no external oxidant, with the triarylphosphine ligand playing a critical role.

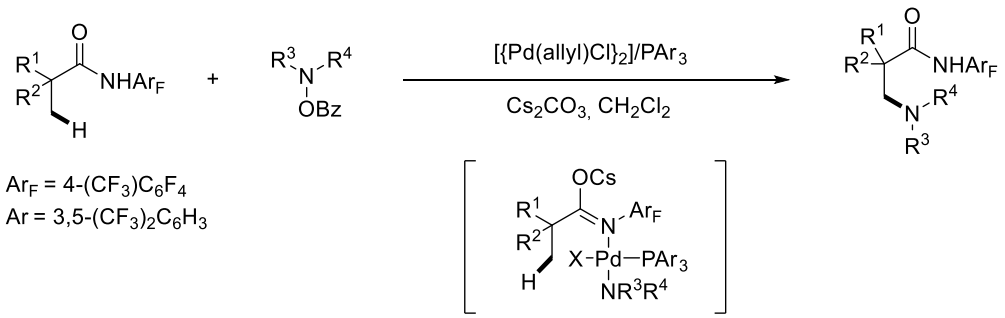

Scheme 2.6 Pd^0/PAr$_3$-catalyzed intermolecular amination of C(sp^3)–H bonds: synthesis of β-amino acids

The field has since evolved, with a growing emphasis on strategies that use native functional groups as directing groups, eliminating the need for additional modifications.

The native aliphatic amine-directed strategy has been particularly effective for sterically hindered amine substrates, where the α-carbon is fully substituted, as in tetramethylpiperidine, which minimizes the formation of stable diamine complexes.[105] However, for less substituted substrates, the efficiency decreases. At present, there are limited reports on using alkyl

carboxylic acids directly as substrates for C–H activation amination.

In 2021, Yu's group reported a Pd^{II}-catalyzed γ-C(sp^3)–H lactamization reaction, enabled by a 2-pyridone ligand (**Scheme 2.7**).[106] This method allowed the direct transformation of naturally occurring amides derived from amino acids into γ-lactams, isoindolinones, and 2-imidazolidinones—all pharmaceutically relevant structures. A key feature of this work was the ligand design; specifically, a C6-substituted 2-pyridone ligand that promoted lactam formation. The study highlighted the broad substrate scope, encompassing diverse amino acid and amide derivatives.

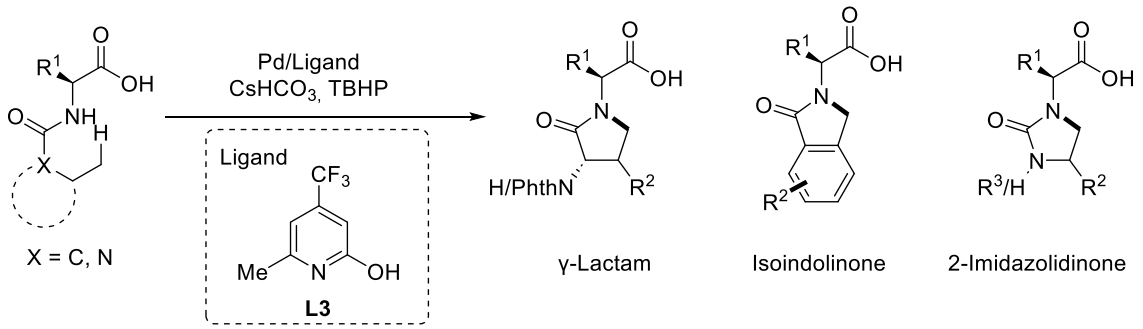

Scheme 2.7 Pd^{II}-catalyzed γ-C(sp^3)–H lactamization reaction

In 2024, the Yu group further advanced the field by developing a Pd-catalyzed C(sp^3)–H lactamization and cyclic amination process to synthesize cyclic β-amino acids, including γ- and δ-lactams, pyrrolidines, and tetrahydroquinolines from N-protected ω-amino acids (**Scheme 2.8**).[107] The breakthrough lay in the use of chloropyridine-pyridone ligands, which addressed coordination challenges inherent in traditional reactions. This approach enabled carboxylate-directed C–H activation and subsequent C–N bond formation.

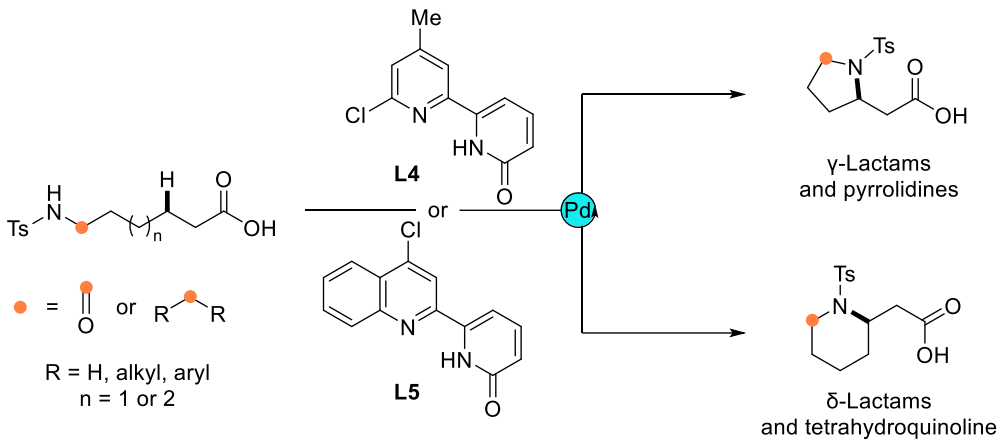

Scheme 2.8 Pd-catalysed methylene C(sp^3)–H lactamization and cycloamination enabled by chlorinated pyridine-pyridone ligands

Despite these advancements, the use of native carboxyl groups as directing groups has mainly been restricted to highly specialized substrates. Therefore, directly employing alkyl carboxylic acids as substrates for introducing nitrogen-containing functional groups to synthesize β-amino acid analogs remains an important, unresolved challenge in the field.

2.2 Project Goals

β-Amino acids and their derivatives have attracted particular attention. Unlike the α-L-amino acids found in proteins in nature, β-amino acids and their derivatives are rare and are often found as key components of bioactive natural products,[108] such as the anticancer agent paclitaxel (taxol) produced by Taxus brevifolia[109] and the anticancer agent bleomycin produced by Streptomyces.[110] In recent years, it has become clear that β-amino acid-based peptides exhibit secondary structures comparable to those of their α-amino acid counterparts, but are less susceptible to protease degradation.

Based on the background research presented earlier, catalytic C–H amination has become an important tool for C–N bond formation. To date, the reported catalytic systems for the synthesis of β-amino acids and their derivatives still require pre-installed directing groups or highly customized substrates, limiting their application in synthesis. In this context, I consider that using readily available alkyl carboxylic acids as substrates could provide a straightforward route for synthesizing β-amino acids and their derivatives (**Scheme 2.9**).

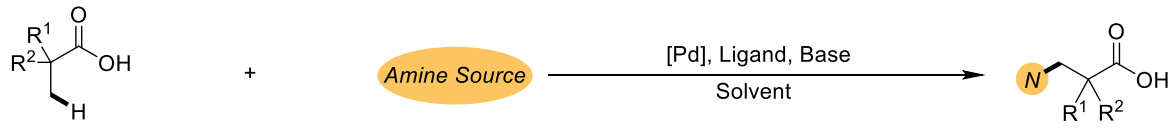

Scheme 2.9 Project goals

2.3 Reaction Design

Based on literature research and our previous work, I first defined two main objectives: (1) to identify suitable ligands, and (2) to identify appropriate amine sources. First, according to the literature, ligands significantly influence the rate of C–H activation, making ligand screening and design a major focus of this project. Second, I aimed to use amine sources that cover diverse structures or could be easily converted to free amines after the reaction, thereby increasing the practical utility of the developed methodology. However, due to the uncertainty regarding which amine sources would be effective,[111] and the fact that different amine sources could involve distinct reaction mechanisms in C–H amination, I conducted an extensive literature survey. I concluded that the Pd(II/IV) cycle would be a favorable tool for developing this transformation,[103] and based on the Pd(II/IV) cycle, I designed two mechanistic blueprints (**Scheme 2.10**).

One approach involves using a hydroxylamine source. The amine source itself acts as an oxidant, facilitating oxidative addition to the Pd^{II} intermediate, attaching the nitrogen-containing fragment to Pd^{IV}, and subsequently undergoing reductive elimination from the high-valent palladium to form the C–N bond and obtain the target product. Another approach involves using free amines. These amine sources have active acidic protons and can coordinate to palladium in anionic form in the presence of a base. The intermediate formed in this way requires an external oxidant to be oxidized into a high-valent palladium intermediate, which then undergoes reductive elimination to form the desired product.

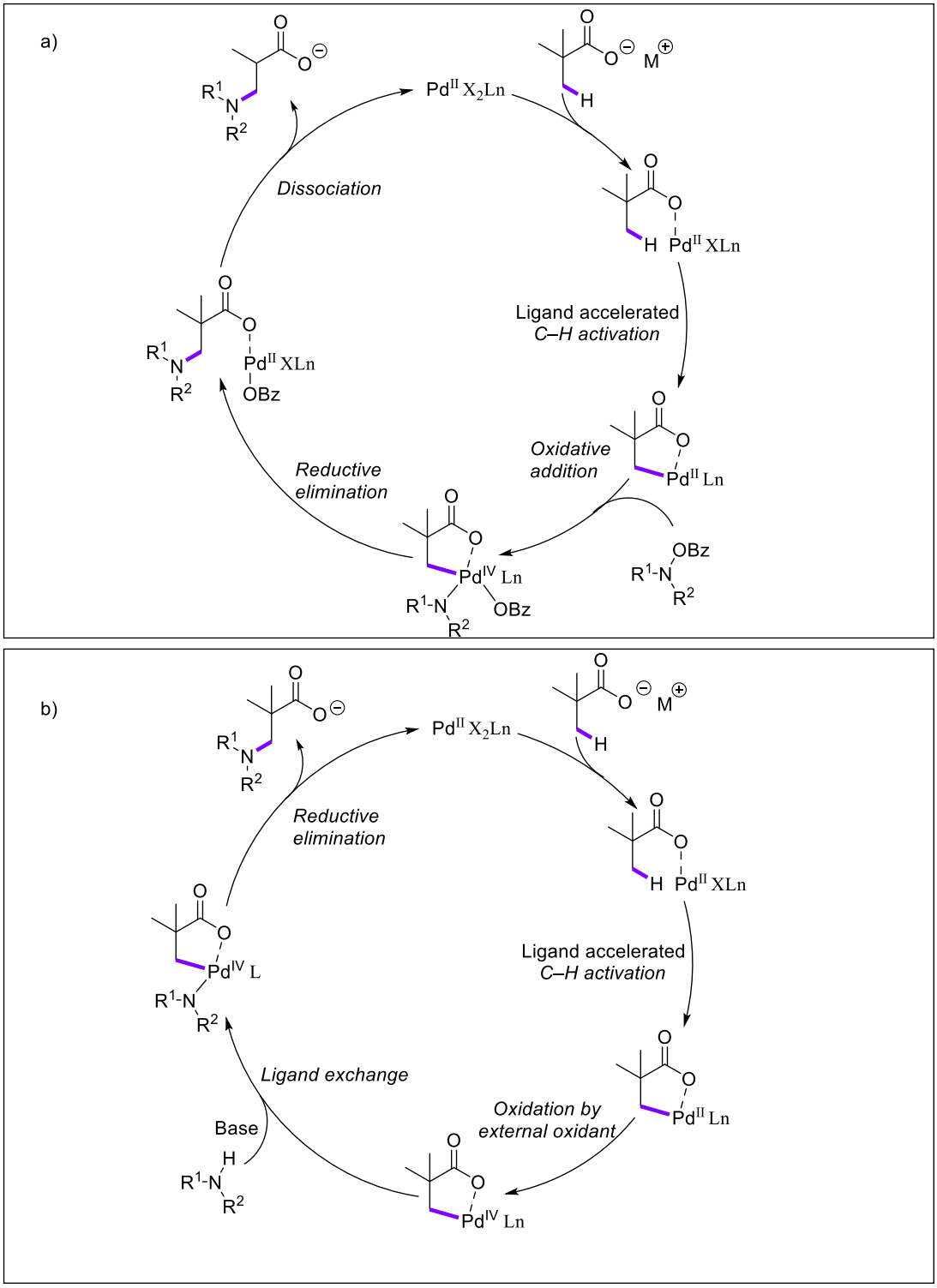

Scheme 2.10 Mechanistic blueprints, a) using hydroxyamine as amine source, b) using free amines as amine source.

2.4 Results and Discussion

2.4.1 The Target Product Synthesized Using Hydroxylamine as Amine Source

First, when using hydroxyamine (morpholino benzoate, **18**) as the amine source, I need to synthesize the desired amination product beforehand to obtain reference NMR chemical shift values.

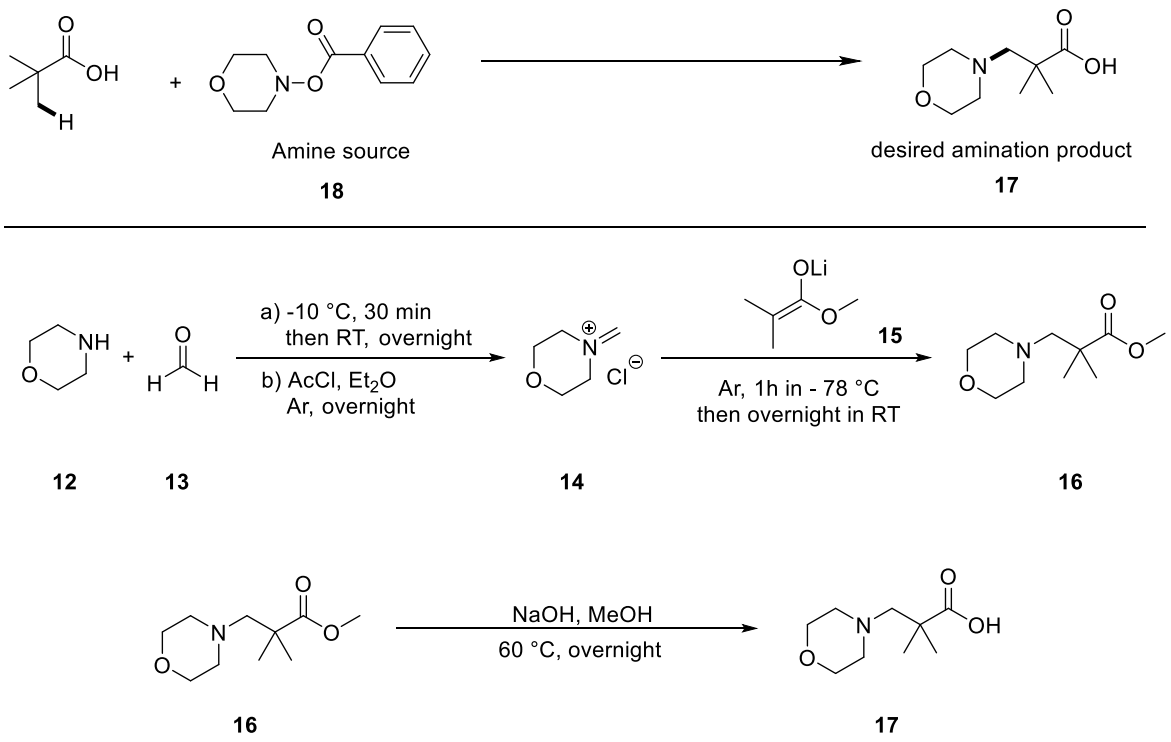

Scheme 2.11 The procedure to synthesis 2,2-dimethyl-3-morpholinopropanoic acid in different method

Initially, morpholine (**12**) reacts with formaldehyde (**13**) to form a morpholinium methyl salt (eschenmoser salt, **14**). Subsequently, the morpholinium methyl salt (**14**) reacts with methyl 2-methylpropanoate (**15**) in the presence of LDA to yield the corresponding ester product (**16**). Finally, hydrolysis of the ester leads to the desired target compound (**17**).

The functionalization of alkyl carboxylic acids via C–H activation often requires the addition of formic or acetic acid post-reaction to neutralize the base and release acidic products. Given that the target compound contains a tertiary amine moiety, I considered the potential influence

of acidic protons on its structure. To investigate this, I analyzed the characteristic peaks of the target compound under varying conditions (**Scheme 2.12**), observing shifts in response. Despite discrepancies between chemical shifts in the mixture and those in the isolated pure compound, the relative distance between two characteristic peaks remained consistently within 0.2 ppm, with peak positions ranging between 2.5 and 3.0 ppm. These data were sufficient to confirm product formation from the crude mixture using NMR analysis.

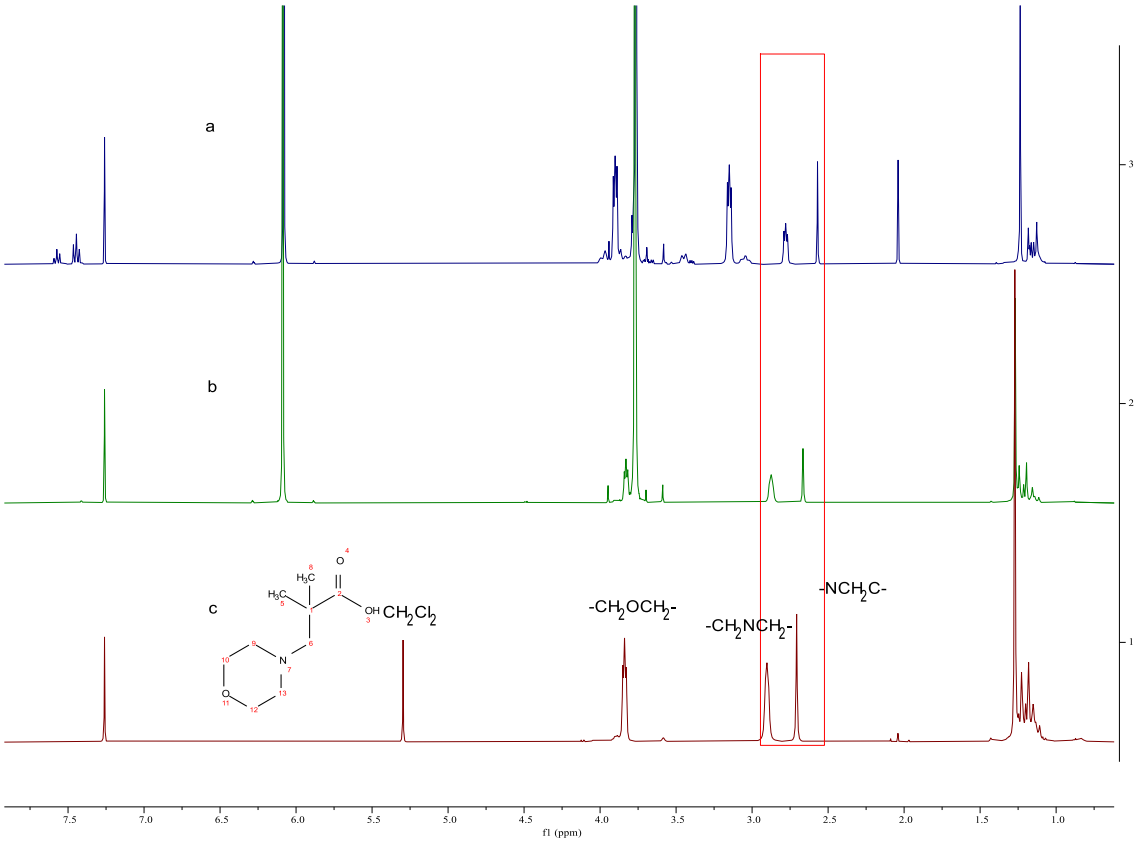

Scheme 2.12 NMR spectra of the target product and the effect of additives: a) Mixture of target product, amine source, formic acid, morpholine and internal standard (trimethoxybenzene (TMB)); b) Mixture of target product and TMB; c) Target Product Only

Following this, I began preliminary exploration of reaction conditions.

2.4.2 Testing of Using Hydroxyamines as Amine Source

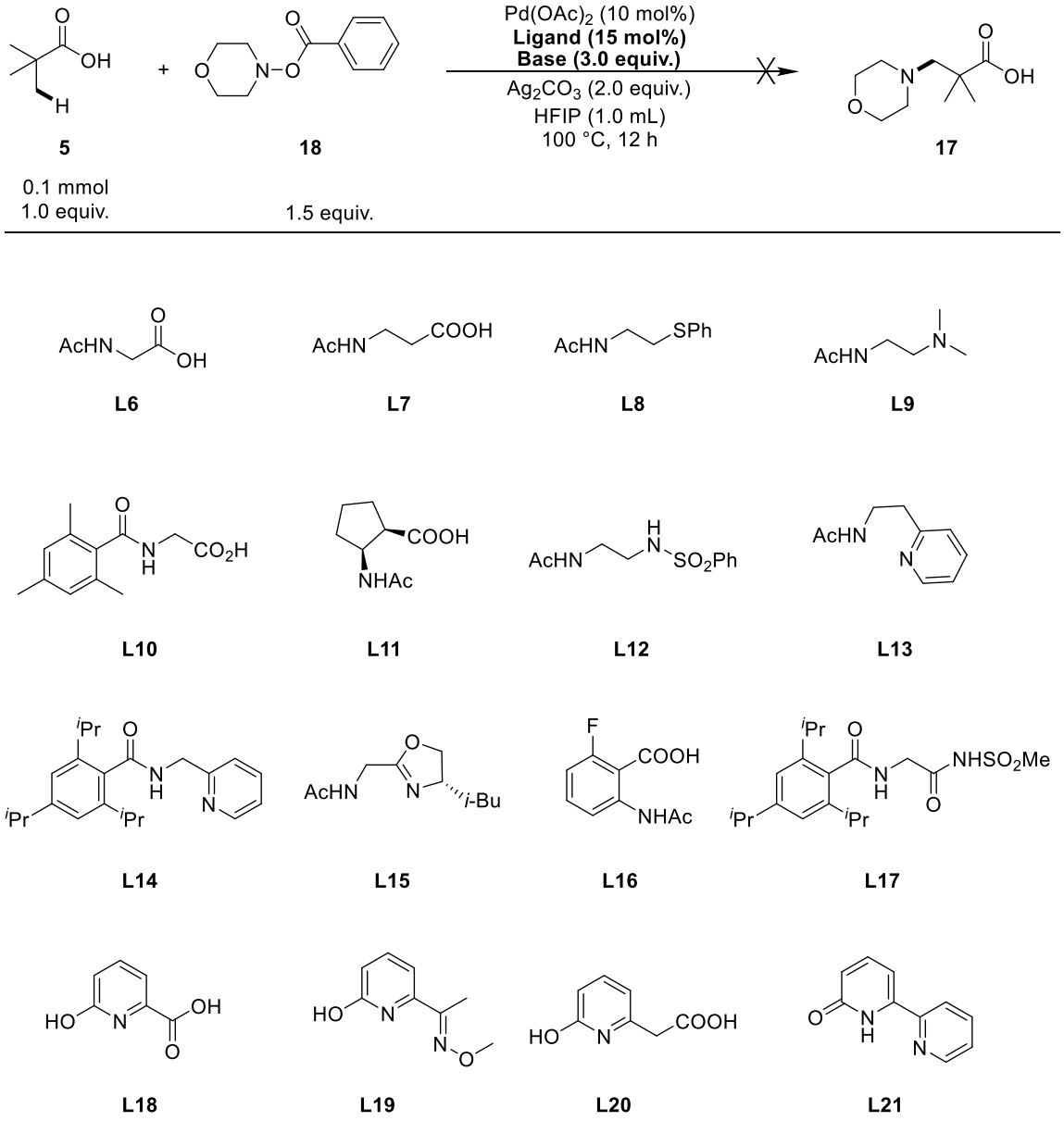

Scheme 2.13 Initial screening of the ligands.

I began by focusing on optimizing the conditions for amination through a comprehensive screening of reaction parameters. Given the critical role of ligands in the C–H activation step, I tested a variety of structurally diverse ligands using palladium acetate as the catalyst and $CsHCO_3$ as the base in HFIP (**Scheme 2.13**). The ligands selected were simpler representatives of their respective structural classes to avoid unpredictable effects of overly complex ligand

structures on catalytic intermediates. However, ligands successfully employed in related C–H activation and functionalization studies, particularly those derived from amino acids, were also included due to their established efficacy.

Despite these efforts, none of the tested ligands facilitated the desired transformation. Further exploration of combinations involving different bases, solvents, and ligands, as well as the exclusion of silver salts (not required for the designed catalytic cycle), also proved unsuccessful. To better understand the results, I analyzed all crude NMR spectra individually. Proton interference from the methyl group in pivalic acid hindered accurate determination of its conversion rate via NMR, so I shifted my focus to monitoring the conversion rate of the amine source. In most cases, partial decomposition of the amine source was observed. Decomposition products, including morpholine and benzoic acid, were identified via NMR. Morpholine likely contributed to palladium deactivation, while benzoic acid, with its more reactive C(sp^2)–H bond, could act as a competing substrate for C–H activation, thereby reducing reaction efficiency.

In a few instances, minor byproducts, such as lactones, were detected, suggesting that C–H activation occurred but that subsequent steps—oxidative addition and reductive elimination—were problematic. According to the proposed Pd(II/IV) catalytic cycle, a suitable oxidant is essential for driving the transformation, while selective C–N bond formation is critical for the reductive elimination step. In this reaction, oxoamines function as both the amine source and oxidant, with their dual functionality reliant on the relatively weak N–O bond.

Based on literature precedents, I hypothesized that modifying the structure of the benzoic acid moiety in the amine source could influence the N–O bond dissociation energy, thereby altering its oxidative properties. Furthermore, structural modifications to the acidic moiety could potentially enhance the selectivity of reductive elimination from the high-valent palladium intermediate. To test these hypotheses, I designed and synthesized a series of hydroxylamine derivatives. These derivatives retained the nitrogen fragment as morpholine while varying the acid moiety to include benzoyl groups substituted with electron-donating and strongly electron-withdrawing groups (**Scheme 2.14**).

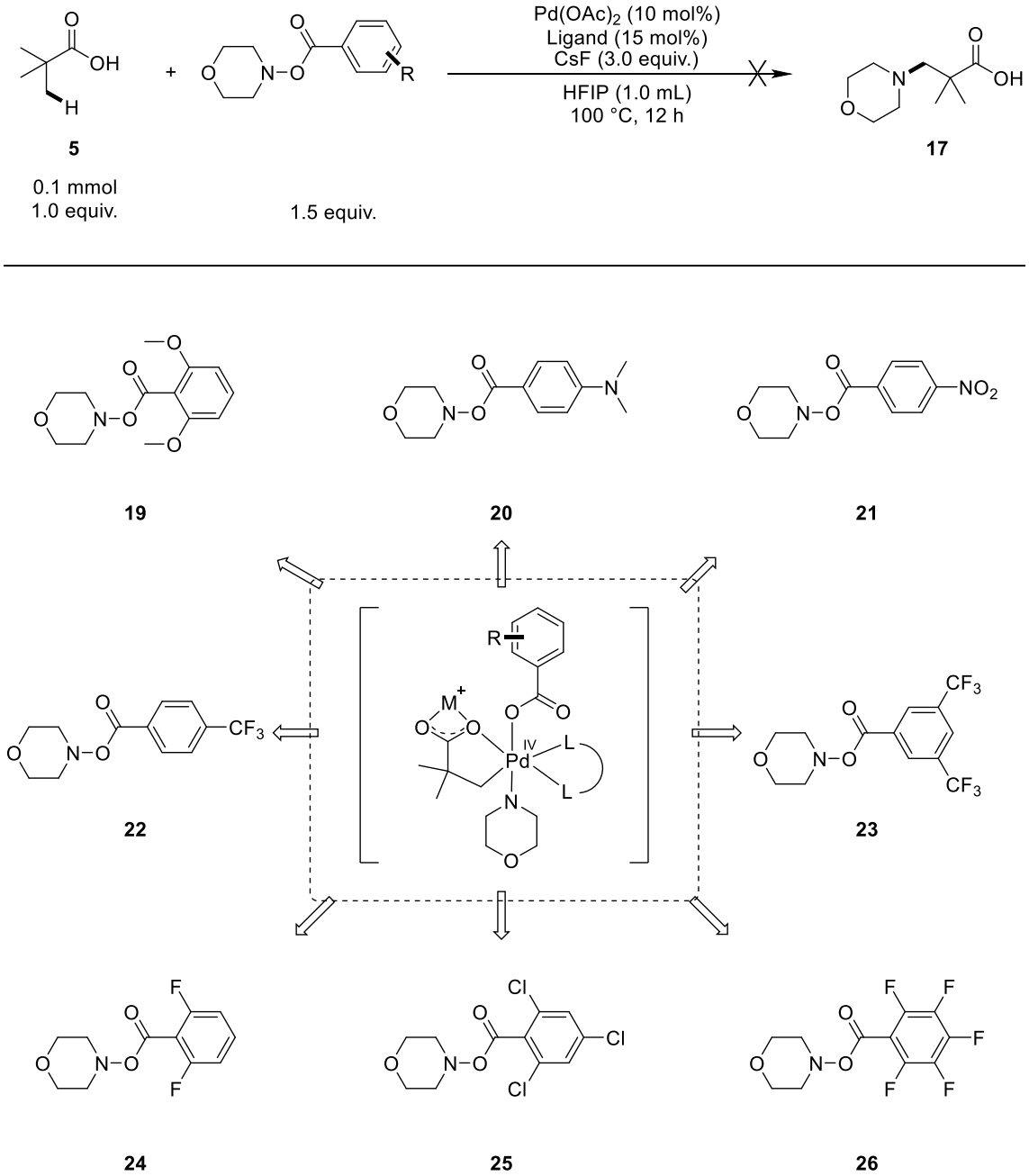

Scheme 2.14 Designed and synthesized hydroxylamine compounds

Subsequently, I substituted the original morpholino benzoate with these newly synthesized, structurally diverse amine sources and proceeded to test various combinations of bases and ligands, following the same systematic screening approach. Unfortunately, these efforts also failed to produce the desired outcome. Analysis of the NMR spectra revealed no significant deviations from the previous results. While the evidence of C–H activation observed earlier

was consistently present, the target amination product remained undetected.

2.4.3 Testing of Using Free Amines as Amine Source

After unsuccessful results with oxidized amine sources, I turned to testing other amine sources. Based on the second mechanistic blueprint, I used amine sources containing N–H[106] bonds. These amine sources lose the active proton on nitrogen during the reaction, so I considered that their reactivity might be influenced by the p*K*a of the amine source itself. To address this, I selected various amine sources with p*K*a values ranging from 4.76 to 15. In addition, considering that these amine sources require the use of external oxidants, I also tested different oxidants, including both inorganic and organic oxidants (**Scheme 2.15**).

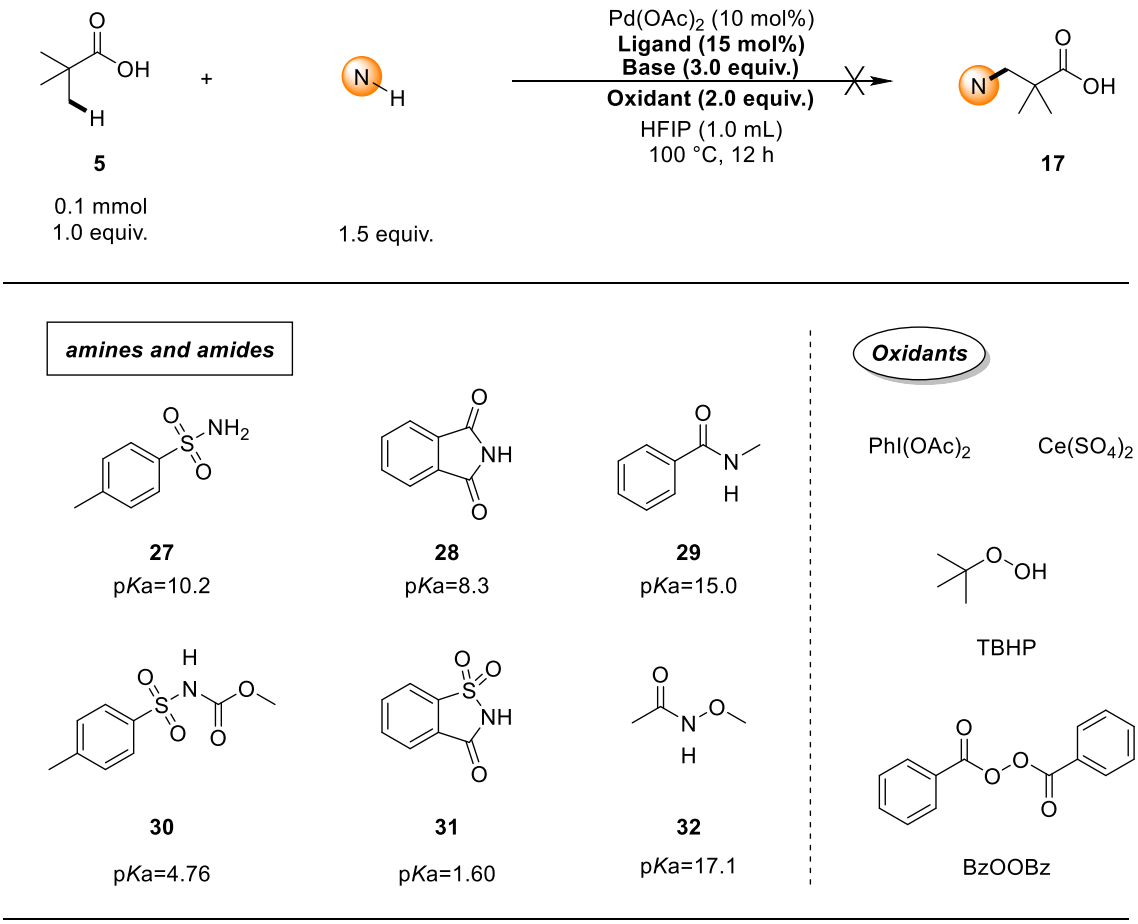

Scheme 2.15 Selected free amine sources and oxidants

However, testing the combinations of these amine sources with different oxidants under various conditions also failed to yield meaningful results. The simplicity of the selected amine sources,

chosen to facilitate the detection of expected products and subsequent transformations, posed a challenge in accurately determining their conversion rates from the crude NMR spectra. This limitation further hindered the extraction of valuable insights from the spectral data.

During our investigation of reaction conditions, a report by Yu captured our attention. Yu described a novel 2-pyridone ligand capable of activating the γ-C(sp³)–H bonds of amino acid-derived amides under Pd^{II} catalysis, resulting in C–N bond formation (**Scheme 2.7**). [106] Inspired by the intermediates proposed in Yu's mechanism, I hypothesized the formation of a similar intermediate for β-C(sp³)–H activation in carboxylic acids (**Scheme 2.16**). In Yu's proposed high-valent palladium intermediates, the Pd center was coordinated to the ligand, the carboxyl oxygen, the amide nitrogen, both components of the oxidant, and the carbon from the activated C–H bond.

Based on this insight, we decided to test a combination of pyridone acid as the ligand, N-methylbenzamide as the amine source, and TBHP as the oxidant.

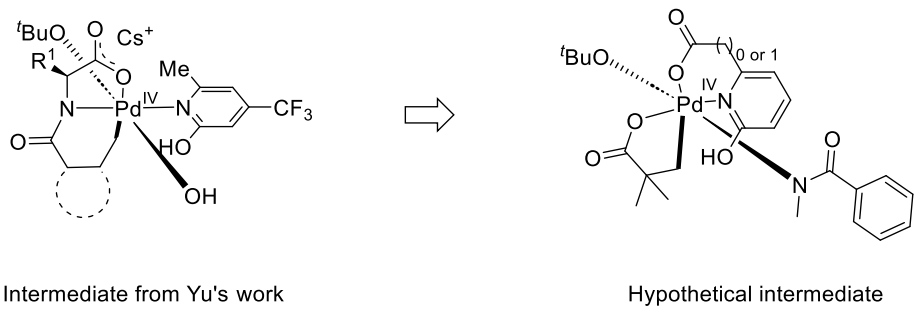

Scheme 2.16 Hypothetical intermediate simplified from Yu's mechanism intermediate

I used N-methylbenzamide as the amine source and tert-butanoic acid as the template substrate, conducting a series of conditions tests with 6–Hydroxypicolinic acid as the ligand (**Table 2.1**). The tests included using different oxidants, different bases, mixed solvents, and the presence of silver salts.

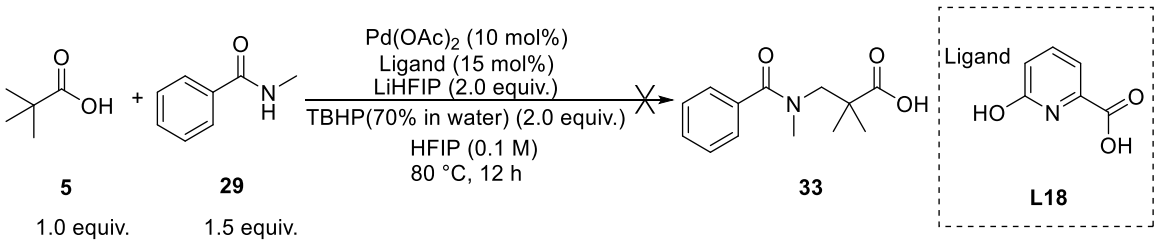

Entry	Condition
1	As Above
2	BQ instead of TBHP
3	$K_2S_2O_8$ instead of TBHP
4	$CsHCO_3$ instead of LiHFIP
5	Na_2HPO_4•$7H_2O$ instead of LiHFIP
6	K_2HPO_4 instead of LiHFIP
7	HFIP: DCE=1:1 instead of HFIP
8	With Ag_2O 1.0 equiv.

Table 2.1 conditions tests with 6-Hydroxypicolinic acid as the ligand

However, the target product did not appear under any conditions. Interestingly, under the conditions of **Entry 4-6**, analysis of the crude NMR spectrum revealed a new set of peaks.

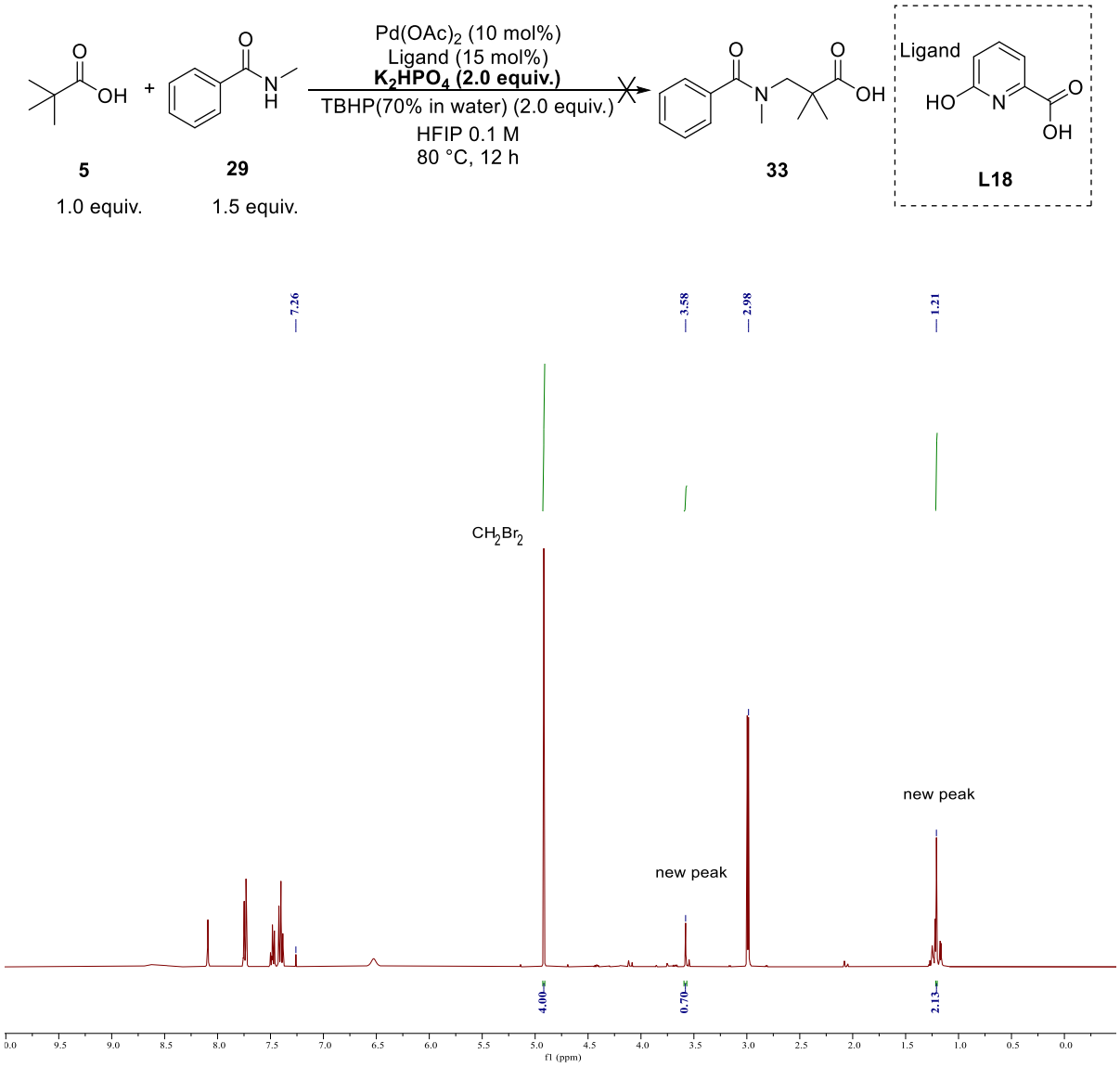

Scheme 2.17 The crude NMR spectrum of under the conditions of **Entry 6**

Using dibromoethane (CH_2Br_2) as an internal standard for integration based on the NMR spectrum, I found that this set of peaks had a relatively high integration value. Assuming that the peak at 3.58 ppm corresponds to a methylene group, a 35% conversion rate of the starting carboxylic acid suggests that the product corresponding to these peaks is present in significant amounts in the mixture. Therefore, I decided to further investigate the identity of this product. First, I conducted a set of control experiments.

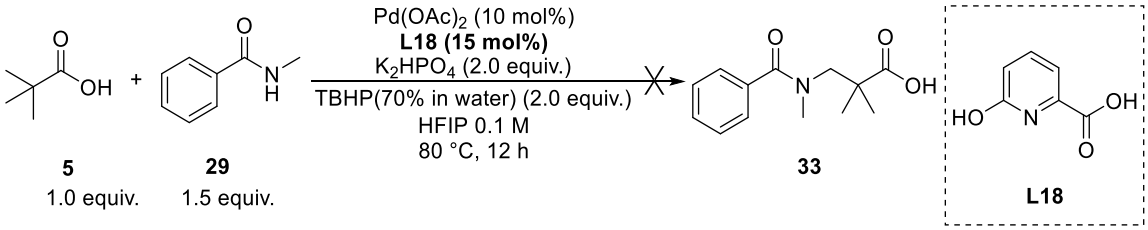

Entry	Condition	^{1}H NMR Yield (peak of δ=3.58)
1	w/o A	Traces (< 5%)
2	w/o B	Traces (< 5%)
3	w/o Pd cat.	Traces (< 5%)
4	w/o K_2HPO_4	Traces (< 5%)
5	w/o Ligand	16%

Table 2.2 Control experiments

From the results of these control experiments, I found that this set of peaks does not appear in the absence of either reactant, indicating that this set of peaks likely corresponds to a product formed after C–H activation. Additionally, the absence of these peaks when no palladium catalyst is used further supports my hypothesis. Interestingly, the peaks also did not appear in the absence of a base, while the effect of the ligand was relatively minor—some product was formed even without the ligand.

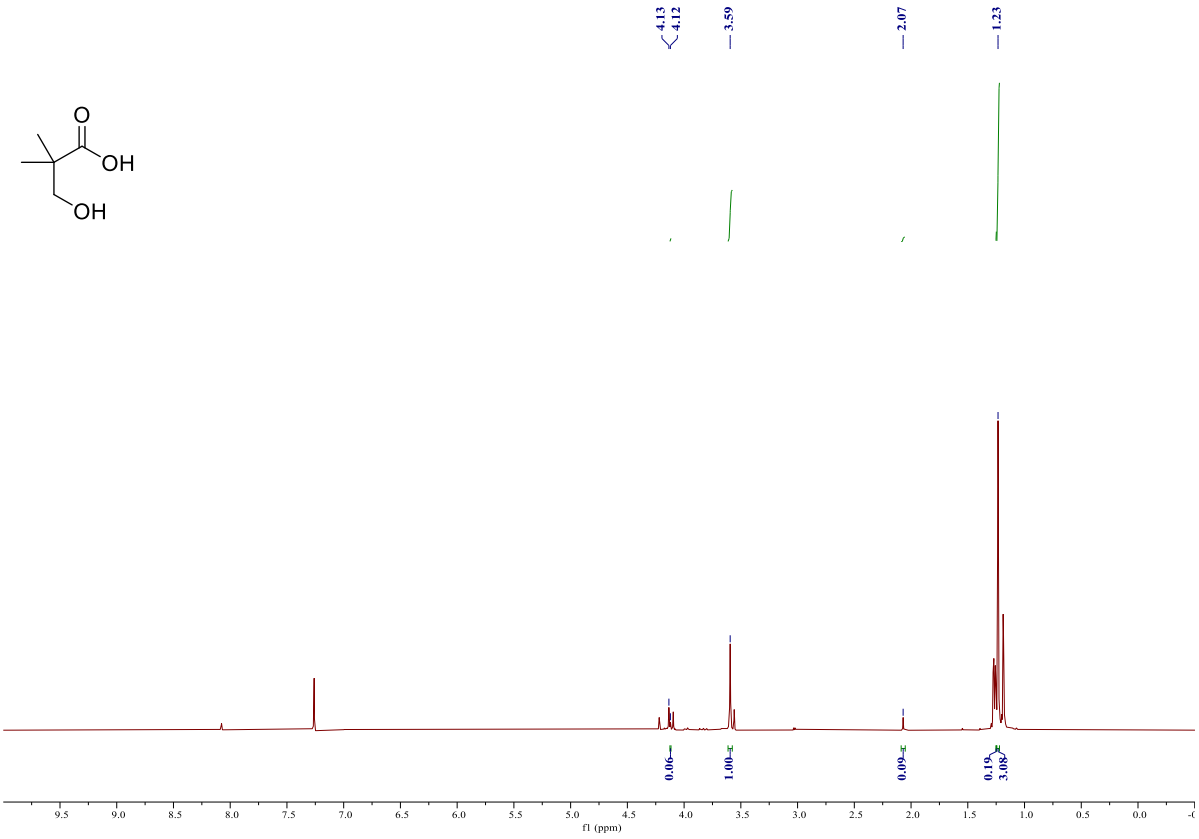

Scheme 2.18 The NMR spectrum of 3–hydroxy-2,2-dimethylpropanoic acid

In the meantime, I also attempted to isolate the compound corresponding to the newly appeared peaks. Based on the control experiments and subsequent comparison of its NMR spectrum (**Scheme 2.18**) with relevant literature, I believe that this product is 3–hydroxy-2,2-dimethylpropanoic acid. Although this was not my target product, the direct formation of a hydroxylated product caught my interest, which has become the third part of this paper.

2.5 Conclusion

In summary, the goal of this project was to develop a method for the direct formation of C–N bonds at the β-position of alkyl carboxylic acids, facilitating the synthesis of β-amino acids and their derivatives. To achieve this transformation, I designed a reaction mechanism based on a Pd(II/IV) cycle and systematically tested various combinations of amine sources and ligands, along with other factors that might influence the reaction outcome. Despite my efforts, I was unable to observe the formation of the desired target product in the NMR spectra of the crude reaction mixtures under the various conditions tested. However, I did identify some intriguing

side reactions during the process. Given the extensive efforts and attempts made, which either yielded no results or led to undesired byproducts, I have decided to pause further development of this project for the time being.

3 The Direct Pd-Catalyzed β-C(sp^3)–H Hydroxylation of Aliphatic Carboxylic Acids

3.1 Background

The hydroxyl group is a versatile functional group that can be readily converted into other common functional groups (such as amines, thioethers, and halides)[112] or used to attach additional fragments for further derivatization (such as sugars and phosphates).[113] Hydroxylation, the process of introducing a hydroxyl group (–OH) into an organic compound, is a powerful method for incorporating oxygen into organic molecules.

Alcohols are omnipresent in plenty of natural products, and bioactive molecules, and the pharmaceutical,[114] bulk, and fine chemical industries produce a large volume of hydroxyl-containing compounds, which are widely used in the synthesis of drugs, agrochemicals, and polymers.[115] In medicinal chemistry, the introduction of hydroxyl groups can significantly enhance binding affinity with targets by strengthening molecular recognition through hydrogen bonding and optimizing structural functionality, and also increase compound solubility, improving absorption and distribution within the body.[116] In polymer chemistry, monomers with hydroxyl (–OH) groups are commonly used to manufacture polyesters, polyamides, and polyurethanes, due to the reactivity of hydroxyl groups allows them to form covalent bonds with other monomers, initiating polymerization.[117]

Hydroxy acids (HAs) represent a class of compounds widely used in numerous cosmetic and therapeutic formulations for their beneficial effects on skin.[118] Among these, β-hydroxy acids (BHAs) and derivatives, characterized by a hydroxyl group at the β-position relative to the carboxyl group, are the second most commonly used type of hydroxy acid (**Scheme 3.1**).[119] Some BHAs, such as β-hydroxybutanoic acid, are present in body tissues as metabolic intermediates and energy sources Additionally, structures derived from β-hydroxy acids, such as β-hydroxy esters, are prevalent as drug precursors or intermediates.[120]

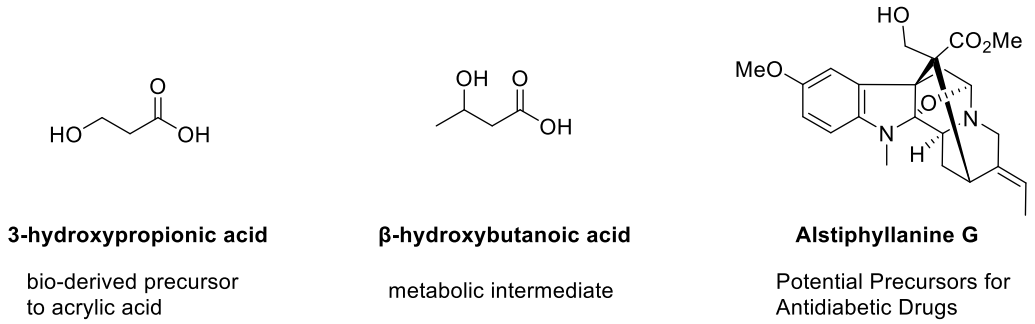

Scheme 3.1 Examples of β–hydroxy acids and derivatives

Over the years, numerous pathways for obtaining hydroxyl groups have been established. However, due to increasing demand, the development of simple and efficient new methods for synthesizing β-hydroxy acids remains a key interest and challenge in both industrial and academic research.

In the late 20th century, Sen and Kao discovered that platinum(II) species, in the presence of platinum(IV) species, can catalyze the hydroxylation of unactivated C–H bonds in aliphatic carboxylic acids in water.[62] Although the reaction lacked selectivity, this pioneering work laid a solid foundation for advancements in this field.[121]

Due to certain limitations of Pt catalysis, researchers have explored Pd complexes as catalysts for hydroxylation. However, direct synthesis of hydroxy acids remains challenging—not only due to the inherent inertness of C–H bonds but also because the alcohol products tend to be more reactive than the alkane substrates, often leading to over-oxidation. Reviewing recent advancements, initial solutions to C–H activation difficulties have employed directing group strategies, enabling β-hydroxylation of carboxylic acids and their derivatives.

In 2015, Rao and colleagues developed a Pd-catalyzed, directing group-assisted hydroxylation of unactivated aliphatic C(sp^3)–H bonds (**Scheme 3.2**), notably using water as the hydroxyl source.[122]

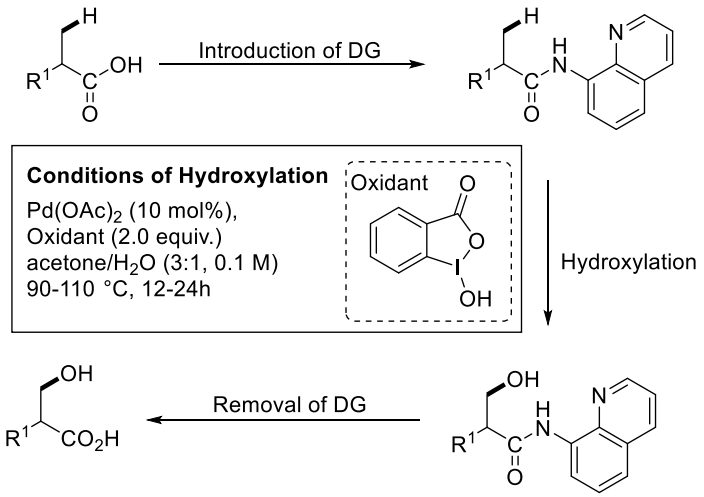

Scheme 3.2 Directing group-assisted hydroxylation of unactivated aliphatic C(sp^3)–H bonds

However, the complex steps of installing and subsequently removing directing groups have prompted the search for new strategies.

In 2019, van Gemmeren's group,[123] and later Yu and co-workers[124] in 2021, reported strategies for Pd-catalyzed direct β-C(sp^3)–H acetoxylation of aliphatic carboxylic acids (**Scheme 3.3**). This approach enables the use of free carboxylic acids in a single step, without the need for installing strong directing groups. The resulting products can be converted to hydroxy acid compounds through hydrolysis.

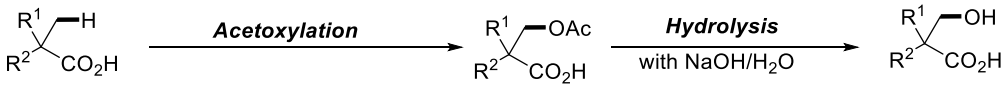

Scheme 3.3 Pd-catalyzed direct β-C(sp^3)–H acetoxylation of aliphatic carboxylic acids

A similar approach can also be achieved through lactonization reactions. In 2020, Yu and colleagues reported a Pd-catalyzed β-C(sp^3)–H lactonization of fatty acids (**Scheme 3.4**), enabled by a mono N-protected β-amino acid-derivated ligand (**L22**). The resulting strained, reactive β-lactone products can be converted to β-hydroxy acids in later stages through hydrolysis.[125]

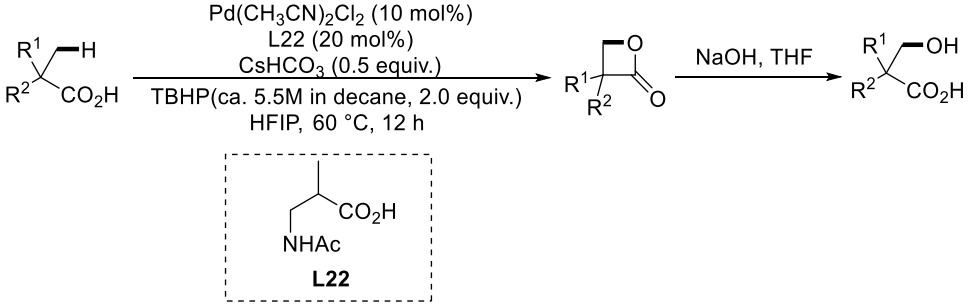

Scheme 3.4 Pd-catalyzed β-C(sp³)–H lactonization of fatty acids

While these approaches provide access to the target compounds, direct β-C(sp³)–H hydroxylation of carboxylic acids would be more convenient and efficient. Building on our prior experience in this field, we aim to develop a one-step method for efficiently obtaining various hydroxy acids directly from their respective acids.

3.2 Project Goals

During our research on the direct C–H amination of alkyl carboxylic acids, we unexpectedly observed a reaction leading to β-hydroxylation. A subsequent literature review revealed that, although there have been some reports on β-C–H activation of alkyl carboxylic acids to construct C–O bonds, none of these methods provide a direct, one-step approach to synthesizing β-hydroxy acids. Motivated by this finding, we decided to investigate this unexpected reaction further, aiming to develop a novel and efficient method for the one-step synthesis of β-hydroxy acids (**Scheme 3.5**).

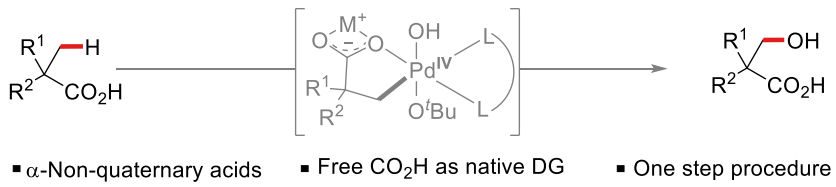

Scheme 3.5 Project goal of the direct Pd-catalyzed β-C(sp³)–H hydroxylation of aliphatic carboxylic acids

3.3 Optimization of the Reaction Conditions

Existing studies have primarily focused on α-quaternary carboxylic acids, while α-non-quaternary carboxylic acids present a greater challenge for C–H activation. This is due to the presence of reactive α-hydrogens, which can lead to β-hydride elimination in the resulting metal complex intermediate, forming undesired unsaturated byproducts.

To address this issue, we selected 2-methylpentanoic acid as a model substrate to optimize conditions that minimize this side reaction. Based on our initial observation of β-hydroxylation, we chose to begin with palladium acetate as the palladium source, potassium hydrogen phosphate as the base, TBHP as the oxidant, DMF as an additive, and HFIP as the solvent. The reaction was conducted at 100 °C to facilitate an efficient screening of suitable ligands (**Scheme 3.6**).

We began by evaluating α-amino acid-derived ligands. The basic N-acetyl α-amino acid ligand (**L6**) yielded 18% product, while introducing a methyl substituent on the backbone (**L23**) slightly improved the yield. However, excessive substitution on the backbone (**L24**) reduced the yield significantly—even tert-butyl substitution (**L25**) resulted in no product formation, whereas benzyl substitution (**L26**) produced yields comparable to methyl substitution. Further modification of the benzyl group on the aromatic ring (**L27, L28**) revealed that ligand **L29** delivered a promising 30% yield.

Next, we focused on modifying the N-protecting group of ligands without backbone substitutions, specifically evaluating their role as internal bases in promoting C–H bond cleavage and C–metal bond formation during the C–H activation step. Ligands with electron-donating benzoyl substituents on the N-protecting group (**L30**) significantly improved the yield, whereas electron-withdrawing benzoyl substituents (**L32, L33**) led to a slight decrease in yield. Based on the comparison of the results of **L30** and **L31**, we considered that, in addition to the electronic effects, the size of the substituent might also be an important factor. Therefore, **L34** was also tested; however, the results were disappointing.

Finally, ligands with simultaneous modifications on both the backbone and the internal base were tested (**L35** – **L40**); however, none outperformed **L29**, which remained the most suitable ligand under the tested conditions.

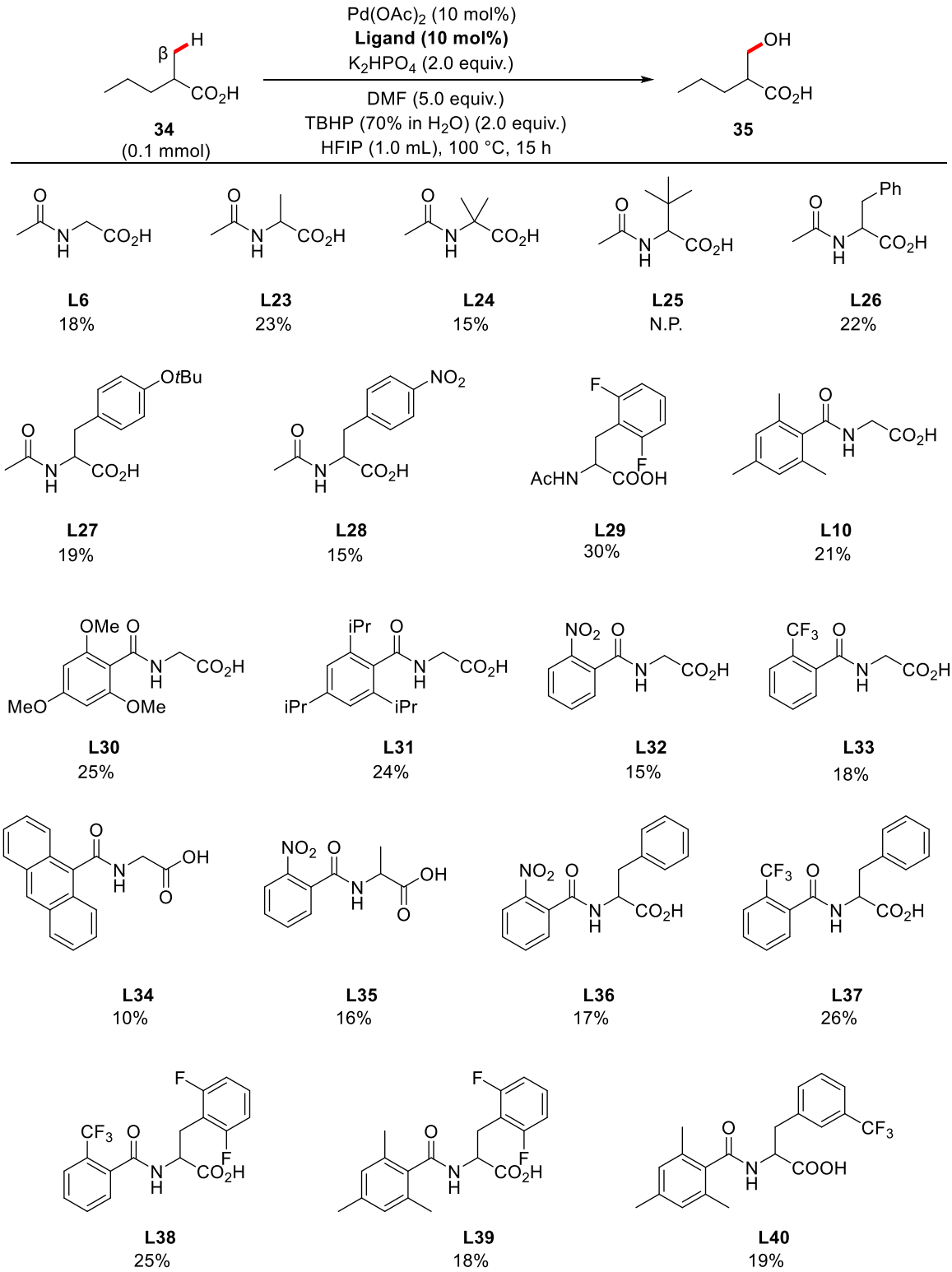

Scheme 3.6 Initial optimization of the ligands. These experiments were carried out together with Sourjya Mal.

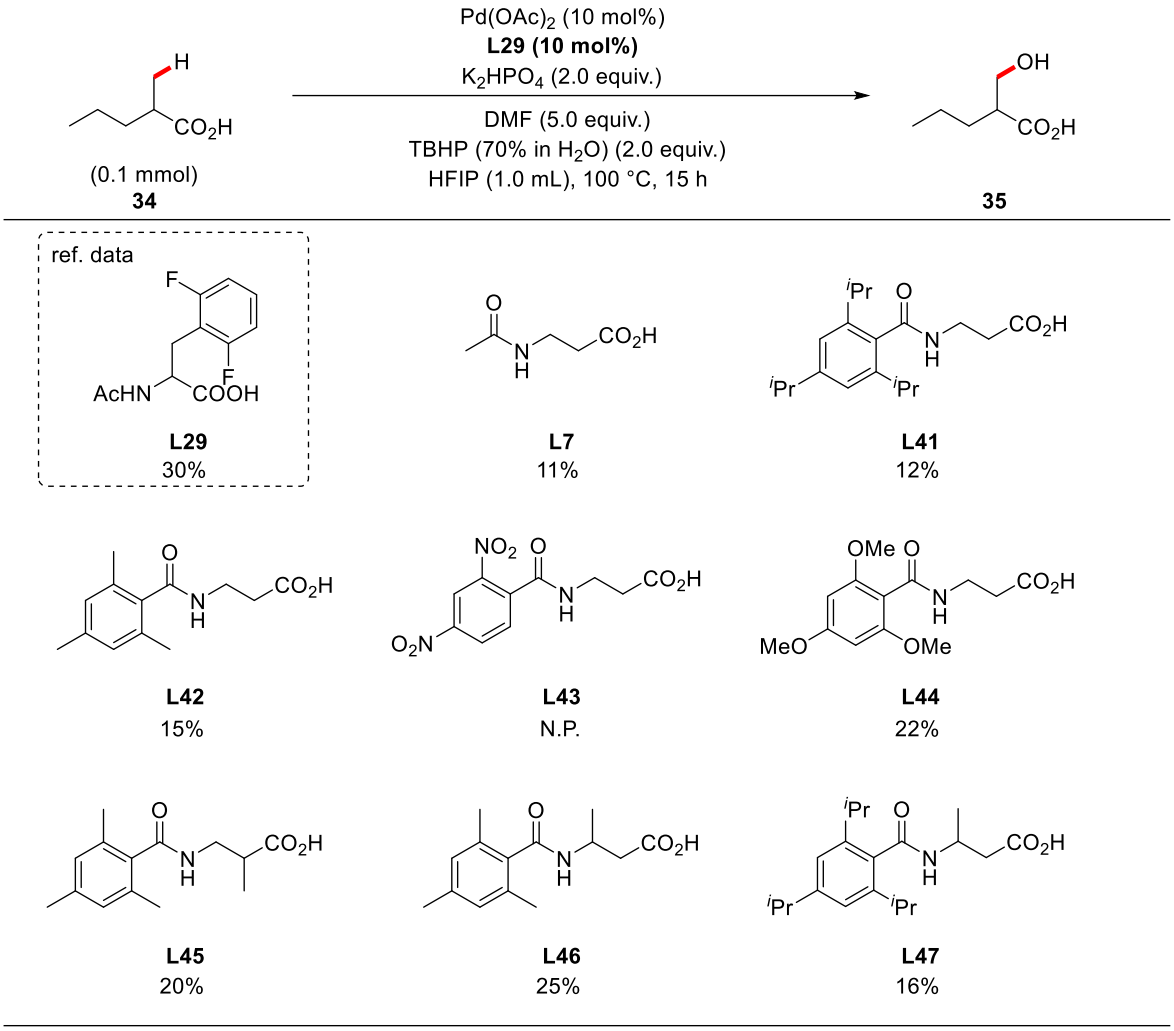

Scheme 3.7 Preliminary screening of β-amino acid derivatives. These experiments were carried out together with Sourjya Mal.

Subsequently, we evaluated β-amino acid-derived ligands (**Scheme 3.7**). The basic N-acetyl β-amino acid ligand (**L7**) yielded only 11% product. When modifying the internal base structures of these ligands (**L41 - L44**), we observed a trend similar to that of α-amino acid-derived ligands: ligands with electron-donating benzoyl substituents on the N-protecting group outperformed those with electron-withdrawing substituents. Simultaneous modifications to both the backbone and the N-protecting group (**L46 - L47**) did not creative more effective ligand.

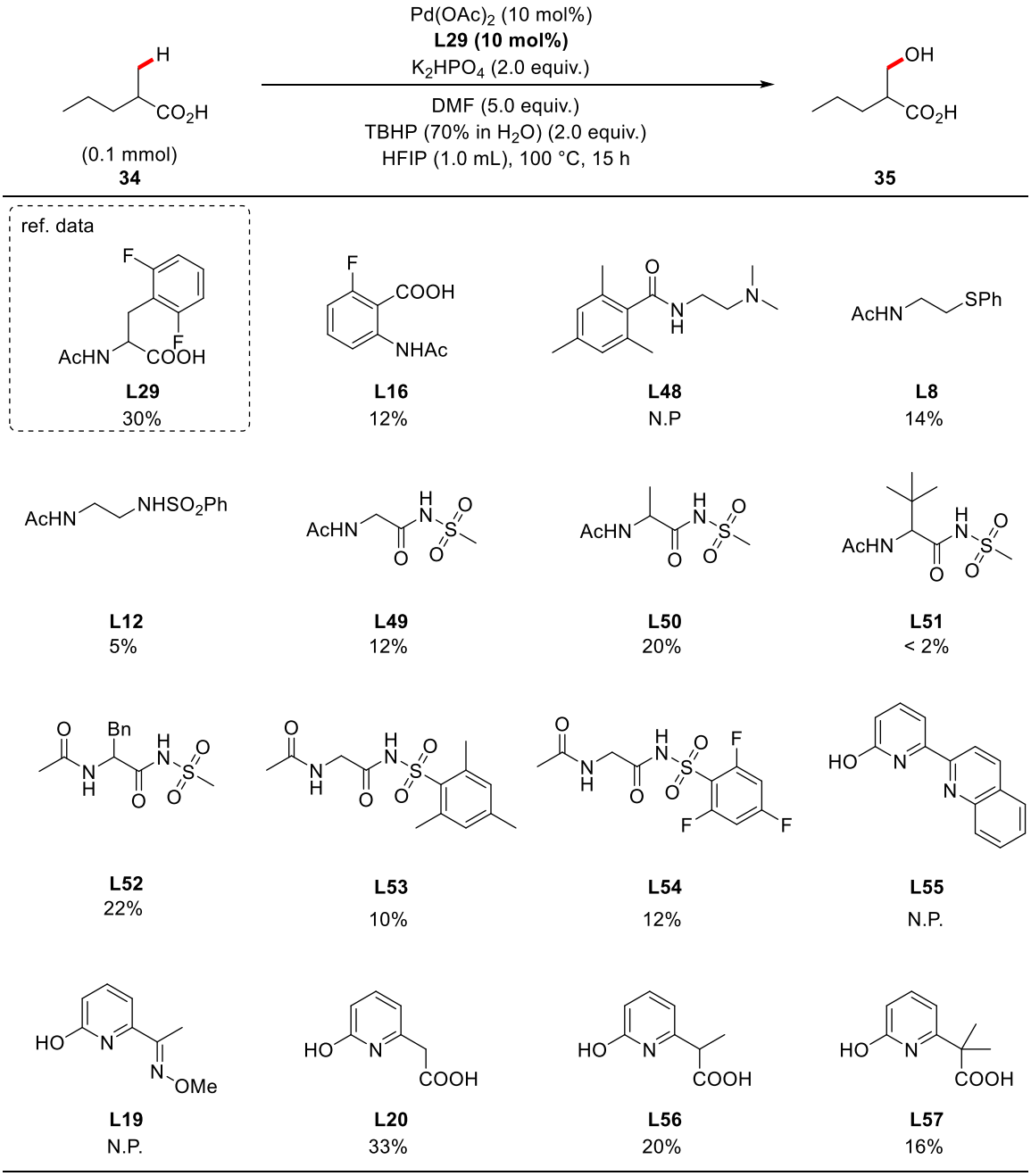

Scheme 3.8 Preliminary screening of different ligand classes. These experiments were carried out together with Sourjya Mal.

We further investigated ligands with different structures (**Scheme 3.8**). Ligands derived from anthranilic acid (**L16**) produced only 12% yield, while **L48**, commonly used in C–H deuteration reactions,[126] were ineffective in promoting C–H hydroxylation. α-Amino amide ligands (**L12, L49 - L54**) were also tested, and a trend similar to α-amino acid ligands was observed: substitutions on the backbone could moderately improve the yield. However, as with

α-amino acid ligands, ligands with tert-butyl substitutions (**L51**) on the backbone impaired the reaction. Finally, we evaluated several pyridone-based ligands. Surprisingly, neither **L55** nor **L19** facilitated the reaction, yielding no product. However, **L20** achieved a superior yield of 33%. Further modifications to this ligand revealed that backbone substitutions (**L56, L57**), rather than enhancing the reaction, reduced the yield. Consequently, we decided to proceed with **L20** as the ligand for further optimization of reaction conditions.

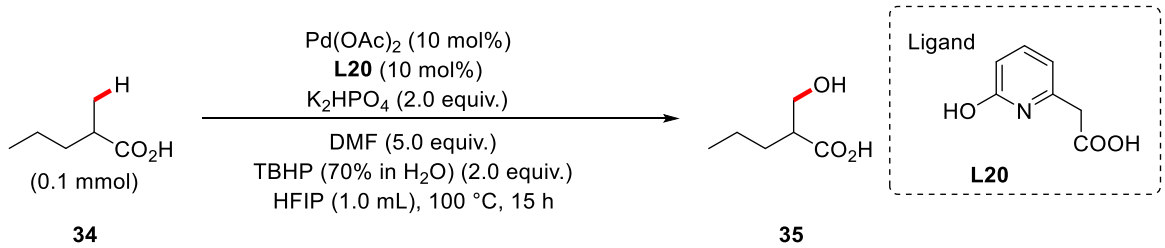

Entry	Variation	NMR Yield
1 (ref. data)	As above	33%
2	w/o $Pd(OAc)_2$	N. P.
3	w/o TBHP	N. P.
4	w/o K_2HPO_4	N. P.
5	w/o Ligand	4%
6	w/o DMF	25%

Table 3.1 Control experiments

We first conducted control experiments under the current conditions. As shown in the **Table 3.1,** the palladium complex, TBHP, and potassium hydrogen phosphate were all critical for the reaction, as the absence of any one of these components completely halted the reaction. In the absence of a ligand, only trace amounts of the product were observed, highlighting the ligand's significant role in promoting the reaction. The use of DMF as an additive was found to be beneficial; without DMF, the yield decreased notably. These results suggest that DMF plays a supportive role, prompting us to explore the effects of other potential additives on the reaction.

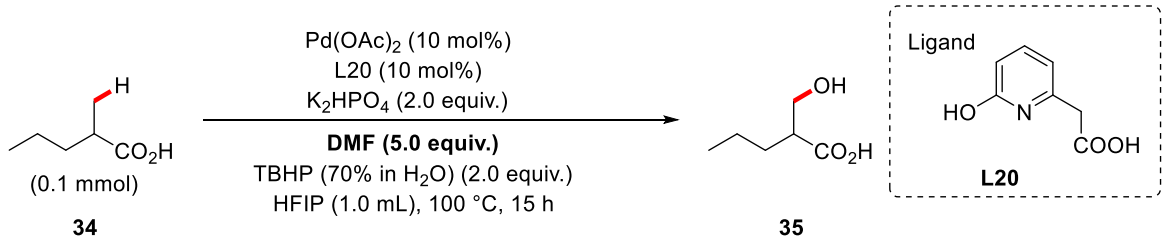

Entry	Additive	NMR Yield
1 (ref. data)	5.0 equiv. DMF	33%
2	2.5 equiv. DMF	29%
3	7.5 equiv. DMF	32%
4	5.0 equiv. DMA	26%
5	5.0 equiv. CH_3CN	17%

Table 3.2 Optimization of additives

We first tested the effect of different equivalents of DMF on the reaction and found that both increasing and decreasing the amount of DMF led to a slight decrease in yield. When DMF was replaced by DMA, which also has an amide structure, the yield decreased significantly. Acetonitrile could also be used as an additive, but replacing DMF with acetonitrile in this reaction resulted in a substantial reduction in yield.

Although DMF is commonly used as a solvent in large volumes or as a reaction partner,[127] in C–H activation, DMF is often used as an additive,[64a, 76a, 128] despite its role being elusive. To date, several hypotheses have been proposed regarding its function. For instance, DMF is known to abstract a proton from carboxylic acids, leading to the formation of a small amount of $DMFH^+$ in excess DMF.[129] It may also act as a mild base or as an unstable ligand.

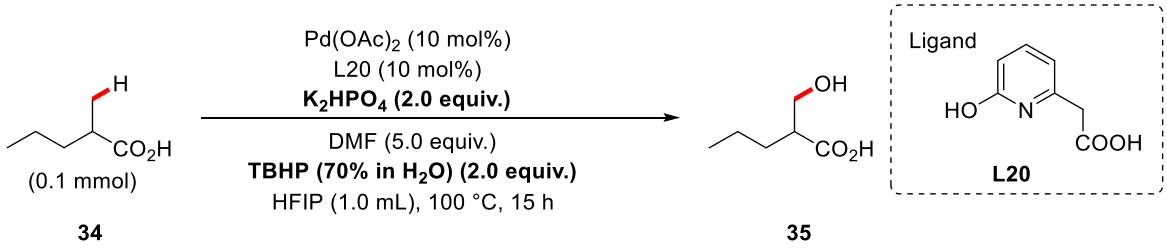

Entry	K_2HPO_4 (equiv.)	TBHP (70% in H_2O) (equiv.)	NMR Yield
1	1.5	2.0	30%
2 (ref. data)	2.0	2.0	33%
3	2.5	2.0	35%
4	3.0	2.0	35%
5	3.5	2.0	35%
6	3.5	3.0	36%
7	3.5	4.0	38%
8	3.5	5.0	40%

Table 3.3 Optimization of base and oxidant amount

We began by examining the effect of the base equivalent while keeping the oxidant fixed at 2.0 equivalents. Increasing the base from 1.5 to 2.5 equivalents resulted in a slight increase in yield, but further increases beyond 2.5 equivalents did not improve the yield. However, NMR analysis revealed that the amount of unreacted starting material increased as the base equivalent was raised. This indicates that while the yield plateaued, the conversion of starting material to the desired product improved with higher base equivalents, reaching its maximum at 3.5 equivalents.

Using 3.5 equivalents of base, we then investigated the effect of the oxidant equivalent. We observed that the yield increased with higher oxidant equivalents, but the conversion efficiency peaked at 4.0 equivalents of oxidant, as shown by the NMR spectra, and decreased thereafter. Based on these results, we selected 3.5 equivalents of base and 4.0 equivalents of oxidant as the optimized conditions for further reaction optimization.

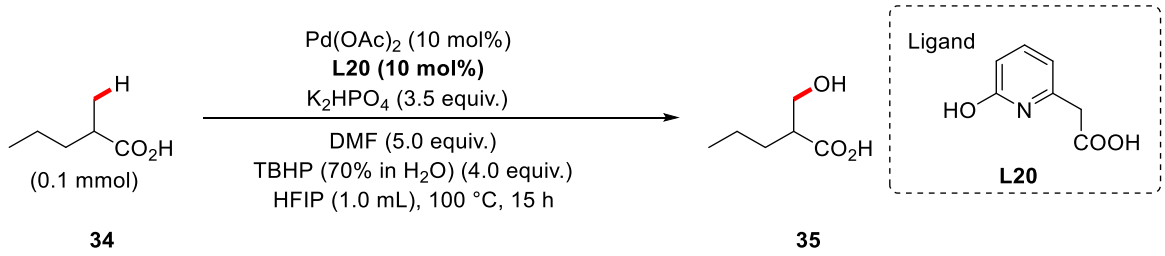

Entry	Ligand Loading	NMR Yield
1 (ref. data)	10 mol%	38%
2	15 mol%	43%
3	20 mol%	45%
4	25 mol%	48%
5	30 mol%	46%

Table 3.4 Screening of ligand loading

The ligand loading has a significant impact on the C–H activation step. Our results showed that increasing the ligand loading notably improved the yield, reaching 48% at a loading of 25 mol%. However, further increasing the ligand equivalent led to a slight decrease in yield. Based on these findings, we selected 25 mol% ligand loading for further optimization of the reaction conditions.

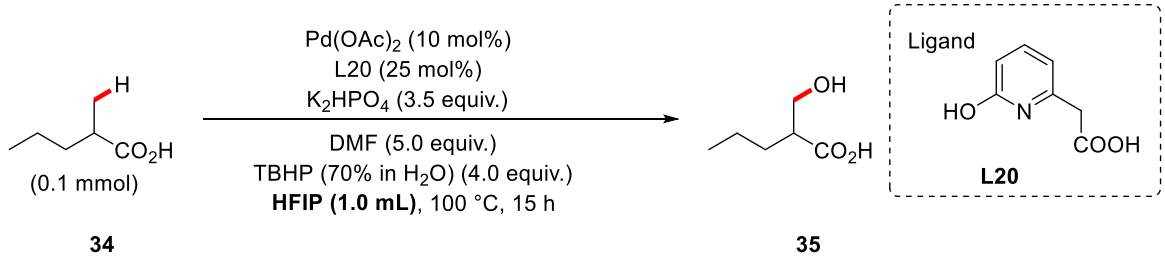

Entry	Volume of HFIP	NMR Yield
1	0.75 mL	40%
2 (ref. data)	1.0 mL	48%
3	1.25 mL	42%
4	1.5 mL	40%
5	2.0 mL	36%

Table 3.5 Screening of solvent volume

The reaction concentration is a critical factor influencing the reaction rate. We tested the effect of HFIP volume on the reaction and found that even a slight increase in HFIP volume led to a decrease in yield. When the volume was increased to 2 mL, the yield dropped to 36%. Based on these results, we opted to maintain the HFIP volume at 1 mL for further optimization of the reaction conditions.

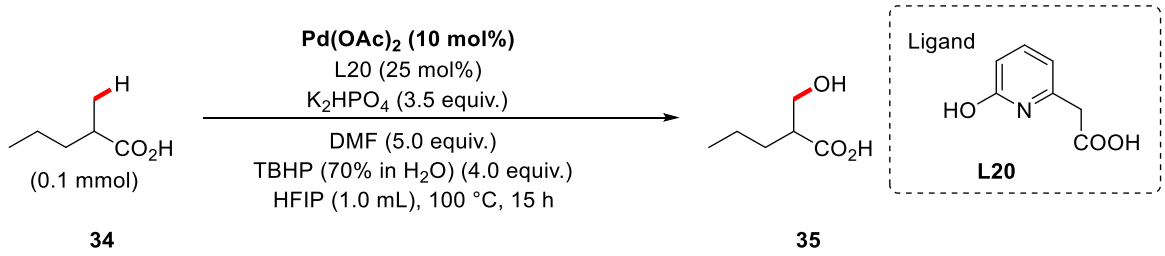

Entry	Pd-source	NMR-Yield
1 (ref. data)	$Pd(OAc)_2$	48%
2	$Pd(CF_3CO_2)_2$	42%
3	$Pd(CH_3CN)_2Cl_2$	42%
4	$PdCl_2$	43%
5	$Pd(acac)_2$	42%

Table 3.6 Screening of different Pd-sources

We investigated the effects of different palladium sources on C–H functionalization reactions. Among the catalysts tested, $Pd(OAc)_2$ demonstrated the highest efficiency, resulting in a product yield of 48%. In comparison, other palladium sources (**entries 2-5**) yielded similar results in the range of 42-43%, which were noticeably lower.

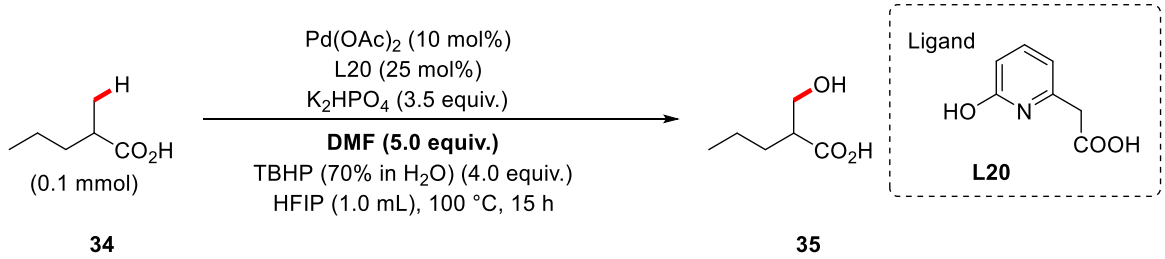

Entry	Additive	NMR Yield
1	No additive	37%
2 (ref. data)	DMF	48%
3	DMA	35%
4	CH_3CN	32%
5	DMPU	41%

Table 3.7 Re-screening of additives

In new conditions, we re-evaluated the use of additives. The yield significantly decreased in the absence of any additives. Replacing the additive with DMA was detrimental to the reaction, and using acetonitrile did not improve the yield. Another amide additive, DMPU, was tested and showed better performance compared to DMA and acetonitrile, but still resulted in a lower yield compared to DMF. Therefore, we continued to use DMF as the additive for optimizing reaction conditions.

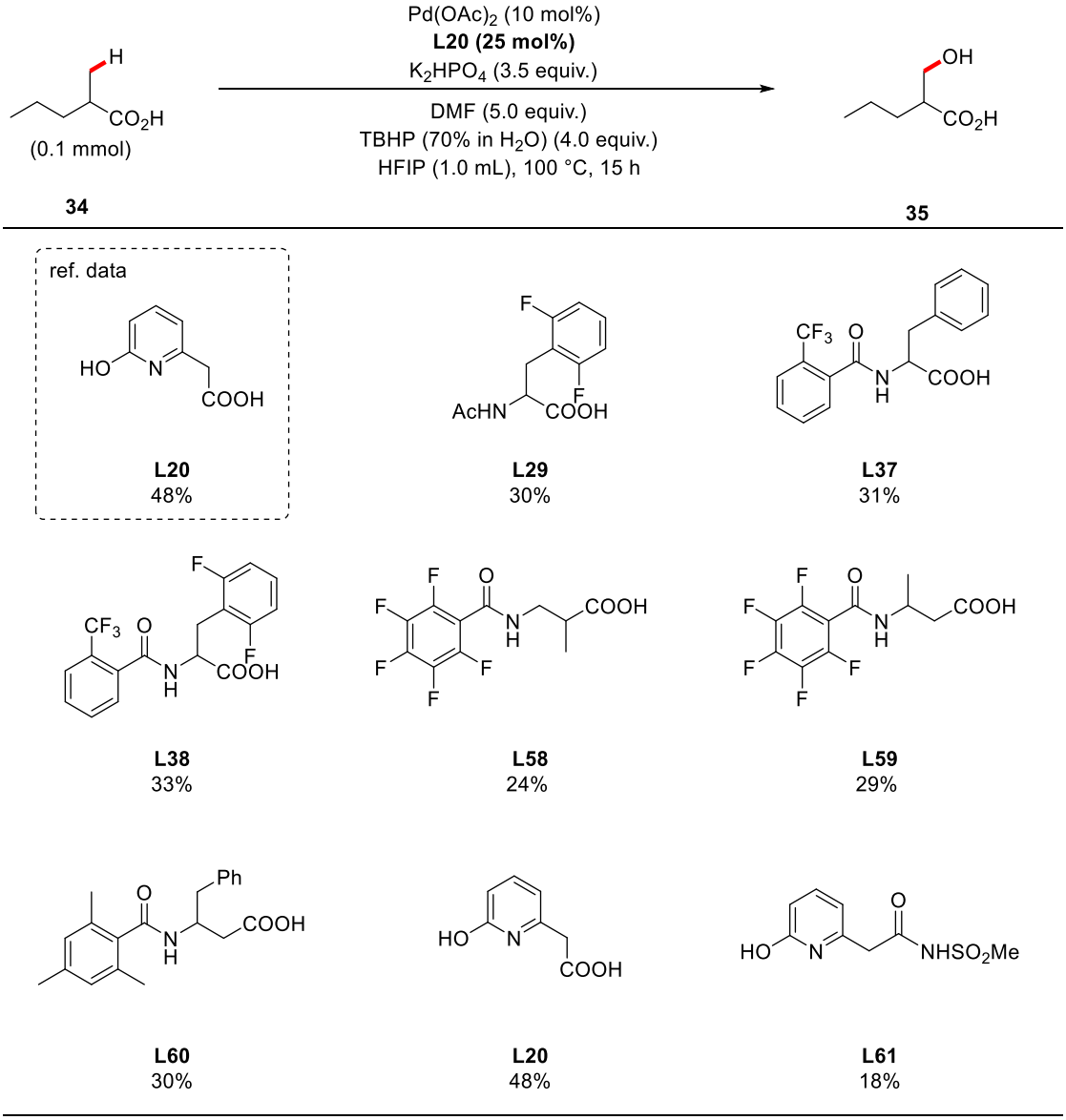

Scheme 3.9 Re-screening of ligands under the new optimized conditions. These experiments were carried out together with Sourjya Mal.

Under the new conditions, we also re-evaluated the ligands. The ligand **L29** that previously gave a yield of 30% under the earlier conditions now still provided a yield of 30%. Interestingly, ligands (**L37, L38**) that were initially less effective than **L29** showed improved yield under the new conditions. Several new β-amino acid derivative ligands (**L58, L60**) were also tested, but their yields ranged between 24% and 30%. Additionally, we designed new ligand (**L61**) by replacing the carboxyl group in **L20** with a protected amide group; however, the new ligand did not provide improved result.

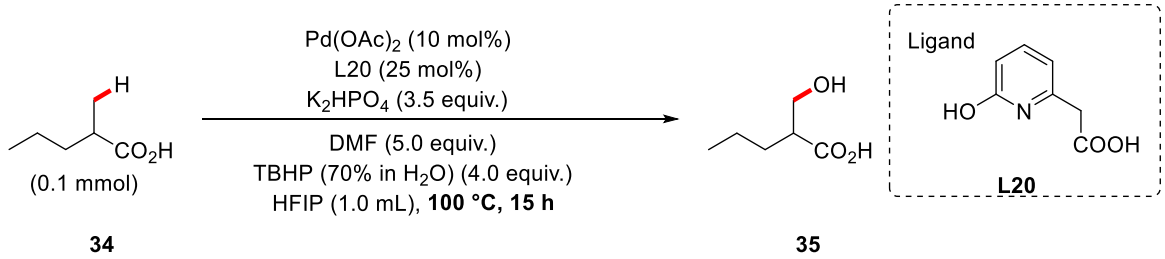

Entry	Temperature	Reaction time	NMR-Yield
1	T = 80 °C	24 h	45%
2		48 h	44%
3		72 h	43%
4	T = 90°C	24 h	41%
5		48 h	45%
6		72 h	46%
7 (ref. data)	T = 100 °C	15 h	48%
8		48 h	46%
9	T = 110 °C	15 h	43%
10		48 h	43%
11	T = 120 °C	15 h	40%
12		48 h	38%

Table 3.8 Temperature and time screening

We also examined the effects of reaction time and temperature on the yield (**Table 3.8**). At 80 °C, the yield slightly decreased as the reaction time increased. At 90 °C, however, the yield gradually increased with longer reaction times. At 100 °C and above, the yield was largely unaffected by reaction time. Based on these results, we selected 100 °C and a reaction time of 15 hours as the optimal conditions.

3.4 Substrate Scope

3.4.1 Scope of the β-C(sp^3)–H Hydroxylation of Aliphatic Carboxylic Acids

Using the optimized conditions, we initially evaluated the performance of various α-non-quaternary carboxylic acids (**Scheme 3.10**). Due to the high polarity of hydroxy acids, we encountered significant difficulties during separation. To address this, the reaction products were converted to the corresponding β–Hydroxy benzyl esters for isolation. Prior to esterification, the hydroxylated mixture required only simple treatment without separation. The excess benzyl alcohol and sufficient reaction time in the esterification process ensured a high conversion rate of the product in the crude mixture.

Under the optimal conditions, the model substrate (**39**) afforded the desired product in a 46% isolated yield. Similar carboxylic acids with different alkyl chain lengths also participated smoothly in the reaction, providing the desired products (**36 – 40**) in good yields. Substrates with branched or substituted structures were also well tolerated (**41 – 43**). Further, alkyl substituents containing halogen atoms also reacted successfully, with the halogen atoms remaining unaffected (**44 – 45, 48**). Alkoxy ethers and phenoxy ethers were also tolerated as functional groups (**46 – 47**). Subsequently, several carboxylic acids with aryl substituents were tested (**49– 54**), and obtained in good yield. Notably, a series of carboxylic acids with competing benzylic C–H bonds at the β-position also afforded the desired products (**50 – 54**) in good yields. These results clearly demonstrate the strong functional group tolerance of this methodology.

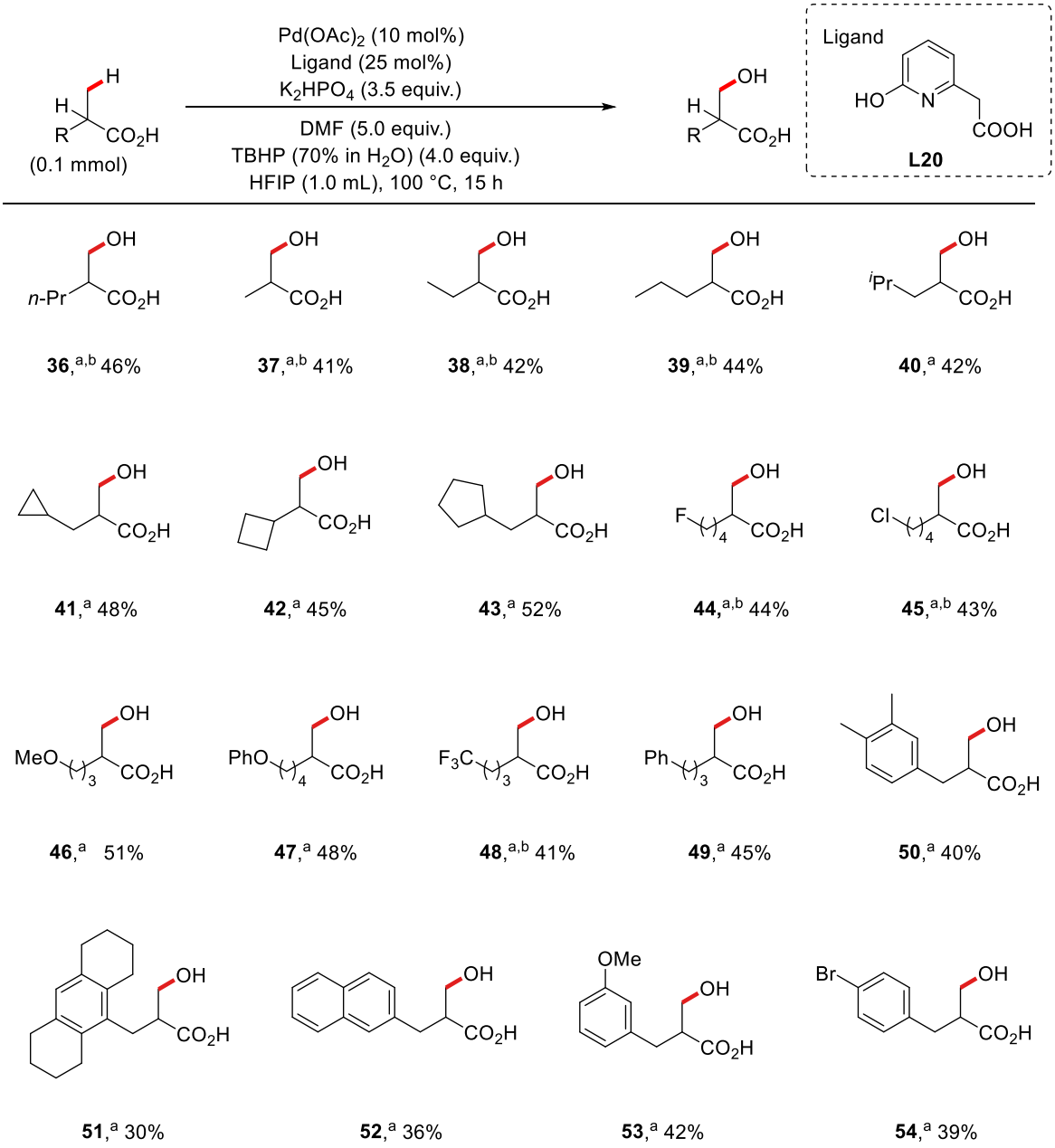

Scheme 3.10 Scope studies of the in α-non-quaternary carboxylic acids substrates. Reactions were conducted on a 0.2 mmol scale. [a] Isolated after conversion to benzyl ester. [b] These products were isolated by Sourjya Mal.

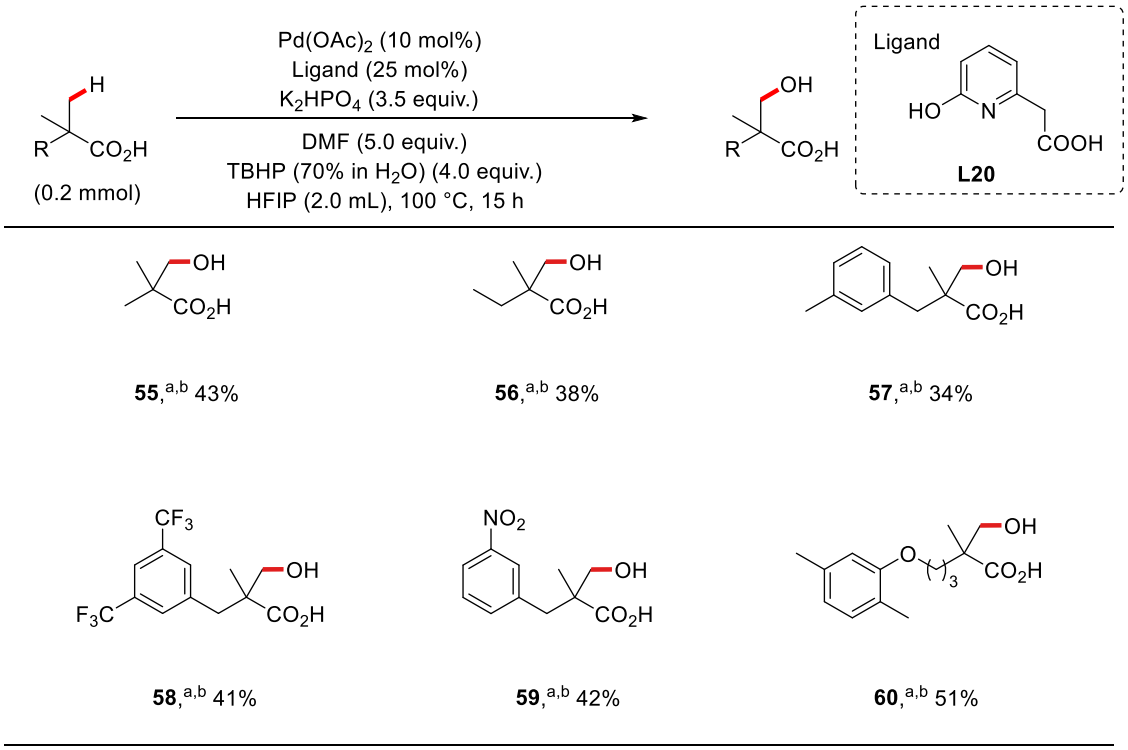

Scheme 3.11 Scope studies of the in α-quaternary carboxylic acids substrates. Reactions were conducted on a 0.2 mmol scale. [a] Isolated after conversion to benzyl ester. [b] These products were isolated by Sourjya Mal.

We also tested several α-quaternary carboxylic acids, which were similarly isolated as benzyl esters. Simple pivalic acid produced the target product (**55**) in a good yield of 43%. Substrates with longer branched chains also underwent the reaction smoothly (**56**). Even in the presence of the Thorpe-Ingold effect, competitive reactions at the β-benzylic C–H bond in the same position were overcome, and these phenylpropionic acid derivatives were obtained in good yields (**57, 58 & 59**). Finally, we tested gemfibrozil, a lipid-regulating drug, and were pleased to observe that the reaction successfully modified the drug, affording the β–Hydroxylated product (**60**).

These findings indicate that the reaction is highly robust across a wide range of substrates, with yields showing only slight variation depending on the substituents. Moreover, its excellent compatibility with diverse functional groups and structural variations underscores the significant potential of this methodology.

3.5 Mechanistic Studies

After developing the conditions for direct β-C–H activation and hydroxylation of alkyl carboxylic acids, and investigating the substrate scope, we considered exploring the mechanistic pathway of this reaction. In fact, the reaction of β-C–H activation followed by lactone formation has been confirmed, although the authors did not observe hydroxylated products under their conditions. It is possible that the four-membered ring lactone could undergo hydrolysis under certain conditions, particularly at high temperatures, which suggests that in our developed reaction, the formation of a lactone intermediate could occur first, followed by hydrolysis to the hydroxylated product (**Pathway B**). On the other hand, direct formation of the hydroxylated product from reductive elimination of a high-valent palladium intermediate (**Pathway A**) is also possible. Therefore, we conducted several control experiments to determine which of these pathways was operative.

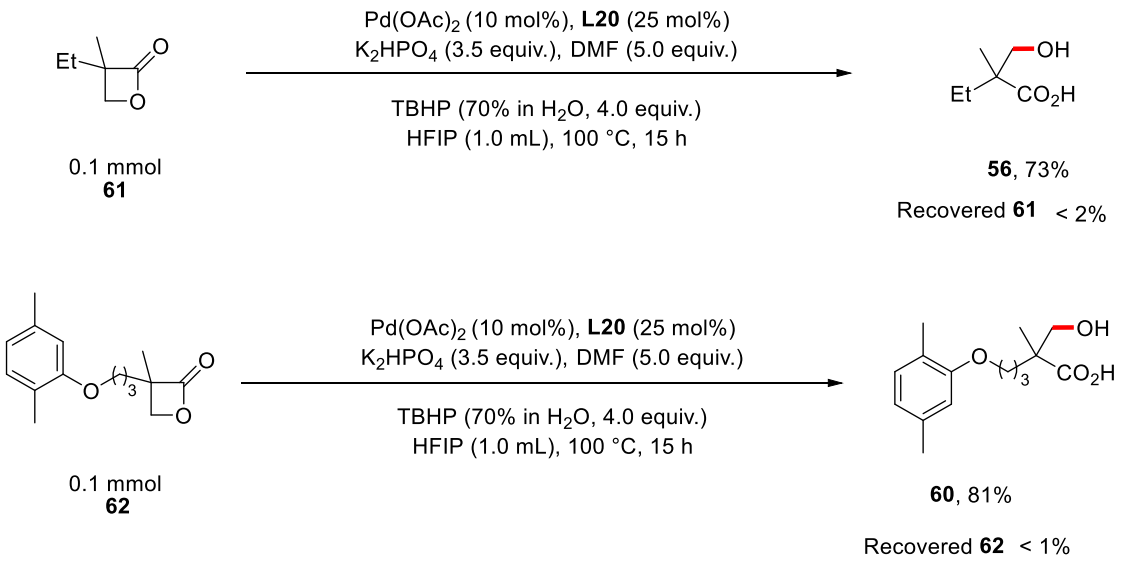

Scheme 3.12 control experiments of decomposing of **61** & **62** in standard conditions. These experiments were carried out by Sourjya Mal.

First, we performed two control experiments (**Scheme 3.12**). When β-lactone **61** was exposed to standard conditions, it yielded **56** (73%), with nearly complete consumption of the starting material. Similar results were observed in the control experiment with lactone **62**. These observations were as expected, as it is known that base (K_2HPO_4) and H_2O can both promote such ring-opening or hydrolysis processes at elevated temperatures. (**61** and **62** were prepared following the literature procedure of Yu *et al.*[125])

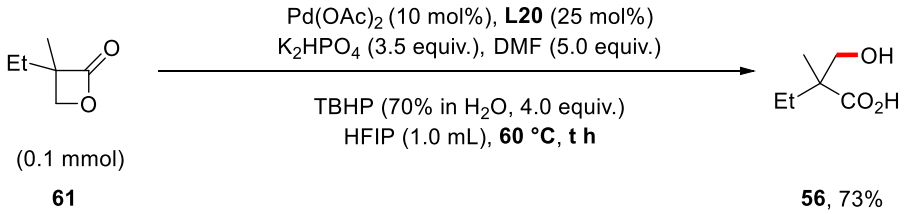

Entry	Reaction Time	NMR Yield of **56**	Recovered **61**
1	1 h	18%	81%
2	2 h	25%	68%
3	3 h	46%	42%
4	4 h	62%	26%

Table 3.9 Hourly monitoring of the decomposition of **61**. These experiments were carried out by Sourjya Mal.

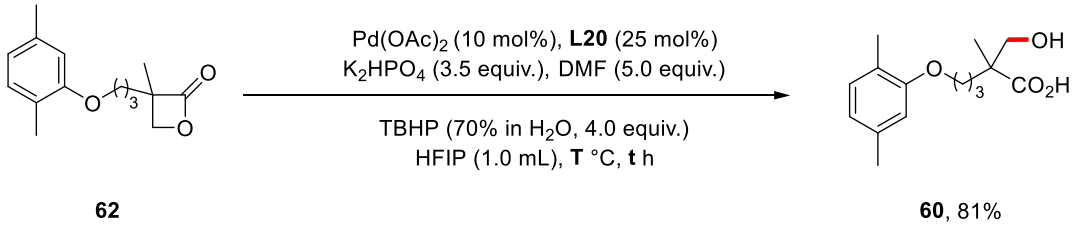

Entry	Temperature	Reaction Time	NMR Yield of **60**	Recovered **62**
1	100 °C	0.5 h	82%	0
2	100 °C	1 h	81%	0
3	80 °C	1 h	82%	0
4	60 °C	1 h	42%	56%
5	60 °C	2 h	62%	33%
6	60 °C	4 h	80%	< 8%

Table 3.10 Hourly monitoring of the decomposition of **62**. These experiments were carried out by Sourjya Mal.

Therefore, we needed to establish milder reaction conditions under which the β-lactone would remain at least partially stable (**Table 3.9 & 3.10**). The decomposition of **61** at 60 °C showed

that over 80% of **61** could still be detected after 1 hour, and even after 4 hours, 26% of the starting material remained, with most of the rest converted into product **56** (62%, **Table 3.9**). For **62**, however, the decomposition rate was much faster; after just one hour at 60 °C, nearly half of the lactone had decomposed to the hydroxy acid, and after four hours, less than 8% of the starting material remained.

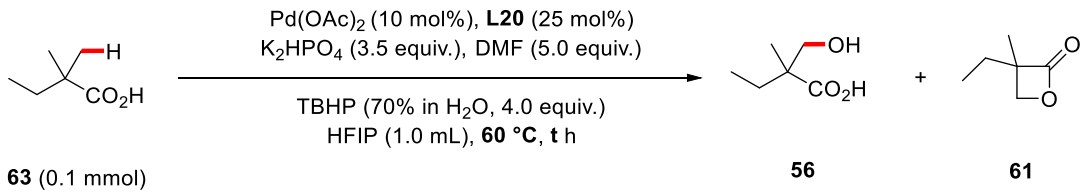

Entry	Reaction Time	NMR Yield of **56**	NMR Yield of **61**
1	1 h	30%	< 2%
2	2 h	42%	< 2%
3	3 h	45%	< 1%
4	4 h	46%	< 1%

Tsble 3.11 Hourly monitoring of the hydroxylation reaction of **63**. These experiments were carried out by Sourjya Mal.

When we applied these modified reaction conditions to substrate 1u, we observed 30% of **56** after 1 hour, with only trace amounts of β-lactone **61**(< 2%) detected. This clearly suggests that **56** could not have formed via **61** as an intermediate, as the relative rates of product formation and **61** decompositions would require significant accumulation of the β-lactone intermediate, allowing us to rule out Pathway B and conclude that the hydroxy acid product was formed directly (Pathway A) rather than through a β-lactone intermediate.

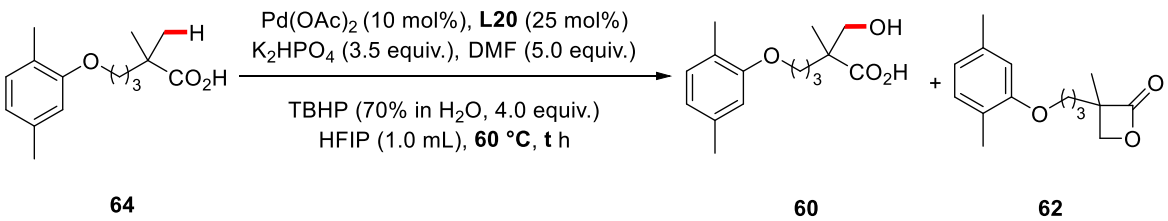

Entry	Reaction Time	NMR Yield of **60**	NMR Yield of **62**
1	1 h	18%	59%
2	2 h	32%	42%
3	3 h	41%	30%
4	4 h	51%	18%

Table 3.12 Hourly monitoring of the hydroxylation reaction of **64**. These experiments were carried out by Sourjya Mal.

Although **62** remained only partially stable at 60 °C, we still studied the hydroxylation of **64** under these conditions. Interestingly, after 1 hour, significant accumulation of **62** was observed, which gradually decomposed to **60** over time (**Table 3.12**), indicating that **64** followed Pathway B. It is worth noting that **64** has a very strong tendency to form β-lactone, as previously reported by the Yu lab, where lactone formation was achieved via C–O reductive elimination from a high-valent Pd^{IV} species, and further supported by our recent fluorination studies, which found that **64** provided **62** as the major product (**Table 3.12**). This is likely due to interactions between the ether moiety (–OAr) and palladium, which favor triggering C–O reductive elimination. Therefore, gemfibrozil (**64**), due to its unique structure compared to other aliphatic carboxylic acids, is the only substrate that follows Pathway B. In contrast, **63**, representative of general aliphatic acids, demonstrated that most acids reported in this study follow **Pathway A**.

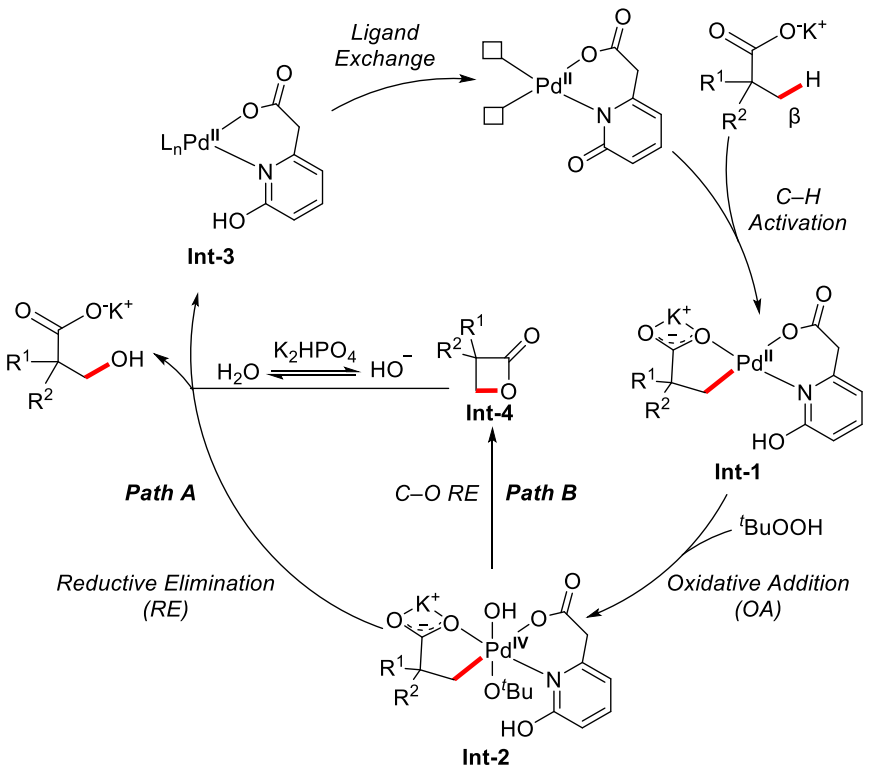

Scheme 3.13 Possible mechanism of the hydroxylation reaction

Based on literature precedent,[76d, 130] we propose that our transformation proceeds via a Pd^{II}/Pd^{IV} catalytic cycle, as shown in **Scheme 3.13**. First, coordination of the external ligand (**L20**) to $Pd(OAc)_2$ generates the active catalyst. The subsequent C–H activation step is accelerated by countercations (K^+) and the ligand, occurring via a concerted metalation-deprotonation (CMD) mechanism[130a] in which the ligand acts as an internal base to generate **Int-1**. Given that the ability of peroxides to oxidize Pd^{II} to Pd^{IV} is well established,[130b-d] **Int-1** is expected to undergo oxidative addition with TBHP to form **Int-2**. From this stage, there are two possible pathways to form the desired product: direct C–O reductive elimination (RE) [130g] or an S_N2-type reaction, both leading to the desired product (**Pathway A**). Alternatively, **Int-2** can undergo C-O RE to form β-lactone **Int-4,**[76d, 125] which then undergoes subsequent S_N2 reaction with $H_2O/HO-$ to yield the desired product.

3.6 Conclusion

In summary, we have developed a robust and effective protocol that enables the direct β-

C(sp^3)–H hydroxylation of aliphatic carboxylic acids. The use of convenient and inexpensive TBHP as an oxidant, along with the appropriate choice of reagents, was crucial in establishing this methodology. The reported synthetic method was demonstrated to be particularly effective for challenging α-non-quaternary carboxylic acids and exhibited considerable functional group tolerance, providing efficient access to a diverse range of β-hydroxy acids in a single step. Additionally, the method showed broad applicability to α-quaternary carboxylic acids and even allowed for the successful modification of complex pharmaceutical substrates such as gemfibrozil. Given the extensive applicability of β-hydroxy acids across various fields, including medicinal chemistry and materials science, we anticipate that the new compound libraries accessible through our method will be valuable for a wide range of applications. Our work highlights the potential for future developments in C–H functionalization, paving the way for new strategies to synthesize complex molecules with high efficiency and selectivity.

4 The Direct Pd-Catalyzed γ-C(sp^3)–H Lactonization of Aliphatic Carboxylic Acids

4.1 Background

γ-Lactones are five-membered heterocyclic compounds with an ester group structure, drawing significant interest in drug development.[131] Several γ-lactone-containing drugs have been FDA-approved for clinical use, including diuretics, anticancer agents, contraceptives, cardiovascular treatments, and glaucoma medications (**Scheme 4.1**).[132] Additionally, γ-lactone is found in various experimental bioactive compounds and synthetic intermediates, and many natural products with this structural feature exhibit diverse biological activities.[133] In organic synthesis, γ-lactones serve as versatile intermediates and are valuable scaffolds, easily converted into hydroxy acids, hydroxy amides, and other biologically active fragments through hydrolysis, substitution, and other transformations.[134]

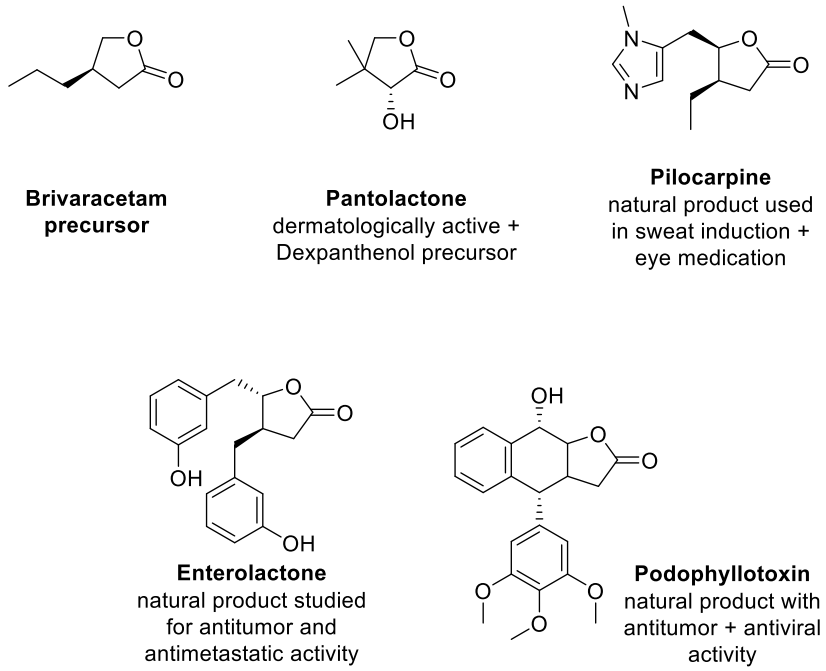

Scheme 4.1 Selected examples of γ-lactones in drug and natural products

From a retrosynthetic analysis perspective, γ-lactone synthesis offers a wide range of methods (**Scheme 4.2**).[135] In general, these methods can be simply classified into intermolecular and

intramolecular reactions. Although the position of the newly formed bond varies in these reactions during the construction of lactones, observations indicate that they all require pre-functionalized or even highly functionalized starting materials. This often leads to tedious synthetic steps and low atom economy,[133] especially in the synthesis of complex pharmaceutical compounds. As lactone-containing compounds continue to be discovered in natural products and synthetic drugs, scientists are dedicated to advancing more efficient synthetic strategies.[133, 136]

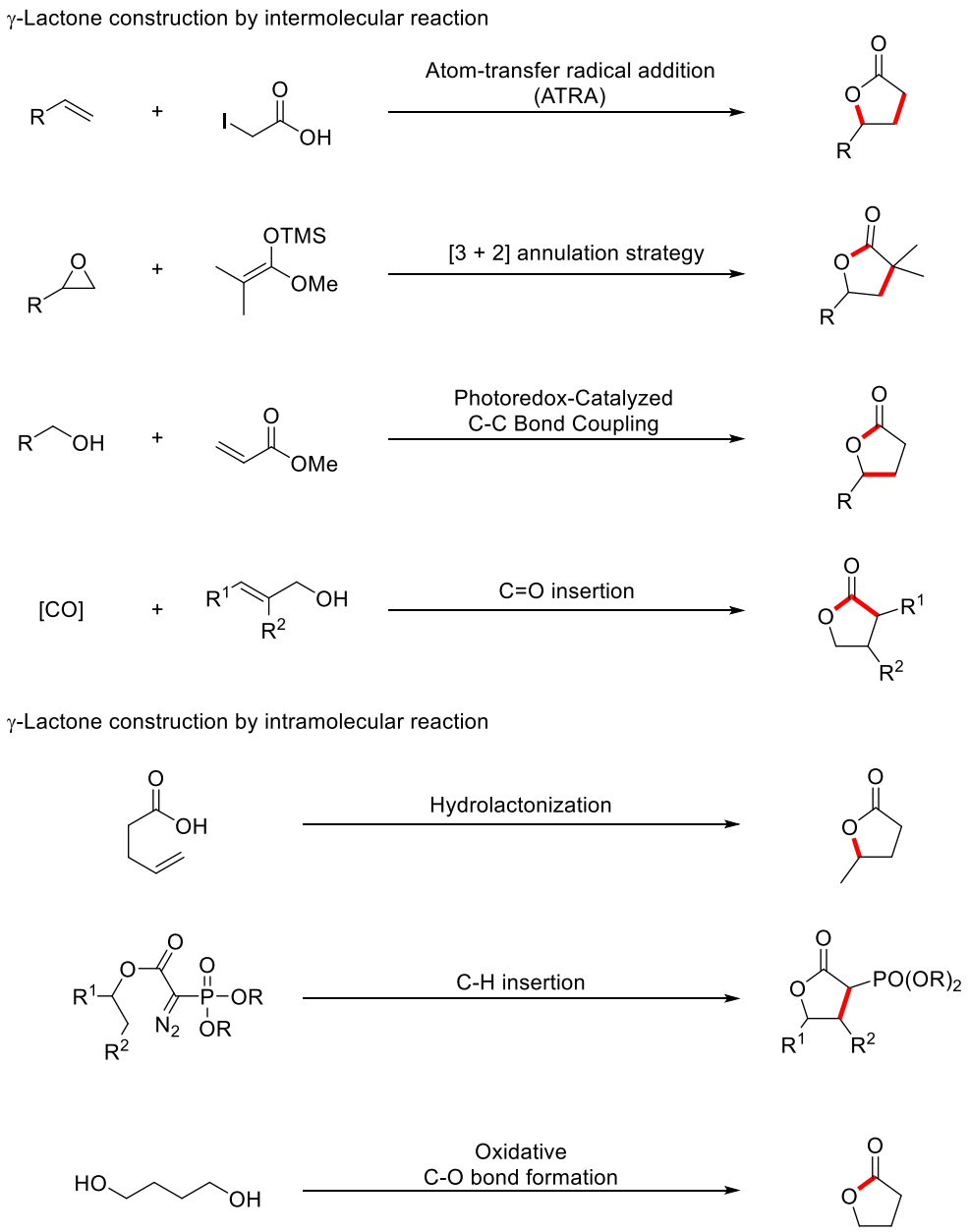

Scheme 4.2 Synthetic methodologies for the synthesis of γ-lactones based on retrosynthetic analysis

Carboxylic acids, with their structural diversity, availability, and accessibility, serve as versatile starting materials for organic synthesis. This makes the direct conversion of carboxylic acids into γ-lactones an appealing alternative to traditional methods. Such a transformation offers an efficient route for rapidly building molecular complexity and expanding compound libraries, particularly valuable for drug discovery and screening. In recent years, various transition metal-catalyzed C–H functionalization strategies have been developed to facilitate lactone synthesis:

a) **Lactonization via C–H homolysis mediated by 3d-metals[137] or enzymes[138] through hydrogen atom transfer (HAT) (Scheme 4.3A):** This approach involves the homolytic cleavage of a C–H bond to generate an alkyl radical intermediate. The intermediate subsequently forms a carbon-oxygen bond under the catalytic influence of a metal or enzyme. The reactivity and regioselectivity of this method are heavily influenced by the bond dissociation energy (BDE) of the C–H bond, with a strong preference for secondary and tertiary C–H bonds due to the higher stability of the resulting radical.[139]

b) **Activation of methylene C–H bonds followed by β-hydride elimination to form an unsaturated carboxylic acid intermediate[140] (Scheme 4.3B):** In this strategy, the activation of methylene C–H bonds leads to β-hydride elimination, producing an unsaturated carboxylic acid intermediate. Cyclization then occurs via addition of the carboxylic acid group to the newly formed double bond, yielding the lactone product. This approach inherently limits selectivity to methylene groups, with the product structure being determined by the position of the double bond formed during elimination.

c) **Formation of metal-cyclized intermediates through activation of benzylic[141] or allylic C–H bonds[89] (Scheme 4.3C):** Here, lactonization proceeds through a mechanism analogous to nucleophilic substitution (SN-type reactions).[142] This method is highly substrate-specific, favoring benzylic and allylic C–H bonds due to their increased acidity and higher reactivity compared to non-activated C–H bonds.

d) **Using substrates with directing[143] or nucleophilic functional groups[124, 144] (Scheme 4.3D)**: This approach involves substrates with added directing groups or internal nucleophilic functional groups to guide the catalytic cycle. While this

enhances selectivity, it limits the substrate scope and increases the number of synthetic steps required, making the process less efficient.

A: Oxidation via Hyrogen Atom Transfer (HAT)

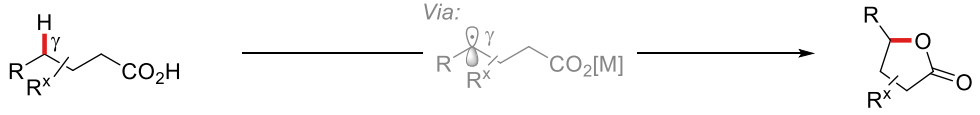

- Known with Mn-, Fe-, Cu-catalysis
- Reactivity trend: C^{tert}–H > C^{sec}–H > C^{prim}–H

B: Lactone Synthesis via Desaturation

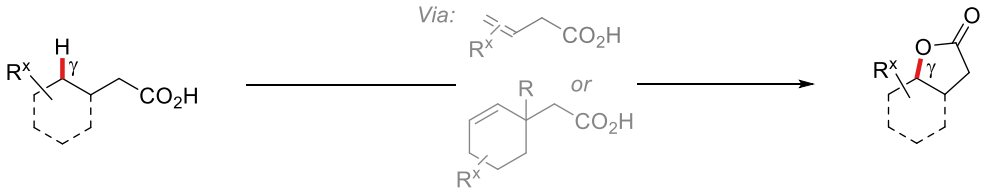

- Desaturation-controlled regioselectivity
- Scope limited by structural requirements of desaturation

C: Lactone Synthesis via Activated C–H Bonds

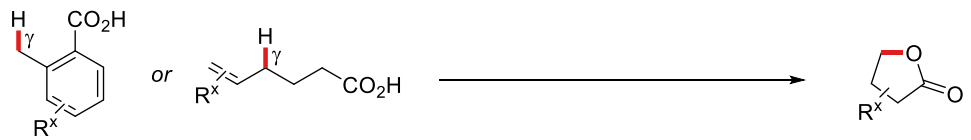

- Limited by need for activated substrates
- S_N-like displacement of Pd proposed for C-O bond-formation

D: Lactone Synthesis via Using Substrates with Directing or Nucleophilic Functional Groups

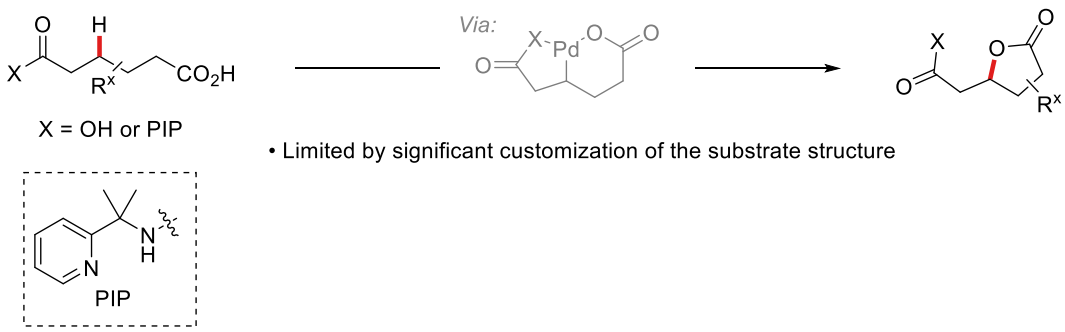

- Limited by significant customization of the substrate structure

Scheme 4.3 Current methods reported for synthesizing γ-lactones from carboxylic acids via C–H cleavage strategies.

4.2 Project Goals

Despite these advancements, a significant challenge remains: developing a broadly applicable method for directly activating unreactive γ-C(sp³)–H bonds, followed by C–O reductive elimination (C–O RE) to form lactones. The C–O RE step, a fundamental yet underexplored process in organometallic chemistry,[130g, 145] has only been successfully coupled with C–H activation in a limited number of cases. To address this gap, we aim to establish a strategy leveraging the weak directing ability of carboxylate groups to activate terminal γ-C(sp³)–H bonds in simple aliphatic acids, followed by C–O reductive elimination to yield the target lactones (**Scheme 4.4**).

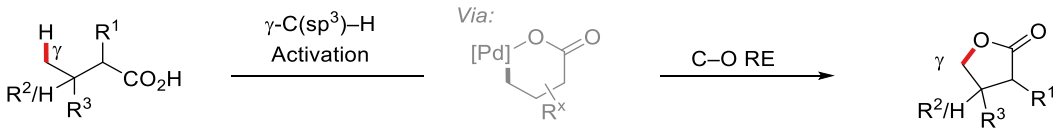

Scheme 4.4 Project Goals of: lactone synthesis via C–O reductive elimination (RE)

Notably, while palladium-catalyzed activation of proximal C(sp³)–H bonds in aliphatic chains is well-established using free carboxylic acids and amines as directing groups, the activation of distal C(sp³)–H bonds remain a significant challenge. Beyond the inherent difficulties of C–H activation, the stability of the intermediate palladacyclic ring formed after γ-C(sp³)–H activation is critical for the success of the subsequent C–O RE step. In particular, six-membered palladacycles formed during γ-C(sp³)–H activation of non-quaternary carboxylic acids often meet competing β–Hydride elimination,[146] thereby undermining the C–O RE process.

Building on our expertise with high-valent palladium chemistry in C–heteroatom bond formation and insights from recent developments,[76e, 94] we propose two key strategies to overcome these challenges. First, selecting an appropriate external ligand[126] will be pivotal for designing a catalyst that facilitates both C–H activation and C–O RE[76c, 76d] while suppressing side reactions. Second, addressing the high activation barrier for the C–O RE step will require the formation of a Pd^{IV} intermediate, from which reductive elimination becomes energetically feasible. The choice of oxidant will therefore play a critical role in enabling this transformation.

4.3 Optimization of the Reaction Conditions

The screening process was divided into two parts, with reaction conditions evaluated separately for β-quaternary carboxylic acids and β-non-quaternary carboxylic acids.

4.3.1 Optimization for β-Quaternary Carboxylic Acids

Building on Yu's recent work[125] and our findings in **Chapter 3**, we began our study using 3,3-dimethylbutanoic acid as a model substrate, selecting $Pd(OAc)_2$ as the core metal catalyst, K_2HPO_4 as the base, and TBHP as the oxidant, with HFIP as the solvent. To address the challenges associated with C–H activation, we initially conducted a ligand screening.

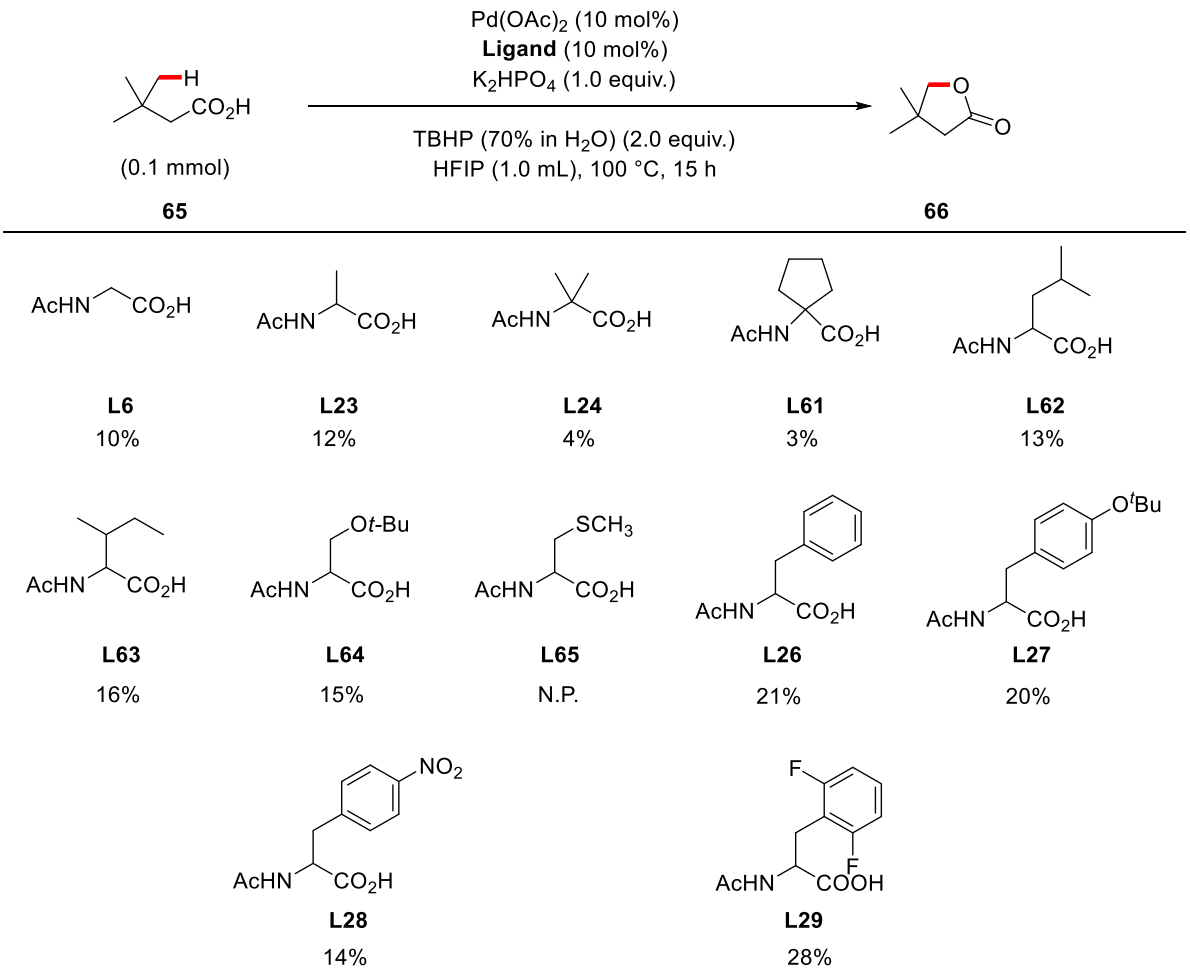

Scheme 4.5 Initial optimization of the ligands. These experiments were carried out together with Sourjya Mal.

We first tested mono-protected α-amino acids as ligands, finding that N-acetylglycine, the basic structure, as ligand produced 10% of the target product in the NMR spectrum. Encouraged by this result, we explored additional α-amino acid-derived ligands. Testing ligands with various substitutions on the backbone revealed that excessive substitution did not improve the yield (**L24**), and minor modifications yielded only slight improvements. Further modification with bulkier substituents on the backbone led to **L29**, which provided the best results.

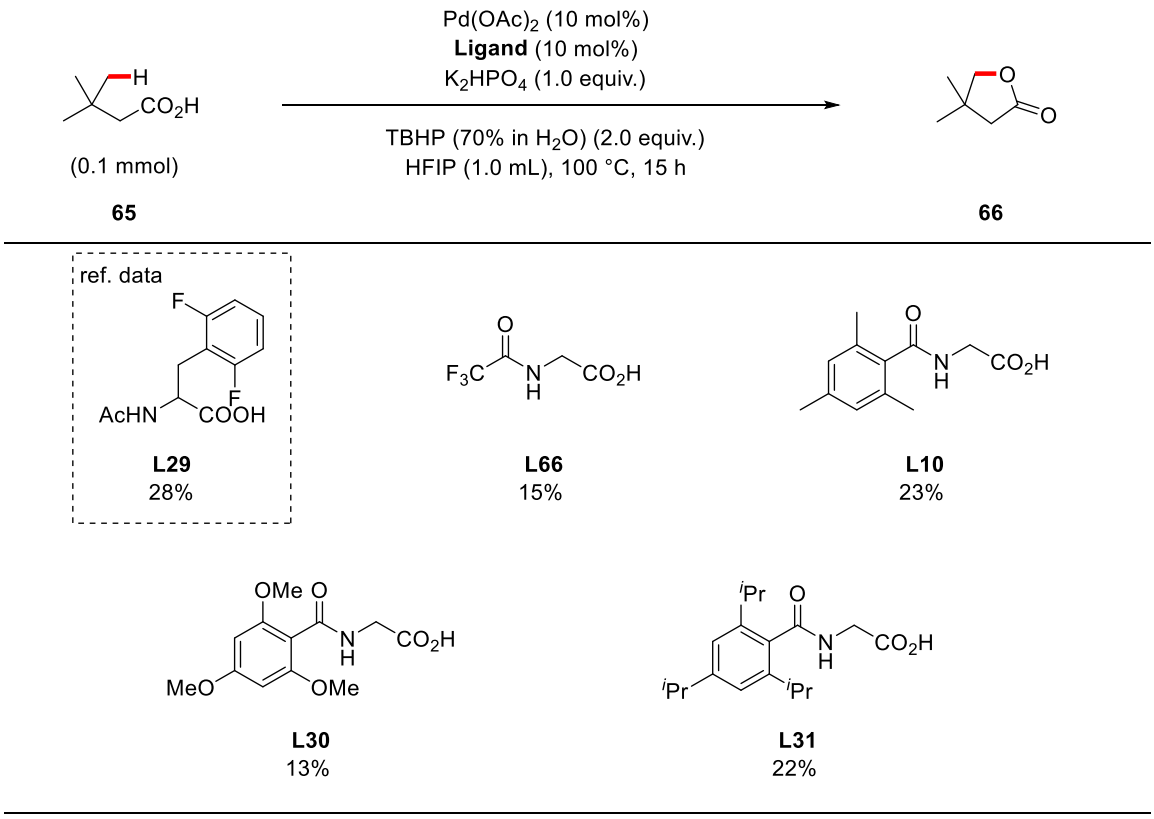

Scheme 4.6 Explored ligands with various N-protecting groups. These experiments were carried out together with Sourjya Mal.

We then explored ligands with various N-protecting groups. Results showed that, compared to basic N-acetylglycine, using a strongly electron-withdrawing trifluoroacetyl group as the nitrogen protecting group (**L66**) provided a modest increase in yield. Further experimentation with benzoyl-based protecting groups revealed that glycine protected with mesityl (trimethylphenyl) benzoyl[126] provided a favorable yield (**L10**).

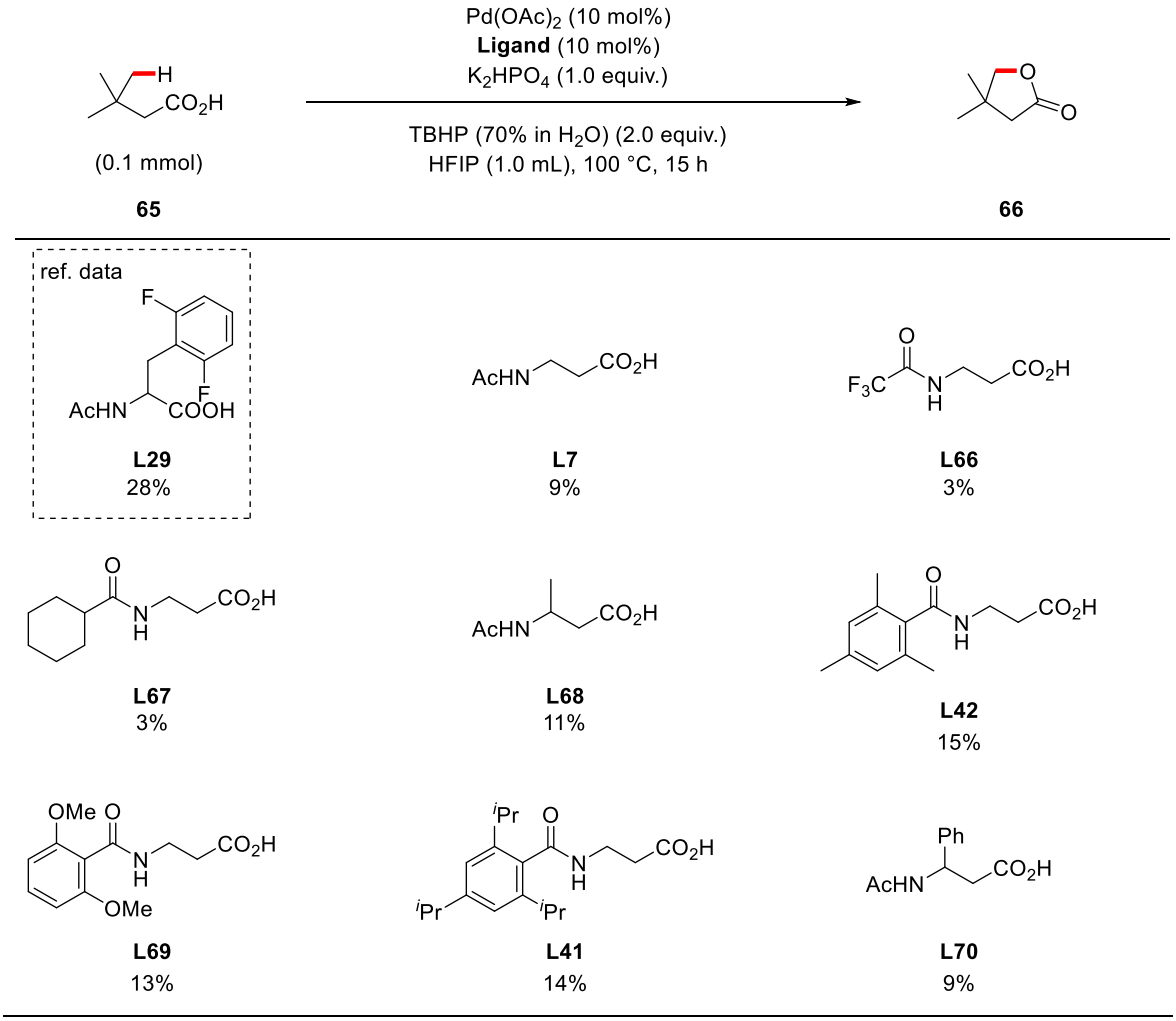

Scheme 4.7 Optimization with β-amino acid derivatives. These experiments were carried out together with Sourjya Mal.

Since further optimization with glycine-derived ligands did not yield better results, we broadened the scope of ligand screening, beginning with β-amino acid derivatives. Compared to the five-membered Pd cycle formed by α-amino acid ligands with the Pd center, the slightly less stable six-membered Pd cycle from β-amino acids may more readily facilitate the dissociation of C–H activation intermediates and subsequent product formation. As shown in the table, basic N-acetyl-β-amino acid provided results similar to those of N-acetylglycine. However, attempts with different protecting groups showed that these β-amino acid ligands generally performed worse than their α-amino acid counterparts.

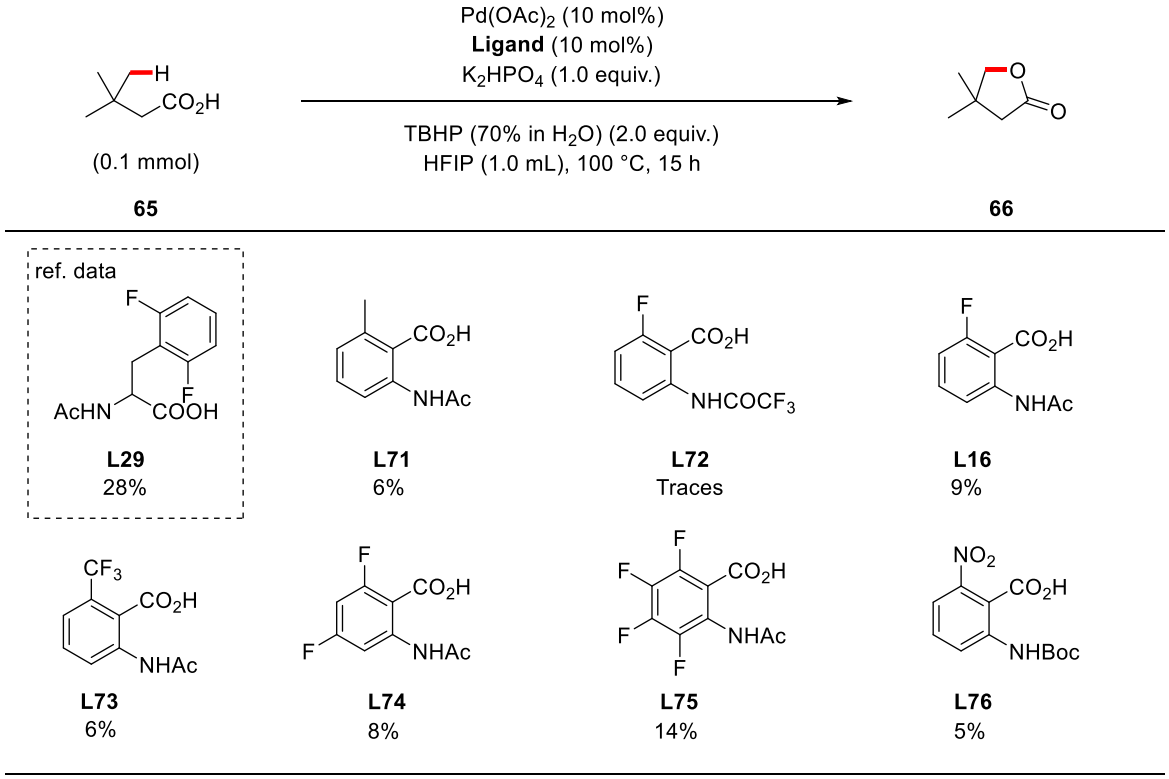

Scheme 4.8 Further optimization with β-amino acid derivatives. These experiments were carried out together with Sourjya Mal.

We then tested *o*-aminobenzoic acid ligands, as this type of ligand had previously shown promising results in γ-position C–H activation.[86] However, after screening various *o*-aminobenzoic acid derivatives, we were unable to identify a ligand that outperformed N-acetylglycine.

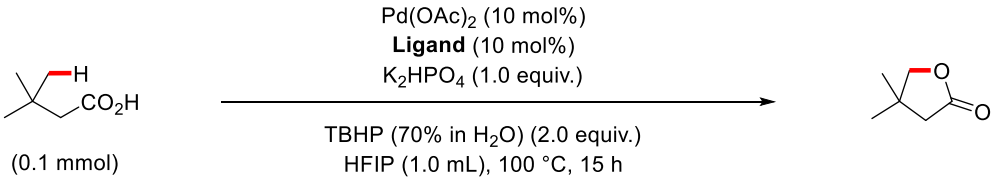

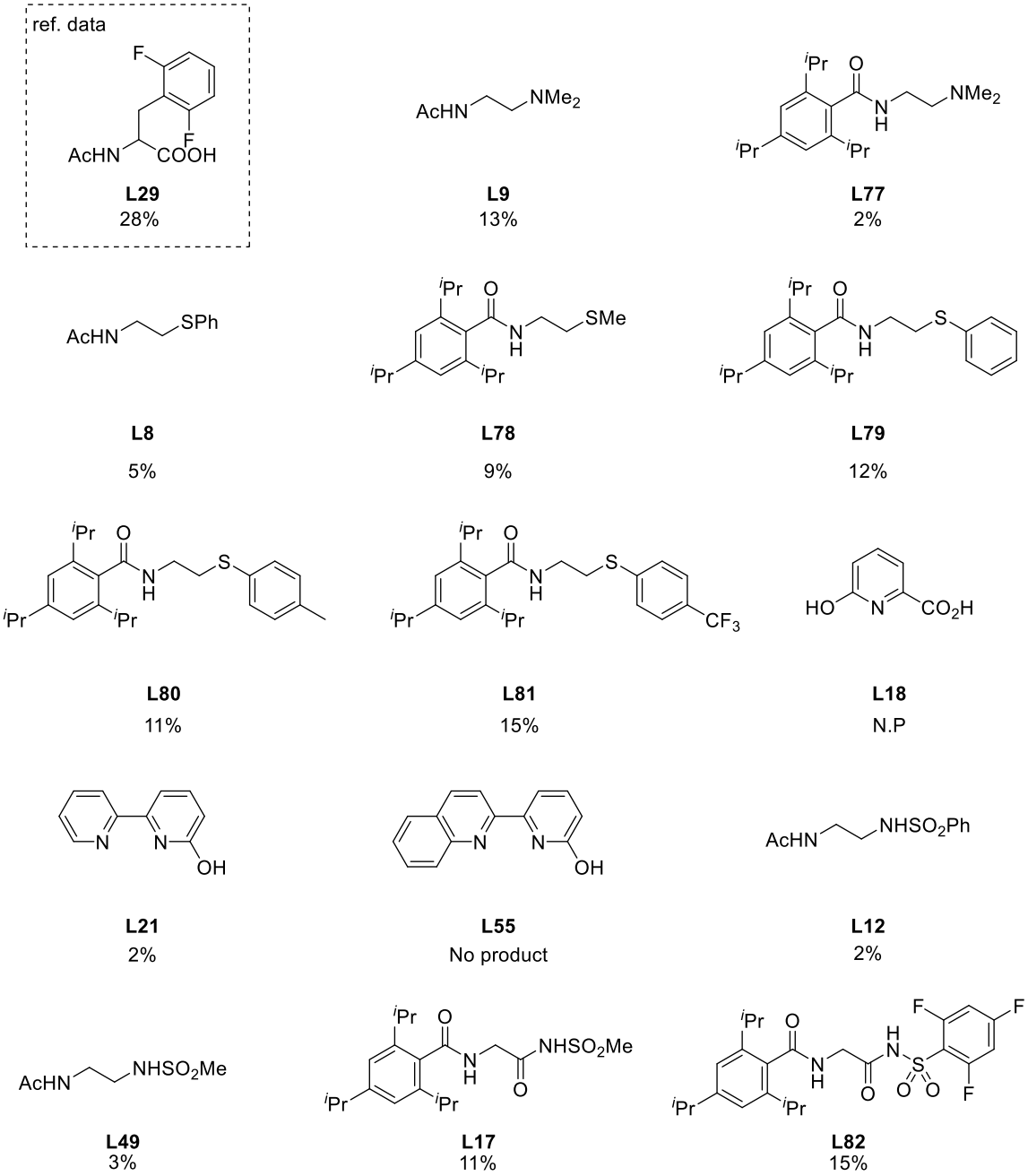

Scheme 4.9 Optimization with ligands of different structures. These experiments were carried out together with Sourjya Mal.

We further tested various ligands with different structures, including ethylenediamine-derived ligands known for their effectiveness in C(sp^3)–H deuteration,[126] thioether ligands capable of γ-position C(sp^3)–H carbonylation of carboxylic acids,[91] N-acylsulfonamide-based N,N-bidentate ligands developed for arene deuteration,[147] and several pyridone ligands.[92, 148] However, the yields achieved with these ligands were significantly lower than those obtained with **L29**. Consequently, we paused further ligand testing and proceeded to co-solvent screening.

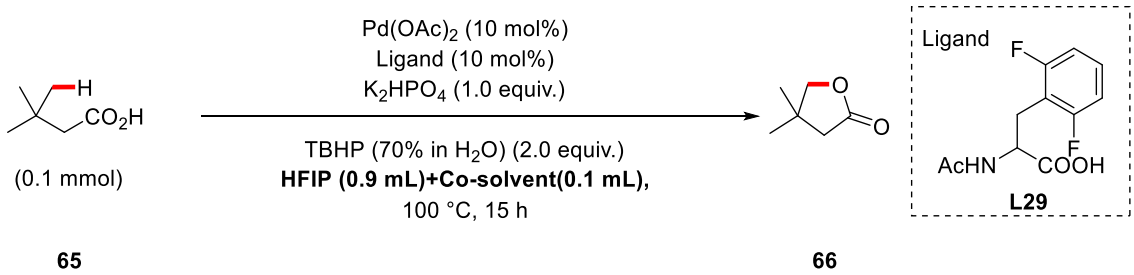

Entry	Co-solvent	NMR Yield
1 (ref. data)	w/o	28%
2	CH_3OH	10%
3	CF_3CH_3OH	21%
4	*t*-AmylOH	18%
5	CH_3CN	Trace
6	$C_2H_4Cl_2$	21%
7	CH_2Cl_2	20%
8	DMF	Trace
9	DMSO	Trace
10	1,4-Dioxane	Trace
11	Toluene	23%
12	THF	20%
13	PhCl	24%

Table 4.1 Screening of co-solvents.

Based on current research, HFIP is typically the preferred solvent for Pd-catalyzed C(sp^3)–H activation; however, some studies have reported improved results with mixed solvents.[92-93, 106, 149] To explore this, we tested several solvent combinations. As shown in the table, mixed alcohol-based solvents (**Entries 2 - 4**) consistently facilitated product formation, whereas acetonitrile (**Entry 5**), even at a volume of 0.1 mL, did not yield favorable results. Mixed halogenated alkanes (**Entry 6 & 7**) showed promise but still produced slightly lower yields than HFIP alone. Combinations with highly polar solvents (**Entry 8 & 9**) performed poorly. While adding 0.1 mL of THF (**Entry 12**) yielded a 20% product, the similar ether solvent 1,4-dioxane (**Entry 10**) surprisingly produced only trace amounts, as observed by NMR. Finally, mixing HFIP with toluene (**Entry 11**) or chlorobenzene (**Entry 13**) didn't influence much compare to using HFIP alone. We therefore proceeded with HFIP as the sole solvent to examine the effect of various oxidants on the reaction.

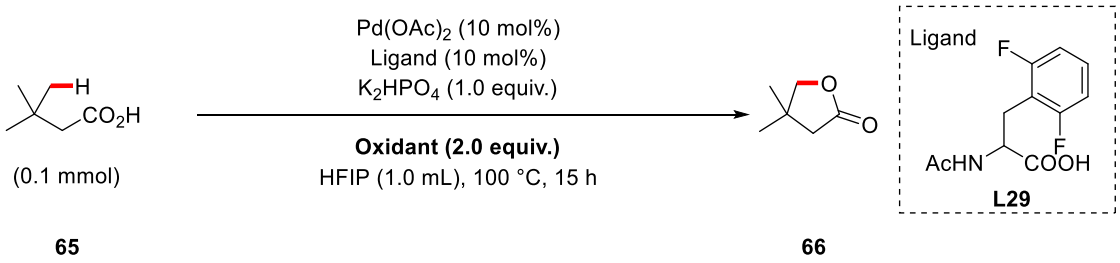

Entry	Oxidant	NMR Yield
1 (ref. data)	TBHP (70% in water)	28%
2	w/o	< 3%
3	TBHP (ca 5.5 M in decane)	27%
4	Cumyl hydroperoxide	6%
5	*m*CPBA	No product
6	AcOO^{t}Bu	No product
7	BzOO^{t}Bu	No product
8	BzOOBz	No product
9	$K_2S_2O_8$	5%
10	$Na_2CO_3 \cdot 1.5H_2O_2$	28%
11	Urea peroxide	8%
12	H_2O_2(30% (w/w) in water)	6%

Table 4.2 Screening of various oxidants

Initially, when no oxidant was used (**Entry 2**), only trace product (<3%) was observed by NMR. These traces may result from oxidation of the Pd^{II} intermediate by atmospheric oxygen, followed by reductive elimination from a high-valent Pd intermediate.[141c, 150] Next, we tested TBHP in decane (**Entry 3**) as an oxidant and found that the solvent carrier had little effect on yield, indicating that the reaction shows some tolerance to water. Other peroxides performed poorly, with no detectable product observed in NMR (**Entries 5 - 8**). Testing the inorganic oxidant $K_2S_2O_8$ (**Entry 9**) yielded only 5% product. However, sodium percarbonate provided

a surprising result, achieving yields comparable to TBHP. Sodium percarbonate (**Entry 10**), an adduct of sodium carbonate and hydrogen peroxide, is a colorless powder that dissolves in water to release carbonate and hydrogen peroxide, offering a highly cost-effective oxidant with basic properties.[151] We then tested other hydrogen peroxide adducts (**Entry 11**), as well as hydrogen peroxide solution (**Entry 12**) itself, but these did not produce improved results.

In light of the newly identified oxidant $Na_2CO_3 \cdot 1.5H_2O_2$ performing equally well to TBHP, we decided to compare the effectiveness of the two oxidants across different ligand conditions.

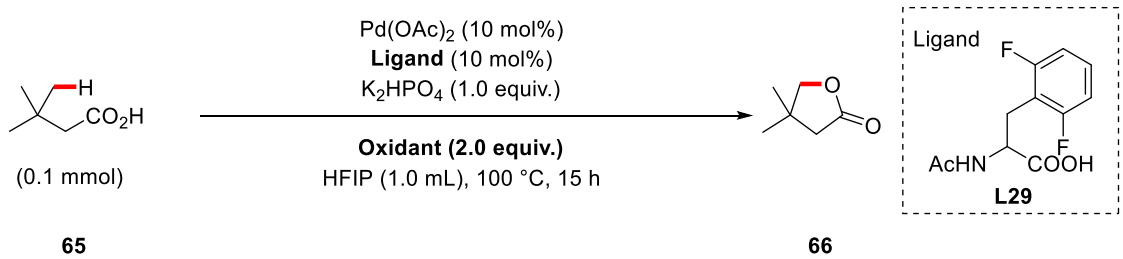

Entry	Ligand	NMR-Yield (%)	
		TBHP (70% in H_2O)	$Na_2CO_3 \cdot 1.5\ H_2O_2$
1	**L6**	10%	16%
2	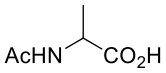 **L23**	12%	18%
3 (ref. data)	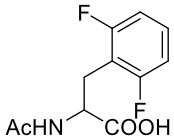 **L29**	28%	30%
4	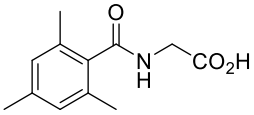 **L10**	23%	20%
5	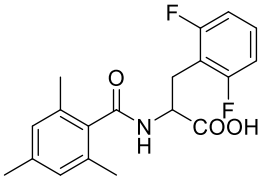 **L39**	30%	34%

Scheme 4.10 Comparison of amino acid derivatives with different oxidants

We first tested several α-amino acid ligands and found that, in most cases, sodium percarbonate as an oxidant produced higher yields than TBHP. Notably, we synthesized ligand **L39**, which combines the backbone and amino-protecting group from **L29** and **L30**. This combination slightly improved yields compared to the original ligands, supporting the logic of this design.

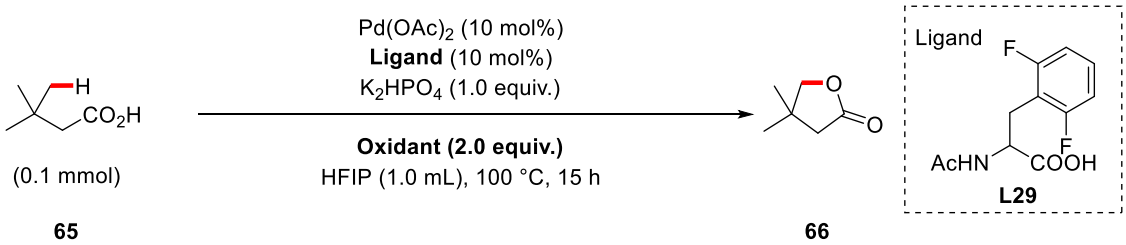

Entry	Ligand	NMR-Yield (%)	
		TBHP (70% in H_2O)	$Na_2CO_3 \cdot 1.5\ H_2O_2$
1 (ref. data)	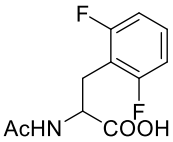 L29	28%	30%
2	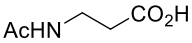 L7	9%	18%
3	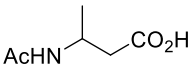 L68	11%	21%
4	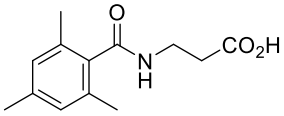 L42	15%	31%
5	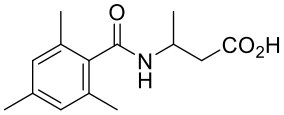 L46	20%	47%
6	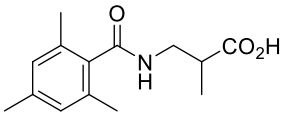 L45	10%	21%
7	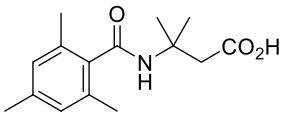 L83	2%	4%

Scheme 4.11 Comparison of amino acid derivatives with different oxidants

We also evaluated a range of β-amino acid ligands, where sodium percarbonate consistently proved to be the superior oxidant. Even the basic N-acetyl-protected β-amino acid achieved an 18% yield by NMR, while the mesityl-protected β-amino acid yielded an impressive 31%. Building on the same design principles established for **L39**, we synthesized a series of β-amino acid-derived ligands by combining favorable backbone and N-protecting groups, along with introducing additional modifications. Remarkably, ligand **L46** with sodium percarbonate as the oxidant achieved a 47% yield. Testing structurally similar ligands highlighted that backbone substitution is critical, as substituting a single methyl group at the α-position of the carboxylic acid(**L45**) or two methyl groups (**L83**) at the β-position reduced yields.

Analysis of the data from both tables demonstrates that ligand design and oxidant selection are key to improving reaction yields. We therefore proceeded with the combination of ligand **L46** and sodium percarbonate for further optimization.

Considering that sodium percarbonate is mildly basic and introduces Na^+ ions into the solution, while K_2HPO_4 is also added as a base, we decided to investigate the effect of varying the relative proportions of these two alkali metal cations on the reaction.

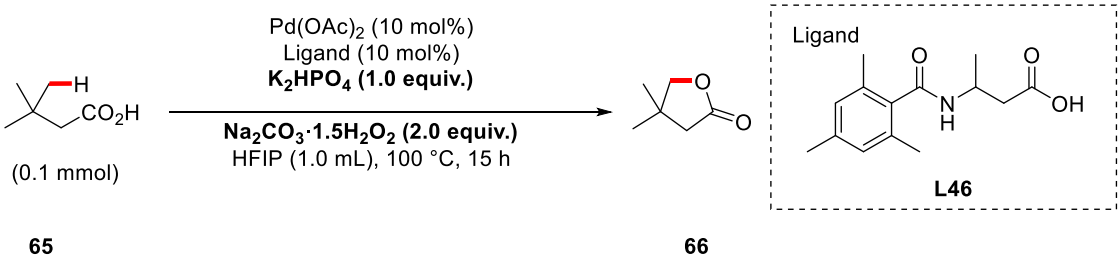

65 **66**

Entry	K_2HPO_4 (equiv.)	$Na_2CO_3 \cdot 1.5H_2O_2$ (equiv.)	NMR Yield
1	1.0	1.5	44%
2	1.6	1.5	14%
3	0.8	2.0	49%
4 (ref. data)	1.0	2.0	47%
5	1.6	2.0	26%
6	0.8	2.5	52%
7	1.0	2.5	50%
8	1.6	2.5	41%
9	0.4	3.0	50%
10	0.8	3.0	52%

Table 4.3 Optimization of base and oxidant amount

Comparing **Entry 1**, **4**, and **7**, we observed that reducing or increasing the oxidant by 0.5 equivalents resulted in a slight decrease and increase in yield, respectively. When using 1.5 equivalents of oxidant, increasing the base equivalents significantly reduced the yield (Entry 2). This trend persisted with 2.0 and 2.5 equivalents of oxidant, suggesting that K_2HPO_4 has a greater impact on the reaction than sodium percarbonate, with higher amounts of K_2HPO_4 having a negative effect. Consequently, we considered slightly reducing the K_2HPO_4

equivalents. Comparing Entry 3 and 4, this adjustment appeared favorable, with a slight increase in yield. Increasing the sodium percarbonate to 2.5 equivalents provided the best result, while further increasing to 3.0 equivalents did not improve the yield. Moreover, reducing the K_2HPO_4 amount at 3.0 equivalents of oxidant lowered the yield. Thus, we identified an optimal ratio of K_2HPO_4 to sodium percarbonate. Based on these results, we proceeded with further conditions optimization.

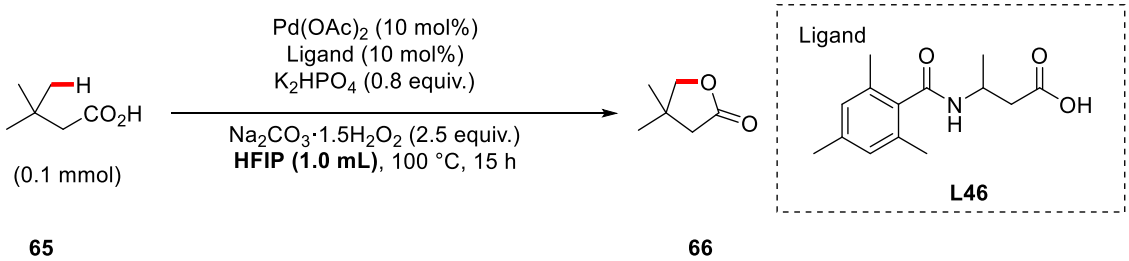

Entry	Solvent Volume	NMR Yield
1	0.5 mL	45%
2	0.8 mL	52%
3 (ref. data)	1.0 mL	52%
4	1.3 mL	54%
5	1.6 mL	55%

Table 4.4 Screening of solvent volume

The concentration of the reaction system is a key factor, as it affects the collision probability of various species. We tested the impact of HFIP volume on the reaction. While the trend of yield increasing with lower concentration was clear, overall, HFIP volume had a minimal effect. In Entry 5, using 1.6 mL of HFIP increased the yield to 55%, representing only a 1% improvement over the 1.3 mL used in Entry 4. Thus, we opted not to increase HFIP volume further and proceeded with 1.6 mL of HFIP for continued optimization under the best conditions.

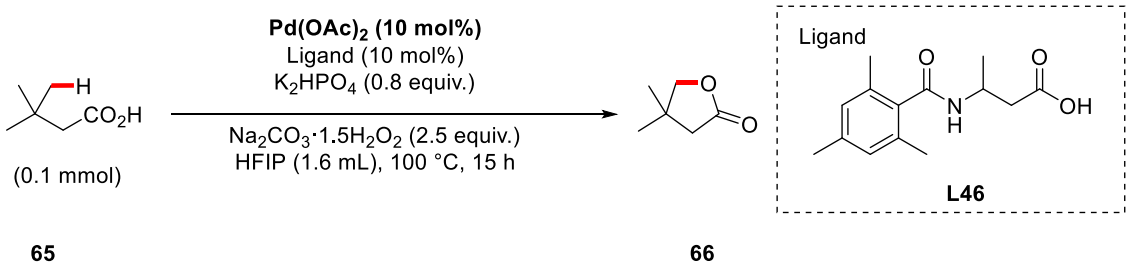

65 **66**

Entry	Pd-sources	NMR Yield
1 (ref. data)	$Pd(OAc)_2$	55%
2	$Pd(CF_3CO_2)_2$	56%
3	$Pd(CH_3CN)_2Cl_2$	60%
4	$PdCl_2$	31%

Table 4.5 Screening of different Pd-sources

The choice of palladium source is also critical, as the dissociation rate of ligands in different Pd sources affects the coordination efficiency of external ligands and thus the efficiency of C–H activation.[124-125, 141c] We tested several commonly used Pd sources for C–H activation, identifying $Pd(CH_3CN)_2Cl_2$ as the most suitable, which increased the yield to 60%.

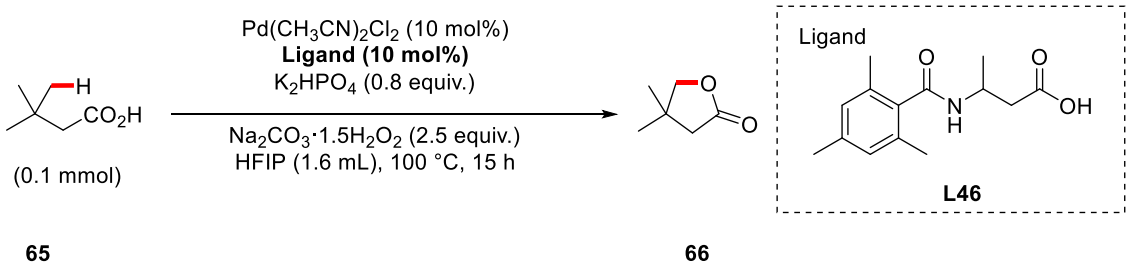

65 **66**

Entry	ligand loading	NMR Yield
1 (ref. data)	10 mol%	60%
2	15 mol%	67%
3	20 mol%	68%
4	25 mol%	68%

Table 4.6 Screening of ligand loading

Similarly, the ligand loading has a significant impact on the C–H activation step. In theory, the maximum amount of a bidentate ligand should be twice that of the Pd catalyst; however, the coordination ability of the ligand and the complexity of the system require thorough screening to determine the optimal ligand loading. Our tests indicated that increasing the ligand loading to 15 mol% raised the yield to 67%, with further increases having minimal effect. To conserve ligand use, we proceeded with 15 mol% for further optimization of reaction conditions.

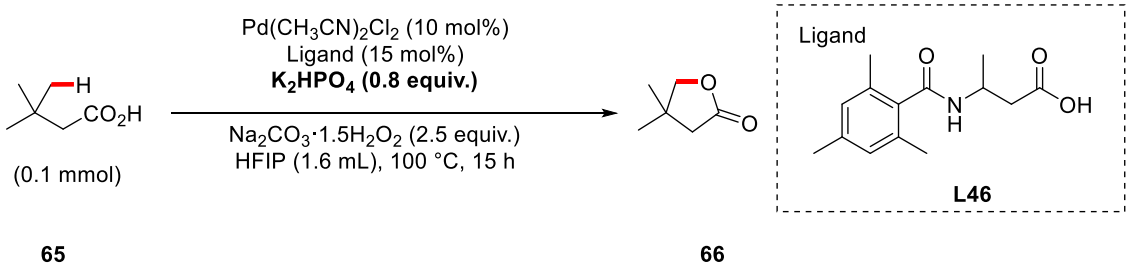

65 **66**

Entry	Base	NMR Yield	Entry	Base	NMR Yield
1	w/o	58%	8	NaHFIP	55%
2 (ref. data)	K_2HPO_4	67%	9	Na_2CO_3	58%
3	KH_2PO_4	49%	10	CsOAc	57%
4	K_3PO_4	60%	11	$CsHCO_3$	60%
5	$KHCO_3$	58%	12	Cs_2CO_3	22%
6	KF	59%	13	CsF	56%
7	Na_2HPO_4	54%	14	Li_2CO_3	56%

Table 4.7 Screening of different bases

From our previous screening, we observed that the base significantly affects reaction yield. Therefore, we expanded the range of bases tested. Initially, we examined the reaction without any base, finding that the yield dropped from 67% to 58%, indicating that while the base influences yield to some extent, it is no longer a critical factor for the reaction. Next, we tested various commonly used bases. The results showed that while K_2HPO_4 remains the most suitable base, other bases—except for Cs_2CO_3—did not lead to a substantial decrease in yield.

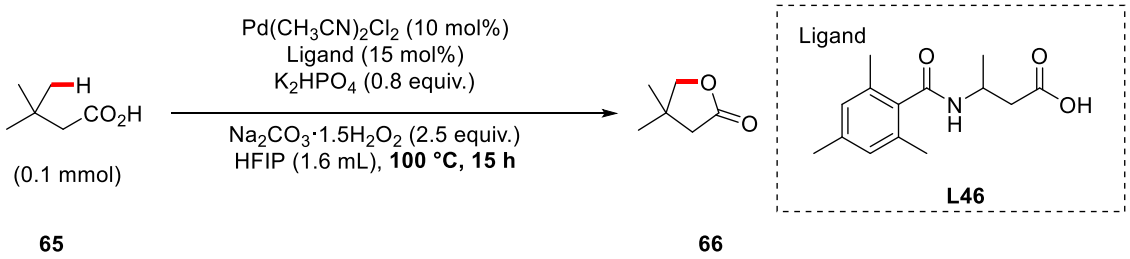

Entry	Temperature	Time	NMR Yield
1	60 °C	15h	43%
2	70 °C	15h	61%
3	80 °C	15h	63%
4	90 °C	15h	63%
5		9h	66%
6 (ref. data)	100 °C	15h	67%
7		30h	67%
8	110 °C	15h	62%

Table 4.8 Temperature and time screening. These experiments were carried out together with Sourjya Mal.

We then examined the effect of reaction temperature and time. The results showed that yield increased as temperature rose from 60 °C to 100 °C, but further increasing the temperature to 110 °C led to a decline in yield. Studying reaction time at 100 °C revealed that a 66% yield was achieved after 9 hours, and extending the reaction time from 15 to 30 hours did not cause decomposition of the desired product. Based on these findings, we selected 100 °C and a reaction time of 15 hours as the optimal conditions for further studies.

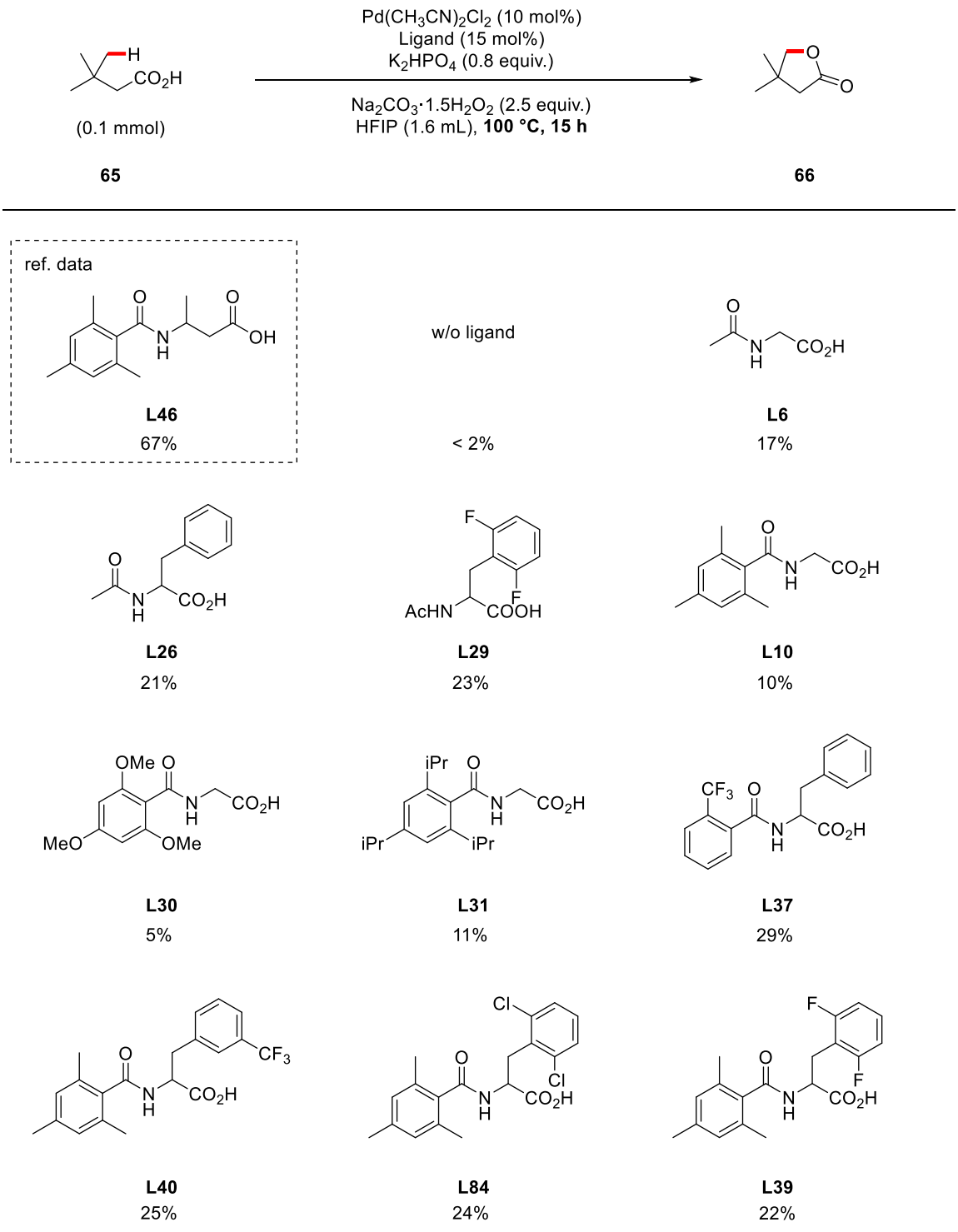

Scheme 4.12 Re-evaluation of ligand structure under the new optimized conditions. These experiments were carried out together with Sourjya Mal.

After thoroughly investigating all potential factors influencing reaction yield, the highest yield we achieved was 67%. Through multiple rounds of screening, the reaction conditions

underwent significant changes. We then decided to re-evaluate the influence of ligands under the current condition, focusing on the influence of substituents on the ligand backbone, and the CMD group. This re-examination aimed to uncover better strategies for ligand design.

First, we performed control experiments and found that the reaction scarcely proceeded without a ligand. Using the basic N-acetylglycine ligand yielded 17% product. Modifications to the backbone of this ligand modestly improved the yield, but changes to the amino protecting group consistently led to reduced yields (**L10, L30 & L31**). Interestingly, while two divergent design strategies produced opposite results, simultaneous modifications to both the backbone and the CMD group consistently gave positive feedback. Under the new reaction conditions, the newly designed ligand **L37** outperformed the previously successful ligand **L29**.

Next, we tested β-amino acid derivate ligands which able to form six-membered Pd cycles with the catalyst. The N-acetyl-β-amino acid (**L7**) as ligand provided a yield comparable to the N-acetyl-α-amino acid (**L6**) as ligand. Modifications to the backbone, such as introducing a methyl substituent at the β-position of the carboxylic group (**L68**), offered little improvement. Testing a series of internal base structures revealed that polysubstituted benzamides were the most suitable internal base structure for the reaction. While modifying the conjugated π-electron structure through substituent design to adjust the CMD ability seemed feasible in previous study, this strategy proved ineffective for this reaction. Strong electron-donating(**L44**) or withdrawing groups substitutions (**L87, L88, L89, L90, L59**) significantly reduced yields, with only mesityl (**L42**) or triisopropyl substitutions (**L41**) providing acceptable results. This behavior contrasted with the observations for α-amino acid ligands. Additionally, modifying the backbone while testing different internal base designs generally improved yields compared to unmodified backbones. Among the various combinations, **L46** consistently delivered the best results.

Through ligand design and conditions optimization, we achieved an NMR yield of 67% for directly obtaining the desired γ-lactone product from simple 3,3-dimethylbutanoic acid in a single step. However, the structural limitations of β-quaternary carboxylic acids prompted us to further address the more challenge γ-C(sp^3)–H activation lactonization of β-non-quaternary carboxylic acids.

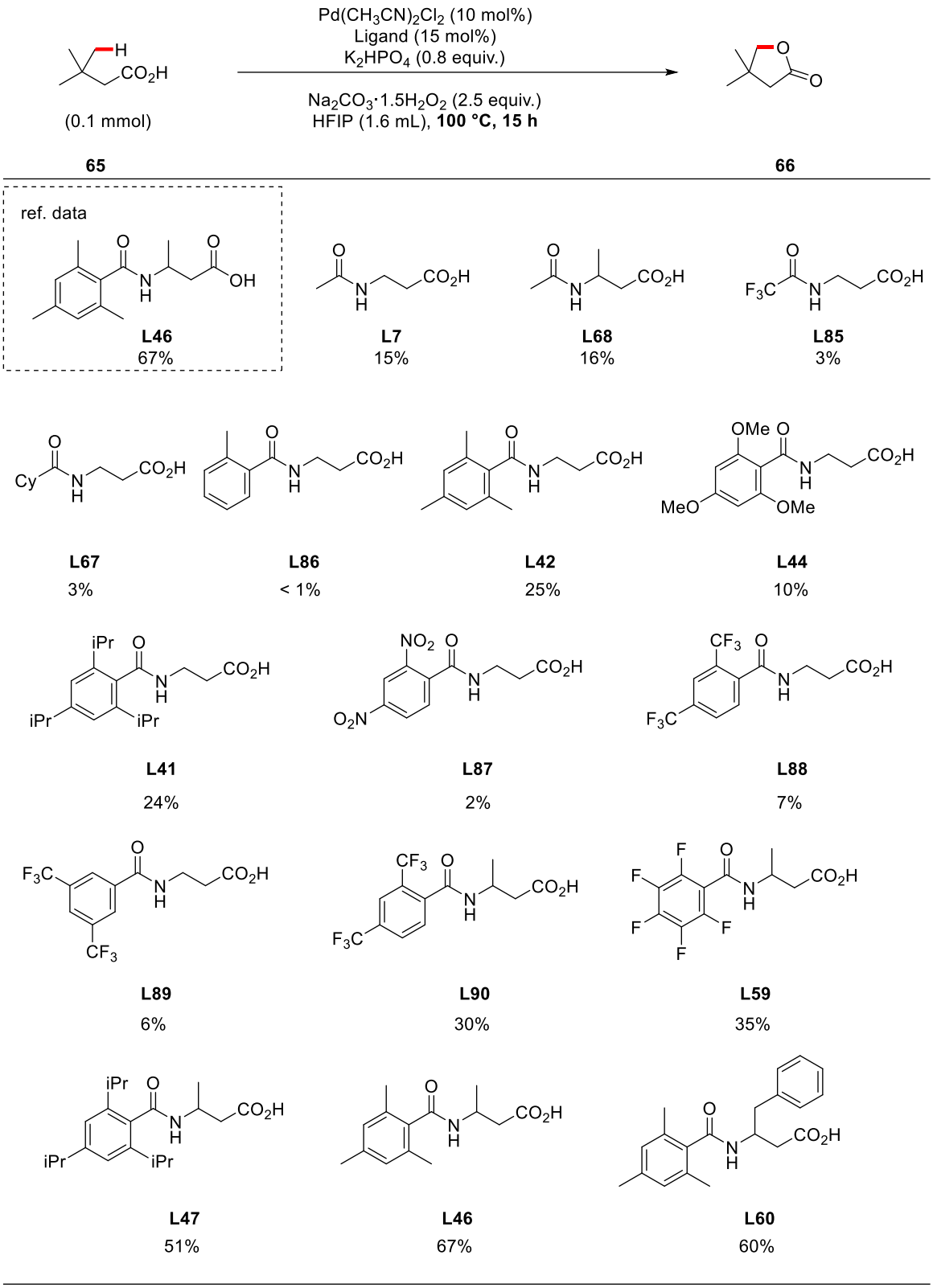

Scheme 4.13 Re-evaluation of β-amino acid derivatives ligands under the new optimized conditions. These experiments were carried out together with Sourjya Mal.

4.3.2 Optimization for β-Non-Quaternary Carboxylic Acids

The γ-position of a β-non-quaternary carboxylic acid is only substituted by two methyl groups, which results in the absence of the Thorpe–Ingold effect,[152] while also being affected by the competing β-hydride elimination pathway.

Initially, we directly applied the conditions used for β-quaternary carboxylic acids to the template substrate, 3-methylbutanoic acid, and obtained 27% of the desired lactone product in the NMR spectrum. Although the yield was not high, obtaining a synthetically useful yield in an initial attempt was encouraging. More notably, achieving selective functionalization of β-quaternary carboxylic acids through palladium-catalyzed γ-C(sp^3)–H activation is known to be highly challenging.

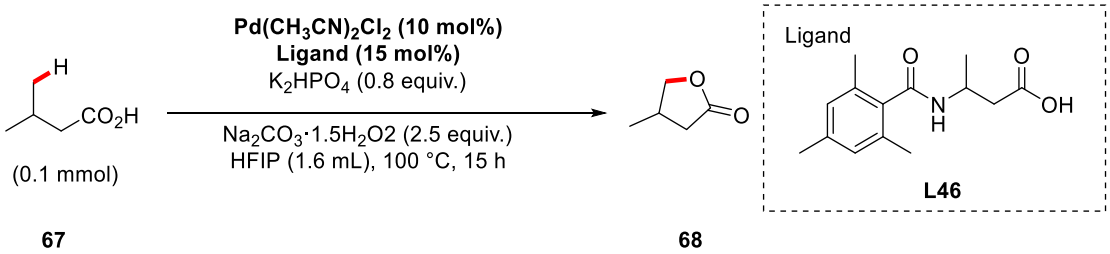

Entry	Pd-sources	Ligand Loading	NMR Yield
1	$Pd(OAc)_2$	15 mol%	25%
2	$Pd(CF_3CO_2)_2$	15 mol%	25%
3 (ref. data)	$Pd(CH_3CN)_2Cl_2$	15 mol%	27%
4	$Pd(CH_3CN)_2Cl_2$	20 mol%	30%
5	$PdCl_2$	15 mol%	5%

Table 4.9 Screening of different Pd-sources and ligand loading

We began by screening Pd sources. Under these conditions, three commonly used Pd sources—$Pd(OAc)_2$, $Pd(CF_3CO_2)_2$, and $Pd(CH_3CN)_2Cl_2$—produced comparable yields, whereas $PdCl_2$ yielded only 5% of the desired product, a significantly lower outcome. Since our screening of β-quaternary carboxylic acids showed that increasing the ligand loading to 20 mol% slightly

improved the yield, we tested this adjustment for β-non-quaternary carboxylic acids as well. The results indicated that increasing the ligand loading from 15 mol% to 20 mol% raised the yield to 30%. Based on these findings, we proceeded with 20 mol% ligand and 10 mol% $Pd(CH_3CN)_2Cl_2$ to further optimize the reaction conditions.

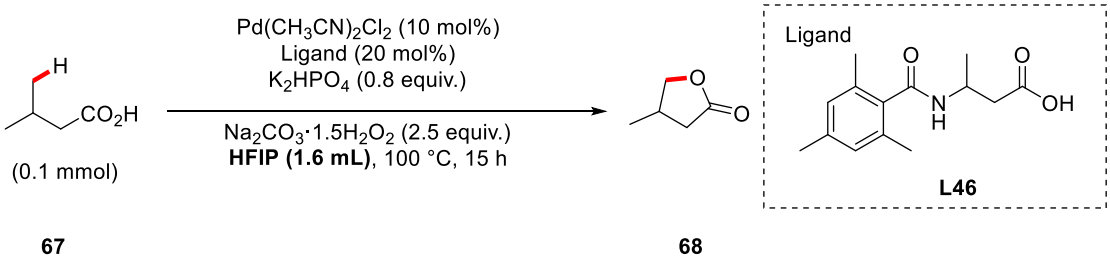

67 68

Entry	Solvent volume	NMR Yield
1 (ref. data)	1.6 mL	30%
2	1.8 mL	32%
3	2.0 mL	33%
4	2.3 mL	34%
5	2.5 mL	36%
6	2.5 mL	40% (with 25 mol% Ligand)

Table 4.10 Screening of solvent volume

Based on our experience with β-quaternary carboxylic acids, the reaction concentration significantly affects the outcome, with increasing the volume of HFIP improving yields. A similar trend was observed with β-non-quaternary carboxylic acid substrates. Increasing the HFIP volume from 1.6 mL to 2.5 mL raised the yield from 30% to 36%. Additionally, further increasing the ligand loading to 25 mol% improved the yield to 40%. These adjustments brought the yield to a moderate level; however, the solvent volume and ligand loading were already quite high, and further increases would likely provide limited benefits. Therefore, we selected a concentration of 0.04 M and a ligand loading of 25 mol% for the next round of

conditions optimization.

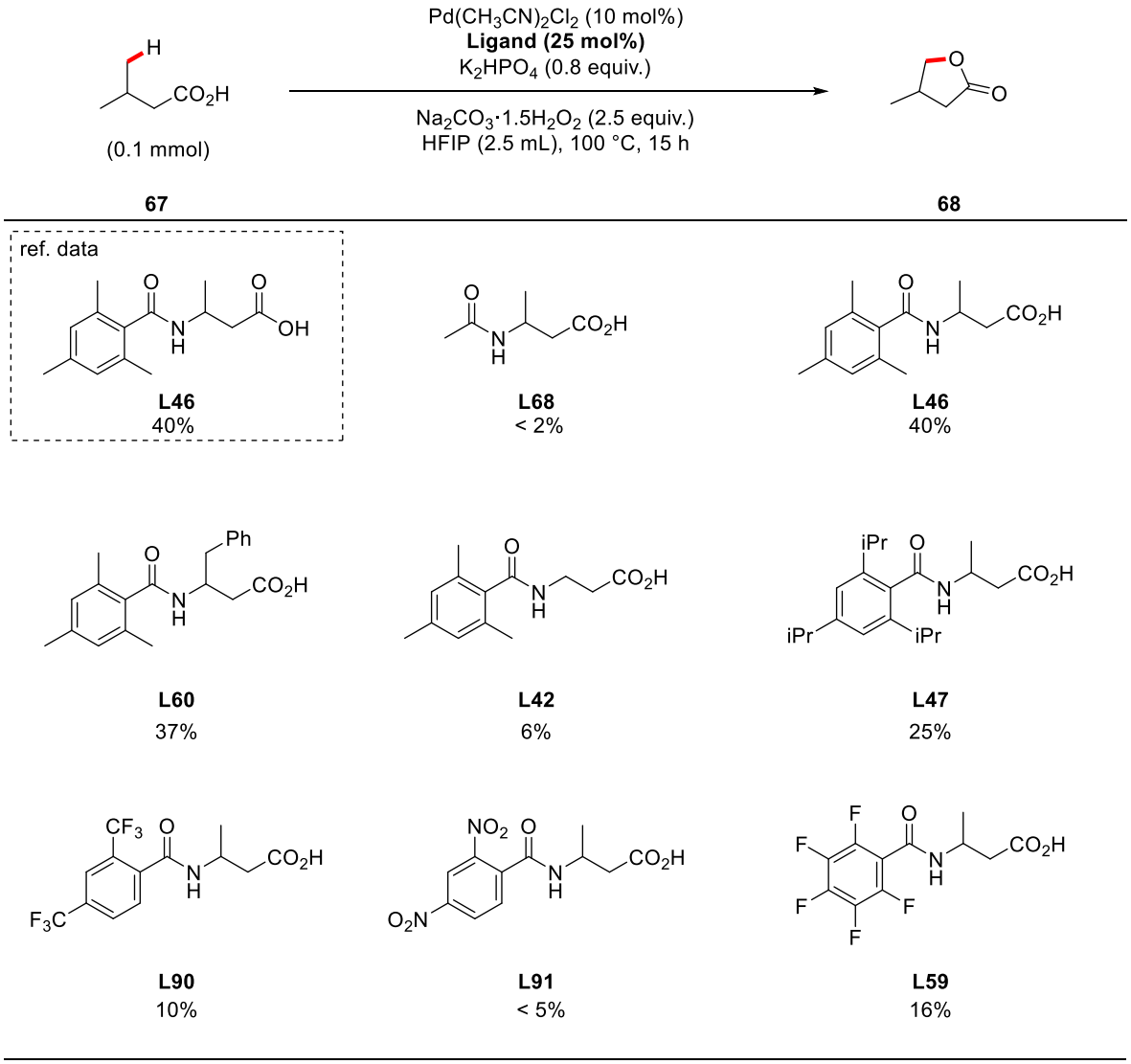

Scheme 4.14 Screening of ligands. These experiments were carried out together with Sourjya Mal.

We then examined the effect of ligand structure on this class of substrates. Retaining the backbone substituents, we first tested N-acetyl-β-amino acid-derived ligands, but the desired product was barely observed by NMR spectrum. Testing with **L42** confirmed that the backbone substituents are crucial for the reaction. Replacing the methyl group on the backbone with a benzyl group (**L60**) resulted in a slight decrease in yield. Finally, the test results consistently demonstrated that the currently used ligand remains the most optimal choice.

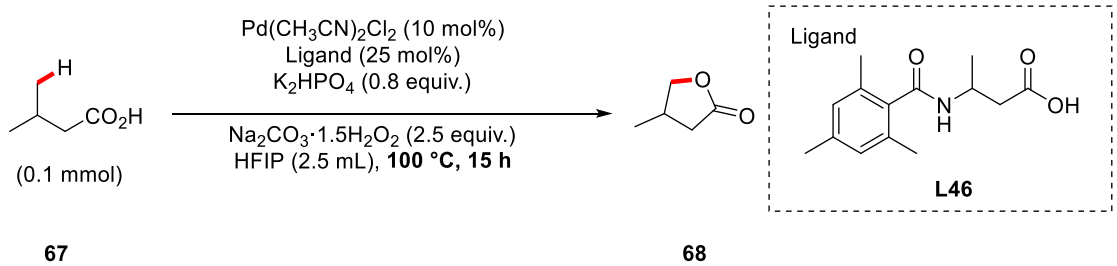

67 **68**

Entry	Temperature	Reaction Time	NMR Yield
1	90 °C	24 h	35%
2		48 h	46%
3		72 h	44%
4 (ref. data)	100 °C	15 h	40%
5		24 h	40%
6		48 h	38%
7		72 h	37%
8	105 °C	12 h	36%
9		18 h	40%
10		24 h	35%

Table 4.11 Temperature and time screening. These experiments were carried out together with Sourjya Mal.

Finally, we optimized the reaction time and temperature. Based on observations during the screening of β-quaternary carboxylic acids, both excessively low and high temperatures negatively impacted the reaction. Therefore, we only tested temperatures of 90 °C, 100 °C, and 105 °C, with reaction times extended to 24 hours or longer. The results showed that at the same reaction time of 24 hours, in the conditions of 100 °C yielded the most product. However, when the reaction time was extended, yields began to decrease at 100 °C, whereas at 90 °C, the yield

reached a maximum of 46% at 48 hours before slightly declining to 44% at 72 hours.

These data suggest that the reaction rate increases with temperature, requiring more than 24 hours to achieve a 40% yield at 90 °C but only 15 hours at 100 °C. However, higher temperatures may also accelerate competing side reactions, reducing selectivity. Additionally, the slight decline in yield over extended reaction times indicates that the product may be somewhat unstable under the reaction conditions.

In summary, a series of screening experiments allowed us to determine the optimal conditions for β-non-quaternary carboxylic acid substrates.

4.4 Substrate Scope

4.4.1 Substrate Scope for β-Quaternary Carboxylic Acids

After establishing the optimal reaction conditions, we evaluated the substrate scope for β-quaternary carboxylic acids.

The isolated yield of the product from the template substrate (**68**) was 49%, which we attribute to the small molecular weight of the product, leading to some loss due to volatility. Modifications to the length or structure of a single alkyl substituent at the β-position did not impact the formation of the lactone product (**69** and **70**), which was consistently obtained in high yields. These alkyl-substituted γ-butyrolactones (GBLs) are known as effective neuropharmaceutical agents.[153] While previous studies often required multiple synthetic steps to access these scaffolds,[154] our method enables their direct synthesis in a single step.

Moreover, substrates with β-position methyl groups replaced by alkyl chains containing heteroatom-functionalized groups, such as phenoxy (**71**), ester (**72**), or TIPS-protected hydroxyl groups (**73**), reacted smoothly to produce the desired lactones in good yields. These functional groups can also serve as handles for further molecular elaboration, facilitating the construction of more complex molecules.

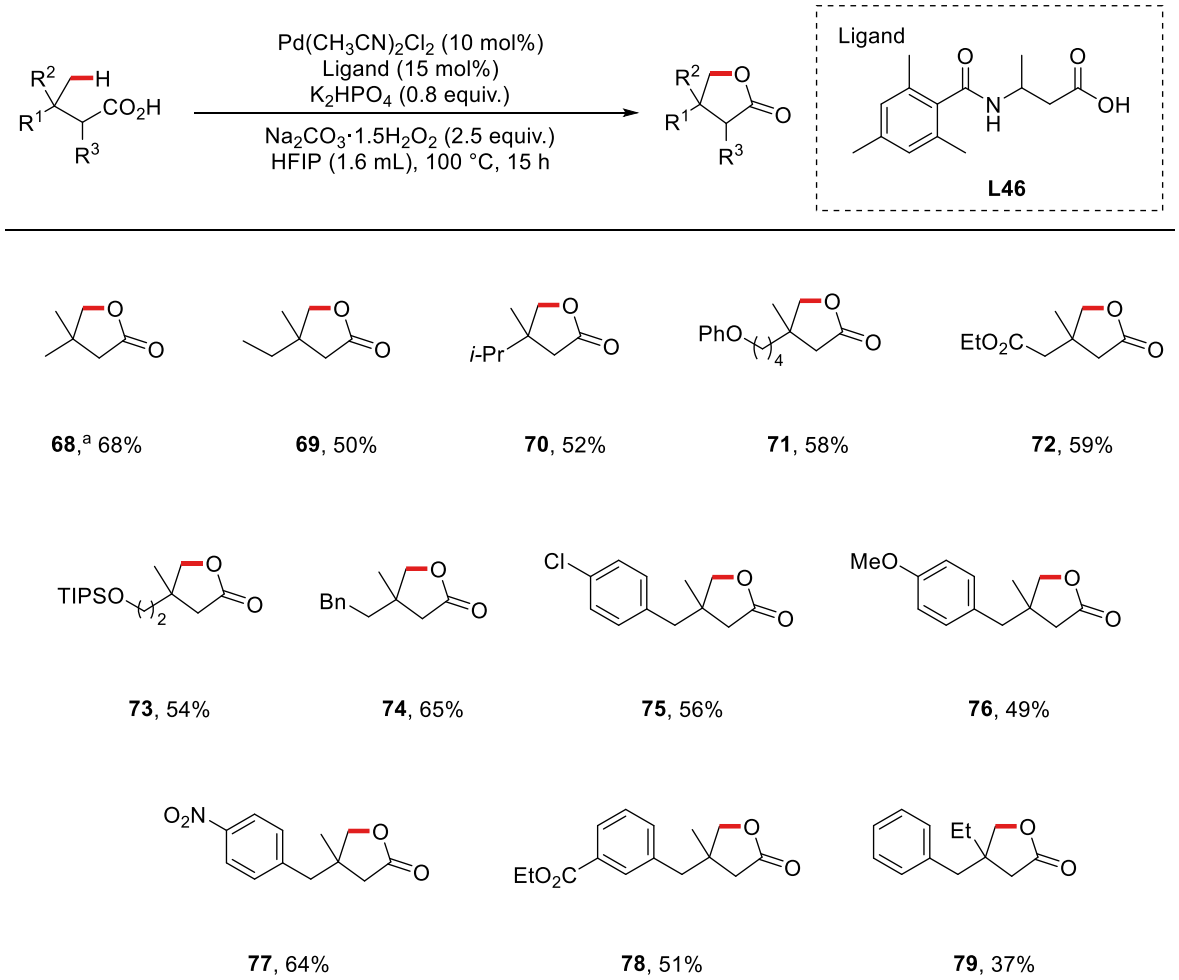

Scheme 4.15 Substrate scope for β-quaternary carboxylic acids. Reactions were conducted on a 0.2 mmol scale. [a] ^{1}H NMR yield calculated using 1,3,5-trimethoxybenzene as internal standard.

A range of aromatic substrates featuring diverse functional groups and electronic properties were evaluated under our reaction conditions and were found to be compatible, producing their respective lactones (**74–79**) in useful yields. Even substrates bearing a single methyl group (**79**) yielded the corresponding lactone product in a moderate yield of 37%. The successful reaction of these multiply substituted substrates significantly broadens the scope of this methodology, underscoring its synthetic practicality. Notably, these aromatic substrates are particularly challenging due to the presence of benzylic C–H bonds at the same γ-position, which are more reactive and prone to side reactions or decomposition. The ability of our method to overcome these challenges highlights its robustness and versatility.

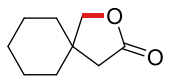

80, 61%

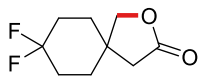

81, 70%

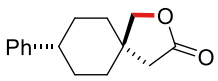

82, 89%

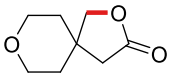

83, 53%

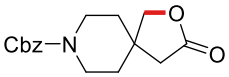

84, 36%

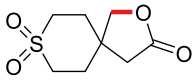

85, 21%

Scheme 4.16 Substrate scope for β-quaternary carboxylic acids for spirocyclic lactones. Reactions were conducted on a 0.2 mmol scale.

Spirocyclic scaffolds are highly valued in medicinal chemistry and are found in various approved drugs and drug candidates. The rigidity of spirocyclic structures can enhance pharmacokinetic properties, influence drug potency, and improve selectivity.[155]

Recognizing the importance of spirocyclic lactones in medicinal chemistry, we applied our method to synthesize a series of β-spiro-γ-lactones. These included compounds such as **80** (61%), fluorinated **81** (70%), and sulfone-substituted **85** (21%), with yields ranging from moderate to excellent. Notably, **82** was obtained with an exceptionally high isolated yield of 89%. Heteroatom-containing spirocyclic substrates also proved compatible with the reaction. For example, the lactone featuring a tetrahydropyran fragment, **83**, was synthesized in 53% yield, while the protected piperidine substrate, a common secondary amine in alkaloids, yielded lactone **84** in 36%.

Importantly, these substrates are challenging to access using previously reported methods. Radical-based pathways for lactone synthesis often struggle with selectivity between methyl and methylene C–H bonds,[156] while approaches relying on vicinal hydrogen elimination typically target γ-secondary positions.[140b] These results highlight the complementarity of our protocol to existing methodologies, providing a valuable alternative for spirocyclic lactone synthesis.

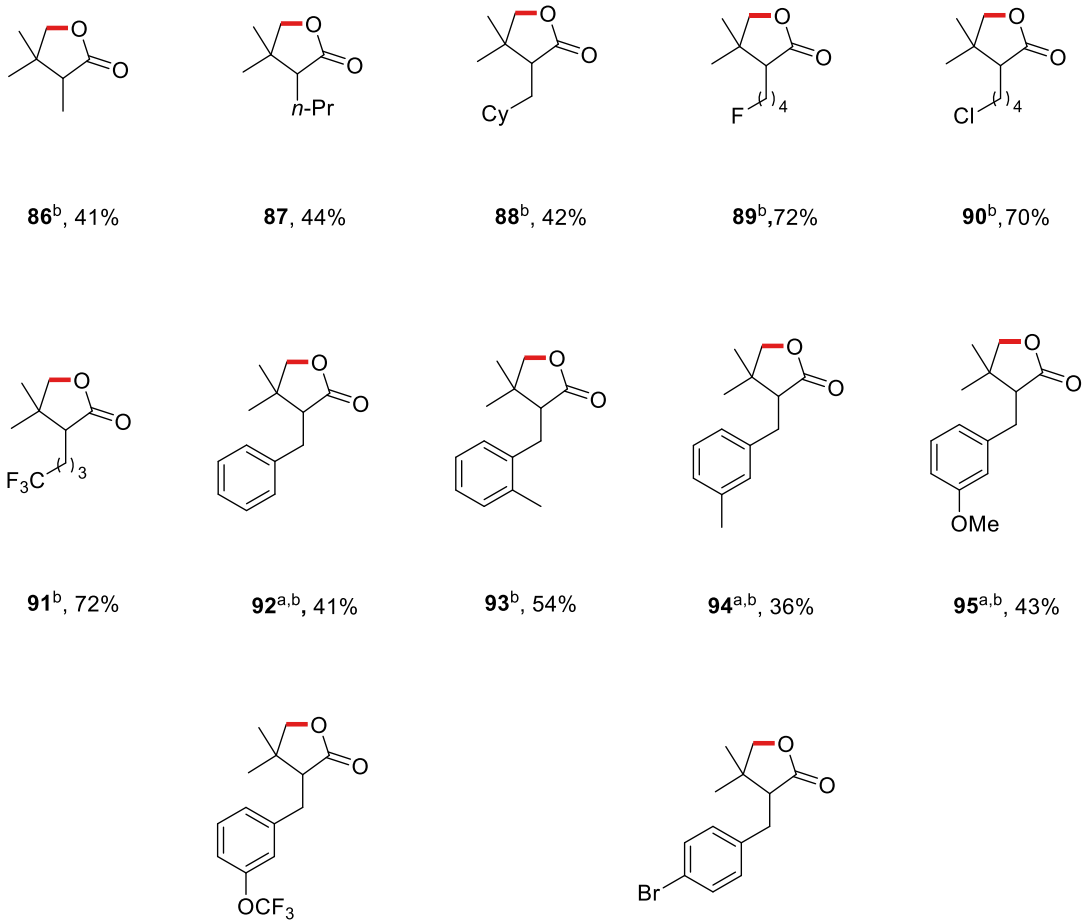

Scheme 4.17 Substrate scope for β-quaternary carboxylic acids with α-substituted. Reactions were conducted on a 0.2 mmol scale. [a] Ag_2CO_3 (1.25 equiv.) was used at 90 °C for 72 h. [b] These products were isolated by Sourjya Mal.

We then explored different substituents at the α-position. Lactones with various substituents, including alkyl chains (**86 & 87**), cycloalkanes (**88**), halides (**89 & 90**), and trifluoromethyl groups (**91**), were obtained in useful yields. Additionally, with minor adjustments to the reaction conditions, lactones containing electron-rich aromatic groups (**92–95**) could also be synthesized. Electron-deficient aromatics, such as **96** (45%) and **97** (44%), exhibited reasonable reactivity under standard reaction conditions.

Notably, in these substrates, activation of the γ-C–H bond had to overcome competition with

decomposition pathways resulting from β-position activation of benzylic C–H bonds.

4.4.1 Substrate Scope for β-Non-Quaternary Carboxylic Acids

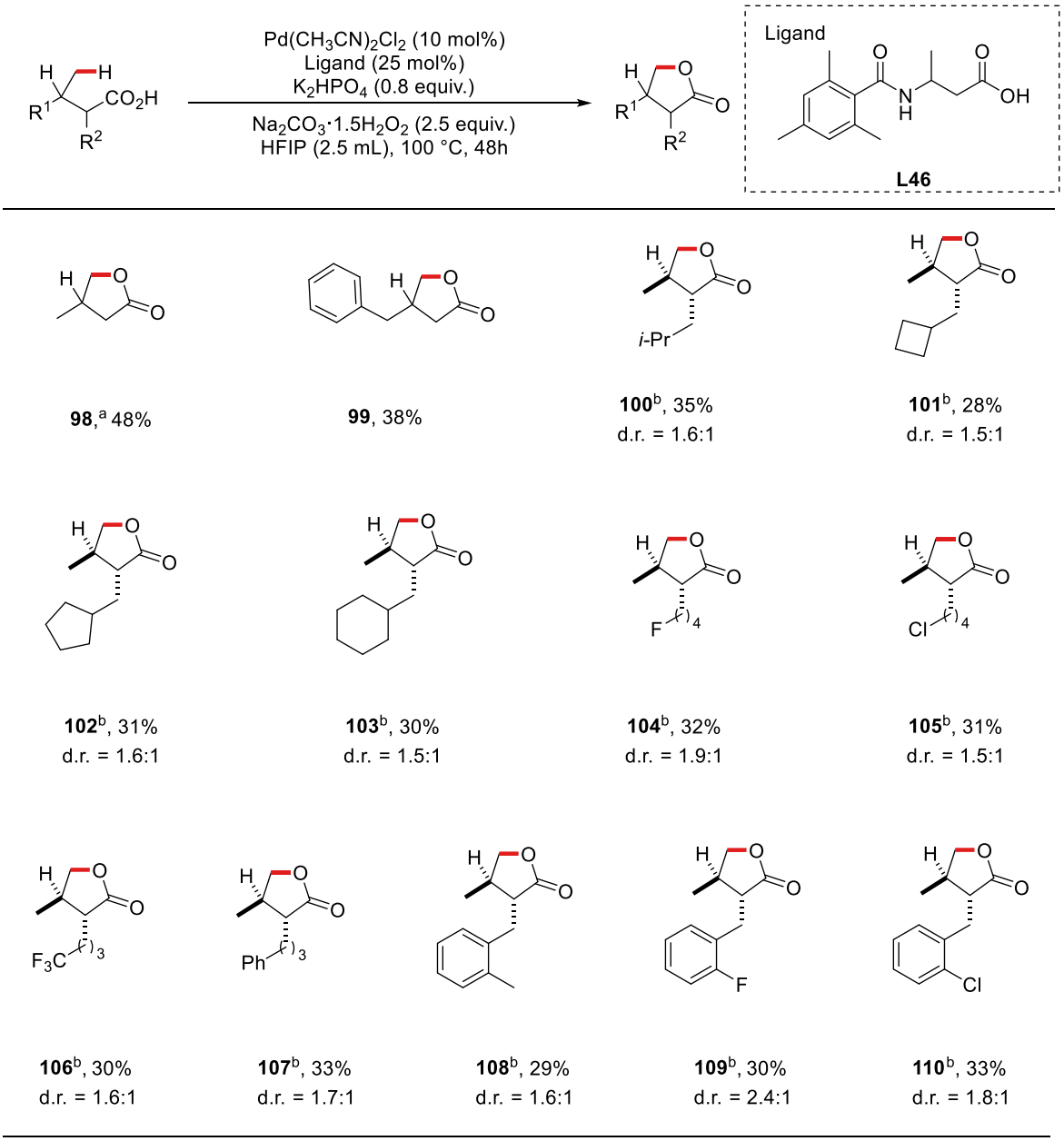

Scheme 4.18 Substrate Scope for β-Non-Quaternary Carboxylic Acids. Reactions were conducted on a 0.2 mmol scale. [a] ^{1}H NMR yield calculated using 1,3,5-trimethoxybenzene as internal standard. [b] These products were isolated by Sourjya Mal.

Next, the challenging β-non-quaternary carboxylic acid substrates were tested. The template substrate faced similar isolation issues as **98** but still achieved a practical isolated yield of 36%.

Despite the potential for competitive benzylic C–H activation, substrates with reactive benzylic positions displayed good tolerance (**99**, 38%).

The vacant α-position accommodated a wide range of structural fragments with excellent substrate compatibility. Cycloalkyl groups (**101 - 103**), halides (**104 & 105**), trifluoromethyl groups (**106**), and phenyl groups (**107**) all afforded the corresponding lactones in useful yields, displaying moderate diastereoselectivity favoring the trans isomer. Additionally, a series of α-benzyl-substituted lactones (**108 - 110**) were successfully synthesized.

4.5 Synthetic Applications

4.5.1 Scale-up Reaction (2.0 mmol scale)

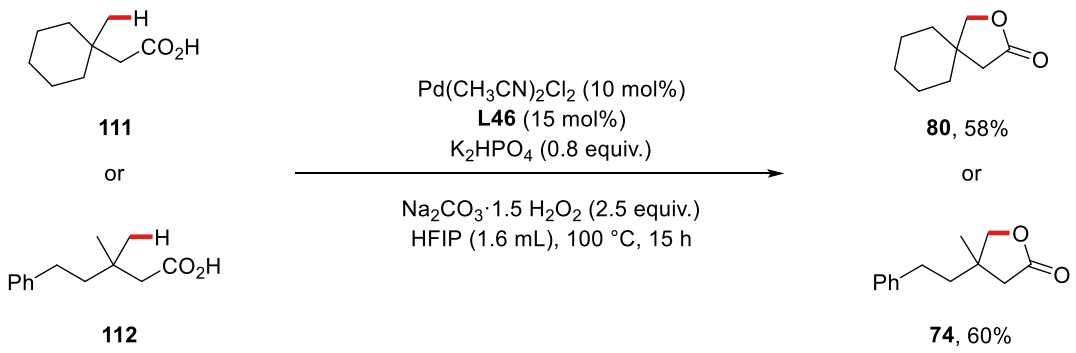

Scheme 4.19 Scalability of the direct *β*-C(sp^3)–H arylation of propanoic acid

To further probe the synthetic utility of our protocol, we first showed that it can be conducted on a preoperatively useful scale. Two representative reactions were performed on a 2.0 mmol scale giving **74** and **80** in 60% and 58% yields respectively.

4.5.2 Derivatization of the Lactone Product

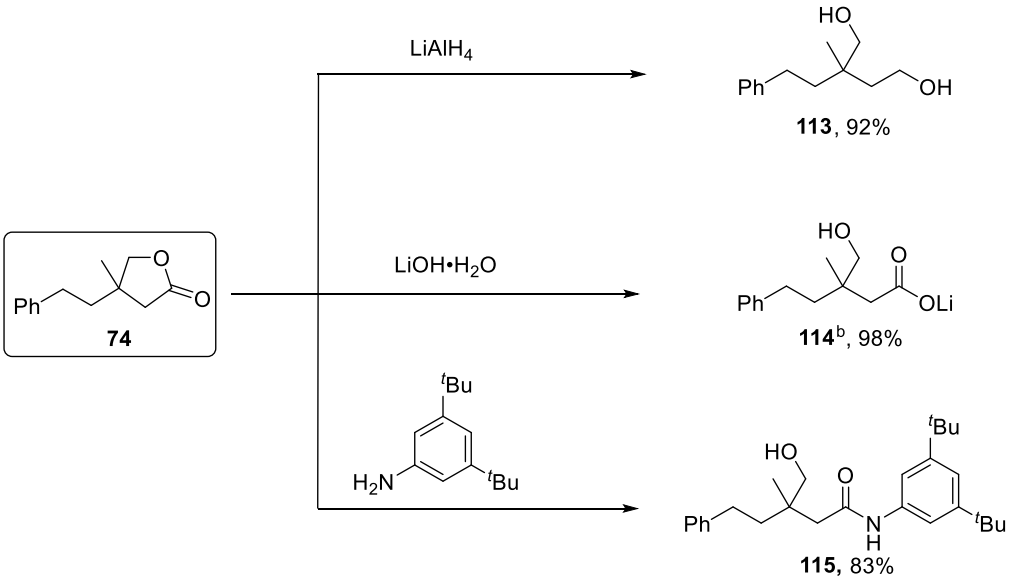

Scheme 4.20 Derivatization of the lactone product. [b] These products were isolated by Sourjya Mal.

We next explored potential derivatizations of the synthesized lactone product, with **74** as the example (**Scheme 4.20**). Reduction of **74** with $LiAlH_4$ yielded 1,4-diol **113** in an excellent yield of 92%. This scaffold is found in biologically active compounds[157] and has widespread applications, including in the polymer industry.[158] Given the significance of hydroxy fatty acids in various fields,[118, 159] **74** was subjected to hydrolysis, producing **114** in 98% yield as its lithium salt. This compound serves as a precursor for photoredox-catalyzed decarboxylative functionalization reactions.[123] Additionally, aminolysis of **74** afforded γ-hydroxy amide **115** in 83% yield.

4.6 Proposed Catalytic Cycle

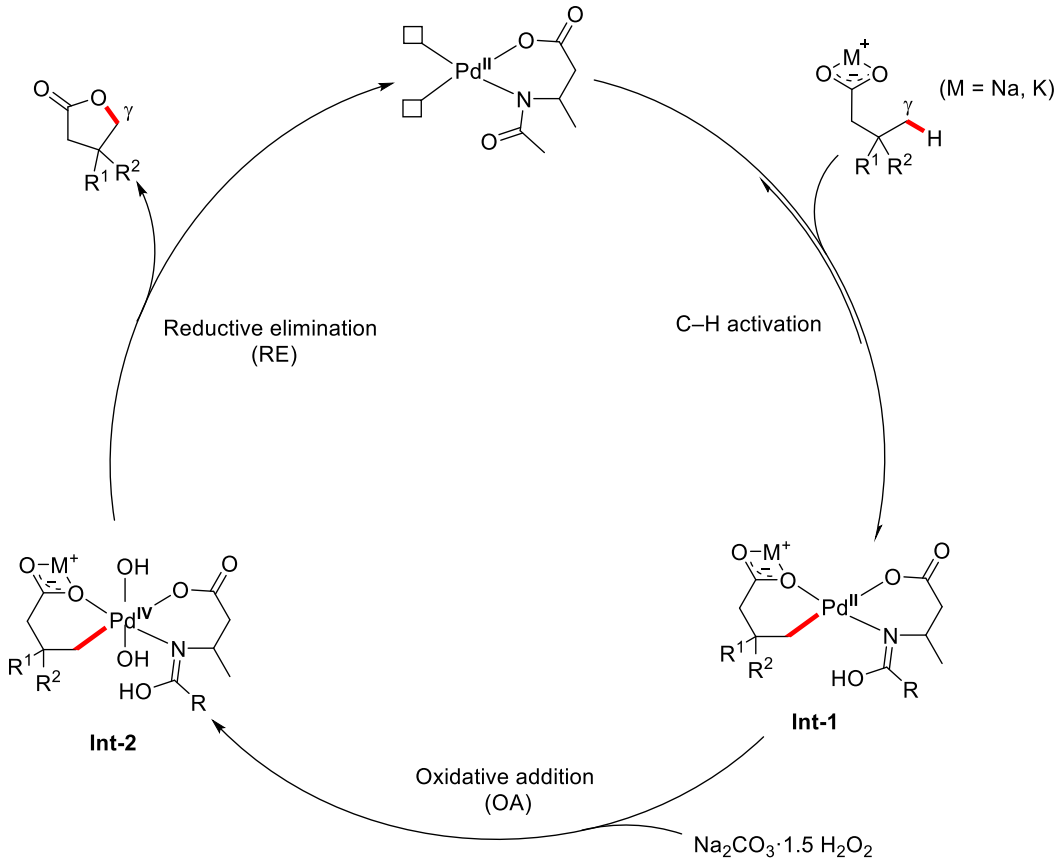

Scheme 4.21 Proposed catalytic cycle of the γ-lactonization of aliphatic carboxylic acids.

Based on relevant literature[76d, 83, 88, 160] and our team's prior work,[87, 90, 161] we propose that the γ-C–H activation lactonization of alkyl carboxylic acids proceeds via a Pd^{II}/Pd^{IV} catalytic cycle, as illustrated in the proposed mechanism. Initially, the external ligand (**L46**) coordinates with the Pd precatalyst to form the active catalyst. The subsequent reversible C–H activation step occurs via a concerted metalation-deprotonation (CMD) pathway,[90, 161] facilitated by the counter cations (Na/K) and the ligand acting as an internal base, generating intermediate Int-1.[130a] Given the well-documented ability of peroxides to oxidize Pd^{II} to Pd^{IV},[54f, 162] Int-1 is expected to undergo oxidative addition of hydrogen peroxide, forming Int-2.[151c, 163] Due to the relative ease of C(sp^3)–O reductive elimination (RE) in high-valent transition metal species,[76d, 130f] Int-2 is anticipated to undergo reductive elimination, yielding the desired γ-lactone and regenerating the active catalyst.

4.7 Limitations

Unsuccessful Substrates

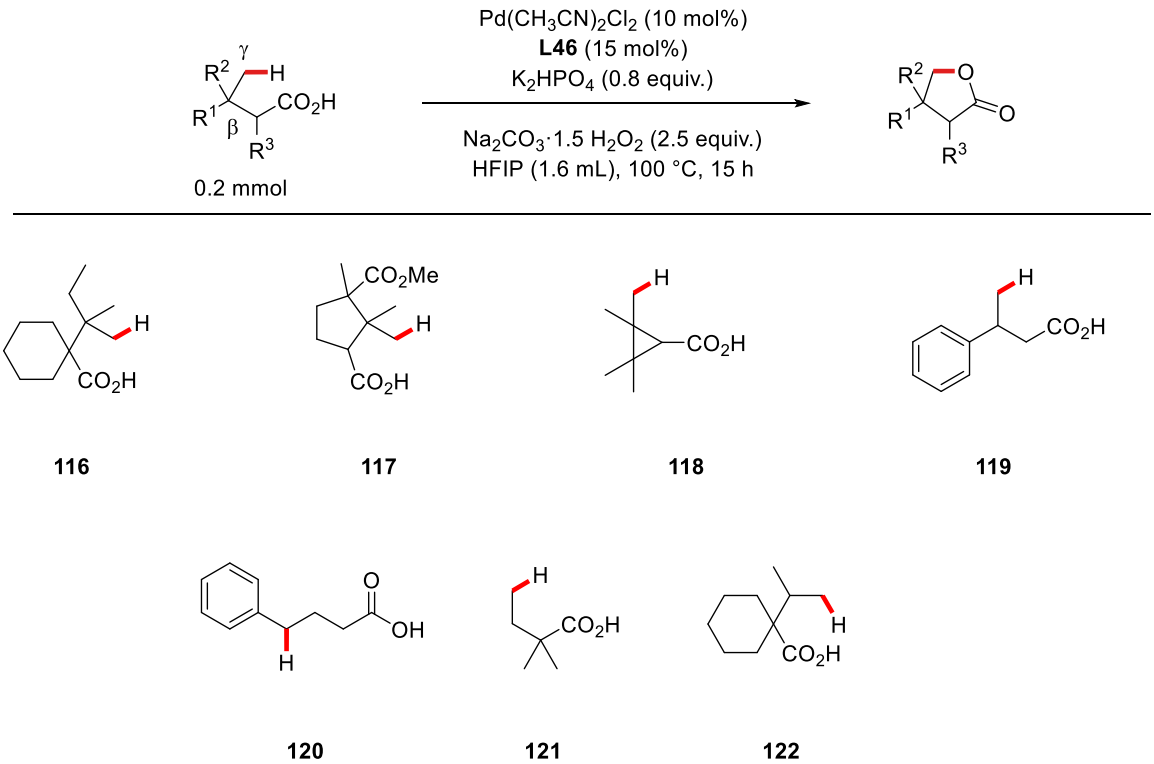

Scheme 4.20 Selected examples of unsuccessful substrates

The unsuccessful outcomes with these substrates can be attributed to the following factors: Substrates **116**, **117**, and **122**, which feature cycloalkane rings at the α-position of $–CO_2H$, are prone to decomposition through dehydrogenation pathway.[164] For substrate **119**, the benzene ring likely suppresses the desired reactivity by promoting competing pathways such as benzylic reactions or ortho-C–H activation. In substrate **121**, the presence of two methyl groups at the α-position of $–CO_2H$ may favor decomposition via a β-C(sp^3)–H activation pathway. For substrate **118**, steric congestion likely inhibits the conformation needed for effective C(sp^3)–H activation. Finally, substrate **120** lacks the Thorpe–Ingold effect, preventing efficient palladium coordination to the target C–H bond.

4.8 Preliminary Evaluation of an Enantioselective Variant

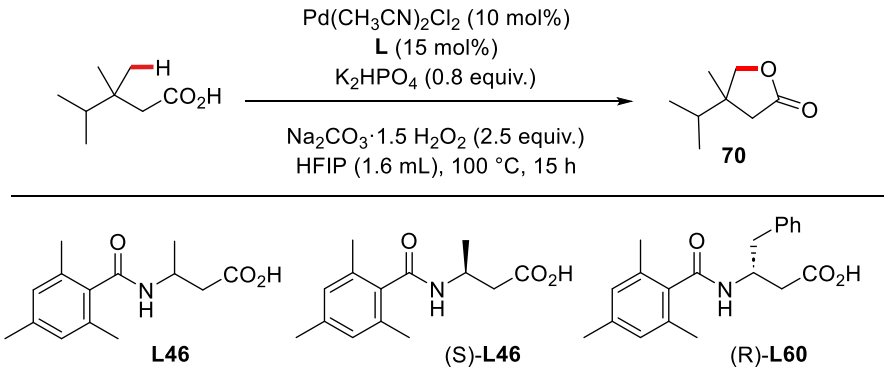

Entry	Ligand	Yield	e.r. [a]
1 (ref. data)	**L46**	52%	50:50
2	**(S)-L46**	50%	63:37
3	**(R)-L60**	44%	33:67

Scheme 4.21 Preliminary evaluation of an enantioselective variant. [a]e.r. were determined from GC using HP-CHIRAL-20B column. Temperature program: Starting at 75 °C for 1 minute, raised to 95 °C at 2 °C /min, hold for 2 minutes. Raised to 110 °C at 0.08 °C /min, hold for 2 minutes. Raised to 200 °C at 20 °C /min, hold for 3 minutes. The analysis time was 210 minutes. Product t_1 = 80.9 min, t_2 = 82.2 min. These experiments were carried out together with Sourjya Mal.

We investigated whether using an enantiopure ligand instead of the original racemic ligand could enable stereocontrol of the lactone product. As shown in the table, the lactone obtained with the racemic ligand exhibited 50:50 er when analyzed using a chiral column. In contrast, employing **(S)-L46** as the ligand made an obvious change in the conformation ratio of the product while maintaining the overall yield, resulting in 63:37 er. When **(R)-L60** was used, a

slight decrease in yield was observed, but the product displayed a further shift in ratio, yielding a 33:67 er.

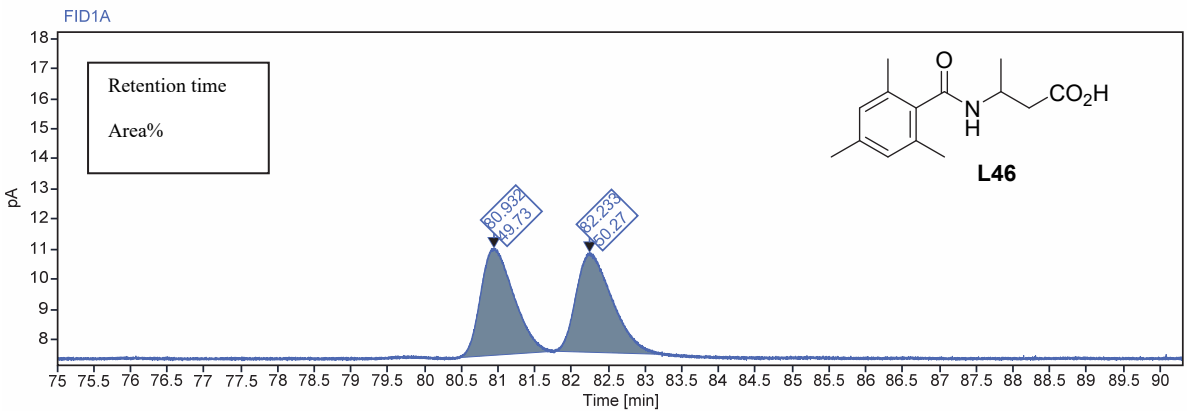

Signal:		FID1A			
RT [min]	**Type**	**Width [min]**	**Area**	**Height**	**Area%**
80.932	MM m	0.37	110.89	3.55	49.73
82.233	MM m	0.40	112.08	3.30	50.27
		Sum	222.97		

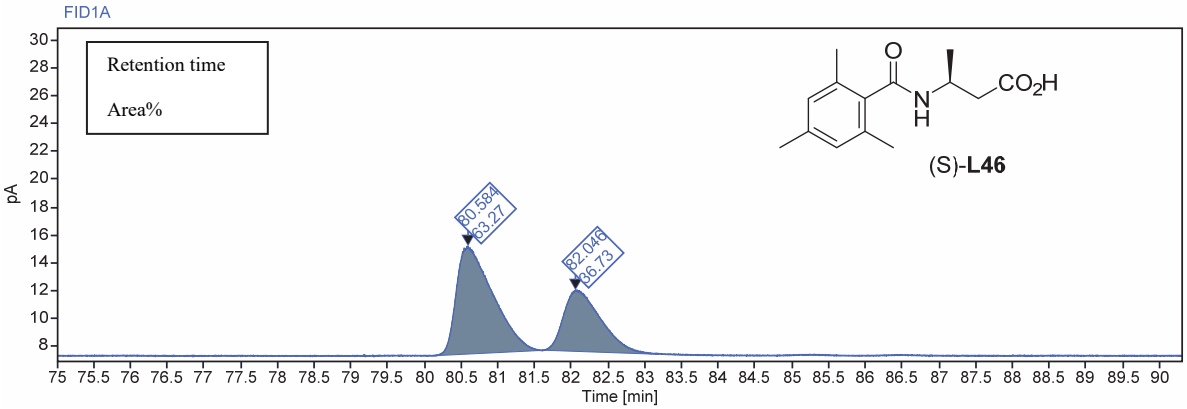

Signal:		FID1A			
RT [min]	**Type**	**Width [min]**	**Area**	**Height**	**Area%**
80.584	MM m	0.40	265.43	7.74	63.27
82.046	MM m	0.59	154.08	4.38	36.73
		Sum	419.51		

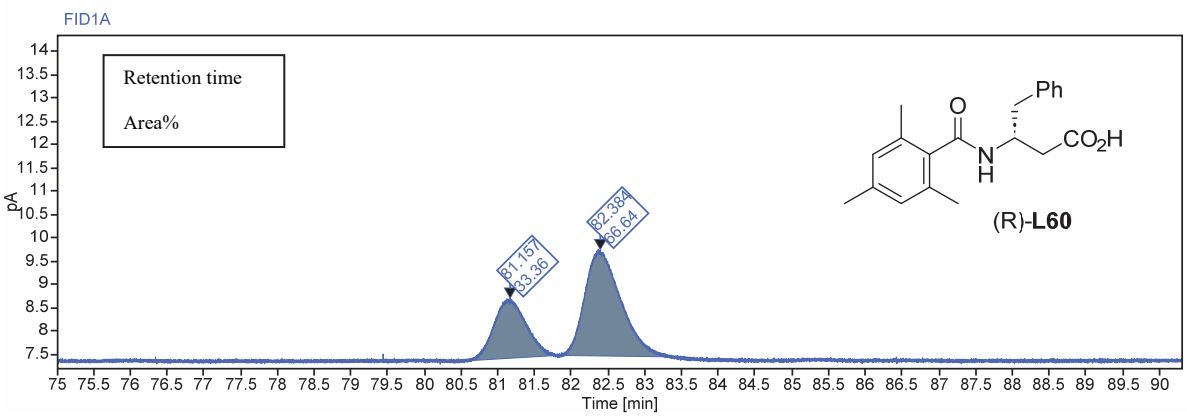

Signal:		FID1A			
RT [min]	**Type**	**Width [min]**	**Area**	**Height**	**Area%**
81.157	MM m	0.35	38.44	1.27	33.36
82.384	MM m	0.40	76.80	2.27	66.64
		Sum	115.24		

4.9 Conclusion

In summary, we have developed Pd^{II}-catalyzed direct γ-C(sp^3)–H lactonization of aliphatic carboxylic acids based on the C–O reductive elimination. The use of sodium percarbonate as an oxidant and the development of a new β-alanine-derived ligand were key to establish this protocol, which converts a wide range of carboxylic acids, including challenging β-non-quaternary acids for the first time, into the corresponding lactones in a single step. Notably, our lactonization protocol is complementary to state-of-the-art methods for the direct lactonization of free carboxylic acids and gives access to a wide library of lactones that were previously only accessible through multi-step synthetic routes. This newly discovered catalyst capable of functionalizing the unprecedented β-non-quaternary acids is expected to significantly advance the substrate accessibility of γ-C(sp^3)–H activation reactions of aliphatic carboxylic acids.

5 Experimental Section

5.1 General Information

Reagents and substrates that are not listed in the experimental section were either previously published or synthesized according to a literature procedure, commercially available, or available in the group from previous projects by coworkers. For the syntheses of starting materials, no attempts of optimization were carried out. The products without literature precedence, were fully characterized.

Reaction Set-up and Working Techniques

Unless otherwise noted, all reactions were conducted in glassware previously dried in an oven at 110 °C. Reaction temperatures are reported as the temperature of the oil bath or the metal block surrounding the reaction vessel.

All reactions were performed using standard laboratory glassware and Schlenk techniques. A silicone oil bath was used for reactions requiring elevated temperatures. Liquids were transferred as follows: for small amounts via Hamilton gas-tight syringes; for large amounts via disposable syringes and cannulas.

Chemicals

Commercial chemicals were obtained from ABCR, Acros Organics, Alfa Aesar, Carbolution, Chempur, Combi-Blocks, Fisher Scientific, Fluka, Fluorochem, Heraeus, Lancaster, Merck, Sigma-Aldrich, Strem Chemicals or TCI Europe and used as received unless otherwise stated. Air or moisture sensitive solid compounds were stored and weighed in a glovebox (MBraun) filled with argon. Air or moisture sensitive liquid compounds were stored in Schlenk flasks and treated under an argon atmosphere using Schlenk techniques.

Solvents

All other dry solvents (< 50 ppm H_2O) were purchased from Acros Organics, Carl Roth or

Sigma-Aldrich and stored over 4 Å molecular sieves under argon in a Schlenk bottle. Pentane, EtOAc, CH_2Cl_2 and Et_2O were distilled prior to use for compound purification techniques such as column chromatography or work-up.

Column and Analytical Thin Layer Chromatography

Flash column chromatography (FCC) was performed using silica gel (60 Å, 0.035–0.070 mm, Acros) and an argon pressure of ~ 0.5 bar. Silica gel 60 F254 aluminum plates (Merck) were used for analytical thin layer chromatography (TLC). The compounds were visualized by the exposure to ultraviolet light (254 nm and 366 nm) and/or by staining. For staining the TLC plates were dipped into a solution of $KMnO_4$ (1 g $KMnO_4$, 6 g K_2CO_3 and 0.1 g KOH in 100 mL H_2O) or bromocresol green (40 mg bromocresol green in 100 mL EtOH; addition of 0.1 M aq. NaOH until the blue colors appears in the solution) and developed with a heat gun if necessary. Flash column chromatography was performed on silica gel (35−70 µm mesh, 60 Å, Acros) with a positive argon overpressure.

NMR Spectroscopy

NMR spectra were measured on a Bruker AV300, DPX300, AV400 or Varian Associated INOVA 500 and a 600 Unity Plus. Chemical shifts δ in ^{1}H and ^{13}C NMR spectra are noted in ppm and calibrated based on residual solvent signals ($CDCl_3$/Chloroform-d: δH = 7.26 ppm, δC = 77.16 ppm; CD_2Cl_2/Methylene Chloride-d_2: δH = 5.30 ppm, δC = 53.84 ppm; CD_3OD/Methanol-d_4: δH = 3.31 ppm, δC = 49.00 ppm; DMSO-d_6: δH = 2.50 ppm, δC = 39.52 ppm). ^{19}F-NMR spectra are not externally calibrated and chemical shifts is givenrelative to CCl_3F as received from the automatic data processing. Chemical shifts are reported with two (1H) or one (all other nuclei) digits after the decimal point. Exceptions are done when required to annotate clearly distinguishable signals observed in very close proximity to one another. NMR-data are reported as follows: chemical shift (multiplicity: s = singlet, d = doublet, t = triplet, q = quartet, quint = quintet, sept = septet, m = multiplet, br = broad), coupling constants (*J*, Hz) and integration). All spectra were processed using the MestReNova program.

Electrospray Ionization-Mass Spectrometry (ESI-MS)

ESI mass spectra or APCI measurements were recorded with a Thermo-Fisher Scientific LTQ

Orbitap LTQ XL with nano spray (alternatively loop injection, syringe pump). ESI mass spectra were measured on a Bruker Daltronics MicroTof with loop injection.

Fourier Transform Infrared Spectroscopy (FT-IR)

Infrared spectra were recorded neat on a Shimadzu FTIR 8400S or a Varian Associates FTIR 3100 Excalibur spectrometer. The wave numbers (ν) of recorded IR-signals are quoted in cm^{-1}.

Gas Chromatography with Flame Ionization Detection (GC-FID)

An Agilent Technologies 7890B GC-system equipped with a HP-CHIRAL-20B column (30 m × 0.25 mm, film thickness: 0.25 µm) and flame ionization detector was used for GC-FID analysis. Temperature program: Starting at 75 °C for 1 minute, raised to 95 °C at 2 °C /min, hold for 2 minutes. Raised to 110 °C at 0.08 °C /min, hold for 2 minutes. Raised to 200 °C at 20 °C /min, hold for 3 minutes. The analysis time was 210 minutes. Product t_1 = 80.9 min, t_2 = 82.2 min.

5.2 Ligand Synthesis

Unless mentioned below, the ligands were commercially available or synthesized using the previously reported protocol.[76e, 147] Some ligands were synthesized by the below procedures.

General Procedure A:

To a solution of the corresponding benzoic acid (10.0 mmol, 1.0 equiv.) in CH_2Cl_2 (40 mL, 0.25 M), $SOCl_2$ (0.87 mL, 12.0 mmol, 1.2 equiv.) was added slowly at 0 °C, followed by DMF (30 µL, 0.39 mmol, 0.04 equiv.) as a catalyst. The mixture was stirred for 4 hours at 50 °C, after which the solvent and volatiles were removed under reduced pressure. The product was used directly in the next step without purification. This crude product was dissolved in CH_2Cl_2 (5 mL) and slowly added to a mixture of ethyl glycinate hydrochloride (1.40 g, 10.0 mmol, 1.0 equiv.) and triethylamine (3.10 mL, 22.0 mmol, 2.2 equiv.) in CH_2Cl_2 (10 mL) at 0 °C. The reaction mixture was stirred for 30 minutes at 0 °C and then allowed to warm to room temperature overnight. The mixture was washed sequentially with 1 M aqueous HCl (2 × 20 mL), saturated aqueous $NaHCO_3$ (2 × 20 mL), and saturated NaCl solution (2 × 20 mL). The combined organic layers were dried over Na_2CO_3, and the solvent was removed under reduced pressure. The resulting product was used directly in the next step without further purification. This product was dissolved in a mixture of MeOH (20 mL) and aqueous NaOH solution (20 wt%, 20 mL) and stirred at 80 °C overnight. MeOH was removed under reduced pressure, and the solution was washed with CH_2Cl_2. The aqueous phase was acidified with concentrated HCl to a pH of 1 and extracted with CH_2Cl_2 (2 × 20 mL). The extracts were concentrated, and the crude product was purified via flash column chromatography.

2-(6–Hydroxypyridin-2-yl)acetic acid (L20)

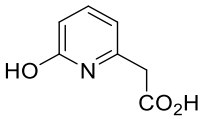

L20

Similar to a procedure by Yu and coworkers.[165] 2,6- difluoropyridine (1.15 g, 10.0 mmol) and acetonitrile (1.23 g, 30.0 mmol) were used. The target compound **L20** was obtained as a colorless solid (0.9 g, 5.9 mmol, 59%).

^{1}H-NMR (500 MHz, DMSO-d6): δ = 12.04 (br, 2H), 7.35 (dd, J = 9.2, 6.7 Hz, 1H), 6.20 (dd,

J = 9.2, 1.1 Hz, 1H), 6.07 (dd, J = 6.8, 1.0 Hz, 1H), 3.50 (s, 2H). ppm

^{13}C-NMR (126 MHz, DMSO-d6): δ = 170.53, 162.90, 142.89, 140.83, 117.56, 105.65, 38.03.ppm

HRMS (ESIpos) m/z: Calcd for $C_7H_8NO_3^+$ 154,0499, Found 154.0496

IR (cm^{-1}): 3707, 2981, 1707, 1618, 1541, 1275, 1260, 1054, 1032, 1012, 764.

3-(2,6-difluorophenyl)-2-(2-(trifluoromethyl)benzamido)propanoic acid (L38)

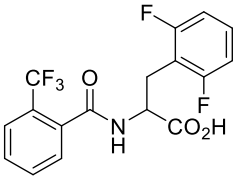

L38

Following the general procedure A, 2-(trifluoromethyl)benzoyl chloride (650 mg, 3.10 mmol) and methyl 2-Amino-3-(2,6-difluorophenyl) propanoate (470 mg, 3.70 mmol) the target compound **L38** was obtained as a colorless solid (750 mg, 2.00 mmol, 64%). A mixture of pentane and EtOAc (50:50 - 60:40 v/v) acidified with HCOOH (0.2 mL for 100 mL of solvent mixture) was used as eluent for silica gel column chromatography.

^{1}H NMR (500 MHz, $(CD_3)_2CO$): δ = 7.89 (d, *J* = 8.3 Hz, 1H), 7.75 – 7.71 (m, 1H), 7.70 – 7.65 (m, 1H), 7.65 – 7.60 (m, 1H), 7.50 – 7.46 (m, 1H), 7.39 – 7.31 (m, 1H), 7.04 – 6.95 (m, 1H), 5.06 – 5.01 (m, 1H), 3.39 (dd, *J* = 13.9, 5.9 Hz, 1H), 3.24 (dd, *J* = 13.9, 9.2 Hz, 1H) ppm

^{13}C NMR (126 MHz, $CDCl_3$): δ = 172.3, 167.9, 163.8 (d, *J* = 8.4 Hz), 161.8 (d, *J* = 8.4 Hz), 137.0, 132.9, 130.7, 130.0 (q, *J* = 5 Hz), 129.4, 127.8, 127.1, 124.6 (q, *J* = 273.0 Hz) 112.1-111.9 (m), 52.5, 25.7 ppm.

HRMS (ESIpos) m/z: Calcd for $C_{17}H_{13}F_5NO_3$ 374.0810, Found 374.0802

IR (cm^{-1}): 3268, 1710, 1654, 1544, 1471, 1315, 1265, 1176, 1035, 978, 784.

3-(2,6-difluorophenyl)-2-(2,4,6-trimethylbenzamido)propanoate (L39)

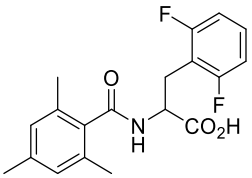

L39

Following the general procedure A, 2,4,6-trimethylbenzoyl chloride (1.3 g, 7.0 mmol) and methyl 2-Amino-3-(2,6-difluorophenyl)propanoate (1.81g, 8.4 mmol) the target compound **L39** was obtained as a colorless solid (1.6 g, 4.6 mmol, 66%).

^{1}H-NMR (500 MHz, $(CD_3)_2CO$): δ = 7.52 (d, J = 9.0 Hz, 1H), 7.40 – 7.30 (m, 1H), 7.05 – 6.96 (m, 2H), 6.84 – 6.75 (m, 2H), 5.18 – 5.10 (m, 1H), 3.42 – 3.34 (m, 1H), 3.21 (dd, J = 14.1, 10.3 Hz, 1H), 2.21 (d, J = 0.7 Hz, 3H), 2.05 (s, 6H). ppm

^{13}C-NMR (126 MHz, $(CD_3)_2CO$): δ = 172.77, 170.55, 162.83 (d, J = 254.3 Hz), 138.54, 136.17, 135.08, 129.89 (t, J = 10.4 Hz), 128.57, 114.45, 112.82 – 111.44 (m), 51.81, 25.58, 21.03, 19.02. ppm

^{19}F NMR (471 MHz, $(CD_3)_2CO$) δ = -114.46.

HRMS (ESIpos) m/z: Calcd for $C_{19}H_{20}F_2NO_3^+$ 348.1406, Found 348.1396

IR (cm^{-1}): 3274, 2921, 1711, 1647, 1535, 1467, 1300, 1266, 1090, 1068, 975, 782.

2-(6–Hydroxypyridin-2-yl)-N-(methylsulfonyl)acetamide (L61)

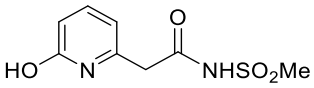

L61

Similar to a procedure by our group.[147] 2-(6-methoxypyridin-2-yl)acetic acid(0.84g, 5.0 mmol) and methanesulfonamide(0.52g, 5.5 mmol) were used, and then hydrolysed by using known procedure. The target compound **L61** was obtained as a colorless solid (0.89 g, 3.9 mmol, 78%).

^{1}H-NMR (500 MHz, DMSO-d6): δ = 11.93 (s, 1H), 11.55 (s, 1H), 7.36 (dd, J = 9.1, 6.7 Hz, 1H), 6.22 (d, J = 9.1 Hz, 1H), 6.07 (s, 1H), 3.56 (s, 2H), 3.24 (s, 3H). ppm

^{13}C-NMR (126 MHz, DMSO-d6): δ = 168.80, 163.35, 141.25, 118.66, 106.22, 41.54, 6.82,

0.58.ppm

HRMS (ESIpos) m/z: Calcd for $C_8H_{11}N_2O_4S^+$ 231.0434, Found 231.0429

IR (cm^{-1}): 3136, 1689, 1671, 1634, 1465, 1356, 1331, 1135, 973, 870, 778.

General procedure B:

Ethyl 3-aminopropanoate hydrochloride (1.3 g, 8.4 mmol, 1.2 equiv.) and triethylamine (2.9 mL, 25 mmol 3.0 equiv.) were dissolved in CH_2Cl_2 (30 mL), the reaction mixture was cooled to 0 °C and the required benzoyl chloride derivative (1.0 equiv, 7.0 mmol) was added dropwise. The reaction mixture was stirred for 30 min at 0 °C and was then allowed to slowly warm to room temperature overnight. The reaction mixture was diluted with CH_2Cl_2 (10 mL), and washed with 1 M aqueous HCl solution (2 × 60 mL), followed by saturated $NaHCO_3$ solution (2 × 60 mL). The combined organic phases were dried over $MgSO_4$ and the solvent was removed under reduced pressure. The product was used in the following step without further purification.

The product from the previous step was dissolved in a mixture (1:1 v/v) of THF (20 mL) and H_2O (20 mL). $LiOH{\cdot}H_2O$ (2.0 equiv.) was added and the reaction mixture was stirred at room temperature for 6 h. THF was removed under reduced pressure and the solution was washed with EtOAc (2 × 10 mL). The aqueous phase was acidified with conc. aq. HCl to reach a pH value of 2-3 and extracted with EtOAc (3 × 10 mL). The extracts were concentrated under reduced pressure and the crude product was purified via silica gel column chromatography using a mixture of pentane and EtOAc (30:70 - 20:80 v/v) acidified with HCOOH (0.2 mL for 100 mL of solvent mixture) as the eluent.

3-(2,4,6-trimethylbenzamido)butanoic acid (L46)

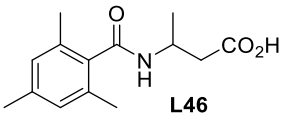

L46

Following the general procedure B, using 2,4,6-trimethylbenzoyl chloride (1.3 g) and methyl 3-aminobutanoate hydrochloride (1.3 g, 8.3 mmol) the target compound **L46** was obtained as a colorless solid (1.2 g, 5.1 mmol, 72%). A mixture of pentane and EtOAc (30:70 - 60:40 v/v) acidified with HCOOH (0.2 mL for 100 mL of solvent mixture) was used as eluent for silica gel column chromatography. This synthesis was carried out by Sourjya Mal.

^{1}H NMR (500 MHz, $(CD_3)_2CO$): δ = 7.20 (d, *J* = 6.4 Hz, 1H (N–H)), 6.80 (s, 2H), 4.51 (m, 1H), 2.70 (dd, *J* = 15.6, 6.6 Hz, 1H), 2.54 (dd, *J* = 15.6, 6.9 Hz, 1H), 2.22 (s, 3H), 2.21 (s, 6H), 1.32 (d, *J* = 6.7 Hz, 3H) ppm.

^{13}C NMR (126 MHz, $(CD_3)_2CO$): δ = 172.7, 169.6, 138.3, 136.9, 134.7, 128.6, 43.2, 40.9, 21.0, 20.5, 19.1 ppm.

HRMS (ESIpos) m/z: Calcd for $C_{14}H_{20}NO_3$ 250.1437, Found 250.1432

IR (cm^{-1}): 3231, 2966, 1714, 1635, 1612, 1546, 1405, 1304, 1228, 1181, 1107, 925, 680.

3-(2,4,6-triisopropylbenzamido)butanoic acid (L47)

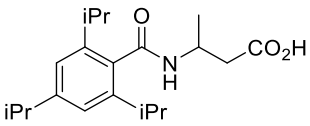

L47

Following the general procedure B, using 2,4,6-triisopropylbenzoyl chloride (2.67g, 10.0 mmol) and methyl 3-aminoisobutanoate hydrochloride (1.53g, 10.0 mmol) the target compound **L47** was obtained as a colorless solid (1.53 g, 4.60 mmol, 46%).

^{1}H-NMR (500 MHz, $(CD_3)_2CO$): δ = 7.28 (d, J = 8.3 Hz, 1H), 7.03 (s, 2H), 4.61 – 4.52 (m, 1H), 3.09 – 2.98 (m, 2H), 2.93 – 2.81 (m, 1H), 2.74 (dd, J = 15.7, 6.4 Hz, 1H), 2.54 (dd, J = 15.7, 7.1 Hz, 1H), 1.33 (d, J = 6.7 Hz, 3H), 1.26 – 1.14 (m, 18H). ppm

^{13}C-NMR (126 MHz, $(CD_3)_2CO$): δ = 172.68, 169.77, 149.87, 145.64, 135.76, 121.27, 43.24, 40.95, 35.16, 31.45, 31.38, 24.87, 24.77, 24.52, 24.38, 20.58. ppm

HRMS (ESIpos) m/z: Calcd for $C_{20}H_{32}NO_3^+$ 334.2377 Found 334.2368

IR (cm^{-1}): 3707, 3265, 2956, 2844, 1697, 1631, 1508, 1454, 1361, 1275, 1032, 750.

3-methyl-3-(2,4,6-trimethylbenzamido)butanoic acid (L83)

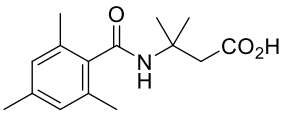

L83

Following the general procedure B, using 2,4,6-trimethylbenzoyl chloride (1.3g 7.0 mmol) and methyl 3-amino-3-methylbutanoate(1.08 g, 8.3 mmol) the target compound **L83** was obtained as a colorless solid (1.14 g, 4.34 mmol, 62%).

^{1}H-NMR (500 MHz, $(CD_3)_2CO$): 7.02 (s, 1H), 6.80 – 6.76 (m, 2H), 2.96 (s, 2H), 2.24 (s, 6H), 2.22 (s, 3H), 1.57 (s, 6H). ppm

^{13}C-NMR (126 MHz, $(CD_3)_2CO$): δ = 172.66, 170.27, 138.12, 137.37, 134.72, 128.55, 52.89, 44.08, 27.20, 21.02, 19.12. ppm

HRMS (ESIpos) m/z: Calcd for $C_{15}H_{22}NO_3^+$ 264.1594, Found 264.1587

IR (cm^{-1}): 3327, 2976, 1729, 1602, 1554, 1354, 1226, 1163, 866, 853, 676.

4-phenyl-3-(2,4,6-trimethylbenzamido)butanoic acid (L60)

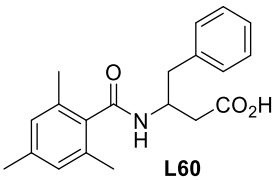

L60

Following the general procedure B, using 2,4,6-trimethylbenzoyl chloride (1.82g, 10.0 mmol) and methyl 3-amino-4-phenylbutanoate hydrochloride(2.75g, 12.0 mmol) the target compound **L60** was obtained as a colorless solid (2.21 g, 6.8 mmol, 68%).

^{1}H-NMR (500 MHz, $(CD_3)_2CO$): δ = 7.38 – 7.28 (m, 4H), 7.27 – 7.20 (m, 1H), 6.76 (h, J = 0.6 Hz, 2H), 4.77 (dddd, J = 13.9, 8.5, 7.4, 6.4 Hz, 1H), 3.02 (d, J = 7.4 Hz, 2H), 2.76 – 2.58 (m, 2H), 2.21 (s, 3H), 2.05 (s, 6H). ppm

^{13}C-NMR (126 MHz, $(CD_3)_2CO$): δ = 172.77, 169.87, 139.73, 138.26, 136.82, 134.82, 130.17,

129.19, 128.51, 127.19, 48.82, 40.87, 39.07, 21.01, 19.06. ppm

HRMS (ESIpos) m/z: Calcd for $C_{20}H_{24}NO_3^+$ 326.1751, Found 326.1741

IR (cm^{-1}): 3680, 2981, 1705, 1627, 1552, 1275, 1260, 1054, 1032, 850, 764.

5.3 Pd-Catalyzed Direct β-C(sp^3)–H-Amination of Free Carboxylic Acids

General procedure C:

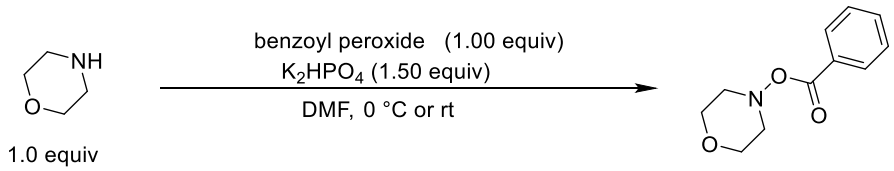

To a reaction flask under argon was added dipotassium hydrogen phosphate (1.5-2.0 equiv.) and benzoyl peroxide (1.0 equiv.), followed by DMF (0.2 M). With vigorous stirring, the secondary amine (1.5 equiv.) was added, and the resulting mixture stirred at 0 °C or room temperature until complete conversion of the benzoyl peroxide, as indicated by TLC. After the reaction was completed, water was added and the mixture was diluted with ethyl acetate. The layers were separated and the organic layer was washed with water and brine, dried over anhydrous MgSO4 and concentrated under reduced pressure. The residue was then chromatographed on silica gel to afford the desired compound.

Morpholino benzoate (18)

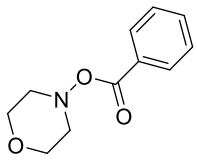

18 Following the general procedure C, purified with flash column chromatography (pentane:EtOAc 3:1) to afford the desired product a colorless solid (81%).

^{1}H NMR (400 MHz, $CDCl_3$): δ 8.08-7.96 (m, 2H), 7.64-7.52 (m, 1H), 7.51-7.39 (m, 2H), 4.07-3.80 (m, 4H), 3.53-3.39 (m, 2H), 3.05 (s, 2H). Analytical data are in accordance with the literature values.[166]

General procedure D:

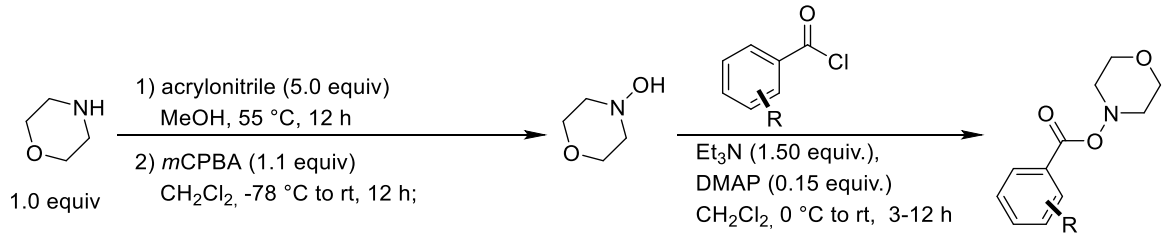

A dry and argon flushed flask equipped with a magnetic stirring bar and a septum, morpholine (1.00 equiv) was dissolved in dry MeOH (0.5 M). To the resulting solution, acrylonitrile (5.00 equiv) was added and the reaction mixture was stirred at 55 °C overnight. The solvent was evaporated and the resulting crude purified by flash column chromatography to afford the 1,4-addition product which used for next step directly without purification.

A dry and argon flushed flask equipped with a magnetic stirring bar and a septum was charged with 1,4-addition product (1.00 equiv) and dissolved in dry CH_2Cl_2 (0.2 M). The solution was cooled to -78 °C and *m*CPBA (1.10 equiv) was added slowly as a solution in dry CH_2Cl_2 (0.2 M). The mixture was stirred at -78 °C for 1 h. Following, the cooling bath was removed and the mixture stirred at rt overnight. The solvent was removed and the acid by-product removed by filtration through a silica plug.

After solvent removal, the resulting N-hydroxylamine (1.00 equiv.) and DMAP (0.15 equiv.) were dissolved in anhydrous CH_2Cl_2 (0.4 M) with stirring. Anhydrous Et_3N (1.50 equiv.) was added, and the solution was cooled to 0 °C, followed by the dropwise addition of acyl chloride (1.05 equiv.) over 5 min. The solution was allowed to slowly warm to rt (3 h) and stirred at this temperature or kept at 5 °C until completion. Next, sat. aq. $NaHCO_3$ solutionwas added, and the mixture was vigorously stirred for 10 min. The organic layer was separated, and the aqueous layer extracted with CH_2Cl_2. The combined organic extracts were washed with brine, dried over Na_2SO_4, filtered, and the volatiles removed. The residue was purified by flash column chromatography on silica gel to afford the desired compound.

Morpholino 2,6-dimethoxybenzoate (19)

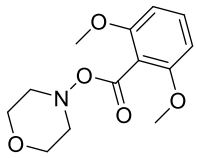

19 Following the general procedure D, using 2,6-dimethoxybenzoyl chloride and flash column chromatographic purification (pentane/EtOAc 1:3) afforded the desired product (89% yield) as an amorphous colorless solid.

^{1}H NMR (400 MHz, $CDCl_3$): δ 7.29 (t, J = 8.4 Hz, 1H), 6.54 (d, J = 8.4 Hz, 2H), 3.93 – 3.86 (m, 4H), 3.81 (s, 6H), 3.47 – 3.43 (m, 2H), 3.02 – 2.97 (m, 2H) ppm. Analytical data are in accordance with the literature values.[167]

Morpholino 4-(dimethylamino)benzoate (20)

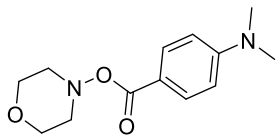

20 Following the general procedure D, using 4-(dimethylamino)benzoyl chloride and flash column chromatographic purification (pentane/EtOAc 2:3) afforded desired product (74% yield) as a gray solid.

^{1}H NMR (400 MHz, $CDCl_3$): δ 7.97 (d, J = 8.8 Hz, 2H), 6.92 (d, J = 8.8 Hz, 2H), 3.97 (d, J = 8.5 Hz, 2H), 3.89–3.82 (m, 5H), 3.44 (d, J = 9.3 Hz, 2H), 3.09–2.94 (m, 2H) ppm. Analytical data are in accordance with the literature values.[167]

Morpholino 4-nitrobenzoate (21)

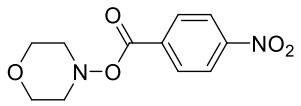

21 Following the general procedure D, using 4-nitrobenzoyl chloride and flash column chromatographic purification (pentane/EtOAc1:3) afforded desired product (79% yield) as a colorless solid.

^{1}H NMR (400 MHz, $CDCl_3$): δ 8.34 – 8.26 (m, 2H), 8.23 – 8.16 (m, 2H), 4.04 – 3.81 (m, 4H), 3.48 (d, J = 10.5 Hz, 2H), 3.09 (t, J = 9.9 Hz, 2H) ppm. Analytical data are in accordance with the literature values.[168]

Morpholino 4-(trifluoromethyl)benzoate (22)

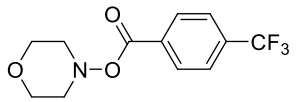

22 Following the general procedure D, using 4-(trifluoromethyl)benzoyl chloride and flash column chromatographic purification (pentane/EtOAc1:3) afforded desired product (66% yield) as a colorless solid.

^{1}H NMR (400 MHz, $CDCl_3$): δ 8.13 (d, J = 8.4 Hz, 2H), 7.72 (d, J = 8.3 Hz, 2H), 4.00 (d, J = 11.5 Hz, 2H), 3.87 (t, J = 11.2 Hz, 2H), 3.47 (d, J = 9.7 Hz, 2H), 3.07 (t, J = 9.3 Hz, 2H) ppm. Analytical data are in accordance with the literature values.[168]

Morpholino 3,5-bis(trifluoromethyl)benzoate (23)

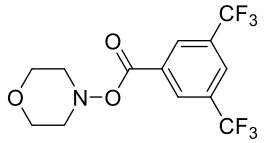

23 Following the general procedure D, using 4-(dimethylamino)benzoyl chloride and flash column chromatographic purification (pentane/EtOAc 1:3) afforded desired

product (63% yield) as a colorless solid.

^{1}H NMR (400 MHz, $CDCl_3$): δ 8.44 – 8.43 (m, 2H), 8.08 – 8.07 (m, 1H), 4.02 – 3.98 (m, 2H), 3.90 – 3.84 (m, 2H), 3.49 – 3.46 (m, 2H), 3.13 – 3.07 (m, 2H) ppm. 13C NMR (101 MHz, CDCl3): δ 162.1, 132.5 (q, J = 34.0 Hz), 131.5, 129.7 (q, J = 4.0 Hz), 127.0 – 126.7 (m), 124.3, 122.9 (q, J = 271.0 Hz), 66.0, 57.4 ppm. Analytical data are in accordance with the literature values.[169]

Morpholino 2,6-difluorobenzoate (24)

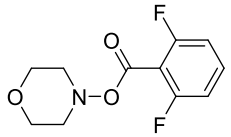

24 Following the general procedure D, using 2,6-difluorobenzoyl chloride and flash column chromatographic purification (pentane/EtOAc 1:3) afforded desired product (78% yield) as a colorless solid.

^{1}H NMR (400 MHz, $CDCl_3$): δ 7.44 (tt, J = 8.5, 6.2 Hz, 1H), 6.97 (t, J = 8.1 Hz, 2H), 3.97 (d, J = 11.6 Hz, 2H), 3.83 (t, J = 11.1 Hz, 2H), 3.47 (d, J = 10.0 Hz, 2H), 3.05 (t, J = 9.1 Hz, 2H). ppm. Analytical data are in accordance with the literature values.[167]

Morpholino2,4,6-trichlorobenzoate (25)

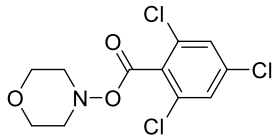

25 Following the general procedure D, using 2,4,6-trichlorobenzoyl chloride and flash column chromatographic purification (pentane/EtOAc 1:4) afforded desired product (83% yield) as a colorless solid.

^{1}H NMR (400 MHz, $CDCl_3$): δ 7.36 (s, 2H), 3.98 – 3.79 (m, 4H), 3.50 – 3.47 (m, 2H), 3.08 – 3.01 (m, 2H) ppm. Analytical data are in accordance with the literature values.[169]

Morpholino 2,3,4,5,6-pentafluorobenzoate (26)

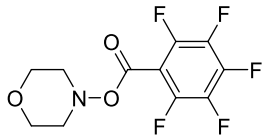

26

Following the general procedure D, using pentafluorobenzoyl chloride and flash column chromatographic purification (pentane/EtOAc 1:4) afforded desired product (81% yield) as a colorless solid.

^{1}H NMR (400 MHz, $CDCl_3$): δ 3.99 – 3.96 (m, 2H), 3.85 – 3.79 (m, 2H), 3.48 – 3.45 (m, 2H), 3.08 – 3.03 (m, 2H) ppm. Analytical data are in accordance with the literature values.[169]

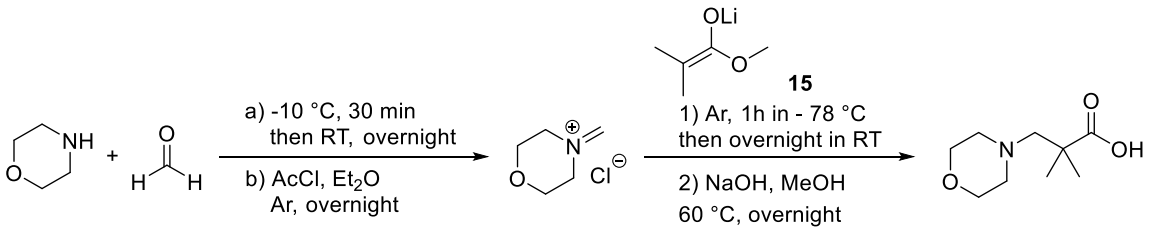

To a round-bottom flask charged with morpholine (2.00 equiv.) and a magnetic stir-bar at 0 °C, an aqueous solution of formaldehyde (37%, 1.00 equiv.) was added dropwise and the resulting biphasic mixture was stirred vigorously at ambient temperature (23 °C) for 12 h. The biphasic mixture was separated, and the aqueous phase was extracted with ethyl acetate (3 ×). The organic phases were combined, dried over anhydrous sodium sulfate and concentrated under reduced pressure, the affording aminals is purity enough for further use. Acetylchloride (1.20 equiv.) in diethylether (2 M) was added drop-wise to an ice cooled suspension of aminals (1.00 equiv.). The mixture was stirred overnight at room temperature. The iminium salt was collected by filtration, washed with diethyl ether and then dried under vacuum.

An oven dried argon filled roundbottom flask was charged with iPr_2NH (1.3 equiv.), THF and n-BuLi (1.2 equiv., 1.6M in hexane) was added slowly. The reaction mixture was stirred at rt for 1 h. The solution was cooled to −78 °C, methylisobutyrate (1.0 equiv.) was added and the mixture was stirred for 1 h. The above iminium salt (1.0 equiv.) was added and the reaction

mixture was stirred overnight while being allowed to warm to rt. water was added to the reaction mixture and the reaction mixture was concentrated under reduced pressure, the residue was transferred to a Schlenk tube with MeOH and aq. NaOH (10 wt%) was added. The reaction mixture was heated to 60 °C and stirred for 16h. The mixture was allowed to cool to rt and was concentrated under reduced pressure. Water was added and the resulting mixture was washed with CH_2Cl_2. The aqueous phase was acidified with HCl (10 wt%) until the pH reached between 1 and 4 and was extracted with CH_2Cl_2 (3 ×). The combined organic phases were dried over $MgSO_4$ and the solvent was removed under reduced pressure. The crude product was purified by silica gel column chromatography.

2,2-Dimethyl-3-morpholinopropanoic acid (17)

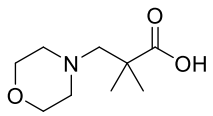

17 . Following the above procedure, purification (CH_2Cl_2: MeOH: AcOH = 90:10:0.3) afforded desired product as a colorless liquid.

^{1}H NMR (400 MHz, $CDCl_3$): δ 3.84 (t, *J* = 4.7 Hz, 4H), 2.90 (t, *J* = 4.6 Hz, 4H), 2.71 (s, 2H), 1.27 (s, 6H) ppm.

5.4 Pd-Catalyzed Direct β-C(sp^3)–H–Hydroxylation of Free Carboxylic Acids

All carboxylic acid substrates were synthesized following the procedures reported in our previous publications.[76e, 123]

General Procedure E of the Hydroxylation of Carboxylic Acids and Isolation as the Corresponding Benzyl Ester

An oven dried 10 mL Schlenk tube was charged with $Pd(OAc)_2$ (4.5 mg, 0.020 mmol, 10 mol%), **L20** (7.6 mg, 0.050 mmol, 25 mol%), K_2HPO_4 (122 mg, 700 µmol, 3.5 equiv.), DMF (77 µL,

1.0 mmol, 5 equiv.), TBHP (70% in H_2O, 116 µL, 800 µmol, 4 equiv.) carboxylic acid (0.200 mmol, 1.0 equiv.) and HFIP (2.0 mL). The reaction mixture was stirred at 100 °C for 15 h in a preheated metal block. The reaction mixture was allowed to cool to rt and formic acid (0.2 mL) was added. The mixture was filtered through a pad of Celite® using CH_2Cl_2 (30 mL) to complete the elution and the volatiles were removed under reduced pressure. Cs_2CO_3 (425 mg, 1.30 mmol, 6.5 equiv.), NaI (15 mg, 0.10 mmol, 0.50 equiv.), benzyl bromide (118 µL, 1.00 mmol, 5.0 equiv.) and acetone (5 mL) were added and the resulting the mixture was stirred at rt for 24 h. The mixture was filtered through a pad of Celite® using CH_2Cl_2 (20 mL) as eluent and all volatiles were removed under reduced pressure. The resulting mixture was diluted with CH_2Cl_2 (10 mL) and was washed with H_2O (4 × 20 mL), the organic layer was concentrated under reduced pressure and subsequent purification by silica gel column chromatography afforded the desired product in the form of benzyl ester.

Benzyl 2-(hydroxymethyl)-4-methylpentanoate

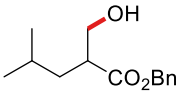

40-Bn

Following the general procedure E, pentane/Et_2O (60:40 v/v) as an eluent, the target compound **40-Bn** was obtained as a colorless oil (19.8 mg, 0.88 mmol, 42%).

^{1}H-NMR (500 MHz, $CDCl_3$): δ = 7.35 (m, 5H), 5.16 (s, 2H), 3.75 (t, J = 5.4 Hz, 2H), 2.72 (m, 1H), 2.12 – 2.05 (m, 1H), 1.64 – 1.53 (m, 2H), 1.38 – 1.30 (m, 1H), 0.91 (d, J = 6.3 Hz, 3H), 0.88 (d, J = 6.3 Hz, 3H).

^{13}C-NMR (126 MHz, $CDCl_3$): δ = 175.51, 135.82, 128.58, 128.26, 128.08, 66.38, 63.52, 45.74, 37.45, 25.87, 22.52, 22.36 ppm

HRMS (ESIpos) m/z: Calcd for $C_{14}H_{24}NO_3$ 254.1750, Found 254.1744

Benzyl 3-cyclopropyl-2-(hydroxymethyl)propanoate

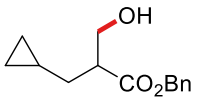

41-Bn

Following the general procedure E, pentane/Et_2O (60/30 v/v) as an eluent, the target compound **41-Bn** was obtained as colorless oil (22.5 mg, 0.96 mmol, 48%).

^{1}H-NMR (500 MHz, $CDCl_3$): δ = 7.40 – 7.30 (m, 5H), 5.17 (s, 2H), 3.92 – 3.77 (m, 2H), 2.76 (m, 1H), 2.17 (t, J = 6.4 Hz, 1H), 1.60 – 1.48 (m, 2H), 0.73 – 0.64 (m, 1H), 0.49 – 0.36 (m, 2H), 0.09 – 0.00 (m, 2H) ppm.

^{13}C-NMR (126 MHz, $CDCl_3$): δ = 175.19, 135.75, 66.43, 62.93, 48.06, 33.54, 8.79, 4.79, 4.43 ppm.

HRMS (ESIpos) m/z: Calcd for $C_{14}H_{22}NO_3$ 252.1594, Found 252.1588

Benzyl 2-cyclobutyl-3–Hydroxypropanoate

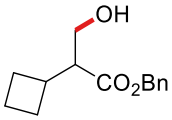

42-Bn

Following the general procedure E, pentane/Et_2O (60/30 v/v) as an eluent, the target compound **42-Bn** was obtained as a colorless oil (21.1 mg,0.9 mmol, 45%).

^{1}H-NMR (500 MHz, $CDCl_3$): δ = 7.40 – 7.29 (m, 5H), 5.15 (q, J = 12.4 Hz, 2H), 3.71 (d, J = 5.4 Hz, 2H), 2.66 – 2.50 (m, 2H), 2.13 – 1.95 (m, 3H), 1.90 – 1.72 (m, 4H) ppm.

^{13}C-NMR (126 MHz, $CDCl_3$): δ = 174.36, 135.83, 66.33, 61.38, 53.66, 34.67, 27.41, 27.29, 18.46 ppm.

HRMS (ESIpos) m/z: Calcd for $C_{14}H_{22}NO_3$ 252.1594, Found 252.1585

Benzyl 3-cyclopentyl-2-(hydroxymethyl)propanoate

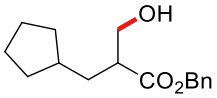

43-Bn

Following the general procedure E, pentane/Et_2O (60/30 v/v) as an eluent, the target compound **43-Bn** was obtained as a colorless oil (27.2 mg, 1.0 mmol, 52%).

^{1}H-NMR (500 MHz, $CDCl_3$): δ = 7.40 – 7.28 (m, 5H), 5.21 – 5.12 (m, 2H), 3.82 – 3.72 (m, 2H), 2.73 – 2.64 (m, 1H), 2.10 (t, J = 6.3 Hz, 1H), 1.84 – 1.67 (m, 4H), 1.65 – 1.43 (m, 5H), 1.11 – 1.00 (m, 2H) ppm.

^{13}C-NMR (126 MHz, $CDCl_3$): δ = 175.49, 135.84, 128.57, 128.26, 128.11, 66.36, 63.46, 47.06, 37.87, 34.73, 32.68, 32.63, 25.04, 25.01 ppm.

HRMS (ESIpos) m/z: Calcd for $C_{16}H_{26}NO_3$ 280.1907, Found 280.1901

Benzyl 2-(hydroxymethyl)-5-methoxypentanoate

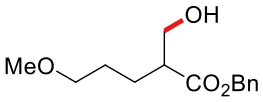

47-Bn

Following the general procedure E, pentane/Et_2O (60/30 v/v) as an eluent, the target compound **47-Bn** was obtained as a colorless oil (25.7 mg, 1.0 mmol, 51%).

^{1}H-NMR (500 MHz, $CDCl_3$): δ = 7.39 – 7.30 (m, 5H), 5.16 (s, 2H), 3.82 – 3.74 (m, 2H), 3.35 (td, J = 6.1, 2.1 Hz, 2H), 3.30 (s, 3H), 2.69 – 2.60 (m, 1H), 1.78 – 1.56 (m, 5H) ppm.

^{13}C-NMR (126 MHz, $CDCl_3$): δ = 174.94, 135.77, 128.60, 128.30, 128.14, 72.24, 66.44, 63.04, 47.29, 30.31, 27.13, 25.08 ppm.

HRMS (ESIpos) m/z: Calcd for $C_{14}H_{21}O_4$ 253.1434, Found 253.1429

Benzyl 2-(hydroxymethyl)-5-phenoxypentanoate

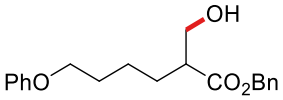

48-Bn

Following the general procedure E, pentane/Et_2O (60:40 v/v) as an eluent, the target compound **48-Bn** was obtained as a colorless oil (31.7 mg, 96.5 µmol, 48%).

^{1}H-NMR (500 MHz, $CDCl_3$): δ = 7.37 – 7.31 (m, 5H), 7.30 – 7.26 (m, 2H), 6.95-6.92 (m, 1H), 6.89 – 6.85 (m, 2H), 5.19 (d, *J* = 12.3 Hz, 1H), 5.16 (d, *J* = 12.3 Hz, 1H), 3.91 (t, *J* = 6.4 Hz, 2H), 3.84 – 3.75 (m, 2H), 2.71 – 2.64 (m, 1H), 1.81 – 1.71 (m, 3H), 1.67-1.60 (m, 1H), 1.53-1.46 (m, 2H) ppm.

^{13}C-NMR (126 MHz, $CDCl_3$): δ = 175.2, 159.1, 135.9, 129.5, 128.7, 128.5, 128.3, 120.7, 114.6, 67.5, 66.6, 63.2, 47.6, 29.3, 28.3, 24.0 ppm.

HRMS (ESIpos) m/z: Calcd for $C_{20}H_{28}F_3O_4N$ 346.2012, Found 346.2010

Benzyl 2-(hydroxymethyl)-5-phenylpentanoate

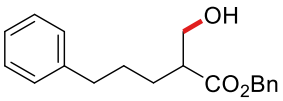

49-Bn

Following the general procedure E, pentane/Et_2O (60/30 v/v) as an eluent, the target compound **49-Bn** was obtained as a colorless oil (26.8 mg, 0.9 mmol, 45%).

^{1}H-NMR (500 MHz, $CDCl_3$): δ = 7.39 – 7.30 (m, 5H), 7.28 – 7.23 (m, 2H), 7.19 – 7.15 (m, 1H), 7.13 – 7.08 (m, 2H), 5.21 – 5.10 (m, 2H), 3.83 – 3.68 (m, 2H), 2.69 – 2.64 (m, 1H), 2.59 (t, J = 7.3 Hz, 2H), 2.13 (s, 1H), 1.72 – 1.54 (m, 4H) ppm.

^{13}C-NMR (126 MHz, $CDCl_3$): δ = 175.07, 141.81, 135.76, 128.62, 128.35, 128.33, 128.20, 125.84, 66.44, 47.40, 35.68, 28.94, 28.08 ppm.

HRMS (ESIpos) m/z: Calcd for $C_{19}H_{23}O_3$ 299.1642, Found 299.1636

Benzyl 2-(3,4-dimethylbenzyl)-3–Hydroxypropanoate

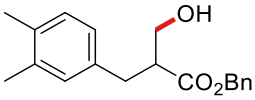

50-Bn

Following the general procedure E, pentane/Et_2O (60/30 v/v) as an eluent, the target compound **50-Bn** was obtained as a colorless oil (23.8 mg, 0.8 mmol, 40%).

^{1}H-NMR (500 MHz, $CDCl_3$): δ = 7.36 – 7.31 (m, 3H), 7.27 – 7.23 (m, 2H), 7.02 (d, J = 7.6 Hz, 1H), 6.93 (d, J = 2.0 Hz, 1H), 6.89 (dd, J = 7.6, 1.9 Hz, 1H), 5.17 – 5.06 (m, 2H), 3.80 – 3.69 (m, 2H), 2.96 (dd, J = 13.1, 6.5 Hz, 1H), 2.92 – 2.85 (m, 1H), 2.80 (dd, J = 13.1, 7.9 Hz, 1H), 2.22 (s, 3H), 2.20 (s, 3H), 2.13 (t, J = 6.4 Hz, 1H) ppm.

^{13}C-NMR (126 MHz, $CDCl_3$): δ = 174.62, 136.63, 135.72, 135.64, 134.69, 130.21, 129.74, 128.54, 128.25, 128.13, 126.27, 66.48, 62.34, 49.22, 33.99, 19.71, 19.32 ppm.

HRMS (ESIpos) m/z: Calcd for $C_{19}H_{23}O_3$ 299.1642, Found 299.1636

Benzyl 3–Hydroxy-2-((1,2,3,4,5,6,7,8-octahydroanthracen-9-yl)methyl)propanoate

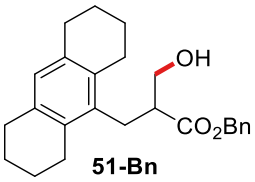

51-Bn

Following the general procedure E, pentane/Et_2O (60/30 v/v) as an eluent, the target compound **51-Bn** was obtained as a colorless oil (22.7 mg, 0.6 mmol, 30%).

^{1}H-NMR (500 MHz, $CDCl_3$): δ = 7.40 – 7.26 (m, 3H), 7.24 – 7.19 (m, 2H), 6.73 (s, 1H), 5.16 – 5.05 (m, 2H), 3.83 – 3.70 (m, 2H), 3.07 – 2.97 (m, 1H), 2.98 – 2.84 (m, 2H), 2.69 (m, 8H), 2.27 (dd, J = 7.1, 5.7 Hz, 1H), 1.82 – 1.65 (m, 8H) ppm.

^{13}C-NMR (126 MHz, $CDCl_3$): δ = 175.21, 135.61, 135.13, 134.72, 133.24, 128.83, 128.51, 128.17, 127.84, 66.48, 62.48, 47.08, 29.94, 26.73, 26.70, 23.73, 22.83 ppm.

HRMS (ESIpos) m/z: Calcd for $C_{25}H_{34}O_3N$ 396.2533, Found 396.2524

Benzyl 3–Hydroxy-2-(naphthalen-2-ylmethyl)propanoate

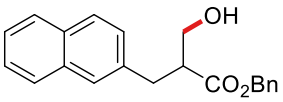

52-Bn

Following the general procedure E, pentane/Et_2O (60/30 v/v) as an eluent, the target compound **52-Bn** was obtained as a colorless oil (23.0 mg, 0.72 mmol, 36%).

^{1}H-NMR (500 MHz, $CDCl_3$): δ = 7.83 – 7.77 (m, 1H), 7.76 – 7.72 (m, 2H), 7.63 – 7.59 (m, 1H), 7.49 – 7.40 (m, 2H), 7.33 – 7.21 (m, 4H), 7.19 – 7.15 (m, 2H), 5.18 – 5.05 (m, 2H), 3.85 – 3.74 (m, 2H), 3.19 (dd, J = 12.9, 6.4 Hz, 1H), 3.10 – 2.91 (m, 2H), 2.18 (s, 1H) ppm.

^{13}C-NMR (126 MHz, $CDCl_3$): δ = 174.45, 135.91, 135.49, 133.50, 132.28, 128.51, 128.26, 128.21, 128.12, 127.61, 127.56, 127.47, 127.22, 126.08, 125.54, 66.58, 62.38, 34.60 ppm.

HRMS (ESIpos) m/z: Calcd for $C_{21}H_{21}O_3$ 321.1485, Found 321.1469

Benzyl 3–Hydroxy-2-(3-methoxybenzyl)propanoate

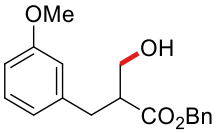

53-Bn

Following the general procedure E, pentane/Et_2O (60/30 v/v) as an eluent, the target compound **53-Bn** was obtained as a colorless oil (25.2 mg, 0.84 mmol, 42%).

^{1}H-NMR (500 MHz, $CDCl_3$): δ = 7.37 – 7.30 (m, 3H), 7.28 – 7.24 (m, 2H), 7.18 (t, J = 7.9 Hz, 1H), 6.78 – 6.70 (m, 3H), 5.18 – 5.09 (m, 2H), 3.82 – 3.70 (m, 5H), 3.02 (dd, J = 13.0, 6.3 Hz, 1H), 2.96 – 2.81 (m, 2H), 2.12 (s, 1H) ppm.

^{13}C-NMR (126 MHz, $CDCl_3$): δ = 174.42, 159.72, 139.98, 135.59, 129.51, 128.57, 128.29, 128.12, 121.29, 114.60, 111.97, 66.55, 62.31, 55.13, 49.03, 34.44 ppm.

HRMS (ESIpos) m/z: Calcd for $C_{18}H_{24}O_4N$ 318.1700, Found 318.1690

Benzyl 2-(4-bromobenzyl)-3–Hydroxypropanoate

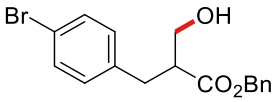

54-Bn

Following the general procedure E, pentane/Et_2O (60/30 v/v) as an eluent, the target compound **54-Bn** was obtained as a colorless oil (27.1 mg, 0.78 mmol, 39%).

^{1}H-NMR (500 MHz, $CDCl_3$): δ = 7.39 – 7.32 (m, 5H), 7.25 – 7.20 (m, 2H), 7.04 – 6.99 (m, 2H), 5.17 – 5.04 (m, 2H), 3.81 – 3.68 (m, 2H), 3.00 – 2.93 (m, 1H), 2.89 – 2.82 (m, 2H), 2.12 (s, 1H) ppm.

^{13}C-NMR (126 MHz, $CDCl_3$): δ = 174.10, 137.36, 135.42, 131.58, 130.70, 128.61, 128.39, 128.25, 66.63, 62.23, 33.81 ppm.

HRMS (ESIpos) m/z: Calcd for $C_{17}H_{21}BrNO_3$ 366.0700, Found 366.0690.

5.5 Pd-Catalyzed Direct γ-C(sp^3)–H-Lactonation of Free Carboxylic Acids

5.5.1 Scope of the Free Carboxylic Acids

General procedure F:

n-BuLi (5.6 mL, 2.5 M solution in hexane, 2.5 equiv.) was added dropwise to a solution of ^{i}Pr$_2$NH (2.0 mL, 14.0 mmol, 2.5 equiv.) in THF (35 mL) at −40 °C. After stirring the resulting solution at −40 °C for 30 min, it was warmed to −20 °C. A solution of carboxylic acid (5.6 mmol, 1.0 equiv.) in DMPU (2.0 mL) was added dropwise at the same temperature and the reaction mixture was stirred at room temperature for 1 h. The reaction mixture was cooled to 0 °C followed by the dropwise addition of the required alkyl or benzyl bromide (11 mmol, 2.0 equiv.) in THF (5 mL). The reaction mixture was stirred at room temperature for 16 h and afterwards was quenched with H_2O (10 mL), THF and hexane were removed under reduced pressure. The resultant mixture was diluted with H_2O (20 mL) and the aqueous solution was extracted with CH_2Cl_2 (2× 20 mL). The aqueous phase was acidified with conc. aq. HCl until

pH 1 and extracted with CH_2Cl_2 (2 x 25 mL). The combined organic phases dried over MgSO4 and all volatiles were removed under reduced pressure. The crude product was purified by column chromatography using CH_2Cl_2: MeOH (99.5:0.5 v/v) acidified with HCOOH (0.1 mL for 100 mL of solvent mixture) as the eluent.

General procedure G:

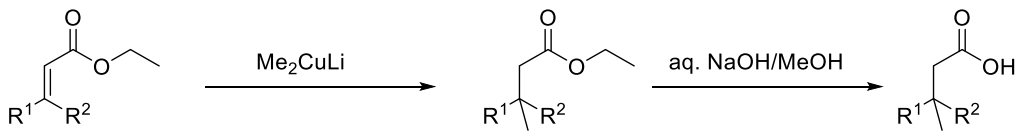

In a dry argon filled schlenk tube CuI (2.0 equiv.) and Et_2O (0.5M) were added and the suspension was cooled to 0 °C. MeLi (1.6 M in Et_2O, 4.0 equiv.) was added dropwise and the mixture was stirred for 10 minutes. The solvent was removed at 0 °C under reduced pressure and CH_2Cl_2 (0.5M) was added. The mixture was stirred for 5 minutes and CH_2Cl_2 was removed at 0 °C under reduced pressure. CH_2Cl_2 (0.2 M) was added and the reaction mixture was cooled to −78 °C. TMSCl (2.0 equiv.) and the α,β-unsaturated carbonyl compound (1.0 equiv.) were added dropwise and the mixture was stirred for 1 h. The reaction mixture was allowed to slowly warm up to r.t. and stirred for 16 h. The reaction was quenched by the addition of sat. aq. NH_4Cl solution and conc. ammonia (aq.) was added. The aqueous phase was extracted with Et_2O and the combined organic phases were washed with brine and dried over $MgSO_4$. All volatiles were removed and the residue was transferred with MeOH (0.5M) to a Schlenk tube and aq. NaOH (10 wt%, 0.5M) was added. The reaction mixture was heated to 60 °C and stirred for 16h. The mixture was allowed to cooldown to r.t. and was concentrated under reduced pressure. Water was added and the aqueous solution was washed with CH_2Cl_2. The aqueous phase was acidified with HCl (10 wt%) until the pH was between 1 and 4. The aqueous phase was extracted with CH_2Cl_2. The combined organic phases were dried over $MgSO_4$·and the solvent was removed under reduced pressure. The crude product was purified by silica gel column chromatography.

General Procedure H:

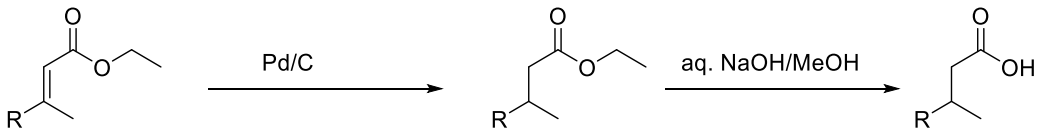

The α,β-unsaturated carbonyl compound was treated with Pd/C (10% by weight) and dissolved in MeOH (25 mL). The resulting mixture was stired under a hydrogen atmosphere (1 atm) at r.t. for 18 h. The reaction mixture was filtered through celite, and the solids thus retained were washed with CH_2Cl_2. The combined filtrates were concentrated in vacuo and the residue was transferred with MeOH (0.5M) to a Schlenk tube and aq. NaOH (10 wt%, 0.5M) was added. The reaction mixture was heated to 60 °C and stirred for 16h. The mixture was allowed to cool down to r.t. and was concentrated under reduced pressure. Water was added and the aqueous solution was washed with CH_2Cl_2. The aqueous phase was acidified with HCl (10 wt%) until the pH was between 1 and 4 and the aqueous phase was extracted withCH_2Cl_2. The combined organic phases were dried over $MgSO_4$ and the solvent was removed under reduced pressure. The crude product was purified by silica gel column chromatography.

3-benzyl-3-methylpentanoic acid

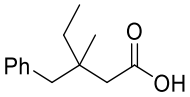

123

Following the general procedure G in 10.0 mmol scale and using ethyl 3-benzylpent-2-enoate (2.18 g, 10.0 mmol), the target compound **123** was obtained as a colorless oil (1.32 g, 6.43 mmol, 64%).

^{1}H NMR (500 MHz, $CDCl_3$): δ 7.29 – 7.25 (m, 2H), 7.23 – 7.17 (m, 3H), 2.77 – 2.65 (m, 2H), 2.29 – 2.17 (m, 2H), 1.52 – 1.33 (m, 2H), 0.99 – 0.92 (m, 6H) ppm

^{13}C NMR (126 MHz, $CDCl_3$): δ = 178.37, 138.29, 130.77, 127.84, 126.10, 44.94, 42.17, 37.02, 31.67, 24.18, 8.28 ppm

HRMS (ESIpos) m/z: Calcd for $C_{13}H_{22}NO_2$ 224.1645, Found 224.1638

IR (cm-1): 2965, 1698, 1453, 1406, 1275, 1219, 934, 748, 701, 599, 491

2-(4,4-difluoro-1-methylcyclohexyl)acetic acid

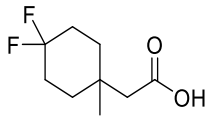

124

Following the general procedure G in 10.0 mmol scale and using ethyl 2-(4,4-difluorocyclohexylidene)acetate (2.04 g, 10.0 mmol), the target compound **124** was obtained as a colorless solid (1.16 g, 6.04 mmol, 60%).

^{1}H NMR (500 MHz, $CDCl_3$): δ 2.33 (s, 2H), 1.98 – 1.86 (m, 4H), 1.68 (dt, J = 13.6, 6.7 Hz, 2H), 1.60 (dt, J = 13.5, 6.1 Hz, 2H), 1.13 (s, 3H) ppm

^{13}C NMR (126 MHz, $CDCl_3$): δ = 177.61, 123.17 (t, J = 241.0 Hz), 44.38, 33.78 (t, J = 4.8 Hz), 32.18, 29.95 (t, J = 24.3 Hz), 23.93 ppm

^{19}F NMR (471 MHz, $CDCl_3$): δ = -96.29 (d, J = 237.2 Hz), -98.39 (d, J = 232.8 Hz) ppm

HRMS (ESIpos) m/z: Calcd for $C_9H_{13}O_2F_2$ 191.0878, Found 191.0880

IR (cm-1): 2971, 2658, 1697, 1451, 1359, 1280, 1175, 1089, 945, 914, 886, 699, 596, 500

2-((1s,4s)-1-methyl-4-phenylcyclohexyl)acetic acid

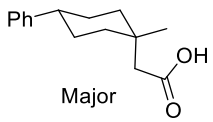

125

Following the general procedure G in 10.0 mmol scale and using ethyl 2-(4-phenylcyclohexylidene)acetate (2.44 g, 10.0 mmol), the target compound **125** was obtained as a colorless solid (1.65 g, 7.10 mmol, 71%).

^{1}H NMR (500 MHz, $CDCl_3$): δ = 7.31 – 7.27 (m, 2H), 7.24 – 7.21 (m, 2H), 7.20 – 7.17 (m, 1H), 2.52 – 2.44 (m, 3H), 1.85 – 1.71 (m, 4H), 1.70 – 1.60 (m, 2H), 1.38 (td, J = 13.5, 3.8 Hz, 2H), 1.12 (s, 3H) ppm (There is another set of peaks belong to the minor diastereomer. The ratio is 97:3, which was determined in the Michael reaction step.)

^{13}C NMR (126 MHz, $CDCl_3$): δ = 178.65, 147.10, 128.36, 126.83, 126.00, 49.57, 44.05, 40.56, 38.19, 32.79, 29.57, 21.70 ppm

HRMS (ESIpos) m/z: Calcd for $C_{15}H_{19}O_2$ 231.1380, Found 231.1386

IR (cm-1): 2924, 1695, 1450, 1317, 1260, 1211, 940, 753, 700, 612, 528, 488

2-(4-methyl-1,1-dioxidotetrahydro-2H-thiopyran-4-yl)acetic acid

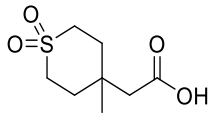

127

Following the general procedure G using in 8.0 mmol scale and using ethyl 2-(1,1-dioxidotetrahydro-4H-thiopyran-4-ylidene)acetate (1.74 g, 8.0 mmol), the target compound **127** was obtained as a colorless solid (1.09 g, 5.29 mmol, 66%).

^{1}H NMR (500 MHz, $CDCl_3$): δ = 3.09 – 2.97 (m, 4H), 2.41 (s, 2H), 2.20 – 2.11 (m, 2H), 2.10 – 2.01 (m, 2H), 1.22 (s, 3H) ppm

^{13}C NMR (126 MHz, $CDCl_3$): δ = 176.26, 47.43, 43.67, 34.87, 31.70, 23.57 ppm

HRMS (ESIpos) m/z: Calcd for $C_8H_{13}O_4S$ 205.0529, Found: 205.0533

IR (cm-1): 2925, 1701, 1414, 1280, 1265, 1139, 1118, 913, 837, 699, 646, 467

3-methyl-4-phenylbutanoic acid

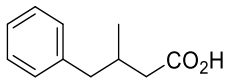

136

Following the general procedure H in 10.0 mmol scale and using ethyl 3-methyl-4-phenylbut-2-enoate (2.04 g, 10.0 mmol), the target compound **136** was obtained as a colorless oil (1.48 g, 8.31 mmol, 83%).

^{1}H-NMR (500 MHz, $(CD_3)_2CO$): δ = 7.30 – 7.26 (m, 2H), 7.22 – 7.14 (m, 3H), 2.65 (dd, J = 13.5, 6.8 Hz, 1H), 2.53 (dd, J = 13.4, 7.4 Hz, 1H), 2.38 (dd, J = 15.0, 5.6 Hz, 1H), 2.32 – 2.24 (m, 1H), 2.20 – 2.14 (m, 1H), 0.98 (d, J = 6.6 Hz, 3H) ppm.

^{13}C-NMR (126 MHz, $(CD_3)_2CO$): δ = 178.65, 140.04, 129.20, 128.29, 126.10, 42.89, 40.59, 32.08, 19.57 ppm.

HRMS (ESIneg) m/z: Calcd for, $C_{11}H_{18}NO_2$, 196.1332, Found 196.1327

IR (cm-1): 2960, 1701, 1453, 1408, 1276, 1260, 1228, 932, 748, 698, 486

5.5.1 Scope of the lactones

General Procedure I: Preperation of β-Quaternary Lactones

An oven dried 10 mL Schlenk tube was charged with $Pd(MeCN)_2Cl_2$ (5.2 mg, 0.020 mmol, 10 mol%), **L46** (7.5 mg, 0.030 mmol, 15 mol%), K_2HPO_4 (27.9 mg, 0.160 mmol, 0.8 equiv.), $Na_2CO_3 \cdot 1.5\ H_2O_2$ (78.4 mg, 0.500 mmol, 2.5 equiv.), carboxylic acid (0.200 mmol, 1.0 equiv.) and HFIP (3.2 mL). The reaction mixture was stirred at 100 °C for 15 h in a preheated metal block. After the mixture was allowed to cool to room temperature, HFIP was removed under reduced pressure, and the resulting mixture was either purified by column chromatography or diluted with CH_2Cl_2 (15 mL), washed with saturated $NaHCO_3$ solution (3× 20 mL), filtered over a short silica plug with CH_2Cl_2 (10 mL) as an eluent and then concentrated under reduced pressure to afford the desired lactone.

4,4-Dimethyldihydrofuran-2(3H)-one

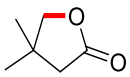

68 Following the general procedure I, pentane/Et_2O (75/25, v/v) as an eluent, the target compound **68** was obtained as a colorless oil (11.2 mg, 0.0982 mmol, 49% yield). (Due to the volatility of the product, the yield was determined by ^{1}H NMR analysis of the crude product using CH_2Br_2 (0.2 mmol, 14 µL) as the internal standard (68% yield).

^{1}H-NMR (500 MHz, $CDCl_3$): δ = 3.98 (s, 2H), 2.33 (s, 2H), 1.20 (s, 6H).

^{13}C-NMR (126 MHz, $CDCl_3$): δ = 177.07, 79.61, 43.08, 36.65, 25.83.

HRMS (ESIpos) m/z: Calcd for $C_6H_{11}O_2$, 115.0754 Found 115.0754

4-Ethyl-4-methyldihydrofuran-2(3H)-one

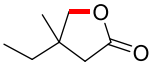

69 Following the general procedure I, pentane/Et_2O (75/25, v/v) as an eluent, the target compound **69** was obtained as a colorless oil (12.8 mg, 0.0994 mmol, 50% yield)).

^{1}H-NMR (500 MHz, $CDCl_3$): δ = 4.04 (d, J = 8.8 Hz, 1H), 3.96 (d, J = 8.8 Hz, 1H), 2.37 (d, J = 17.2 Hz, 1H), 2.27 (d, J = 17.2 Hz, 1H), 1.51 (q, J = 7.4 Hz, 2H), 1.15 (s, 3H), 0.92 (t, J = 7.5 Hz, 3H).

^{13}C-NMR (126 MHz, $CDCl_3$): δ = 177.11, 78.40, 41.32, 40.01, 31.70, 23.17, 8.83.

HRMS (ESIpos) m/z: Calcd for $C_7H_{13}O_2$, 129.0910, Found 129.0909

4-Isopropyl-4-methyldihydrofuran-2(3H)-one

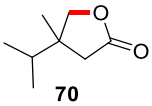

70 Following the general procedure I, pentane/Et_2O (80/20, v/v) as an eluent, the target compound **70** was obtained as a colorless oil (14.8 mg, 0.104 mmol, 52%).

^{1}H-NMR (500 MHz, $CDCl_3$): δ = 4.04 (dd, J = 8.9, 0.7 Hz, 1H), 3.98 (dd, J = 8.9, 0.6 Hz, 1H), 2.38 (d, J = 17.2 Hz, 1H), 2.24 (dd, J = 17.2, 0.6 Hz, 1H), 1.73 (hept, J = 6.8 Hz, 1H), 1.08 (t, J = 0.6 Hz, 3H), 0.92 (d, J = 6.9 Hz, 3H), 0.88 (d, J = 6.9 Hz, 3H).

^{13}C-NMR (126 MHz, $CDCl_3$): δ = 177.20, 78.68, 43.17, 41.50, 35.77, 19.01, 18.16, 17.34.

HRMS (ESIpos) m/z: Calcd for $C_8H_{15}O_2$, 143.1067, Found 143.1063

4-Methyl-4-(2-((triisopropylsilyl)oxy)ethyl)dihydrofuran-2(3H)-one

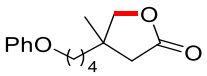

71 Following the general procedure I, pentane/Et_2O (75/25 v/v) as an eluent, the target compound **71** was obtained as a red solid (28.8 mg, 0.116 mmol, 58%).

^{1}H-NMR (500 MHz, $CDCl_3$): δ = 7.32 – 7.24 (m, 2H), 6.98 – 6.91 (m, 1H), 6.91 – 6.82 (m, 2H), 4.04 (d, J = 8.9 Hz, 1H), 4.00 – 3.94 (m, 3H), 2.39 (d, J = 17.2 Hz, 1H), 2.28 (d, J = 17.2

Hz, 1H), 1.84 – 1.75 (m, 2H), 1.56 – 1.42 (m, 4H), 1.18 (s, 3H).ppm

^{13}C-NMR (126 MHz, $CDCl_3$): δ = 177.05, 159.00, 129.58, 120.81, 114.55, 78.69, 67.35, 41.82, 39.90, 39.03, 29.78, 23.72, 21.46.ppm

HRMS (ESIpos) m/z: Calcd for $C_{15}H_{21}O_3$ 249.1485, Found 249.1483

Ethyl 2-(3-methyl-5-oxotetrahydrofuran-3-yl)acetate

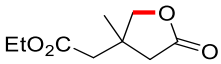

72 Following the general procedure I, pentane/Et_2O (50/50, v/v) as an eluent, the target compound **72** was obtained as a colorless oil (21.9 mg, 0.118 mmol, 59%).

^{1}H-NMR (500 MHz, $CDCl_3$): δ = 4.24 (d, J = 9.2 Hz, 1H), 4.16 (q, J = 7.0 Hz, 2H), 4.11 (d, J = 9.2 Hz, 1H), 2.60 (d, J = 17.4 Hz, 1H), 2.50 (d, J = 2.6 Hz, 2H), 2.39 (d, J = 17.4 Hz, 1H), 1.31 – 1.24 (m, 6H).

^{13}C-NMR (126 MHz, $CDCl_3$): δ = 176.08, 170.46, 77.88, 60.83, 42.93, 41.64, 38.36, 23.97, 14.17.

HRMS (ESIpos) m/z: Calcd for $C_9H_{15}O_4$, 187.0965, Found 187.0960

2-(2-(3-Methyl-5-oxotetrahydrofuran-3-yl)ethyl)isoindoline-1,3-dione

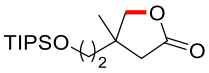

73 Following the general procedure I, pentane/Et_2O (80/20, v/v) as an eluent, the target compound **73** was obtained as a coloureless oil (32.4 mg, 0.108 mmol, 54%).

^{1}H-NMR (500 MHz, $CDCl_3$): δ = 4.14 (d, J = 9.1 Hz, 1H), 4.01 (d, J = 9.1 Hz, 1H), 3.87 – 3.75 (m, 2H), 2.49 (d, J = 17.2 Hz, 1H), 2.27 (dd, J = 17.2, 0.7 Hz, 1H), 1.76 – 1.63 (m, 2H), 1.15 – 0.97 (m, 24H).ppm

^{13}C-NMR (126 MHz, $CDCl_3$): δ = 177.16, 79.45, 59.88, 42.71, 41.24, 39.05, 23.36, 18.09, 11.91.ppm

HRMS (ESIpos) m/z: Calcd for $C_{16}H_{33}O_3Si$ 301.2194, Found 301.2187

4-Benzyl-4-methyldihydrofuran-2(3H)-one

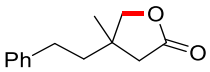

74

Following the general procedure I, pentane/Et_2O (50/50, v/v) as an eluent, the target compound **74** was obtained as a brown oil (26.5 mg, 0.130 mmol, 65%).

^{1}H-NMR (600 MHz, $CDCl_3$): δ = 7.31 – 7.28 (m, 2H), 7.24 – 7.18 (m, 1H), 7.18 – 7.16 (m, 2H), 4.07 (d, J = 8.9 Hz, 1H), 3.99 (d, J = 8.9 Hz, 1H), 2.65 – 2.61 (m, 2H), 2.43 (d, J = 17.2 Hz, 1H), 2.31 (d, J = 17.2 Hz, 1H), 1.84 – 1.76 (m, 2H), 1.26 (s, 3H).

^{13}C-NMR (126 MHz, $CDCl_3$): δ = 176.90, 141.31, 128.75, 128.32, 126.39, 78.69, 41.90, 41.29, 40.03, 31.22, 23.75.

HRMS (ESIpos) m/z: Calcd for $C_{13}H_{17}O_2$, 205.1223, Found 205.1224

4-(4-Chlorobenzyl)-4-methyldihydrofuran-2(3H)-one

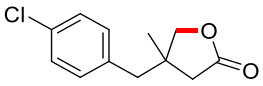

75

Following the general procedure I, pentane/Et_2O (50/50, v/v) as an eluent, the target compound **75** was obtained as a colorless solid (25.1 mg, 0.112 mmol, 56%).

^{1}H-NMR (500 MHz, $CDCl_3$): δ = 7.31 – 7.27 (m, 2H), 7.07 – 7.04 (m, 2H), 4.15 (d, J = 8.9 Hz, 1H), 3.91 (d, J = 9.0 Hz, 1H), 2.73 (s, 2H), 2.49 (d, J = 17.0 Hz, 1H), 2.23 (d, J = 17.0 Hz, 1H), 1.14 (s, 3H).

^{13}C-NMR (126 MHz, $CDCl_3$): δ = 176.33, 135.03, 133.01, 131.29, 128.67, 77.41, 43.71, 41.28, 40.82, 23.47.

HRMS (ESIpos) m/z: Calcd for $C_{12}H_{14}ClO_2$ 225.0677, Found 225.0673

4-(4-methoxybenzyl)-4-methyldihydrofuran-2(3H)-one

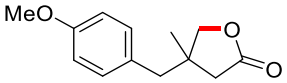

76

Following the general procedure I, pentane/Et_2O (35/65, v/v) as an eluent, the target compound **76** was obtained as a colorless oil (21.6 mg, 0.981 mmol, 49%).

^{1}H-NMR (500 MHz, $CDCl_3$): δ = 7.04 (d, J = 8.6 Hz, 2H), 6.85 (s, 2H), 4.17 (d, J = 8.9 Hz, 1H), 3.90 (d, J = 8.9 Hz, 1H), 3.80 (s, 3H), 2.70 (s, 2H), 2.50 (d, J = 17.0 Hz, 1H), 2.22 (d, J = 17.0 Hz, 1H), 1.15 (s, 3H).

^{13}C-NMR (126 MHz, $CDCl_3$): δ = 176.74, 158.61, 131.03, 128.61, 113.89, 77.56, 55.27, 43.52, 41.27, 40.98, 23.66.

HRMS (ESIpos) m/z: Calcd for $C_{13}H_{17}O_3$ 221.1172, Found 221.1169.

4-Methyl-4-(4-nitrobenzyl)dihydrofuran-2(3H)-one

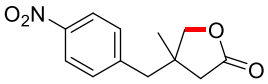

77

Following the general procedure I, pentane/Et_2O (33/67, v/v) as an eluent, the target compound **77** was obtained as a colorless solid (30.1 mg, 0.128 mmol, 64%).

^{1}H-NMR (500 MHz, $CDCl_3$): δ = 8.15 (ddd, J = 8.1, 2.3, 1.2 Hz, 1H), 7.53 (t, J = 7.8 Hz, 1H), 7.48 (dt, J = 7.6, 1.5 Hz, 2H), 4.18 (d, J = 9.0 Hz, 1H), 3.96 (d, J = 9.0 Hz, 1H), 2.89 (s, 2H), 2.52 (d, J = 17.0 Hz, 1H), 2.29 (d, J = 17.0 Hz, 1H), 1.18 (s, 3H).

^{13}C-NMR (126 MHz, $CDCl_3$): δ = 175.86, 148.32, 138.61, 136.04, 129.57, 124.60, 122.25, 77.23, 43.99, 41.26, 40.85, 23.44.

HRMS (ESIpos) m/z: Calcd for $C_{12}H_{14}NO_4$ 236.0917, Found 236.0916

Ethyl 4-((3-methyl-5-oxotetrahydrofuran-3-yl)methyl)benzoate

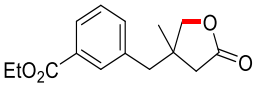

78 Following the general procedure I, pentane/Et_2O (60/40, v/v) as an eluent, the target compound **78** was obtained as a colorless oil (26.7 mg, 0.102 mmol, 51%).

^{1}H-NMR (500 MHz, $CDCl_3$): δ = 7.95 (dt, J = 7.8, 1.5 Hz, 1H), 7.81 (t, J = 1.8 Hz, 1H), 7.40 (t, J = 7.7 Hz, 1H), 7.31 (dt, J = 7.6, 1.6 Hz, 1H), 4.37 (q, J = 7.1 Hz, 2H), 4.18 (d, J = 8.9 Hz, 1H), 3.92 (d, J = 8.9 Hz, 1H), 2.81 (s, 2H), 2.52 (d, J = 17.1 Hz, 1H), 2.24 (d, J = 17.0 Hz, 1H), 1.39 (t, J = 7.1 Hz, 3H), 1.15 (s, 3H).

^{13}C-NMR (126 MHz, $CDCl_3$): δ = 176.46, 166.46, 137.04, 134.46, 130.98, 130.95, 128.68, 128.33, 77.54, 61.25, 44.22, 41.44, 40.96, 23.74, 14.44.

HRMS (ESIpos) m/z: Calcd for $C_{15}H_{19}O_4$ 263.1278, Found 263.1275

4-Benzyl-4-ethyldihydrofuran-2(3H)-one

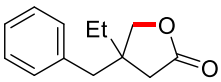

79 Following the general procedure I, pentane/Et_2O (50/50, v/v) as an eluent, the target compound **79** was obtained as a colorless oil (15.1 mg, 0.0739 mmol, 37%).

^{1}H-NMR (500 MHz, $CDCl_3$): δ = 7.36 – 7.30 (m, 2H), 7.29 – 7.25 (m, 1H), 7.15 – 7.09 (m, 2H), 4.18 (d, J = 9.1 Hz, 1H), 4.00 (d, J = 9.1 Hz, 1H), 2.77 (s, 2H), 2.48 (d, J = 17.3 Hz, 1H), 2.30 (d, J = 17.3 Hz, 1H), 1.50 (q, J = 7.5 Hz, 2H), 1.01 (t, J = 7.5 Hz, 3H).

^{13}C-NMR (126 MHz, $CDCl_3$): δ = 176.78, 136.50, 130.10, 128.54, 126.95, 75.81, 44.12, 41.35, 39.02, 28.96, 8.64.

HRMS (ESIpos) m/z: Calcd for $C_{13}H_{17}O_2$ 205.1223, Found 205.1220

2-Oxaspiro[4.5]decan-3-one

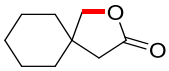

80 Following the general procedure I, pentane/Et_2O (50/50, v/v) as an eluent, the target compound **80** was obtained as a colorless oil (18.8 mg, 0.122 mmol, 61%).

^{1}H-NMR (500 MHz, $CDCl_3$): δ = 4.04 (s, 2H), 2.36 (s, 2H), 1.58 – 1.36 (m, 10H).

^{13}C-NMR (126 MHz, $CDCl_3$): δ = 177.08, 78.23, 40.72, 40.32, 35.18, 22.84.

HRMS (ESIpos) m/z: Calcd for $C_9H_{15}O_2$ 155.1067, Found 155.1065

8,8-Difluoro-2-oxaspiro[4.5]decan-3-one

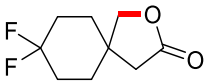

81 Following the general procedure I, pentane/Et_2O (50/50, v/v) as an eluent, the target compound **81** was obtained as a colorless oil (26.6 mg, 0.140 mmol, 70%).

^{1}H-NMR (500 MHz, $CDCl_3$): δ = 4.10 (s, 2H), 2.44 (s, 2H), 2.06 – 1.83 (m, 4H), 1.83 – 1.73 (m, 4H).

^{13}C-NMR (126 MHz, $CDCl_3$): δ = 175.82, 122.28 (t, J = 241.5 Hz), 76.90, 39.54, 39.41, 31.29 (t, J = 4.9 Hz), 30.84 (t, J = 24.8 Hz).

^{19}F-NMR (471 MHz, $CDCl_3$) δ = -97.59 (d, J = 251.0 Hz), -99.93 (d, J = 240.9 Hz).

HRMS (ESIpos) m/z: Calcd for $C_9H_{13}F_2O_2$ 191.0878, Found 191.0877

8-Phenyl-2-oxaspiro[4.5]decan-3-one

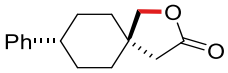

82 Following the general procedure I, pentane/Et_2O (50/50, v/v) as an eluent, the target compound **82** was obtained as a gray solid (40.9 mg, 0.178 mmol, 89%).

^{1}H-NMR (500 MHz, $CDCl_3$): δ = 7. 34 – 7.28 (m 2H), 7.25 – 7.16 (m, 3H), 4.04 (s, 2H), 2. 58 – 2.47 (m, 3H), 1.98 – 1.88 (m, 2H), 1.88 – 1.81 (m, 2H), 1.62 – 1.47 (m, 4H). ppm (There is another set of peaks belong to the minor diastereomer. The ratio is 97:3, which was

determined from starting material.)

^{13}C-NMR (126 MHz, $CDCl_3$): δ = 176.72, 146.02, 128.51, 126.65, 126.34, 79.70, 43.63, 40.13, 38.61, 35.28, 30.48.ppm

HRMS (ESIpos) m/z: Calcd for $C_{15}H_{19}O_2$ 231.1380, Found 231.1378

2,8-Dioxaspiro[4.5]decan-3-one

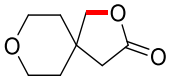

83 Following the general procedure I, pentane/Et_2O (40/60, v/v) as an eluent, the target compound **83** was obtained as a colorless oil (16.5 mg, 0.106 mmol, 53%).

^{1}H-NMR (500 MHz, $CDCl_3$): δ = 4.12 (s, 2H), 3.74 (ddd, J = 12.0, 6.1, 4.0 Hz, 2H), 3.63 (ddd, J = 11.8, 7.9, 3.5 Hz, 2H), 2.47 (s, 2H), 1.76 – 1.62 (m, 4H).

^{13}C-NMR (126 MHz, $CDCl_3$): δ = 175.95, 77.53, 64.57, 39.95, 38.18, 34.98, 30.31.

HRMS (ESIpos) m/z: Calcd for $C_8H_{13}O_3$ 157.0859, Found 157.0856

Benzyl 3-oxo-2-oxa-8-azaspiro[4.5]decane-8-carboxylate

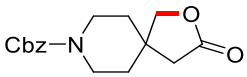

84 Following the general procedure I, pentane/Et_2O (30/70, v/v) as an eluent, the target compound **84** was obtained as a colorless oil (20.8 mg, 0.0719 mmol, 36%).

^{1}H-NMR (600 MHz, $CDCl_3$): δ = 7.41 – 7.29 (m, 5H), 5.13 (s, 2H), 4.09 (s, 2H), 3.71 – 3.64 (m, 2H), 3.38 – 3.31 (m, 2H), 2.44 (s, 2H), 1.55 (s, 4H).

^{13}C-NMR (151 MHz, $CDCl_3$): δ = 176.72, 155.51, 136.96, 128.63, 128.12, 128.00, 67.23, 45.04, 40.11, 36.68, 31.84, 23.97.ppm

HRMS (ESIpos) m/z: Calcd for $C_{16}H_{23}N_2O_4$ 307.1652, Found 307.1644

2-Oxa-8-thiaspiro[4.5]decan-3-one 8,8-dioxide

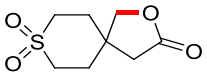

85 Following the general procedure I, pentane/Et_2O (40/60, v/v) as an eluent, the target compound **85** was obtained as a colorless oil (8.6 mg). The sample was found to contain grease. Taking its amount into consideration, the isolated sample contains 18% of desired product.

^{1}H-NMR (500 MHz, $CDCl_3$): δ = 4.15 (s, 2H), 3.11 – 2.98 (m, 4H), 2.52 (s, 2H), 2.33 – 2.16 (m, 4H).

^{13}C-NMR (126 MHz, $CDCl_3$): δ = 174.37, 76.03, 48.18, 39.10, 38.90, 32.62.

HRMS (ESIpos) m/z: Calcd for $C_8H_{16}O_4NS$ 222.0795, Found 222.0789

4,4-Dimethyl-3-propyldihydrofuran-2(3H)-one

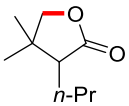

87 Following the general procedure I, pentane/Et_2O (75/25, v/v) as an eluent, the target compound **87** was obtained as a colorless oil (13.7 mg, 0.0878 mmol, 44%).

^{1}H-NMR (500 MHz, $CDCl_3$): δ = 3.91 (d, J = 8.6 Hz, 1H), 3.83 (dd, J = 8.6, 0.7 Hz, 1H), 2.16 (dd, J = 7.7, 6.1 Hz, 1H), 1.74 – 1.58 (m, 2H), 1.52 – 1.33 (m, 2H), 1.17 (s, 3H), 1.01 (s, 3H), 0.96 (t, J = 7.2 Hz, 3H).

^{13}C-NMR (126 MHz, $CDCl_3$): δ = 179.13, 77.95, 49.89, 39.86, 27.28, 24.85, 21.03, 20.87.

HRMS (ESIpos) m/z: Calcd for $C_9H_{17}O_2$ 157.1223, Found 157.1222.

General Procedure J: **Preperation of β-Non-Quaternary Lactones**

An oven dried 10 mL Schlenk tube was charged with $Pd(MeCN)_2Cl_2$ (5.2 mg, 0.020 mmol, 10 mol%), **L46** (12.5 mg, 500 µmol, 25 mol%), K_2HPO_4 (27.9 mg, 0.160 mmol, 0.8 equiv.), $Na_2CO_3 \cdot 1.5\ H_2O_2$ (78.4 mg, 0.500 mmol, 2.5 equiv.), carboxylic acid (0.200 mmol, 1.0 equiv.) and HFIP (5.0 mL). The reaction mixture was stirred at 90 °C for 48 h in a preheated metal block. After the mixture was allowed to cool to room temperature, HFIP was removed under reduced pressure, and the resulting mixture was either purified by column chromatography or diluted with CH_2Cl_2 (15 mL), washed with saturated $NaHCO_3$ solution (3× 20 mL), filtered over a short silica plug with CH_2Cl_2 (10 mL) as an eluent and then concentrated under reduced pressure to afford the desired lactone. The diastereomeric ratio was determined by ^{1}H-NMR analysis of the crude reaction mixture using CH_2Br_2 as internal standard.

4-Methyldihydrofuran-2(3H)-one

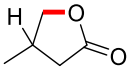

98 Following the general procedure J, purification by diluting with CH_2Cl_2 and washing with saturated $NaHCO_3$, afforded the target compound **98** as a colorless oil (7.2 mg, 71.9 µmol, 36%). Due to the volatility of the product, a ^{1}H-NMR yield (48%) was determined from the crude reaction mixture using CH_2Br_2 (34.8 mg, 0.200 mmol) as internal standard.

^{1}H-NMR (500 MHz, $CDCl_3$): δ = 4.45 – 4.37 (m, 1H), 3.89 – 3.84 (m, 1H), 2.68 – 2.59 (m, 2H), 2.17 – 2.10 (m, 1H), 1.16 (d, *J* = 6.5 Hz, 3H) ppm.

^{13}C-NMR (126 MHz, $CDCl_3$): δ = 177.43, 74.83, 36.26, 30.52, 18.05 ppm.

HRMS (ESIpos) m/z: Calcd for $C_5H_9O_2$ 101.0597, Found 101.0599

4-Benzyldihydrofuran-2(3H)-one

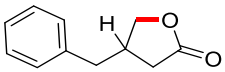

99 Following the general procedure J (35.6 mg), using pentane/Et_2O (60/40, v/v) as an eluent, the target compound **99** was obtained as a colorless oil (13.4 mg, 0.0761

mmol, 38%).

^{1}H-NMR (500 MHz, $CDCl_3$): δ = 7.36 – 7.28 (m, 2H), 7.27 – 7.23 (m, 1H), 7.19 – 7.12 (m, 2H), 4.34 (dd, J = 9.2, 6.9 Hz, 1H), 4.04 (dd, J = 9.2, 6.2 Hz, 1H), 2.93 – 2.81 (m, 1H), 2.80 – 2.73 (m, 2H), 2.61 (dd, J = 17.5, 8.0 Hz, 1H), 2.30 (dd, J = 17.5, 7.0 Hz, 1H).

^{13}C-NMR (126 MHz, $CDCl_3$): δ = 176.79, 138.20, 128.81, 128.65, 126.83, 72.64, 38.96, 37.18, 34.25.

HRMS (ESIpos) m/z: Calcd for $C_{11}H_{13}O_2$ 177.0910, Found 177.0910

General procedure K: Scale-up reaction

An oven dried 100 mL Schlenk tube was charged with $Pd(MeCN)_2Cl_2$ (52.0 mg, 0.200 mmol, 10 mol%), **L46** (100.0 mg, 400.0 µmol, 20 mol%), K_2HPO_4 (279.0 mg, 1.600 mmol, 0.8 equiv.), $Na_2CO_3 \cdot 1.5\ H_2O_2$ (784.0 mg, 5.000 mmol, 2.5 equiv.), carboxylic acid (2.00 mmol, 1.0 equiv.) and HFIP (32 mL). The reaction mixture was placed in a preheated metal block and stirred at 100 °C for 15 h. After the mixture was allowed to cool to room temperature, HFIP was removed under reduced pressure, and the resulting mixture was purified by column chromatography.

2-Oxaspiro[4.5]decan-3-one

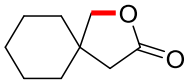

Following the general procedure K**,** the desired product was obtained as a colorless oil (178.2 mg, 1.156 mmol, 58%).

4-Benzyl-4-methyldihydrofuran-2(3H)-one

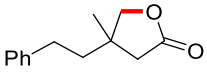

Following the general procedure K**,** the desired product was obtained as a colorless oil (244.6 mg, 1.197 mmol, 60%).

2-methyl-2-phenethylbutane-1,4-diol

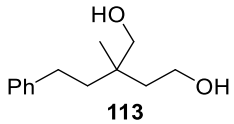

113

2-methyl-2-phenethylbutane-1,4-diol (**113**) was prepared according to a modified version of a reported literature procedure. 4-Benzyl-4-methyldihydrofuran-2(3H)-one (**74**) (612 mg, 0.300 mmol, 1 equiv.) in dry THF (1.5 mL) was added dropwise to a suspension of $LiAlH_4$ (11.4 mg, 0.300 mmol, 1 equiv.) in dry THF (1.5 mL) at 0 °C. The resulting mixture was stirred at room temperature for 12 h, diluted with diethyl ether and quenched with water. The resulting mixture was stirred at room temperature for 1 h. After filtration through a pad of Celite, the filtrate was dried over $MgSO_4$ and concentrated to give a residue, which was further purified by silica-gel chromatography using EtOAc:Pentane=1:2 as eluent to afford the target compound **113** as a colourless oil (57.4 mg, 0.280 mmol, 92%).

^{1}H-NMR (500 MHz, $CDCl_3$): δ = 7.34 – 7.21 (m, 2H), 7.20 – 7.13 (m, 3H), 4.07 – 3.52 (m, 4H), 3.52 – 3.35 (m, 2H), 2.63 – 2.50 (m, 2H), 1.70 – 1.54 (m, 4H), 0.95 (s, 3H) ppm.

^{13}C-NMR (126 MHz, $CDCl_3$): δ = 143.06, 128.50, 128.42, 125.83, 69.92, 58.71, 41.07, 39.75, 37.69, 30.09, 22.40 ppm.

HRMS (ESI) m/z: Calcd for $C_{13}H_{21}O_2$ 209.1536, Found 209.1531

N-(3,5-di-*tert*-butylphenyl)-3-(hydroxymethyl)-3-methyl-5-phenylpentanamide

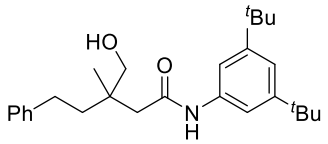

115

N-(3,5-di-*tert*-butylphenyl)-3-(hydroxymethyl)-3-methyl-5-phenylpentanamide(**115**) was prepared according to a modified version of a literature procedure.[170] *n*-BuLi (2.5 M in hexanes, 2.6 mL, 6.6 mmol, 2.2 equiv.) was added to a solution of 3,5-di-*tert*-butylaniline (677 mg, 3.30 mmol, 1.1 equiv.) in THF (2.5 mL) at 0 °C. The resulting reaction mixture was stirred at 0 °C for 1h, and then cooled down to −78 °C. 4-Benzyl-4-methyldihydrofuran-2(3H)-one (**74**) (612 mg, 0.300 mmol, 1 equiv.).in THF (1.0 mL) was added drop-wise. The reaction mixture was stirred for 1 h at the same temperature. The reaction was quenched with saturated NH_4Cl and extracted with ethyl acetate (3 × 10 mL). The

combined organic extracts were dried over Na_2SO_4 and concentrated under reduced pressure. The crude reaction mixture was purified by silica gel chromatography using EtOAc:Pentane=1:4 as eluent to afford the target compound **115** as a colourless oil (101.8 mg, 0.2487 mmol, 83%).

^{1}H-NMR (500 MHz, $CDCl_3$): δ = 7.71 (s, 1H), 7.36 (d, J = 1.8 Hz, 2H), 7.30 – 7.25 (m, 2H), 7.23 – 7.16 (m, 4H), 3.74 (s, 1H), 3.63 – 3.51 (m, 2H), 2.70 – 2.63 (m, 2H), 2.48 – 2.36 (m, 2H), 1.75 – 1.69 (m, 2H), 1.32 (s, 18H), 1.09 (s, 3H) ppm.

^{13}C-NMR (126 MHz, $CDCl_3$): δ = 170.80, 151.77, 142.65, 137.14, 128.57, 128.52, 125.97, 118.96, 114.86, 69.73, 46.69, 40.27, 39.02, 35.05, 31.52, 30.32, 22.65 ppm.

HRMS (ESIpos) m/z: Calcd for $C_{27}H_{40}NO_2$ 410.3045, Found 410.3053

6 References

[1] a) M.-L. Sun, Y. Han, X. Yu, K. Wang, L. Lin, R. Ledesma-Amaro, X.-J. Ji, *Green Chem.* **2024**, *26*, 5202; b) S. Nam, D. Mooney, *Chem. Rev.* **2021**, *121*, 11336; c) D. R. Hill, A. D. Huters, T. B. Towne, R. E. Reddy, J. L. Fogle, E. A. Voight, P. R. Kym, *Chem. Rev.* **2023**, *123*, 13693; d) S. Malik, K. Muhammad, Y. Waheed, *Molecules* **2023**, *28*, 661; e) F. Gomollón-Bel, *Chem. Int.* **2020**, *42*, 3.

[2] G. Rothenberg, in *Catalysis: Concepts and Green Applications,* **2008**, pp. 1.

[3] W. N. R. W. Isahak, A. Al-Amiery, *Green. Technol. Sustain.* **2024**, *2*, 100078.

[4] F. A. Carey, R. J. Sundberg, in *Advanced Organic Chemistry,* **1983**, pp. 95.

[5] A. S. Goldman, K. I. Goldberg, in *Activation and Functionalization of C—H Bonds,* **2004**, pp. 1.

[6] K. Godula, D. Sames, *Science* **2006**, *312*, 67.

[7] a) J. H. Docherty, T. M. Lister, G. McArthur, M. T. Findlay, P. Domingo-Legarda, J. Kenyon, S. Choudhary, I. Larrosa, *Chem. Rev.* **2023**, *123*, 7692; b) T. Dalton, T. Faber, F. Glorius, *Acs Cent. Sci.* **2021**, *7*, 245; c) J. F. Hartwig, *J. Am. Chem. Soc.* **2015**, *138*, 2.

[8] K. M. Altus, J. A. Love, *Commun. Chem.* **2021**, *4*, 173.

[9] J. Zhang, M. Rueping, *Chem. Soc. Rev.* **2023**, *52*, 4099.

[10] a) J. C. K. Chu, T. Rovis, *Angew. Chem. Int. Ed.* **2018**, *57*, 62; b) J. A. Labinger, J. E. Bercaw, *Nature* **2002**, *417*, 507.

[11] a) A. E. Shilov, A. A. Shteinman, *Coord. Chem. Rev.* **1977**, *24*, 97; b) J. A. Labinger, *Chem. Rev.* **2017**, *117*, 8483.

[12] a) P. Gandeepan, T. Müller, D. Zell, G. Cera, S. Warratz, L. Ackermann, *Chem. Rev.* **2019**, *119*, 2192; b) L. Lukasevics, A. Cizikovs, L. Grigorjeva, *Chem. Commun.* **2021**, *57*, 10827.

[13] a) V. Butera, *Physical Chemistry Chemical Physics* **2024**, *26*, 7950; b) L.-L. Zhang, L. Zhang, S.-J. Li, D.-C. Fang, *Dalton Trans.* **2018**, *47*, 6102.

[14] A. H. Janowicz, R. G. Bergman, *J. Am. Chem. Soc.* **1982**, *104*, 352.

[15] a) P. L. Watson, *J. Am. Chem. Soc.* **1983**, *105*, 6491; b) M. E. Thompson, S. M. Baxter, A. R. Bulls, B. J. Burger, M. C. Nolan, B. D. Santarsiero, W.

P. Schaefer, J. E. Bercaw, *J. Am. Chem. Soc.* **1987**, *109*, 203.

[16] I. P. Rothwell, *Acc. Chem. Res.* **1988**, *21*, 153.

[17] a) M. Lafrance, C. N. Rowley, T. K. Woo, K. Fagnou, *J. Am. Chem. Soc.* **2006**, *128*, 8754; b) Y. Boutadla, D. L. Davies, S. A. Macgregor, A. I. Poblador-Bahamonde, *Dalton Trans.* **2009**, 5820; c) D. Lapointe, K. Fagnou, *Chem. Lett.* **2010**, *39*, 1118.

[18] S. Winstein, T. G. Traylor, *J. Am. Chem. Soc.* **1955**, *77*, 3747.

[19] J. M. Davidson, C. Triggs, *J. Chem. Soc. A* **1968**, 1324.

[20] D. L. Davies, S. A. Macgregor, C. L. McMullin, *Chem. Rev.* **2017**, *117*, 8649.

[21] D. H. Ess, S. M. Bischof, J. Oxgaard, R. A. Periana, W. A. Goddard, III, *Organometallics* **2008**, *27*, 6440.

[22] a) L. Wang, B. P. Carrow, *Acs Catal.* **2019**, *9*, 6821; b) D. H. Ess, W. A. Goddard, III, R. A. Periana, *Organometallics* **2010**, *29*, 6459.

[23] A. Biffis, P. Centomo, A. Del Zotto, M. Zecca, *Chem. Rev.* **2018**, *118*, 2249.

[24] T. W. Lyons, M. S. Sanford, *Chem. Rev.* **2010**, *110*, 1147.

[25] A. G. Constable, W. S. McDonald, L. C. Sawkins, B. L. Shaw, *J. Chem. Soc., Chem. Commun.* **1978**, 1061.

[26] E.-i. Negishi, in *Handbook of Organopalladium Chemistry for Organic Synthesis,* **2002**, pp. 17.

[27] K. M. Engle, T.-S. Mei, M. Wasa, J.-Q. Yu, *Acc. Chem. Res.* **2012**, *45*, 788.

[28] B. Biswas, M. Sugimoto, S. Sakaki, *Organometallics* **2000**, *19*, 3895.

[29] a) M. Aufiero, T. Scattolin, F. Proutière, F. Schoenebeck, *Organometallics* **2015**, *34*, 5191; b) L. M. Mirica, J. R. Khusnutdinova, *Coord. Chem. Rev.* **2013**, *257*, 299; c) D. C. Powers, T. Ritter, in *Higher Oxidation State Organopalladium and Platinum Chemistry,* **2011**, pp. 129.

[30] G. Dyker, *Angew. Chem. Int. Ed.* **1994**, *33*, 103.

[31] O. Baudoin, A. Herrbach, F. Guéritte, *Angew. Chem. Int. Ed.* **2003**, *42*, 5736.

[32] P. Muller, *Pure Appl. Chem.* **1994**, *66*, 1077.

[33] P. B. Armentrout, J. Simons, *J. Am. Chem. Soc.* **1992**, *114*, 8627.

[34] a) S. J. Blanksby, G. B. Ellison, *Acc. Chem. Res.* **2003**, *36*, 255; b) M. Díaz-

Requejo, P. J. Pérez, *Chem. Rev.* **2008**, *108*, 3379.

[35] a) A. R. Dick, M. S. Sanford, *Tetrahedron* **2006**, *62*, 2439; b) B. Hashiguchi, S. Bischof, M. M. Konnick, R. Periana, *Acc. Chem. Res.* **2012**, *45*, 885; c) O. Baudoin, *Chem. Soc. Rev.* **2011**, *40*, 4902.

[36] O. Baudoin, *Acc. Chem. Res.* **2017**, *50*, 1114.

[37] a) V. V. Dunina, O. A. Zalevskaya, V. M. Potapov, *Russ. Chem. Rev.* **1988**, *57*, 250; b) E. C. Constable, *Polyhedron* **1984**, *3*, 1037; c) A. G. Constable, W. S. McDonald, L. C. Sawkins, B. L. Shaw, *J. Chem. Soc., Dalton Trans.* **1980**, 1992; d) L. V. Desai, K. L. Hull, M. S. Sanford, *J. Am. Chem. Soc.* **2004**, *126*, 9542.

[38] a) J. Dupont, C. S. Consorti, J. Spencer, *Chem. Rev.* **2005**, *105*, 2527; b) J. Liu, Y. Xie, W. Zeng, D. Lin, Y. Deng, X. Lu, *J. Org. Chem.* **2015**, *80*, 4618; c) Q. Zhang, X.-S. Yin, S. Zhao, S.-L. Fang, B.-F. Shi, Q. Zhang, *Chem. Commun.* **2014**, *50*, 8353; d) L. Hu, G. Meng, J.-Q. Yu, *J. Am. Chem. Soc.* **2022**, *144*, 20550.

[39] J. He, S. Li, Y. Deng, H. Fu, B. N. Laforteza, J. E. Spangler, A. Homs, J.-Q. Yu, *Science* **2014**, *343*, 1216.

[40] R. de Jesus, K. Hiesinger, M. van Gemmeren, *Angew. Chem. Int. Ed.* **2023**, *62*, e202306659.

[41] a) N. Rodríguez, L. J. Goossen, *Chem. Soc. Rev.* **2011**, *40*, 5030; b) L. J. Gooßen, N. Rodríguez, K. Gooßen, *Angew. Chem. Int. Ed.* **2008**, *47*, 3100; c) S. Mondal, S. Mandal, S. Mondal, S. P. Midya, P. Ghosh, *Chem. Commun.* **2024**, *60*, 9645.

[42] C. T. Bedford, in *Organic Reaction Mechanisms 2018,* **2021**, pp. 51.

[43] a) M. Solmi, M. Schmitz, W. Leitner, in *Studies in Surface Science and Catalysis,* **2019**, pp. 105; b) Y. Zhang, Y. Wang, Q. Qian, Y. Li, B. B. Asare Bediako, J. Zhang, J. Yang, Z. Li, B. Han, *Green Chem.* **2022**, *24*, 1973; c) R. Sang, P. Kucmierczyk, R. Dühren, R. Razzaq, K. Dong, J. Liu, R. Franke, R. Jackstell, M. Beller, *Angew. Chem. Int. Ed.* **2019**, *58*, 14365.

[44] C. Anyaegbu, G. Vidali, D. Haridas, J. F. Hooper, *Polym. Chem.* **2024**, *15*, 2537.

[45] a) C. Lamberth, J. Dinges, in *Bioactive Carboxylic Compound Classes: Pharmaceuticals and Agrochemicals,* **2016**, pp. 1; b) M. Lackinger, W. Heckl, *Langmuir* **2009**, *25*, 11307; c) J. Iglesias, I. Martínez-Salazar, P. Maireles-Torres, D. Martin Alonso, R. Mariscal, M. López Granados, *Chem. Soc. Rev.* **2020**, *49*, 5704.

[46] A. Varenikov, E. Shapiro, M. Gandelman, *Chem. Rev.* **2020**, *121*, 412.

[47] a) L. Li, Y. Yao, N. Fu, *Eur. J. Org. Chem.* **2023**, *26*, e202300166; b) N. A. Nguyen, J. H. Forstater, J. A. McIntosh, *JACS Au* **2024**, *4*, 2715; c) S. B. Beil, T. Q. Chen, N. E. Intermaggio, D. W. C. MacMillan, *Acc. Chem. Res.* **2022**, *55*, 3481.

[48] W. Bi, Y. Tang, X. Li, C. Dai, C. Song, X. Guo, X. Ma, *Commun. Chem.* **2022**, *5*, 124.

[49] V. Soni, B. Punji, in *Strategies for Palladium-Catalyzed Non-Directed and Directed C–H Bond Functionalization,* **2017**, pp. 357.

[50] a) S. Murahashi, *J. Am. Chem. Soc.* **1955**, *77*, 6403; b) D. R. Fahey, *J. Organomet. Chem.* **1971**, *27*, 283; c) L. N. Lewis, J. F. Smith, *J. Am. Chem. Soc.* **1986**, *108*, 2728; d) S. Murai, F. Kakiuchi, S. Sekine, Y. Tanaka, A. Kamatani, M. Sonoda, N. Chatani, *Nature* **1993**, *366*, 529.

[51] T. Rogge, N. Kaplaneris, N. Chatani, J. Kim, S. Chang, B. Punji, L. L. Schafer, D. G. Musaev, J. Wencel-Delord, C. A. Roberts, R. Sarpong, Z. E. Wilson, M. A. Brimble, M. J. Johansson, L. Ackermann, *Nat. Rev. Methods* **2021**, *1*, 43.

[52] D. Shabashov, O. Daugulis, *J. Am. Chem. Soc.* **2010**, *132*, 3965.

[53] V. G. Zaitsev, D. Shabashov, O. Daugulis, *J. Am. Chem. Soc.* **2005**, *127*, 13154.

[54] a) L. V. Desai, K. L. Hull, M. S. Sanford, *J. Am. Chem. Soc.* **2004**, *126*, 9542; b) R. Giri, X. Chen, J.-Q. Yu, *Angew. Chem. Int. Ed.* **2005**, *44*, 2112; c) J. J. Neumann, S. Rakshit, T. Dröge, F. Glorius, *Angew. Chem. Int. Ed.* **2009**, *48*, 6892; d) M. Wasa, K. M. Engle, J.-Q. Yu, *J. Am. Chem. Soc.* **2009**, *131*, 9886; e) Z. Ren, F. Mo, G. Dong, *J. Am. Chem. Soc.* **2012**, *134*, 16991; f) R. Giri, J. Liang, J.-G. Lei, J.-J. Li, D.-H. Wang, X. Chen, I. C. Naggar, C. Guo, B. M. Foxman, J.-Q. Yu, *Angew. Chem. Int. Ed.* **2005**, *44*, 7420.

[55] a) R. L. Carvalho, R. G. Almeida, K. Murali, L. A. Machado, L. F. Pedrosa, P. Dolui, D. Maiti, E. N. da Silva Júnior, *Org. Biomol. Chem.* **2021**, *19*, 525; b) L. S. Fitzgerald, M. L. O'Duill, *Chem. Eur. J.* **2021**, *27*, 8411.

[56] B. Liu, A. M. Romine, C. Z. Rubel, K. M. Engle, B.-F. Shi, *Chem. Rev.* **2021**, *121*, 14957.

[57] a) C.-H. Jun, D.-Y. Lee, J.-B. Hong, *Tetrahedron Lett.* **1997**, *38*, 6673; b) F.-L. Zhang, K. Hong, T.-J. Li, H. Park, J.-Q. Yu, *Science* **2016**, *351*, 252.

[58] a) H. Ha, J. Lee, M. H. Park, B. Jung, M. Kim, *Bull. Korean Chem. Soc.* **2020**, *41*, 582; b) J. Das, W. Ali, D. Maiti, *Trends Chem.* **2023**, *5*, 551; c) N. Goswami, T. Bhattacharya, D. Maiti, *Nat. Rev. Chem.* **2021**, *5*, 646; d) P. Gandeepan, L. Ackermann, *Chem* **2018**, *4*, 199.

[59] a) J. I. Higham, J. A. Bull, J. I. Higham, *Org. Biomol. Chem.* **2020**, *18*, 7291; b) B. Niu, K. Yang, B. Lawrence, H. Ge, *ChemSusChem* **2019**, *12*, 2955.

[60] a) B.-B. Gou, H.-F. Liu, J. Chen, L. Zhou, *Org. Lett.* **2019**, *21*, 7084; b) X.-L. Zhang, G.-F. Pan, X.-Q. Zhu, R.-L. Guo, Y.-R. Gao, Y.-Q. Wang, *Org. Lett.* **2019**, *21*, 2731; c) C. Dong, L. Wu, J. Yao, K. Wei, *Org. Lett.* **2019**, *21*, 2085; d) S. St John-Campbell, A. J. P. White, J. A. Bull, *Org. Lett.* **2020**, *22*, 1807; e) Y.-Q. Chen, Z. Wang, Y. Wu, S. R. Wisniewski, J. X. Qiao, W. R. Ewing, M. D. Eastgate, J.-Q. Yu, *J. Am. Chem. Soc.* **2018**, *140*, 17884; f) B. Li, B. Lawrence, G. Li, H. Ge, *Angew. Chem. Int. Ed.* **2020**, *59*, 3078.

[61] a) Z. Wang, Y. Fu, Q. Zhang, H. Liu, J. Wang, *J. Org. Chem.* **2020**, *85*, 7683; b) Y.-Q. Chen, Y. Wu, Z. Wang, J. X. Qiao, J.-Q. Yu, *Acs Catal.* **2020**, *10*, 5657; c) B. Su, A. Bunescu, Y. Qiu, S. J. Zuend, M. Ernst, J. F. Hartwig, *J. Am. Chem. Soc.* **2020**, *142*, 7912.

[62] L.-C. Kao, A. Sen, *J. Chem. Soc., Chem. Commun.* **1991**, 1242.

[63] R. Giri, N. Maugel, J.-J. Li, D.-H. Wang, S. P. Breazzano, L. B. Saunders, J.-Q. Yu, *J. Am. Chem. Soc.* **2007**, *129*, 3510.

[64] a) T.-S. Mei, R. Giri, N. Maugel, J.-Q. Yu, *Angew. Chem. Int. Ed.* **2008**, *47*, 5215; b) D.-H. Wang, T.-S. Mei, J.-Q. Yu, *J. Am. Chem. Soc.* **2008**, *130*, 17676.

[65] a) B. A. Arndtsen, R. G. Bergman, T. A. Mobley, T. H. Peterson, *Acc. Chem. Res.* **1995**, *28*, 154; b) T. A. Stephenson, S. M. Morehouse, A. R. Powell, J. P. Heffer, G. Wilkinson, *J. Chem. Soc.* **1965**, 3632; c) S. Hermans, M. Wenkin, M. Devillers, *J. Mol. Catal. A: Chem.* **1998**, *136*, 59.

[66] a) S. S. Ng, W. H. Pang, O. Y. Yuen, C. M. So, *Org. Chem. Front.* **2023**, *10*, 4408; b) L.-C. Campeau, N. Hazari, *Organometallics* **2018**, *38*, 3.

[67] a) T. Jankech, I. Gerhardtova, P. Majerova, J. Piestansky, J. Jampilek, A. Kovac, *Anal. Chim. Acta* **2024**, *1300*, 342435; b) A. L. Clevenger, R. M. Stolley, J. Aderibigbe, J. Louie, *Chem. Rev.* **2020**, *120*, 6124.

[68] D.-H. Wang, K. M. Engle, B.-F. Shi, J.-Q. Yu, *Science* **2010**, *327*, 315.

[69] a) B.-F. Shi, Y.-H. Zhang, J. K. Lam, D.-H. Wang, J.-Q. Yu, *J. Am. Chem.*

Soc. **2009**, *132*, 460; b) B.-F. Shi, N. Maugel, Y. H. Zhang, J.-Q. Yu, *Angew. Chem. Int. Ed.* **2008**, *47*, 4882.

[70] a) K. M. Engle, D.-H. Wang, J.-Q. Yu, *J. Am. Chem. Soc.* **2010**, *132*, 14137; b) D. G. Musaev, A. Kaledin, B.-F. Shi, J.-Q. Yu, *J. Am. Chem. Soc.* **2012**, *134*, 1690.

[71] K. Wu, N. Lam, D. A. Strassfeld, Z. Fan, J. X. Qiao, T. Liu, D. Stamos, J.-Q. Yu, *Angew. Chem. Int. Ed.* **2024**, *63*, e202400509.

[72] a) K. S. L. Chan, M. Wasa, L. Chu, B. N. Laforteza, M. Miura, J.-Q. Yu, *Nat. Chem.* **2014**, *6*, 146; b) G. Chen, W. Gong, Z. Zhuang, M. S. Andrä, Y.-Q. Chen, X. Hong, Y.-F. Yang, T. Liu, K. N. Houk, J.-Q. Yu, *Science* **2016**, *353*, 1023.

[73] a) A. Uttry, M. van Gemmeren, *Synthesis* **2019**, *52*, 479; b) J. Das, D. K. Mal, S. Maji, D. Maiti, *Acs Catal.* **2021**, *11*, 4205; c) S. Dutta, T. Bhattacharya, F. J. Geffers, M. Bürger, D. Maiti, D. B. Werz, *Chem. Sci.* **2022**, *13*, 2551.

[74] Q. Shao, K. Wu, Z. Zhuang, S. Qian, J.-Q. Yu, *Acc. Chem. Res.* **2020**, *53*, 833.

[75] G.-J. Cheng, Y.-F. Yang, P. Liu, P. Chen, T.-Y. Sun, G. Li, X. Zhang, K. N. Houk, J.-Q. Yu, Y.-D. Wu, *J. Am. Chem. Soc.* **2014**, *136*, 894.

[76] a) T.-S. Mei, X. Wang, J.-Q. Yu, *J. Am. Chem. Soc.* **2009**, *131*, 10806; b) K. M. Engle, T. S. Mei, X. Wang, J.-Q. Yu, *Angew. Chem. Int. Ed.* **2011**, *50*, 1478; c) Z. Zhuang, J.-Q. Yu, *Nature* **2019**, *577*, 656; d) L.-P. Xu, Z. Zhuang, S. Qian, J.-Q. Yu, D. G. Musaev, *Acs Catal.* **2022**, *12*, 4848; e) S. Mal, F. Jurk, K. Hiesinger, M. van Gemmeren, *Nat. Synth.* **2024**, *3*, 1292.

[77] a) I. Colomer, A. Chamberlain, M. B. Haughey, T. Donohoe, *Nat. Rev. Chem.* **2017**, *1*, 1; b) T. Bhattacharya, A. Ghosh, D. Maiti, *Chem. Sci.* **2021**, *12*, 3857.

[78] a) K. L. Bay, Y.-F. Yang, K. N. Houk, *J. Organomet. Chem.* **2018**, *864*, 19; b) I. Pérez-Ortega, A. C. Albéniz, *Dalton Trans.* **2023**, *52*, 1425.

[79] a) J. Grover, A. T. Sebastian, S. Maiti, A. C. Bissember, D. Maiti, *Chem. Soc. Rev.* **2025**, *54*, 2006; b) S. Saha, J. Das, S. A. Al-Thabaiti, S. M. Albukhari, Q. A. Alsulami, D. Maiti, *Catal. Sci. Technol.* **2023**, *13*, 11.

[80] Y. Zhu, X. Chen, C. Yuan, G. Li, J. Zhang, Y. Zhao, *Nature Commun.* **2017**, *8*, 14904.

[81] G. Chen, Z. Zhuang, G.-C. Li, T. G. Saint-Denis, Y. Hsiao, C. L. Joe, J.-Q.

Yu, *Angew. Chem. Int. Ed.* **2017**, *56*, 1506.

[82] K. K. Ghosh, M. van Gemmeren, *Chem. Eur. J.* **2017**, *23*, 17697.

[83] G. Meng, L. Hu, M. Tomanik, J.-Q. Yu, *Angew. Chem. Int. Ed.* **2023**, *62*, e202214459.

[84] G. Kang, D. A. Strassfeld, T. Sheng, C.-Y. Chen, J.-Q. Yu, *Nature* **2023**, *618*, 519.

[85] Z. Zhuang, C.-B. Yu, G. Chen, Q.-F. Wu, Y. Hsiao, C. Joe, J. X. Qiao, M. Poss, J.-Q. Yu, *J. Am. Chem. Soc.* **2018**, *140*, 10363.

[86] K. K. Ghosh, A. Uttry, A. Mondal, F. Ghiringhelli, P. Wedi, M. van Gemmeren, *Angew. Chem. Int. Ed.* **2020**, *59*, 12848.

[87] J. Das, P. Dolui, W. Ali, J. P. Biswas, H. B. Chandrashekar, G. Prakash, D. Maiti, *Chem. Sci.* **2020**, *11*, 9697.

[88] H. S. Park, Z. Fan, R.-Y. Zhu, J.-Q. Yu, *Angew. Chem. Int. Ed.* **2020**, *59*, 12853.

[89] J. Das, T. Pal, W. Ali, S. R. Sahoo, D. Maiti, *Acs Catal.* **2022**, *12*, 11169.

[90] F. Ghiringhelli, A. Uttry, K. K. Ghosh, M. van Gemmeren, *Angew. Chem. Int. Ed.* **2020**, *59*, 23127.

[91] Z. Zhuang, A. N. Herron, J.-Q. Yu, *Angew. Chem. Int. Ed.* **2021**, *60*, 16382.

[92] Z. Wang, L. Hu, N. Chekshin, Z. Zhuang, S. Qian, J. X. Qiao, J.-Q. Yu, *Science* **2021**, *374*, 1281.

[93] T. Sheng, Z. Zhuang, Z. Wang, L. Hu, A. N. Herron, J. X. Qiao, J.-Q. Yu, *J. Am. Chem. Soc.* **2022**, *144*, 12924.

[94] L. Hu, G. Meng, X. Chen, J. S. Yoon, J.-R. Shan, N. Chekshin, D. A. Strassfeld, T. Sheng, Z. Zhuang, R. Jazzar, G. Bertrand, K. Houk, J.-Q. Yu, *J. Am. Chem. Soc.* **2023**, *145*, 16297.

[95] a) N. A. McGrath, M. Brichacek, J. T. Njardarson, *J. Chem. Educ.* **2010**, *87*, 1348; b) J. Kim, M. Movassaghi, *Acc. Chem. Res.* **2015**, *48*, 1159.

[96] a) C. M. Marshall, J. G. Federice, C. N. Bell, P. B. Cox, J. T. Njardarson, *J. Med. Chem.* **2024**, *67*, 11622; b) S. P. France, E. A. Lindsey, E. L. McInturff, S. Berritt, D. W. Carney, J. C. DeForest, S. J. Fink, A. C. Flick, T. S. Gibson, K. Gray, A. M. Johnson, C. A. Leverett, Y. Liu, S. Mahapatra, R. B. Watson, *J. Med. Chem.* **2024**, *67*, 4376.

[97] a) L.-L. Li, E. W.-G. Diau, *Chem. Soc. Rev.* **2013**, *42*, 291; b) M. M. Lee,

J. Teuscher, T. Miyasaka, T. N. Murakami, H. J. Snaith, *Science* **2012**, *338*, 643.

[98] J. F. Hartwig, *Nature* **2008**, *455*, 314.

[99] Y. Park, Y. Kim, S. Chang, *Chem. Rev.* **2017**, *117*, 9247.

[100] a) M. Suginome, L. Uehlin, M. Murakami, *J. Am. Chem. Soc.* **2004**, *126*, 13196; b) Y. Tanaka, T. Hasui, M. Suginome, *Synlett* **2008**, *2008*, 1239.

[101] A. Yu. Rulev, *Eur. J. Org. Chem.* **2023**, *26*, e202300451.

[102] F. Collet, R. H. Dodd, P. Dauban, *Chem. Commun.* **2009**, 5061.

[103] Y. N. Timsina, B. F. Gupton, K. C. Ellis, *Acs Catal.* **2018**, *8*, 5732.

[104] H.-Y. Thu, W.-Y. Yu, C.-M. Che, *J. Am. Chem. Soc.* **2006**, *128*, 9048.

[105] a) A. McNally, B. Haffemayer, B. S. L. Collins, M. J. Gaunt, *Nature* **2014**, *510*, 129; b) A. P. Smalley, M. J. Gaunt, *J. Am. Chem. Soc.* **2015**, *137*, 10632; c) A. P. Smalley, J. D. Cuthbertson, M. J. Gaunt, *J. Am. Chem. Soc.* **2017**, *139*, 1412.

[106] S. Liu, Z. Zhuang, J. X. Qiao, K.-S. Yeung, S. Su, E. C. Cherney, Z. Ruan, W. R. Ewing, M. A. Poss, J.-Q. Yu, *J. Am. Chem. Soc.* **2021**, *143*, 21657.

[107] H. S. S. Chan, Y. Lu, J.-Q. Yu, *Nat. Synth.* **2024**, *3*, 752.

[108] F. Kudo, A. Miyanaga, T. Eguchi, *Nat. Prod. Rep.* **2014**, *31*, 1056.

[109] S. Zhang, T. Ye, Y. Liu, G. Hou, Q. Wang, F. Zhao, F. Li, Q. Meng, *Molecules* **2023**, *28*, 7517.

[110] H. Umezawa, in *Mechanism of Action of Antimicrobial and Antitumor Agents,* **1975**, pp. 21.

[111] Y. Park, Y. Kim, S. Chang, *Chem. Rev.* **2017**, *117*, 9247.

[112] a) T. Mandal, S. Mallick, M. Islam, S. De Sarkar, *Acs Catal.* **2024**, *14*, 13451; b) A. Cook, S. G. Newman, *Chem. Rev.* **2024**, *124*, 6078.

[113] a) Y. Yang, X. Zhang, B. Yu, *Nat. Prod. Rep.* **2015**, *32*, 1331; b) M. Ociepa, K. W. Knouse, D. He, J. C. Vantourout, D. T. Flood, N. M. Padial, J. S. Chen, B. B. Sanchez, E. J. Sturgell, B. Zheng, S. Qiu, M. A. Schmidt, M. D. Eastgate, P. S. Baran, *Org. Lett.* **2021**, *23*, 9337; c) J. Dhineshkumar, K. R. Prabhu, *Org. Lett.* **2013**, *15*, 6062.

[114] S. Bera, L. M. Kabadwal, D. Banerjee, *Chem. Soc. Rev.* **2024**, *53*, 4607.

[115] a) P. Ertl, T. Schuhmann, *J. Nat. Prod.* **2019**, *82*, 1258; b) A. G. Atanasov,

S. B. Zotchev, V. M. Dirsch, I. E. Orhan, M. Banach, J. M. Rollinger, D. Barreca, W. Weckwerth, R. Bauer, E. A. Bayer, M. Majeed, A. Bishayee, V. Bochkov, G. K. Bonn, N. Braidy, F. Bucar, A. Cifuentes, G. D'Onofrio, M. Bodkin, M. Diederich, A. T. Dinkova-Kostova, T. Efferth, K. El Bairi, N. Arkells, T.-P. Fan, B. L. Fiebich, M. Freissmuth, M. I. Georgiev, S. Gibbons, K. M. Godfrey, C. W. Gruber, J. Heer, L. A. Huber, E. Ibanez, A. Kijjoa, A. K. Kiss, A. Lu, F. A. Macias, M. J. S. Miller, A. Mocan, R. Müller, F. Nicoletti, G. Perry, V. Pittalà, L. Rastrelli, M. Ristow, G. L. Russo, A. S. Silva, D. Schuster, H. Sheridan, K. Skalicka-Woźniak, L. Skaltsounis, E. Sobarzo-Sánchez, D. S. Bredt, H. Stuppner, A. Sureda, N. T. Tzvetkov, R. A. Vacca, B. B. Aggarwal, M. Battino, F. Giampieri, M. Wink, J.-L. Wolfender, J. Xiao, A. W. K. Yeung, G. Lizard, M. A. Popp, M. Heinrich, I. Berindan-Neagoe, M. Stadler, M. Daglia, R. Verpoorte, C. T. Supuran, T. the International Natural Product Sciences, *Nat. Rev. Drug Discov.* **2021**, *20*, 200.

[116] J. Cramer, C. P. Sager, B. Ernst, *J. Med. Chem.* **2019**, *62*, 8915.

[117] C. Shi, E. C. Quinn, W. T. Diment, E. Y. X. Chen, *Chem. Rev.* **2024**, *124*, 4393.

[118] B. A. Green, R. J. Yu, E. J. Van Scott, *Clin. Dermatol.* **2009**, *27*, 495.

[119] A. Kornhauser, S. G. Coelho, V. J. Hearing, *Clin Cosmet Investig Dermatol.* **2010**, *3*, 135.

[120] H. Arai, Y. Hirasawa, A. Rahman, I. Kusumawati, N. C. Zaini, S. Sato, C. Aoyama, J. Takeo, H. Morita, *Biorg. Med. Chem.* **2010**, *18*, 2152.

[121] M. Janssen, D. E. De Vos, *Chem. Eur. J.* **2019**, *25*, 10724.

[122] J. Hu, T. Lan, Y. Sun, H. Chen, J. Yao, Y. Rao, *Chem. Commun.* **2015**, *51*, 14929.

[123] K. K. Ghosh, A. Uttry, A. Koldemir, M. Ong, M. van Gemmeren, *Org. Lett.* **2019**, *21*, 7154.

[124] Z. Zhuang, A. N. Herron, Z. Fan, J.-Q. Yu, *J. Am. Chem. Soc.* **2020**, *142*, 6769.

[125] Z. Zhuang, J.-Q. Yu, *Nature* **2020**, *577*, 656.

[126] A. Uttry, S. Mal, M. van Gemmeren, *J. Am. Chem. Soc.* **2021**, *143*, 10895.

[127] Majid M. Heravi, M. Ghavidel, L. Mohammadkhani, *RSC Adv.* **2018**, *8*, 27832.

[128] a) C. J. Vickers, T.-S. Mei, J.-Q. Yu, *Org. Lett.* **2010**, *12*, 2511; b) X. Wang,

D. Leow, J.-Q. Yu, *J. Am. Chem. Soc.* **2011**, *133*, 13864; c) X.-G. Zhang, H.-X. Dai, M. Wasa, J.-Q. Yu, *J. Am. Chem. Soc.* **2012**, *134*, 11948; d) P. S. Thuy-Boun, G. Villa, D. Dang, P. Richardson, S. Su, J.-Q. Yu, *J. Am. Chem. Soc.* **2013**, *135*, 17508.

[129] a) A. G. Gonzalez, D. Rosales, J. L. Gomez Ariza, J. Fernandez Sanz, *J. Phys. Org. Chem.* **1991**, *4*, 87; b) M. Witt, H.-F. Grützmacher, *J. Am. Soc. Mass. Spectrom.* **2002**, *13*, 1273.

[130] a) K. M. Engle, *Pure Appl. Chem.* **2016**, *88*, 119; b) G. Koten, P. L. Alsters, H. T. Teunissen, J. Boersma, A. L. Spek, *Organometallics* **1993**, *12*, 4691; c) A. J. Canty, H. Jin, B. W. Skelton, A. H. White, *Inorg. Chem.* **1998**, *37*, 3975; d) R. Giri, J. Liang, J.-G. Lei, J.-J. Li, D.-H. Wang, X. Chen, I. C. Naggar, C. Guo, B. M. Foxman, J.-Q. Yu, *Angew. Chem. Int. Ed.* **2005**, *44*, 7420; e) A. N. Vedernikov, in *Top.Organomet.Chem,* **2010**, pp. 101; f) N. M. Camasso, M. H. Pérez-Temprano, M. S. Sanford, *J. Am. Chem. Soc.* **2014**, *136*, 12771; g) A. R. Dick, K. L. Hull, M. S. Sanford, *J. Am. Chem. Soc.* **2004**, *126*, 2300.

[131] S. Schulz, S. Hötling, *Nat. Prod. Rep.* **2015**, *32*, 1042.

[132] S. K. Sartori, M. A. N. Diaz, G. Diaz-Muñoz, *Tetrahedron* **2021**, *84*, 132001.

[133] J. Hur, J. Jang, J. Sim, *Int. J. Mol. Sci.* **2021**, *22*, 2769.

[134] M. A. F. Delgove, M. T. Elford, K. V. Bernaerts, S. M. A. D. Wildeman, *Org. Process Res. Dev.* **2018**, *22*, 803.

[135] a) J. L. Jeffrey, J. A. Terrett, D. W. C. MacMillan, *Science* **2015**, *349*, 1532; b) M. Keshavarz, A. Zarei Ahmady, A. Mostoufi, N. Mohtasham, *Molecules* **2017**, *22*, 1385; c) I. Triandafillidi, M. G. Kokotou, C. G. Kokotos, *Org. Lett.* **2018**, *20*, 36; d) D. C. Davis, K. L. Walker, C. Hu, R. N. Zare, R. M. Waymouth, M. Dai, *J. Am. Chem. Soc.* **2016**, *138*, 10693; e) Y. Ueki, H. Ito, I. Usui, B. Breit, *Chem. Eur. J.* **2011**, *17*, 8555; f) C. You, S. Li, X. Li, H. Lv, X. Zhang, *Acs Catal.* **2019**, *9*, 8529; g) D. W. Hwang, P. Kashinathan, J. M. Lee, J. H. Lee, U. h. Lee, J.-S. Hwang, Y. K. Hwang, J.-S. Chang, *Green Chem.* **2011**, *13*, 1672; h) D. J. Wackelin, R. Mao, K. M. Sicinski, Y. Zhao, A. Das, K. Chen, F. H. Arnold, *J. Am. Chem. Soc.* **2024**, *146*, 1580; i) C. M. Johansen, E. A. Boyd, D. E. Tarnopol, J. C. Peters, *J. Am. Chem. Soc.* **2024**, *146*, 25456; j) J. Yu, Q. Zhang, B. Zhao, T. Wang, Y. Zheng, B. Wang, Y. Zhang, X. Huang, *Angew. Chem. Int. Ed.* **2024**, *63*, e202402673.

[136] R. R. A. Kitson, A. Millemaggi, R. J. K. Taylor, *Angew. Chem. Int. Ed.*

2009, *48*, 9426.

[137] a) G. I. Nikishin, I. V. Svitanko, E. I. Troyansky, *J. Chem. Soc., Perkin Trans. 2* **1983**, *14*, 595; b) M. Cianfanelli, G. Olivo, M. Milan, R. J. M. Klein Gebbink, X. Ribas, M. Bietti, M. Costas, *J. Am. Chem. Soc.* **2019**, *142*, 1584; c) L. Vicens, M. Bietti, M. Costas, *Angew. Chem. Int. Ed.* **2020**, *60*, 4740; d) A. Call, M. Cianfanelli, P. Besalú-Sala, G. Olivo, A. Palone, L. Vicens, X. Ribas, J. Luis, M. Bietti, M. Costas, *J. Am. Chem. Soc.* **2022**, *144*, 19542; e) A. Call, G. Capocasa, A. Palone, L. Vicens, E. Aparicio, N. Choukairi Afailal, N. Siakavaras, M. E. López Saló, M. Bietti, M. Costas, *J. Am. Chem. Soc.* **2023**, *145*, 18094; f) M. A. Bigi, S. A. Reed, M. C. White, *J. Am. Chem. Soc.* **2012**, *134*, 9721; g) S. Zhou, Z.-J. Zhang, J.-Q. Yu, *Nature* **2024**, *629*, 363; h) V. I. Kurganskiy, R. V. Ottenbacher, M. V. Shashkov, E. P. Talsi, D. G. Samsonenko, K. P. Bryliakov, *Org. Lett.* **2022**, *24*, 8764.

[138] Q. Ma, W. Shan, X. Chu, H. Xu, Z. Chen, F. Li, J.-L. Liao, C. He, W. J. Bai, X.-Q. Wang, *Nat. Synth.* **2023**, *3*, 123.

[139] J. Hioe, H. Zipse, *Org. Biomol. Chem.* **2010**, *8*, 3609.

[140] a) M. E. Hoque, J.-Q. Yu, *Angew. Chem. Int. Ed.* **2023**, *62*, e202312331; b) J. Das, W. Ali, A. Ghosh, T. Pal, A. Mandal, C. Teja, S. Dutta, R. Pothikumar, H. Ge, X. Zhang, D. Maiti, *Nat. Chem.* **2023**, *15*, 1626.

[141] a) J. M. Lee, S. Chang, *Tetrahedron Lett.* **2006**, *47*, 1375; b) P. Novák, A. Correa, J. Gallardo-Donaire, R. Martin, *Angew. Chem. Int. Ed.* **2011**, *50*, 12236; c) S. Qian, Z.-Q. Li, M. Li, S. R. Wisniewski, J. X. Qiao, J. M. Richter, W. R. Ewing, M. D. Eastgate, J. S. Chen, J.-Q. Yu, *Org. Lett.* **2020**, *22*, 3960.

[142] L.-P. Xu, S. Qian, Z. Zhuang, J.-Q. Yu, D. Musaev, *Nature Commun.* **2022**, *13*, 315.

[143] B.-F. Shi, B. Liu, *Synlett* **2016**, *27*, 2396.

[144] H. S. S. Chan, J. Yang, J.-Q. Yu, *Science* **2022**, *376*, 1481.

[145] N. M. Camasso, M. H. Pérez-Temprano, M. Sanford, *J. Am. Chem. Soc.* **2014**, *136*, 12771.

[146] J. He, M. Wasa, K. S. L. Chan, Q. Shao, J.-Q. Yu, *Chem. Rev.* **2016**, *117*, 8754.

[147] M. Farizyan, A. Mondal, S. Mal, F. Deufel, M. van Gemmeren, *J. Am. Chem. Soc.* **2021**, *143*, 16370.

[148] Z. Li, Z. Wang, N. Chekshin, S. Qian, J. X. Qiao, P. T. Cheng, K.-S. Yeung, W. R. Ewing, J.-Q. Yu, *Science* **2021**, *372*, 1452.

[149] Y. Xue, H. S. Park, C. Jiang, J.-Q. Yu, *Acs Catal.* **2021**, *11*, 14188.

[150] P. Novák, A. Correa, J. Gallardo-Donaire, R. Martin, *Angew. Chem. Int. Ed.* **2011**, *50*, 12236.

[151] a) A. McKillop, W. R. Sanderson, *Tetrahedron* **1995**, *51*, 6145; b) H. Yao, D. E. Richardson, *J. Am. Chem. Soc.* **2000**, *122*, 3220; c) Z. Zhuang, A. N. Herron, S. Liu, J.-Q. Yu, *J. Am. Chem. Soc.* **2021**, *143*, 687.

[152] a) M. E. Jung, G. Piizzi, *Chem. Rev.* **2005**, *105*, 1735; b) T. C. Bruice, W. C. Bradbury, *J. Am. Chem. Soc.* **1965**, *87*, 4838.

[153] a) D. K. Naritoku, J. A. Levine, D. F. Covey, J. A. Ferrendelli, *Biochem. Pharmacol.* **1987**, *36*, 797; b) J. A. Levine, J. A. Ferrendelli, D. F. Covey, *Biochem. Pharmacol.* **1985**, *34*, 4187.

[154] a) D. J. Canney, J. A. Levine, H.-F. Lu, D. F. Covey, *Synth. Commun.* **1990**, *20*, 2065; b) E. L. Grimm, H. U. Reissig, *J. Org. Chem.* **1985**, *50*, 242.

[155] a) K. Hiesinger, D. Dar'in, E. Proschak, M. Krasavin, *J. Med. Chem.* **2021**, *64*, 150; b) S. S. Thorat, R. Kontham, *Org. Biomol. Chem.* **2019**, *17*, 7270.

[156] A. Call, M. Cianfanelli, P. Besalú-Sala, G. Olivo, A. Palone, L. Vicens, X. Ribas, J. M. Luis, M. Bietti, M. Costas, *J. Am. Chem. Soc.* **2022**, *144*, 19542.

[157] R. Alfaro, A. Parra, J. Alemán, M. Tortosa, *Synlett* **2013**, *24*, 804.

[158] Y. Zhu, J. Yang, F. Mei, X. Li, C. Zhao, *Green Chem.* **2022**, *24*, 6450.

[159] S. Serra, D. De Simeis, A. Castagna, M. Valentino, *Catalysts* **2020**, *10*, 154.

[160] a) P. Dolui, J. Das, H. B. Chandrashekar, S. S. Anjana, D. Maiti, *Angew. Chem. Int. Ed.* **2019**, *58*, 13773; b) L. Liu, Y.-H. Liu, B.-F. Shi, *Chem. Sci.* **2020**, *11*, 290.

[161] K. K. Ghosh, A. Uttry, A. Mondal, F. Ghiringhelli, P. Wedi, M. van Gemmeren, *Angew. Chem. Int. Ed.* **2020**, *59*, 12848.

[162] a) P. L. Alsters, H. T. Teunissen, J. Boersma, A. L. Spek, G. van Koten, *Organometallics* **1993**, *12*, 4691; b) A. J. Canty, H. Jin, B. W. Skelton, A. H. White, *Inorg. Chem.* **1998**, *37*, 3975.

[163] a) W. Oloo, P. Y. Zavalij, J. Zhang, E. Khaskin, A. N. Vedernikov, *J. Am. Chem. Soc.* **2010**, *132*, 14400; b) E. Abada, P. Y. Zavalij, A. N. Vedernikov, *J. Am. Chem. Soc.* **2017**, *139*, 643.

[164] a) G. Meng, L. Hu, H. S. S. Chan, J. X. Qiao, J.-Q. Yu, *J. Am. Chem. Soc.* **2023**, *145*, 13003; b) T. Pal, P. Ghosh, M. Islam, S. Guin, S. Maji, S. Dutta, J. Das, H. Ge, D. Maiti, *Nature Commun.* **2024**, *15*, 5370; c) T. Sheng, G. Kang, Z. Zhuang, N. Chekshin, Z. Wang, L. Hu, J.-Q. Yu, *J. Am. Chem. Soc.* **2023**, *145*, 20951.

[165] Z. Li, H. S. Park, J. X. Qiao, K.-S. Yeung, J.-Q. Yu, *J. Am. Chem. Soc.* **2022**, *144*, 18109.

[166] Q. Gou, G. Liu, Z. N. Liu, J. Qin, *Chem. Eur. J.* **2015**, *21*, 15491.

[167] T. Kang, N. Kim, P. T. Cheng, H. Zhang, K. Foo, K. M. Engle, *J. Am. Chem. Soc.* **2021**, *143*, 13962.

[168] B.-S. Zhang, Y. Li, Y. An, Z. Zhang, C. Liu, X. Wang, Y. M. Liang, *Acs Catal.* **2018**, *8*, 11827.

[169] L. Talavera, R. R. A. Freund, H. Zhang, M. Wakeling, M. Jensen, R. Martin, *Acs Catal.* **2023**, *13*, 5538.

[170] Y. Zheng, X. Nie, Y. Long, L. Ji, H. Fu, X. Zheng, H. Chen, R. Li, *Chem. Commun.* **2019**, *55*, 12384.